Sheffield Hallam University

A Sheffield Hallam University thesis

ProQuest Number: 10694073

ProQuest 10694073

ProQuest LLC.
789 East Eisenhower Parkway
P.O. Box 1346
Ann Arbor, MI 48106 – 1346

J.E. Abram

W 1 3

ABSTRACT

Low weld tensile strengths are shown to be a feature of hot gas
welded clear unplasticised polyvinyl chloride (UPVC). Typical
weld strengths are 20-30 MPa compared to 45 MPa for hot gas
welded filled UPVC and 61 MPa for hot tool welded clear UPVC.
A short mechanical, microstructural and chemical analysis
revealed only minor differences between clear sheet and rod.
An examination of weld fracture surfaces revealed the presence
of unfused regions (flaws) which act as fracture initiation sites.
In over 80% of the surfaces studied fracture occurred at such
sites, at or close to the weld surface. These regions were
observed for both hot gas welded clear and filled UPVC but not
in hot tool welded clear UPVC. It was concluded that these
regions were a feature of hot gas welding and that clear UPVC
was more sensitive to them than filled UPVC. A range of linear
elastic fracture mechanics (LEFM) test techniques were used to
establish that clear UPVC had a K_{IC} of 2.1 MPam$^{\frac{1}{2}}$, which dropped
to 1.5 MPam$^{\frac{1}{2}}$ after welding. The filled UPVC examined was too
tough to allow K_{IC} to be measured. However, embrittlement of the
welded filled UPVC was indicated, as only brittle fracture, with
no plastic zone, occurred. A simplistic LEFM analysis based on
measured flaw sizes and failure stresses for welds confirmed the
embrittlement of hot gas welded clear UPVC. Two approaches were
tried to improve weld strengths: 1) to reduce the size and number
of flaws and 2) to increase the toughness of the weld rod. An
initial study indicated that changes to the rod lubricant system
and the inclusion of 10 phr methyl methacrylate-butadiene-styrene
in the rod composition led to improved and more consistent weld
strengths. However, improvements were limited to weld strengths
of 32 MPa and to achieve any further improvement the clear sheet
toughness would need to be increased.

HOT GAS WELDS IN

UNPLASTICISED POLYVINYL CHLORIDE

A thesis submitted to the Council for National Academic

Awards in partial fulfilment for the degree of

DOCTOR OF PHILOSOPHY

by

John   Edward   Abram

Collaborating Establishment:-   Sponsoring Establishment:-

British Nuclear Fuels Ltd.,   Department of Metallurgy,

Sellafield,   Sheffield City Polytechnic,

Cumbria.   Sheffield, South Yorkshire,

                                       February, 1983.

Preface

All the work reported in this thesis was carried out during
the period for which the candidate was registered for a higher
degree. No part of this thesis has been submitted for a degree
at any other polytechnic, university or college.

During the period 1977 - 1978 the following modules of the
postgraduate course "Metallurgical Process and Management" were
attended:-

1) Numerical Methods and Programming

2) Metals and Competitive Materials

3) Accountancy

4) Economics

A two week period of welding training was received at British
Nuclear Fuels Ltd, Sellafield, in May 1977.

Over the period 1980 - 1982 two papers based on this work have
been published:-

1) J. Abram, D.W. Clegg and D.V. Quayle, "The Strength of
    Welds in UPVC", Plastics and Rubber International, 7 (1982),
    58.

2) J. Abram, D.W. Clegg and D.V. Quayle, "The Mechanical
    Properties of Welds in UPVC", Proc. 3rd Polytechnic
    Symposium on Manufacturing Engineering, Wolverhampton,
    May, 1982, p. 168.

    (See Appendix for copies.)

HOT GAS WELDS IN UNPLASTICISED POLYVINYL CHLORIDE

J.E. Abram

ABSTRACT

Low weld tensile strengths are shown to be a feature of hot gas welded clear unplasticised polyvinyl chloride (UPVC). Typical weld strengths are 20-30 MPa compared to 45 MPa for hot gas welded filled UPVC and 61 MPa for hot tool welded clear UPVC. A short mechanical, microstructural and chemical analysis revealed only minor differences between clear sheet and rod. An examination of weld fracture surfaces revealed the presence of unfused regions (flaws) which act as fracture initiation sites. In over 80% of the surfaces studied fracture occurred at such sites, at or close to the weld surface. These regions were observed for both hot gas welded clear and filled UPVC but not in hot tool welded clear UPVC. It was concluded that these regions were a feature of hot gas welding and that clear UPVC was more sensitive to them than filled UPVC. A range of linear elastic fracture mechanics (LEFM) test techniques were used to establish that clear UPVC had a K_{IC} of 2.1 MPam$^{\frac{1}{2}}$, which dropped to 1.5 MPam$^{\frac{1}{2}}$ after welding. The filled UPVC examined was too tough to allow K_{IC} to be measured. However, embrittlement of the welded filled UPVC was indicated, as only brittle fracture, with no plastic zone, occurred. A simplistic LEFM analysis based on measured flaw sizes and failure stresses for welds confirmed the embrittlement of hot gas welded clear UPVC. Two approaches were tried to improve weld strengths: 1) to reduce the size and number of flaws and 2) to increase the toughness of the weld rod. An initial study indicated that changes to the rod lubricant system and the inclusion of 10 phr methyl methacrylate-butadiene-styrene in the rod composition led to improved and more consistent weld strengths. However, improvements were limited to weld strengths of 32 MPa and to achieve any further improvement the clear sheet toughness would need to be increased.

CONTENTS

1. Introduction

It is normal when dealing with hazardous chemicals, such as those present during the reprocessing of low level radioactive waste, to handle them in airtight glove boxes. By using such boxes the need for special protective clothing or remote handling facilities is minimised.

These boxes need to be made from materials which are resistant both to the chemicals contained inside them and to accidental damage which would lead to leaks. In the past, such boxes have been produced as welded stainless steel boxes, into the sides of which are incorporated the glove and viewing ports. This construction is adequate for the smaller sized boxes with sides up to 1m long. However, larger boxes suffer several drawbacks:

1) To obtain adequate viewing of the interior, large sections of the wall have to be replaced by transparent material. This makes the maintaining of an airtight environment difficult due to the large amount of sealing around each viewport. It further leads to weakness in the overall structure resulting from the number of holes that are cut in the walls.

2) Even with a large number of viewports it is virtually impossible to eliminate all the blind spots in the box, i.e. areas into which the handler cannot readily see.

3) The welded construction of these boxes leaves sharp corners which act as dirt traps and are difficult to keep clean. Further the welds along the base of the box are particularly vulnerable to attack by spilled chemicals.

4) In the case where they are used for the reprocessing of radioactive materials, the disposal of contaminated boxes at the end of their useful life is very expensive.

British Nuclear Fuels Ltd, Windscale site (now Sellafield, and hereafter referred to as BNFL) decided upon a new approach. To overcome the first two drawbacks, a totally transparent material, which could be easily cut or sealed, was required. The third drawback could be overcome if the material was easily shaped so that the sharp corners could be rounded out. Further, with a

material which was easily moulded, the base of the box could be moulded as a shallow tray thereby lifting vulnerbale joints above any spilled chemicals. The fourth drawback could be overcome if the material was easily destroyed, say by ashing, with any contamination being recovered from the residue.

One class of materials which satisfies the above requirements are the glassy amorphous thermoplastics, such as polystyrene, polymethyl methacrylate, rigid polyvinyl chloride, and polycarbonate. However, the other requirements of a glove box material, the good chemical resistance and toughness, reduced the choice to clear rigid polyvinyl chloride. This material is better known as clear unplasticised polyvinyl chloride, clear UPVC.

To fabricate UPVC structures, four methods of jointing are available:

1) mechanical fixation, screws, bolts, clips, etc.
2) adhesive bonding
3) solvent welding
4) thermal welding

The first two methods introduce a second material into the structure, which may be attacked by the chemicals, and are not particularly successful in producing airtight seals. The third method of solvent welding involves the use of large quantities of organic solvents which introduce unacceptable health and fire hazards. However, thermal welding methods are well established in the plastics fabrication industries, being capable of producing strong, airtight joints with little or no operator risk.

1.1. Thermal Welding of UPVC

UPVC does not become completely fluid when heated. However, if parts are heated to between 175-190°C and moderate pressure applied, then fusion joints can be formed.

The methods of supplying heat to the parts include ultrasonic, friction, radio frequency electric fields, heated tools and hot

gas jets [1]. For large structures and thicker sheets only
the last two are applicable, this work being concerned mainly
with the last method.

1.1.1. Hot Tool Welding

This technique, sometimes known as hot plate welding, uses
a heated tool, normally a round or square sheet of metal with a
non-stick surface, as the heat source. The tool is heated either
electrically or by hot air to 175 - 190°C and the parts to be
joined are lightly pressed against its surface. When these are
softened and a bead has formed, the pressure is relaxed and
the heat allowed to 'soak in' for a short period, approximately
45 seconds. The parts are then rapidly brought together and held
under pressure until cool, see fig. 1.

The technique is used mainly for the jointing of pipe systems
and is ideal where many welds of the same type are required.
It is easily automated and, once the correct weld conditions have
been determined, high strength welds are readily reproduced.
Typical weld efficiencies quoted for UPVC are 70 - 100% [1].

1.1.2. Hot Gas Welding

Hot gas welding is analagous to oxyacetylene welding in metals
in that rod, of the same material as that being joined, under the
action of heat and pressure is laid into a groove prepared between
the parts and a fusion joint with both of them formed. Unlike
metal welding, where a naked flame is used, a heated jet of gas,
either air or nitrogen, supplies the heat. Also neither the rod
nor the parts go fluid; pressure is required to form a good fusion
joint and there is no flux to aid welding. However, similar
types of welds are used, i.e. butt, lap and fillet welds, see fig. 2.
Like metal welding, the weld efficiencies achieved are dependent
on the skill of the welder. An experienced welder should achieve
weld efficiencies of 70-90% [1]. However, values as low as 30%
are not uncommon for inexperienced welders.

The feature of this method of welding is the range and the size

of structures which can be fabricated using it. Typical uses include ventilator ducting, fume extraction systems and tank lining.

Some automation has been developed, but only finds a use where simple straight line welding is required, for example in floor covering.

1.2. Construction of Glove Boxes

The hot tool welding method would seem to offer the best fabrication route, requiring less skill and time than hot gas welding whilst producing stronger welds. However, two drawbacks are apparent when considering glove box construction:

1) when two lengths of sheet need to be joined, to make a side wall, the weld would have to be completed at every point along the length at the same time. If a weld length of 2m was required, the hot tool would have to be of a similar or larger size. This presents problems in terms of the power requirements to heat the tool and in the accurate control of the temperature along the tool.

2) hot tool welding is best suited to cases where a large number of identical welds need to be made. This is not the case in glove box construction in which each glove box is tailor-made for a specific job. Further, in each box there is a large number of different welds used. They range from simple straight butt welds to corner welds, to fillet welds, these being used to fabricate shelves or support structures inside the box.

These present no obstacles to hot gas welding, which was therefore, adopted as the main fabrication method.

However, during routine testing at BNFL, the efficiency of hot gas welded clear UPVC sheet was found to be typically only 40%, far short of the 70-90% efficiencies quoted in the literature. The following research investigation was inspired by a need to:

1) determine the reasons for the low weld efficiencies achieved by the BNFL welders.

2) determine the ways to improve the weld efficiencies.

A more detailed description of the hot gas welding methods
is given next , along with guidelines and typical conditions
used. However,details of the research into hot gas welding,as
reported in the literature, are given in section 2.6.

1.3. General Practice and Guidelines for Hot Gas Welding

Hot gas welding is really still an art and as such the
experience and skill of the welder is considered the main factor
controlling the strength of the finished weld. It is normal,
therefore, to find the practice and conditions for welding being
given only as guidelines, with the final details being determined
by the welder to suit both him and the material. The following
concerns the practice for the welding together of two UPVC sheets
using a butt weld.

As in all types of welding,cleanliness is important both in
the welding gas and the surfaces to be joined.

A groove is formed between the sheets by chamfering the edges
to give an included angle of 60-70°. The chamfered surfaces and
the rod are wiped clean and any grease or oil removed with a
volatile solvent. The sheets are then clamped leaving a gap, not
greater than 1mm, between them, see fig. 3.

The rod, known as either weld or filler rod, is normally
supplied with a circular cross section of 3mm diameter. Rod with
2,4 and 5mm diameter is sometimes used and the use of triangular
and cloverleaf cross-sections is becoming more common. Prior to
welding, one end of the rod is cut to a 30° angle to aid the
start of the weld.

The gas jet is heated and directed by a hand held welding
torch, or gun, in which the gas either passes over electrically
heated elements or through gas heated coils, see fig. 4. The
electric torch is more common today and recent versions contain
heater control systems which allow particular gas temperatures
to be selected and maintained without having to alter the gas flow

conditions. The torch may also be supplied with a small fan
compressor built into the handle, this supplies air as the
welding gas, at a sufficient flow rate and pressure for most
welding. A wide range of nozzles may be fitted to the torch
depending on the type of welding being done, these being either
a push or screw fit.

The following gas conditions may be taken as being typical of
those used in industry, although individual welders may use
slightly different ones:-

Gas   : Dry, oil-free air or nitrogen
Flow   : 15-40 litre/min
Pressure   : 20-100KPa
Optimum Temperature: 300°C measured 3mm from the nozzle end.

The gas temperature should be monitored at a set distance
from the nozzle but the usual practice of experienced welders is
to play the gas jet over the palm of their hand from a distance
of 3 - 4 inches. The welder then varies either the gas flow
rate or the heater power to get the 'right' temperature.

With both types of torch a period of 5 - 10 minutes should
be allowed after turning on, for the welding gas temperature to
stabilise. With the electric torch, the gas should be flowing
all the time power is on, and should be left on for 5 - 10 minutes
after power is switched off to avoid damaging the heater elements.

There are three types of hot gas welding: tack, hand, and
speed. Tack welding provides a temporary weld with sufficient
strength to hold pieces in place until a more permanent weld is
carried out. Nozzle A in fig. 5 is used and the blade is drawn
along the root of the groove causing a weak fusion joint to be
formed.

Hand welding is the basic method of hot gas welding. Both hands
are used, the torch being held in one hand and the rod fed into
the groove with the other. A simple round nozzle, B in fig. 5

is used. The hot gas is directed into the groove and at the
tip of the rod, the cut end, which is held vertically
above the start of the weld. The rod is pressed into the groove
and once softened and fused with the sheet will begin to bend
through 90° and lay horizontally in the groove. If correct
conditions are maintained, a bow wave of softened material should
be observed at the bottom of the rod. As this happens, the
torch is advanced along the groove, continuing to heat the base
of the rod and the groove, see fig. 6. A pendulum action is
commonly used, the jet being directed in an arc from a point
just in front of the weld bow wave to a point on the rod just
above the bow wave and back again. The full cycle is normally
repeated between one and three times a second. Once started,
typical speeds of 100-200mm/min are obtainable. After finishing
a run, a short time is allowed for the weld to cool. Degraded
material is then removed from the weld by scraping and the next
run started.

Speed welding is used for long straight runs with Nozzle C,
see fig. 5, fixed to the torch. This nozzle has a preheating
guide tube down which the weld rod is fed prior to entering the
heating zone of the gas jet. The shoe at the end of the tube is
used to force the rod into the groove and maintains the torch
a uniform distance from the weld. Typical speeds are 1-2m/min
and this technique has the advantage of freeing one of the
welder's hands to hold the parts together.

For both hand and speed welding it is usual to use sufficient
weld runs to overfill the groove by 30%, see fig. 7. Dressing
of the weld, that is the removal of excess weld material above the
surface of the sheet, is not normally carried out except for
aethestic reasons.

1.4. Weld Efficiency

The determination of weld efficiencies is carried out in the
same way for both hot tool and hot gas welds. Two sheets of UPVC
are welded and the resultant plate is cut across the weld into
narrow parallel sided test pieces. These are then tested in tension

and the resulting load at failure recorded. The load at
failure, normally yield , of similar sized samples of
unwelded material is also determined. The ratio of welded
to unwelded failure load is then expressed in percent and is
called the weld efficiency, weld factor or weld quality.

2. Literature

In the following chapter a review of the literature relevant to the work carried out will be given. As such it has been divided into six main sections. The first two are brief reviews of the polymerisation of polyvinyl chloride, the physical properties of the polymer and the additives and processing required to convert the polymer into a finished product. The third is a review of the mechanical properties of unplasticised polyvinyl chloride and the factors which affect them. Section four covers fracture and fractography, whilst section five reviews the subject of fracture mechanics and its application to polymers. The final section reviews the research carried out and gives a more detailed description of hot gas welding as applied to unplasticised polyvinyl chloride.

2.1. Polyvinyl Chloride Polymer

The polymerisation, processing and properties of polyvinyl chloride have been extensively reviewed [2-5], and as part of this work is concerned with a materials characterisation, a brief summary is included.

It is important to understand the difference between a polyvinyl chloride product and the polymer polyvinyl chloride. The product is made from a mix of polymer plus additives which has undergone some processing. Different products may contain a different molecular weight polymer, and the additives and the processing may also be changed. A variation in any of these three parameters may affect the mechanical and physical properties of the product [6]. Therefore, whenever comparing results from different polyvinyl chloride products, allowances need to be made not only for differences in the testing conditions but also on the processing history of the material.

In the following, PVC will refer to the polymer, polyvinyl chloride, whilst UPVC and PPVC will refer to unplasticised and plasticised polyvinyl chloride products respectively.

2.1.1. Polymerisation

It is standard commerical practice to convert vinyl chloride monomer to PVC by addition polymerisation using free radical mechanisms either in bulk, emulsion or suspension [7]. Bulk polymerised PVC (B-PVC) is the purest of the three since little or no polymerising aids are used. It is little used in industry due to problems of controlling the exothermic reaction during polymerisation [8]. Emulsion polymerised PVC (E-PVC) is the least pure due to the difficulties of removing the emulsifying agents. However, particle morphology considerations [7] have meant it is used extensively in the PVC industry. Suspension polymerised PVC (S-PVC) is the main polymer type used in UPVC products due to reasonable purity and ease of manufacture [7].

Owing to processing requirements [9] only a limited range of molecular weights are used in PVC. In S-PVC the molecular weight is determined by the polymerisation temperature and in commercial practice a temperature of $50^{o}C$ is used [10,11]. PVC so produced is generally atatic, amphorphous and linear. The number of short chain branches is typically 5×10^{-3} per monomer unit with the number of long chain branches approximately 0.5×10^{-3} per monomer unit [11].

These polymers are thought to be approximately 10% crystalline [11], but there is a debate over this figure [12] and the exact nature of the crystalline phase is uncertain. The crystallinity can be increased by lowering the polymerisation temperature but even when polymerised at $-40^{o}C$ the level of crystallinity is still only 20-25% [10,11]. The increased crystallinity improves the heat and solvent resistance of PVC but also increases the processing

difficulties and is not generally used in industry [13].

2.1.2. Molecular Weight

The statistical nature of the addition polymerisation means polymers are produced with a range of molecular weights. The molecular weight may be defined with respect to either number, viscosity, weight or z average, $\bar{M}_n$, $\bar{M}_v$, $\bar{M}_w$, $\bar{M}_z$, respectively. These are single value parameters, with the ratio of $\bar{M}_w/\bar{M}_n$ sometimes used as a measure of the width of the distribution. [14]. Although the first three molecular weights can be determined experimentally from fundamental properties of the polymer, it is normal commercial practice to characterise the polymer using a simple relative viscosity measurement [15, 16]. The measurements are transformed into a single value parameter usually reported as the K number which is dependent not only on molecular weight but also the solvent and the temperature of the test. The relationship between $\bar{M}_n$, $\bar{M}_w$ and K for a range of solvents and test temperatures has been given [17], see Table 1.

A more versatile method which will give all four molecular weight averages is that of gel permeation chromatography (GPC), [18,19]. However, this method is again only relative, needing to be calibrated using known molecular weight polymer

A study of several industrially available PVC's [20], has shown that the value of $\bar{M}_w/\bar{M}_n$ is typically 2.2.

2.1.3. Glass Transition Temperature, T_g, and other Transitions

An amorphous polymer is considered to be either glassy or rubbery depending on where its glass transition temperature T_g, lies with respect to the testing temperature. In the former case it lies far above and for the latter it lies far below. The glass transition occurs when, with increasing temperature, the polymer chain which was frozen becomes capable of extensive carbon-carbon bond rotations and hence becomes flexible [21]. This transition has been observed to affect many of the polymer's properties, i.e. mechanical, dielectric and thermal. However, this

transition is rate-dependent with the transition occurring at lower temperatures for 'slow' mechanical tests than for high frequency dielectric tests.

It is also common to find other transitions occurring at lower temperatures than T_g, these being labelled β, δ, γ and ξ in order of decreasing temperature of transition. These are usually associated with either side group rotations or short chain segmental local mode rotations [21].

The glass transition temperature of PVC is dependent on molecular weight but for molecular weights used commercially the difference is negligible [22]. For industrially available PVC the T_g, determined using a slow thermal method is $78^{\circ}C$. The β transition is usually quoted as lying between $-40^{\circ} - 0^{\circ}C$ as the frequency Hz used in the test changes from 100Hz to 2200Hz [22,23]. However, there is evidence of a small transition lying between the glass transition and the β transition which only appears for PVC quenched from above the T_g [23,24].

2.1.4. Degradation of PVC

PVC is renowned for its susceptibility to degrade when subjected to typical processing temperatures. Degradation manifests itself by the elimination of hydrogen chloride from the polymer chain, and in many cases, the discolouration of the material. Despite extensive research the mechanisms of thermally activated degradation have not been fully clarified [25-28]. The main problem is that the degradation process is extremely sensitive to many factors including : the presence or absence of oxygen; the effects of mechanical working; the presence of defects in the polymer chain; and the presence of polymerisation additives. Further, the relevance of the literature concerning PVC degradation is limited since every commercially used PVC product contains additives designed to prevent or slow down the degradation process.

In general, PVC degradation involves not only the elimination of hydrogen chloride but also the competing reactions of chain scission and crosslinking. One of these will dominate depending

on the factors listed above. In the absence of oxygen, PVC degrades by the elimination of hydrogen chloride by a zipper-like reaction which leaves short sequences of polyene structures, the cause of the colour formation. This process leads mainly to the crosslinking of the polymer chains. When again oxygen is present, the polyene structures left when hydrogen chloride is eliminated, are rapidly oxidised, preventing the colour formation, into hydro-peroxides or peroxides. The presence of the peroxides leads mainly to chain scission.

Most research has been carried out on the chemical nature of the degradation process with the industrial interest centred on the prevention of the discolouration of the material. As such, little work has been reported on the effects of degradation on the physical properties of PVC, though it is generally stated that discolouration must have proceeded considerably before the mechanical properties would be affected [25, 9].

PVC is not only prone to thermally activated degradation but also to photo-oxidation and ionising radiation-induced degradation. However, as above, the mechanisms are poorly understood and little work on the effects on physical properties has been published.

2.2. Additives and Processing

As previously stated, to produce a finished product, polymer and additives are mixed and then processed. The additives are added either to aid processing or to modify the polymer's properties. Processing is the means whereby the mixture of polymer and additives are first converted into a homogeneous melt which is then moulded into the shape required for the product. It is normal industrial practice to quote the amount of additive present in a PVC product in terms of the parts per hundred resin (phr), where resin refers to the polymer.

2.2.1. Additives

The additives which are required in the processing of PVC are thermal stabilisers and lubricants. These are normally selected

to have the minimum effect on the properties of the product.
Additives used to modify the properties of the product include
U-V absorbers, pigments, fillers, impact modifiers and, in
the case of PPVC, plasticisers [6, 30-32].

The thermal requirements for processing UPVC are such that
unstabilised PVC would rapidly degrade. The stabilisers
generally employed are based on lead, tin, barium-cadmium, and
cadmium-zinc organo-metallic compounds [33]. However, when
clarity is an important requirement for the finished product,
organotin compounds are used. For exceptional clarity the
choice is further limited to the sulphur containing organotin
compounds [34].

Lubricants are generally classed as either internal or
external depending on the function they fulfil. This classification
is based on their compatibility with PVC. Those which are more
compatible are classed as internal lubricants and function to
control the mixing and shear heating. Those which are less
compatible are classed as external lubricants and act to prevent
PVC sticking to the hot metal of the processing equipment.

This categorisation is only a guide since no lubricant is
either completely compatible or non-compatible and each lubricant
will act in both modes to some degree. The details of lubricant
action are poorly understood and the types and levels of lubricants
required for a particular processing system are usually determined
by trial and error [35]. Furthermore, because of the time and
cost of these trials, details of the lubricant system and
indeed the composition in general are rarely reported.

Commonly used external lubricants are synthetic waxes; fatty
esters, ethers and alcohols; low-molecular weight polythylenes;
and lead stearate. Internal lubricants include long chain fatty
acids, calcium stearates, alkylated fatty acids, and long chain
alkyl amines [30].

Pure PVC is not thought to be susceptible to U-V attack.
However, PVC which has undergone processing and therefore may be

slightly degraded or PVC which contains traces of polymerisation additives is known to degrade during exposure to U-V radiation. This degradation is mainly observed as embrittlement in clear products and embrittlement and discolouration in filled products[29,36] U-V absorbers are, therefore, added to the composition. For clear products these are usually either derivatives of 2- hydroxy-benzo-phenuone, 2-(2H-benzotriazol -2-yl) - phenols or phenyl esters. Filled products may also incorporate these, though more use is made of titanium dioxide and carbon black [30].

Pigments are generally used to colour the product although they are sometimes used to give further protection against U-V attack.

Fillers are generally added to UPVC composition to reduce costs. Typical fillers are the clays, calcium carbonate and titanium dioxide at loadings up to 30% by weight [30].

Impact modifiers improve the toughness of UPVC products by introducing a second phase of rubbery material such as acrylonitrile-butadiene-styrene (ABS) terpolymers, methyl methacrylate-butadiene-styrene (MBS) terpolymers,chlorinated polyethylene and ethylene-vinyl acetate (EVA) copolymers. These are usually added at the 5-10% level and tend to reduce the yield stress from 55MPa to 42MPa [30]. The impact strength may also be improved if precipitated calcium carbonate, with a particle size less than $0.1\mu m$, is used as the filler [37].

The mechanical and physical properties of a PVC product are most dramatically changed when plasticisers are added to the composition. The addition of 30phr dioctyl phthalate (DOP) may reduce the polymer yield stress to values lower than 25MPa. The product so formed is no longer a glassy material but a rubbery flexible material. The range of materials used as plasticisers is extensive and the levels at which they are used varies between 20-100phr [38].

The main point concerning additives is that not only is there

an extensive choice of materials to perform a wide range of
functions but that each material acts not just in one mode,
but to a degree, in two or more. The selection of additives
for a particular composition is therefore very complicated
and the final choice is only arrived at after several trials.

Typical formulations for a clear UPVC extruder composition
and calendering composition are given in Table 2.

2.2.2. Processing

Many routes are available to the processor, to convert a
mixture of polymer and additives into a homogeneous melt and
then from a melt into a particular shaped object. Some of the
more common ones include extrusion, calendering, compression
moulding, blow moulding and injection moulding.[39].

For this work the two methods of importance are extrusion
and calendering. These two, in essence, are very similar
processes requiring similar molecular weight polymer and similar
additives. They also introduce similar levels of orientation
and similar thermal histories, when compared to injection
moulding [39].

To manufacture weld rod a simple extrusion process would be
used, whilst to manufacture sheet a calendering process followed
by a press lamination process would be used. To manufacture
the thickness of sheet used, foils of UPVC, approximately 0.5-1.0mm
thick, are first calendered. Then the number of foils required
to make up the thickness of sheet desired are stacked in a press,
heated to about 180°C and are then pressed together until they
have fused.

It has been noted [40,41] that two-roll milling, a standard
industrial method of mixing polymer and additives prior to both
extrusion and calendering, may result in a reduction in the
polymer molecular weight. Typically, the reduction was found to
be 20% for PVC milled for 5 minutes at 190°C [41].

2.3. Mechanical Properties of UPVC

Commercially available clear UPVC is described as a glassy, amorphous thermoplastic, at ambient temperatures. Other important materials in this class are polymethyl methacrylate (PMMA), polystyrene (PS) and polycarbonate (PC).

The mechanical properties of this class of materials are sensitive not only to the temperature and rate of testing but also to the presence of additives and the thermal history of the material. There has been no full assessment of the effect of additives or thermal history for the as-supplied commercial materials although it has been suggested that they would only produce variations in properties of up to 20% [42]. However this value still means caution is required when comparing mechanical data obtained from different grades of material.

2.3.1. Temperature and Rate of Testing

As with all thermoplastics the mechanical properties of UPVC vary with the temperature and rate of testing. There is also a slight dependence on pressure but it has been shown that it requires an increase in pressure of 1000 atmospheres to raise the T_g by $11^{\circ}C$ [43] and therefore pressure may be ignored as far as normal testing is concerned.

The effects of temperature and rate have been studied by Vincent [44] and Bauwens et al [45]. It is concluded that the tensile yield stress increases between 0.7 - 0.9 MPa for each $1^{\circ}C$ decrease in temperature and increases between 1.7 - 2.7MPa each time the strain rate is doubled. The Bauwens et al study used the Eyring rate theory [46] to analyse their data. They found that as the temperature decreased or the strain rate increased more account had to be taken of the β transition. They showed that at any temperature a test done below a certain rate was dominated by the glass transition, whilst above that rate it was controlled by both the glass and the β transition. In their study they found that at $0^{\circ}C$ and $23^{\circ}C$ the critical strain rates were $0.008s^{-1}$ and $0.04s^{-1}$ respectively.

The temperature dependence of the yield stress in the glass transition controlled region is confirmed by Williams and Isherwood [47], and Rawson and Rider [48]. In the same region the rate dependence is confirmed by Pezzin et al [49] and Shinozaki et al [50].

Williams and Isherwood [47] and Harrell and Chartoff [23] both report a decrease in tensile modulus of 0.01 - 0.02 GPa with an increase in test temperature of $1^{O}C$. Pezzin et al [49] and Shinozaki et al [50] have shown that a doubling of strain rate increases the tensile modulus by 0.03 - 0.05 GPa.

From these studies, UPVC is found to have a tensile yield stress of 55 - 65MPa and a tensile modulus of 2.7 - 4.1 GPa when tested at $20^{O}C$ using a strain rate of 10^{-3} s^{-1}.

The brittle strength of UPVC, and thermoplastics in general, is less sensitive than yield stress to changes in test temperature and strain rate [51]. This reduced dependence on temperature means that as the temperature is reduced, the yield stress increases and the probability of brittle failure increases. The brittle-ductile transition [52] occurs when the temperature is such that half the specimens tested fail in a brittle manner, see fig. 8. In amphorous polymers this transition has been associated with the β transition [53, 54]. In the case of UPVC the β transition occurs between -40 - $0^{O}C$ as does the brittle-ductile transition.

2.3.2. Molecular Weight Dependence

The properties of UPVC are dependent on molecular weight and possibly molecular weight distribution. However, as most commercially available UPVC is processed from PVC having $\bar{M}_w/\bar{M}_n$ ≈ 2.2 [20], the effects of molecular weight distribution are not discussed.

The T_g of PVC increases rapidly with molecular weight

but plateaus at $T_g = 78^{\circ}C$ for molecular weights exceeding $\bar{M}_n = 10,000$ [22]. The yield stress for UPVC with $\bar{M}_w = 50,000 - 500,000$ has been shown to be "sensibly" constant although energy-to-break and flexural brittle strength increase for $\bar{M}_w$ less than 200,000 [44]. Pezzin and Zinelli [41] reported no molecular weight dependence for either yield stress or tensile modulus for $\bar{M}_w$ greater than 70,000 but were unable to test UPVC with $\bar{M}_w = 26,000$ due to difficulties of processing. Shinozaki et al [50] reported a constant yield stress for a range of commercially available UPVC's, with different molecular weights, but a slight decrease in tensile modulus with increasing molecular weight.

Other properties shown to be dependent on molecular weight are time-to-rupture under fatigue loading [55], discontinuous growth band formation during fatigue testing [56], craze stability [57,58], heat stability, impact strength and softening point [59].

2.3.3. Effects of Additives

It has been shown that the presence of some soluble, liquid additives increase certain properties such as yield stress, whilst insoluble, solid additives lead to a decrease [60], see fig. 9.

The clearest example of how additives affect the properties of PVC is seen when plasticisers are added to the composition. The addition of 50phr of di-octyl phthalate (DOP) to PVC reduces the material yield stress to 21MPa whilst increasing the elongation-to-break to 290 %[38]. This is achieved by depressing the polymer T_g either closer to or below room temperature.

However, some plasticisers exhibit anomalous behaviour in that when at low concentrations, less than 10phr, they increase the yield stress and reduce the elongation-to-break, but still depress the polymer T_g [61]. This effect has been called anti-plasticisation. Mascia [62] has studied this effect in PVC, using tri-cresyl phosphate (TCP), by examining the

dynamic response and creep response at various temperatures.
He showed that the anti-plasticisation effect is absent for
material tested at or above 40°C. Indeed above 40°C the
material showed the typical plasticisation effect. This
confirmed the results of work carried out by Peukert [63]
on plasticised weld rod.

The effects of the presence of particulate fillers on the
mechanical properties of UPVC have been extensively studied.
Vincent [44] examined the effects of adding titanium dioxide,
calcium stearate, PMMA butadiene-methyl methacrylate copolymer,
and vinyl acetate on the yield stress, impact strength and
elongation-to-break. Increasing the loading of titanium
dioxide increased the impact strength and decreased the yield
stress. At 30phr the impact strength had increased 150%
whilst the yield stress had decreased 10%. The addition of
up to 2phr calcium stearate lead to a reduction in yield stress
of 15%. When PMMA or vinyl acetate were blended or copolymerised
with UPVC the yield stress increased and the impact strength
decreased. However, when butadiene-methyl methacrylate was
blended with UPVC the yield stress decreased and the impact
strength increased. Similar effects were shown by Weldon [59]
when calcium stearate and vinyl acetate were added to UPVC.

Studies of the effects on mechanical properties of adding
calcium carbonate to UPVC are complicated by particle size and
agglomeration effects [64]. The major effect of particle size
is that the impact strength increases as the size decreases.
A 20% loading of calcium carbonate has been shown to increase
the notched Charpy impact strength from $6.5KJ/m^2$ to $9.6KJ/m^2$
for a particle size of 2.4µm but will increase it to $36KJ/m^2$
for a particle size of 0.07µm [64]. However, at this loading the
yield stress drops by 14% and 21% respectively.

Baum [65] has studied the weathering of UPVC stabilised with
three different organotin compounds with and without particulate
U-V stabilisers. He reported that the yield stress for unweathered
material was significantly less for the UPVC containing the
U-V stabilisers.

The increase in yield stress for a UPVC composition containing soluble additives is noted in one of the supplier's literature [66]. The specific example quoted being a liquid organotin stabiliser as used in clear sheet. It is further noted that there is an attendant increase in brittleness when such additives are used, This is also reported by workers [67] studying the creep and fatigue response of various grades of UPVC,

Dunlop et al [68] whilst studying the effects of plasticisers on the T_g of PVC showed that the addition of a liquid organotin stabiliser at the 2phr level reduced the PVC T_g to 69°C, They considered it to be a plasticising additive. A barium-cadmium particulate stabiliser only reduced the T_g to 77°C. Similar findings were reported by Duiser and Keijzer [69] who found that the T_g of a PVC composition containing 2phr of liquid organotin stabiliser was reduced at 65°C,

2.3.4. Thermal History and Orientation

Turner [70] reported a marked reduction in the long term creep compliance of UPVC when conditioned at 60°C for 12 weeks prior to testing. He reported that rapid cooling from above T_g then restored the compliance. Dunn and Turner [71] monitored the short term modulus, 100 sec. creep modulus at 0.2% strain, after various times of conditioning at 60°C. They found a 70% increase after 6.6 years, and also report that conditioning at 20°C for 3.5 years raised the modulus by 8%. Mascia [62] reports a similar trend in the results for creep compliance and sheer modulus, when comparing unconditioned UPVC with UPVC kept at 60°C for 3 months prior to testing.

Wright [72] studied the effects of annealing UPVC for different lengths of time, at various temperatures between 40°C and 60°C. He reported the expected improvemrnt in creep modulus with increasing anneal time for the longer duration annealed material. A further improvement was obtained when a delay time was introduced between annealing and testing. In all cases, though, this improvement was only towards the creep modulus obtained for UPVC conditioned at 20°C for 2 years, However, he also

reported an anomalous effect for the high temperature, short
duration annealed material in that as the time of the anneal increased
the creep modulus was initially observed to drop before showing
the usual improvement.

Struik [73] also reports an improvement in creep modulus with
prolonged storage at $20^{\circ}C$ when compared with the values obtained
from material quenched from $90^{\circ}C$.

Illers [74] reports an increase in density and yield stress
and a reduction in elongation-to-break for UPVC annealed at $70^{\circ}C$
compared to material quenched from above T_g. Mills [75] and
Cross and Howard [76] have shown that quenching UPVC from above T_g
produces a material which at low strain rates will yield in a
uniform manner without showing any signs of necking. This yield
occurred at a lower stress than for unquenched material. They found
this state to be unstable in that when increasing delay times were
introduced between quenching and testing the material behaviour
gradually returned to that of unquenched material. Rider and
Hargreaves [77] report a drop of 10% in yield stress for UPVC
annealed at $71^{\circ}C$ but give no details of the cooling rates used.
Shinozaki et al [50] annealed injection moulded UPVC specimens at
$110^{\circ}C$ and found that both tensile modulus and yield stress increased
with annealing times up to 20 minutes but they then remained
constant. The increase in modulus and yield stress was between
10-20% whilst elongation-to-break decreased from 140% to 80%.
Again, no details were given for cooling rates from the annealing
temperature.

The methods of differential scanning calorimetry (DSC) have
been used extensively to study the effects of varying thermal
history on UPVC. Illers [74,78], McKinney and Foltz [79], and
Gray and Gilbert [80] all report the presence of an endothermic
peak super-imposed over the glass transition for UPVC annealed
below T_g. The area under this peak is dependent on the rate of
cooling and heating and the time and temperature of the anneal.
Heating to above T_g and quenching removed the peak.

Wolpert et al [81] studied the effects of using different heating and cooling rates on the T_g for a range of thermoplastics including PVC. They showed that similar rates for cooling and heating produced the standard glass transition with faster rates moving the transition to higher temperatures. Slow cooling and fast heating produced the endothermal peak super-imposed over the glass transition. Fast cooling and slow heating produced a small exothermic peak super-imposed just prior to the glass transition, see fig. 10. These extra peaks were explained as being due to the rate effects varying the relaxation of free volume. Illers [78] and Gray and Gilbert [80] explain exothermic peaks super-imposed on the curve between T_g at $200^{\circ}C$ as being caused by crystallinity formed during annealing treatments above T_g of previously quenched PVC, the exothermic peak occurring between $10-20^{\circ}C$ lower than the annealing temperature.

The effect of orientation on UPVC has been studied by Rider and Hargreaves [77]. They examined the yield stress dependence on draw ratio, draw direction and draw temperature, either $71^{\circ}C$ or $90^{\circ}C$. The lower temperature drawn material had a yield stress up to 200% greater than the undrawn material, when tested in the draw direction for draw ratios in the range 0 - 7. In the same range the high temperature drawn material's yield stress only increased up to 50%. Both high and low temperature drawn material had yield stresses lower than the undrawn material when tested at $90^{\circ}C$ to the draw direction, see fig.11.. Rawson and Rider [48] found no change in the temperature dependence of the yield stress for the hot drawn material compared to the undrawn sheet. However, they report a slight anisotropy in the yield stress for the as-received sheet (less than 8%) which was not observed by Rider and Hargreaves.

Rawson and Rider [82] extended their study to include the effects of hot drawing on tensile modulus using an ultrasonic method [83] to determine the elastic constants of the materials. They reported a linear relationship between tensile modulus and yield stress for a range of draw directions and birefringence, birefringence being used as a measure of draw ratio.

Brady and Jabarin [84] studied the effects of cold drawing (23°C) UPVC. They observed that the temperature at which shrinkage occurred was reduced from 70°C, for undrawn material, to 45°C. However, the yield stress increased from 72MPa to 88.3MPa. To try to preserve the improved mechanical properties whilst improving the shrinkage temperature, they studied the effects of two annealing treatments. Both were carried out at 70°C for 3 days. In the first, the sample was constrained in its drawn state, whilst the second was unconstrained. Undrawn sheet was also annealed at 70°C for 3 days, unconstrained for use as a comparison. Their results, for each treatment, for the shrinkage temperature, yield stress, modulus, total shrinkage and T_g are given in table 3.

2.4. Fracture and Fractography

A material may fracture in either of two modes, ductile or brittle. Ductile failure is usually observed as slow tearing with large deformations and is associated with yielding of the bulk polymer. Brittle failure, however, is usually a low stress, low energy and small scale deformation process resulting in planar surfaces covered with cleavage type features.

2.4.1. Crazing and Brittle Fracture

Brittle failure in glassy thermoplastics is usually preceded by craze formation through which the crack grows, in either a slow stable manner or a fast catastrophic fashion [85].

The crazing behaviour and craze morphology have been extensively studied but the complete details have not been fully established. Craze formation is dependent on many factors including: the level and duration of applied stress, temperature, polymer, molecular weight and the presence of orientation in the polymer [58]. Crazing develops under a tensile stress only, the plane of the craze being normal to the stress direction. The crazes usually initiate at surfaces but can develop internally from notches or inclusions. Crazes tend to be wedge shaped, the distance between the craze walls increasing with distance from the craze tip,

however, the wedge angle is only 1-2°. At the tip of the craze the wedge shape sometimes gives way to a cusp-like form [85]. Kambour [86] showed the craze to consist of 40-60% void with polymer highly orientated between the voids. The fracture surfaces of some polymers show interference colours [87]. This is caused by a residual layer of craze material left on the surface as the crack moves first along the centre of the craze. Then as the crack accelerates, the crack moves away from the centre of the craze and begins to jump between the craze/solid interfaces. This mode of craze/crack growth has been demonstrated by Doyle et al [88] and Beahan et al [89] using transmission electron microscopy. As the crack continues to accelerate, the fracture mode abruptly changes and the crack begins to bifurcate, that is move on two or more planes. This results in exceptionally rough fracture surfaces and may lead to the ejection of large pieces of the specimen [90]. Why this happens is uncertain but it appears to be related to the velocity and energy of the crack [91].

UPVC was originally thought not to craze as no interference colours were seen on the fracture surfaces [87]. Later work by Gotham [92], and Cornes and Howard [93] showed that UPVC did indeed craze. Mills and Walker [94] have characterised crazes in monotonically loaded UPVC. They reported crazes up to 500μm long with thicknesses between 6.3 - 8.9μm at the crack tip.

2.4.2. Fractography

Fractography is an important tool in studying fracture behaviour, both in terms of the initiation and the propagation of cracks [95].

The gross features of a brittle fracture surface are defined as the mirror, the mist, and the hackle zones [91,96]. The mirror region is a highly reflective smooth region at and around the fracture initiation site, the mist surrounds the mirror zone and is a more rough surface which then becomes the hackle zone, a very rough shattered surface. However, within

each of these regions there are further finer features.

It is generally considered that the mirror region corresponds to slow crack growth through the preceding craze, the mist is a transition zone and the hackle is the fast fracture region [97]. Within the mirror zone penny shaped features may be observed [94], these being formed either by void coalescence or by secondary fractures in advance of the main crack. The features most studied in the transition zone are the patch or mackerel patterns observed on the fracture surfaces of PS. These patterns have been attributed to the craze wedge first separating from one craze/solid interface, then from the other [97]. The hackle zone contains four main features, rough shatter bands, fine striations, river markings and Wallner lines. The shatter bands and the fine striations are thought to be essentially similar [88] with the shatter bands, being caused by excess energy in the crack. This causes the crack not to move through the preceding craze, thereby leaving a striation, but into the bundle of crazes which surround the crack tip, hence leaving a shatter band. River markings are seen when the crack has been moving on two or more different levels which gradually meet as the crack advances [98]. Wallner lines are perturbations of the crack caused by the interference between stress waves reflected by the specimen surfaces and the crack front [99]. These are normally observed as curved bands of roughened material which show in some cases, an unexplained periodicity. Where two or more sets are present definite over-lapping may be seen. These lines have been used as a means of determining the crack velocity, when the stress wave velocity is known and have been shown to occur when the crack is moving with a velocity close to its maximum [98]. Ultrasonic pulses have been used to artificially modulate the crack front to allow crack velocity determinations in glassy thermoplastics [100].

The fine striations observed on PS fracture surfaces have also been observed on UPVC [56, 57, 98, 101], styrene-diene triblock copolymers [102] and polymethyl-α-cyanoacrylate adhesive [103] fracture surfaces. They are all characterised by spacings typically 10-30μm with a high degree of regularity in size and

spacing. They lie parallel to the crack front and do not overlap, as do Wallner lines, they have a well defined leading edge behind which lies a craze band which fades into a featureless zone approximately equal in length to the craze band. Similar lines have been seen on the fracture surfaces of PC [104] but with a much larger spacing.

2.5. Fracture Mechanics

In the engineering context the study of brittle failure is through the theories of fracture mechanics [105-107]. For the case where failure occurs at loads low compared to the yield stress and when the material is approximately obeying Hooke's law, a linear elastic fracture mechanics (LEFM) approach may be used.

2.5.1. Fracture Mechanics Theory

Inglis [108] has shown that for a small elliptical hole in a uniformly stressed, linear elastic plate, the stresses around the hole are modified so that a maximum local stress, σ_L, is observed at point C, see fig. 12, equal to

$$\sigma_L = \sigma_A \ [1 + 2 \ (a/\rho)^{\frac{1}{2}}] \qquad -(1)$$

Where σ_A is the applied stress, 2a is the major axis length and ρ is the radius of curvature of the ellipse at point C.

Griffiths [109, 110] used Inglis's analysis with an energy balance criterion for failure to derive the failure stress σ_F , for a line crack (the limiting case of an ellipse) as

$$\sigma_F = (2E \ \gamma/\pi a)^{\frac{1}{2}} \qquad -(2)$$

in plane stress, or
$$\sigma_F = (2E \ \gamma/\pi a(1 - \nu^2) \ )^{\frac{1}{2}} \qquad -(3)$$

in plane strain E is the material's Young's Modulus, γ is the surface energy, 2a, the crack length and ν Poisson's ratio.

Irwin [111], using a stress analysis approach showed the stresses around the crack tip to have the following form

$$\sigma_{ij} = Kf(r) \; g_{ij} \; (\theta) \qquad\qquad -(4)$$

Where K is termed the stress intensity factor and $f(r)$ and $g_{ij}(o)$ are radial and angular functions. K is defined as

$$K = \sigma_A \sqrt{\pi a} \qquad\qquad -(5)$$

K is usually referred to the mode of opening of the crack, i.e, K_I is the K relevant to Mode I opening, see fig. 13.

Irwin suggested that fracture occurs when K reaches a critical value K_c, this value being a constant for the material, that is the same way as yield stress is a constant, i.e., allowing for rate and temperature dependence.

The equivalence of Griffith's and Irwin's approach was demonstrated by Irwin who introduced the strain energy release rate parameter G. At the instance of fracture, this parameter has a constant value G_c, which equals the surface energy term γ, of Griffiths which, substituted into (2) and (3) and using (5) gives

$$K_c = \sigma_F \sqrt{\pi a} = (E \; G_c)^{\frac{1}{2}} \qquad\qquad -(6)$$

for plane stress and

$$K_c = (E \; G_c / (1 - \nu^2))^{\frac{1}{2}} \qquad\qquad -(7)$$

for plane strain.

Irwin [111] and Orowan [112] suggested that plastic work, γ_p done at the crack tip should be included in the surface energy term and that in engineering materials γ_p is very much greater than γ. Irwin went on to show that this work was independent of the external conditions, provided the volume of plastically deformed material was small, with respect to the specimen

dimensions, and therefore could be used in place of γ.
The zone of plastically deformed material has been analysed
by Dugdale [113] who showed that it extended beyond the crack
tip by an amount Δa, given by

$$\frac{\Delta a}{a} = sec \left(\pi \sigma A / 2\sigma_y \right) - 1$$

-(8)

Where σ_y is the yield stress.

2.5.2. Fracture Mechanics Testing

To allow for the finite size of test specimens equation (5)
is modified by the inclusion of a geometric factor, Y, such that

$$K_c = \sigma_F Y \sqrt{a}$$

-(9)

These geometric factors have been determined for a number of
test geometries [114, 115].

The dependence of G_{IC} and K_{IC} on specimen thickness is
simplified through the plane strain/plane stress approximations,
that is thick/thin plate respectively, and in practice the approx-
imation is determined empirically. The surface of the specimen
is assumed to be in plane stress and this state is assumed to
continue into the sample for a depth approximately equal to the
plastic zone size Δa. Provided the sample is thicker than 2Δa the
middle is assumed to be in plane strain.

The usual parameter studied in fracture mechanics is the
plane strain fracture toughness, K_{IC}, for mode I opening. The
plane strain state prevents the relaxation of the strain by
through-the-thickness yielding and leads to a brittle, flat
fracture at relatively low loads.

A G_{IC} versus thickness plot for aluminium is shown in fig. 14.
[116].

The insensitivty of G_{IC} to specimen thickness in the plane
strain regions allows tests to be done under more controlled
conditions. If specimen thicknesses less than those necessary
for plane strain testing are used then large differences in
G_{IC} are caused by small variations in thickness.

In metals, the minimum thickness conditions for plane strain
testing is given by [114].

$$b \geq 2.5 (K_{IC}/ \sigma_y)^2$$ -(10)

The condition is semi-empirical, based on results for
aluminium and a value judgement that fifty times the plastic
zone size is sufficient thickness to ensure minimal effects
due to the plane stress surface region [117].

Other specimen dimensions such as crack length and distance
from the crack tip to the opposite edge of the specimen should
also be greater than (10) for valid plane strain testing [114].

Plane strain fracture toughness testing may be divided into
two sections. The first section uses methods and specimens which
give one result per test specimen and the second uses methods
and specimens which give more than one result per specimen.

In the first category are tests using single edge notch (SEN),
double edge notch (DEN) and the centre notch (CN) specimens in
tension and the SEN specimen in bend, see fig. 15. The feature
of these is that once the crack propagates, it is unable to
come to rest again within the sample and hence completely
fractures the specimen. The fracture toughness, K_{IC}, is
determined through (9) using standard geometric factors [114,115].

In the second category samples are used which are sufficiently
large that under fixed grip (constant displacement) testing the
propagating crack is able to come to rest within the sample. If
the grip separation is increased until the crack propagates again
and is then held constant, the crack may again come to rest within

the sample. With the correct design and a suitable material this procedure may be repeated many times before the crack completely separates the sample. Using this type of testing, two types of behaviour are observed: slow stable crack growth and fast stick-slip fracture; typical load-extension curves are shown in fig. 16. During testing, the grip displacement is increased at a constant rate. With some designs and materials the crack grows so slowly that the movement of the grips serves to drive the crack forward without it stopping, thus giving slow crack growth. However, with other designs and materials the crack movement is so fast that the grips are effectively frozen during propagation and therefore no further work is done on the sample. This results in stick-slip fracture.

Specimens for this type of test are shown in fig. 17 and they are known as double cantilever beam (DCB), tapered double cantilever beam (TDCB), compact tension (CT) and double torsion (DT) specimens.

For each specimen type, an appropriate geometric factor has been determined [118,119,114,120] thus permitting a direct calculation of K_{IC}. However all four specimens can also be used to determine G_{IC} using compliance methods. If a calibration curve of compliance against crack length is produced then G_{IC} can be calculated from [121].

$$G_{IC} = \frac{P_f^2}{2b} \times \frac{dc}{da} \qquad -(11)$$

Where P_f is the failure load, c is the specimen compliance and dc/da is the rate of change of compliance with crack length, at that crack length, and b is the specimen thickness, see fig. 17. The compliance calibration curve is produced by measuring the specimen compliance, that is the deflection of the ends of the beams divided by the load, for a range of different crack lengths.

When using either the DCB or CT specimens, both the load

and the crack length are required before G_{IC} can be calculated.
By careful design the dc/da term can be made constant for a range
of crack lengths and therefore whilst the crack is within
that region only the load at failure is required in the calculation
of the G_{IC} [121]. To produce a constant dc/da, the DCB design is
modified to a taper. Strictly it should be contoured, but a
simple taper is a reasonable approximation for a limited size
of cracks [122].

In almost all of the multi-result tests the specimens are
grooved along their centre line to guide the crack and to
prevent it wandering out of the side of the specimen.

The two types of crack behaviour, i.e. slow or fast crack
growth, provide different information about the crack. When
slow crack growth occurs, data may be obtained about crack
propagation and about the way in which cracks, too small to
produce catastrophic failure, may grow to a critical size. Fast
catastrophic failure only gives information on the crack
initiation behaviour [123].

Mai et al [124] have analysed the various TDCB designs and
have shown that crack growth is more stable, when smaller taper
angles are used. They also show that arm break-off becomes
more common when smaller taper angles are used, and therefore
specimen grooving becomes essential. Arm break-off may be reduced
if designs with smaller e/w values are used, where w is the
specimen length and e is the extra beam length necessary to
bring the taper to its apex. They suggest that the most stable
crack growth will occur for TDCB's which are reverse loaded,
that is loaded at the end away from the apex.

Kobayashi and Broughtman [125] have suggested that the
bonding of stiff side plates to the specimen may reduce the
incidence of arm break-off. They developed the technique to
permit a fracture mechanics analysis to be carried out on a
rubber modified acrylic, PMMA was used for the side plates.

One important requirement for reliable fracture mechanics

testing is the need for reproducible, sharp, starter cracks. Marshall et al [126] have demonstrated the need for care when notching PS. They showed that slow razor notched, impact razor notch and fatigue notched PS TDCBs' gave K_{IC} values of 1.87, 1.32 and 0.45 $MPam^{\frac{1}{2}}$ respectively. They found that both forms of razor notching and low frequency fatigue notching (less than 30Hz) produced a bundle of crazes at the crack tip. These crazes acted as energy sinks prior to crack propagation. High frequency fatigue notching (greater than 30Hz) lead to the creation and growth of a single craze at the crack tip thereby lowering the fracture surface energy. Razor notching of PMMA was found to be adequate as only a single craze formed at the crack tip.

2.5.3. Fracture Mechanics and Polymers

The methods of LEFM have been applied to many glassy polymers, in particular PMMA [127-132], PS [126,127,130,134-136], PC [135-139], epoxy resins [121,140-147] and UPVC [47,56,57,93,94,148-156].

The majority of work has concentrated on either PMMA or epoxy resins. PMMA has been considered an ideal material with which to use LEFM, since in many tests considerable spans of slow stable crack growth can be achieved. This permits the evaluation of K_I for both crack initiation and propagation over a wide range of test rates and temperatures; typical curves are shown in fig. 18 and fig. 19 [131, 132].

The epoxy resins have been studied because of their extensive use as adhesives and as the matrix material in many fibre composites. They also provide a means of evaluating the effects of chemical structure on fracture behaviour. It is possible, by the careful selection of catalyst or hardener, to vary the crosslink density of the cured resin, and therefore to examine how crosslinking affects fracture behaviour. The dependence of K on crosshead speed and test temperature has been studied and typical curves are given in fig. 20 and fig. 21 [147]. At low crosshead speeds, crack propagation is stick-slip. However, as the crosshead speed increases, the K_{IC} decreases, and when it equals

the arrest value of K, K_{Ia}, then crack propagation is slow and continuous. At high temperatures K_{IC} is very much larger than K_{Ia} and crack propagation is stick-slip; but as the temperature decreases, K_{IC} decreases until equal to K_{Ia}, and again slow continuous crack propagation is observed.

A comparison between PMMA and epoxy resins is made difficult since different aspects of K are reported. However, it would seem that with PMMA, slow stable crack propagation is favoured by slow crosshead speeds and high temperatures whilst the reverse applies for epoxy resins.

In the case of UPVC various factors affecting K_{IC} and G_{IC}, such as specimen dimensions, rate and temperature of testing, composition and orientation have been studied.

Cornes and Howard [93] reported a value of 2.45 KN/m and for K_{IC} of 2.9 $MPam^{\frac{1}{2}}$ for 1 and 2mm thick clear rigid PVC SEN'S tested at -40°C. At the same temperature, using a notched three-point bend test, Williams et al [123] reported an identical value for G_{IC}, although no information was given concerning the sheet thickness.

Guild et al [148] used UPVC with PMMA to study the effects on fracture behaviour of bonding together different materials. Using a grooved DCB method with a nett section thickness of 1.5mm, UPVC was reported to have a K_{IC} of 3.56 $\pm$ 0.20 $MPam^{\frac{1}{2}}$. Initial notching was carried out with a Stanley knife.

Mills [149], using centre notched specimens and a photoelastic analysis, studied the effects of annealing and quenching on K_{IC} for 1 and 2mm thick UPVC sheet. The annealed and as-received sheet fractured in a brittle manner with K_{IC} = 2.0 $\pm$ 0.2 $MPam^{\frac{1}{2}}$. Quenched 1mm sheet failed by shear yielding, but 80% of the quenched 2mm sheet failed in a brittle manner.

Mills and Walker[94] used clear rigid UPVC SENS with thicknesses 1,2,3 and 6mm to study craze growth and the effects of thermal

history on K_{IC}. They reported that as-received sheet had a K_{IC} of 2.00 $MPam^{\frac{1}{2}}$. After quenching, the 2mm sheet had a K_{IC} of 2.57 $\pm$ 0.24 $MPam^{\frac{1}{2}}$ whilst 3 and 6mm sheet had a K_{IC} of 1.95 $\pm$ 0.16 $MPam^{\frac{1}{2}}$. The quenched 2mm sheet had a K_{IC} of 1.94 $\pm$0.17 $MPam^{\frac{1}{2}}$ when tested 21 days after quenching. They investigated the method of notching and found that fatigue notching did not produce significantly lower values for K_{IC} than razor notching. Poor alignment of the loading system and the notch was blamed for higher values of K_{IC} recorded (up to 2.9 $MPam^{\frac{1}{2}}$). They concluded that using the energy balance approach of Griffiths implies slow stable crack growth is possible with the material. They, however, proposed a theory of advance fracture formation which would tend to prevent slow stable crack growth, which they failed to observe. They suggest analyses should be presented in terms of the critical stress intensity factor, K_{IC}, and not fracture surface energies, G_{IC}.

Brown and Chin [150] used 6mm thick UPVC and a compact tension test method to determine a value for K_{IC} of 1.3 $MPam^{\frac{1}{2}}$. They did not observe any stable crack growth and no shear lips were seen on the fracture surfaces.

Green and Pratt [151] reported a dynamic K_{IC} of 2 $MPam^{\frac{1}{2}}$ for cracks in UPVC travelling at speeds between 510-590 m/s. At velocities above 590 m/s the crack bifurcated and an approximate K_{IC} of 2.6 $MPam^{\frac{1}{2}}$ was estimated. The UPVC used formed a large craze bundle, approximately 300-400μm, during notching. In propagating through this bundle, the crack accelerated to speeds of greater than 500 m/s and they were unable to report values of K_{IC} for crack velocities less than 500 m/s. They suggest that although the grade of UPVC used has a low dynamic toughness the presence of the craze bundle would lead to a more useful toughness under practical conditions of loading. However, once fracture had started it would be more catastrophic than PMMA.

Plati and Williams [152] used an instrumented impact tester to determine G_{IC} for UPVC. Over the temperature range -100 to

$+60^\circ C$, using notches with a 50µm radius, G_{IC} was found to be between 1.3 and 1.4 KN/M. When tested at $20^\circ C$ using notch tip radii of 250µm and 500µm, G_{IC} rose to 2.0 and 3.8 KN/m respectively.

Radon [153] and Johnson and Radon [154] used impact and slow bend tests to study the temperature dependence of K_{IC} for UPVC. They report maxima in the curves of K_{IC} versus temperature which varied with testing speed. They suggest that these maxima correspond to an effect due to the β transition.

Miller et al [155] orientated UPVC by hot drawing and then examined the effects of differing degrees of orientation on fracture surface energy using a grooved DCB method. They reported slow stable crack growth, with a resultant non-reflective surface, and a diminishing fracture surface energy with increasing orientation. Above a certain orientation, indicated by a birefringence of 2×10^{-3}, the crack growth propagated in a jerky manner with a highly reflective fracture surface. For undrawn material of 1mm thickness a value of fracture surface energy of 3.6KN/m was determined.

Skibo et al [56, 101] used LEFM to study the effects of molecular weight and plasticiser on the properties of PVC. They showed that for unplasticised PVC, K_{IC} varied from $0.7 - 2.4$ MPam$^{\frac{1}{2}}$ for $\bar{M}w$ from $0.605 \times 10^{5} - 2.25 \times 10^{5}$, when 6.4mm thick sheets were tested.

The effects of specimen dimensions and notching method on K_{IC} have been studied using a pipe grade UPVC [156]. It was concluded that, provided the size requirements recommended for metals, i.e that the important sample dimensions are greater than $2.5 (K_{IC}/\sigma_y)^2$, are met, then LEFM may be used. Further, that razor blade pre-cracking produces acceptable crack tips under these test conditions.

Chauffoureaux [64] reports the results of impact tests on DEN specimens of UPVC containing differing amounts of two

calcium carbonates of different particle size. The unfilled UPVC had a K_{IC} of 2.3 MPam$^{\frac{1}{2}}$ and the 20% by weight filled UPVC, fine particle size, had a K_{IC} of 2.7 MPam$^{\frac{1}{2}}$. It is, however, pointed out that the filled UPVC fracture surfaces showed evidence of plastic yielding at the notch tip which may invalidate the results for the filled materials.

2.6. Hot Gas Welding of UPVC

The basic techniques of hot gas welding of thermoplastics were patented independently by Reinhardt in the U.S.A. [158] and Henning in Germany [159] between 1937 and 1938. However, almost all the development work and later studies were carried out in Germany. Except for improvements in equipment and the introduction of speed welding, there has been little change in the methods of hot gas welding since they were first patented. As such it still remains a skill which is learnt by experience over months and years of welding.

In general the literature concerning hot gas welding of UPVC contains recommendations for good welding procedure with little research or explanation of why one set of conditions are better than another.

2.6.1. Sheet Preparation

Voigt [154] gave recommendations for the preparation of the groove formed between two sheets to be butt welded. The groove was to be a single-vee configuration for thin sheet and a double-vee for sheet thicker than 6mm; the included angle of each vee should be 60°- 70°. The use of a double-vee groove for thick sheets was to save both time and material, as it required more rods to fill a single large vee than two smaller vee's. When using a single-vee groove special attention is drawn to the need to ensure good root penetration, this being helped by leaving a slight gap, 0.5 - 1.0mm, between the bevelled edges of the sheets. It is further advised that an extra reinforcing weld rod should be welded along the root from the reverse side of the groove.

These sheet preparations have been accepted as standard ever
since.

2.6.2. Welding Gas

Many authors have reported the values for various parameters
of the welding gas used during welding, or have recommended
certain values to be used, and these are listed in table 4.

Henning [160] reported the effects on weld strength when
different welding gases were tried. He used air, nitrogen,
hydrogen, carbon dioxide and oxygen and reported that all the
gases bar air produced nearly 100% efficient welds. The welds
produced using air as the welding gas were only 75% efficient.
Connors [161] found only minor differences in weld efficiencies
between welds produced using either nitrogen or air. However,
his average efficiencies were only 53%.

Connors [162] examined the effects on gas temperature due to changes
in flow rate, pressure and power, for both electrically heated
and gas heated welding torches. He observed that a drop in gas
pressure from 55KPa to 28KPa caused the gas temperature to
increase up to $60^{o}C$. He strongly recommended that monitoring
devices, for all four parameters, be used to ensure constant
welding gas conditions.

Neumann [163] has observed a $100^{o}C$ drop in gas temperature
when the measuring position was changed from the nozzle tip to
approximately 12mm away from the nozzle tip.

2.6.3. Weld Rod

Weld rod comes in both unplasticised and slightly plastic-
ised forms. Originally the weld rod was plasticised to improve
extrudability [159] but improvements in thermal stabilisers and
extruders have allowed unplasticised rod to be produced. In
Europe the plasticised rod is still in common use [164] and
typically contains 10phr tricresyl phosphate [165]. At this

level it is acting as an anti-plasticiser [62]. Peukerts [63] has reported that welds made with plasticised rods are stronger than those made with unplasticised rods when tested at temperatures less than 40°C, but that their efficiencies drop below those of unplasticised rod welds when tested above 40°C. Plasticised rods were also observed to char more easily at higher weld temperatures.

Voigt [159] examined the effect of weld rod shape on weld efficiencies. He tried rods with circular, hexagonal, square and triangular cross sections and found that the weld efficiencies decreased in that order from 85% for welds with circular rod to 50% for welds with triangular rod.

2.6.4. Welding Technique

It is suggested [159,165] that good welding technique is indicated when a bow wave of softened material is observed at the junction of rod and sheet during welding, see fig. 22. Further along the line of the welded rod and to either side of the rod, a small ripple of material should be seen, see fig. 23.

During welding, the weld rod should be pushed vertically into the groove with a force of approximately 1-2Kgs. [165]. If the weld rod is pushed into the groove at an acute angle, see fig. 24, stretching of the rod will occur. Stretching may also occur if too great a force is used [159]. This may cause the rod to fracture as it cools or as a second weld rod is welded over the first, see fig. 25, [165]. It is recommended that the rod length is measured before and after welding, so that the length of rod used to produce a certain length of weld can be determined and hence the degree of stretch in the rod can be calculated. Some stretching is considered unavoidable and up to 15% stretch is considered harmless [165]. The effects of pushing the rod into the groove at angles other than 90° on the weld strength have been reported [1], see fig. 26.

In the introduction, see section 1.3, the torch action

during welding, is described as simply being advanced along
the weld. Some authors prefer the use of a pendulum action [159,165].
For this the gas jet is continuously directed through a short arc
first onto the rod then back to the groove thereby giving a more
uniform heating between the rod and the sheet.

The effects of improper heating of the parts on the weld
efficiencies and associated characteristic features of the
resultant weld have been described [159], see table 5,

2.6.5. Testing of Welds

Two tests are commonly used to ascertain the quality of
the weld: firstly, a visual examination of a polished cross-
section of the weld [159,161], and secondly, tensile testing
of samples cut across the weld [161,166,167].

UPVC does not go completely fluid during welding and
examination of the polished cross-section of the weld usually
reveals that the weld rods and sheet have retained, to a degree,
their original shapes [159,161]. The weld rods during welding
soften and as they are pushed into the groove they tend to
distort their cross-section to match with the groove configuration.
This distortion has been taken as a sign that a good welding
technique has been used. Examples of typical cross-sections
are given in figs. 27-30. Fig. 27 shows the cross-section of
a satisfactory double-vee butt weld. Note the homogeneity
through the weld and the distortion of the groove wall and rods.
Figs. 28-30 show the cross-section for some typical faults in
hot gas welding of UPVC. In the first, fig. 28, the temperature
was too low: there is no deformation of the rods and little or
no fusion. Fig. 29 shows the cross-section of a weld for which
the temperature was too high and the materials have charred.
Fig. 30 shows a double-vee butt weld in which no root penetration
has occurred.

Voigt [159] examined the cross-sections of hot gas welds in
clear UPVC using polarised light and observed complex fringe

patterns. These he suggested were indicative of the large residual strains caused by thermally induced shrinkage of the rods across the weld.

The second means of assessing the quality of the weld is to conduct tensile tests on specimens cut across the weld with the weld perpendicular to the direction of loading. This has been commonly used and the method is the subject of ASTM D1789-77 [167] and BS 4994 [166]. In the literature, as in the standard, the weld efficiency is calculated from the ratio of weld failure strength to unwelded sheet failure strength, with failure strength defined as being the maximum load sustained by the sample divided by the sheet thickness and specimen width.

ASTM D1789-77 [167] defines a satisfactory weld as one with a weld efficiency greater than 75%, whilst BS 4994 [166] requires efficiencies greater than 90%. In the literature weld efficiencies range from 100% [165] to 50% [161] and it is suggested [163] that weld efficiencies of as low as 30% are common for inexperienced welders. However, interpreting the literature values for weld efficiencies is made difficult as the definition of weld efficiency fails to take into account the different weld configurations and differing degrees of filling of the weld groove used by different welders.

A comparison of the different weld configurations used showed that the single-vee weld with a backing run was strongest, 90% efficient; a double-vee butt weld had an efficiency of 80% while a single-vee butt weld without a backing run was only 70% efficient [163]. The same author claimed that the dressing of a weld, i.e, the removal of welded material in excess of the sheet thickness, lead to a 25% reduction in efficiency.

The effects of storage at temperatures between $80^{o}C$ and $180^{o}C$ for times between 15 minutes and 24 hours on the efficiency of welded sheet and unwelded sheet have been studied. Prior to testing, the materials were either slow-cooled or quenched to

the testing temperature. Henning [160] reported that both slow-cooled welded and unwelded sheets had tensile strengths up to 10% less than the untreated materials. The quenched unwelded sheet had a tensile strength up to 15% less than the untreated sheet but the quenched welded sheet showed no reduction in tensile strength.

The effect of various chemical environments on weld efficiency have been studied by Connors [161] and Henning [160]. Connor's results are given in table 6. His examples were immersed for 10 days in the reagents. Only the sulphuric acid immersion shows an improved weld efficiency. However, Henning, who used very much more concentrated reagents at higher temperatures, found that out of sulphuric, hydrochloric, and nitric acids and sodium hydroxide only the hydrochloric acid caused the weld efficiencies to drop. For the other reagents weld efficiencies increased on average 25% over the first ten days of immersion after which they remained reasonably constant [160].

Henning [160] further showed that over the temperature range $0^\circ C$ - $40^\circ C$ weld strengths for welds using unplasticised rod remained nearly constant whilst for welds using plasticised rod the strengths dropped at approximately the same rate as the sheet yield stress.

A more recent study by Alf et al [168] has confirmed most of the previously described trends in weld strength and efficiency behaviour as far as temperature and weld configuration effects are concerned. They extended their study to include long term mechanical tests, i.e, creep, and fatigue tests. In the short term, weld efficiency dropped as the sheet thickness increased and varied with temperature as in fig. 31. From fig. 31, the scatter of results at $20^\circ C$ gives efficiencies between 70% and 90%.

For the higher efficiency welds cracks were noticed to start in the weld prior to the main failure. The creep and fatigue results showed a similar dependence on weld configuration to that seen during short term testing. They found that dressing

the welds prior to short term testing did not effect the average efficiency but did increase the scatter. However, dressing the welds gave significantly better results during fatigue testing. For this work they used two types of welds: one was produced by a skilled welder, whilst the other was produced by a semi-automatic welding rig set up to produce welds with reproducible efficiencies of 60%. For all types of tests the machine welds were found to be poorer than the hand welds, particularly so in the fatigue tests.

The main observation made during mechanical testing of hot gas welds in UPVC by many authors [159, 161, 165, 168,169] is the extreme brittleness of the welds. This is attributed to the notch sensitivity of the sheet material and to the presence of strain left in the weld during the cooling process after welding.

3. Experimental

The work described in this and the subsequent chapters is
shown diagrammatically in fig. 32. The first step in the programme,
after a period of welding training, was to prepare and test hot
gas welds to establish the level of weld strengths attainable
with clear UPVC. For comparison, hot gas welds in filled UPVC
and hot tool welds in clear UPVC were prepared by the author and
hot gas welds in clear UPVC were prepared by experienced industrial
welders.

The standard materials, of sheet and rod, were then subjected
to a characterisation programme which included mechanical testing,
microstructural analysis and chemical analysis. This programme
being carried out to ensure that there was no basic incompatibility
between the materials which could result in poor weld strengths.

At the same time, weld fracture surfaces were examined and the
importance of notches and flaws within the weld zone became
increasingly apparent. The notch sensitivity of both clear and
filled UPVC was examined using the methods of linear elastic
fracture mechanics. The effect of welding on the notch sensitivity
was also examined.

From above, it was decided that there were two possible ways
to improve weld strengths, these being the removal of the flaws
in the weld zone and the reduction of the materials' notch
sensitivity. The work to examine the two approaches concentrated
mainly on modifying the chemical composition of the weld rod.
Weld rods of various compositions were prepared, in conjunction
with I.C.I. and hot gas welds produced and tested.

However, for the purposes of writing, the work is reported in
the order of materials characterisation, standard welds, fracture
mechanics and modified weld rod composition and weld procedure.

During the course of this work a range of commercially available
materials were used. The majority of the work was carried out
using I.C.I. Darvic clear 025 sheet, hereafter referred to as

clear sheet, which was supplied in 10, 9.5, 6 and 3mm thicknesses
and as sheets 2438mm x 1219mm. A characteristic feature of the
sheet was its blue mauve colouring. For most of the welding a water
clear weld rod was used, which came supplied in 2Kg loads of 1m long,
3mm diameter circular cross-section rods. This rod is hereafter
referred to as clear rod.

Other sheets used were I.C.I. industrial grade Darvic 909,
6mm thick, and Placon, a 10mm thick water-clear grade supplied by
the Plastics Construction (Northern)Ltd. The industrial grade
Darvic 909 is hereafter referred to as filled UPVC.

Two other weld rods were used, both I.C.I. materials, one was
supplied as 3mm diameter circular cross-section rod and one with
a triangular cross-section, base width 5.5mm and height 2.8mm.
The circular rod was supplied in a continuous coil whilst the
triangular rod was supplied in 1m lengths. Both materials had a
blue mauve colouring similar to the I.C.I. clear sheet.

3.1. Mechanical Properties of the As-Received Materials

The mechanical properties of the sheet materials were charact-
erised by the determination of yield stress in tension, tensile
modulus and flexural modulus. However,only the clear rod was
examined in this work since the form of the other rods prevented
them being tested.

All mechanical testing was carried out using either a floor
model TT-CM Instron or a table-top model TT-1112 Instron. Prior
to testing, the machines were allowed to stabilise and then were
calibrated, in the case of the floor model by dead weight loading
and for the table top model by a built-in electronic calibration
system.

All tests were carried out in ambient conditions as the
Instrons were not in environment controlled laboratories. Except
where otherwise stated, all testing was carried out using a

crosshead rate of 5mm/min. Where parallel sided samples, with
no shoulders,were used the gauge length refers to the original
grip separation distance. Where dumbbell specimens were used
the gauge length refers to the length of the parallel sided
centre section of the specimen. The cross-sectional area of all
specimens were determined, prior to testing, using a micrometer.

3.1.1. Yield Stress Determination for UPVC Sheet Materials

Sixteen specimens of clear sheet were prepared and tested in
accordance with BS 2782 Method 320A [170], but with a thickness
of 10mm.

Due to the time required to prepare such specimens subsequent
test specimens were prepared with a simple parallel sided
geometry without the use of shoulders, see fig. 33. These
specimens were cut from the sheet using either a bandsaw or a
circular saw. The machined surfaces were smoothed using a
range of emery papers down to the 600 grade.

Initially this specimen design was required for the tensile
modulus testing. During that test programme the sheet yield stress
was also determined and a difference observed between those results
and those obtained using the dumbbell specimen of BS 2782. A
short series of trials were then conducted to evaluate the cause.
Possible causes considered were orientation, cross-section, ageing,
strain rate and temperature.

To test for orientation effects specimens were taken parallel
to both the length and the width of the sheet. To check if
changes in cross-sectional area would cause the difference the
area was varied between 50mm^2 and 250mm^2, for subsequent tests
the cross-sectional area was maintained at 150mm^2. It was
thought possible that changes in the delay time between machining
and testing might be important. This was tested for by carrying
out tests on specimens machined less than an hour before and by
testing others left for 35 days after machining. The strain
rate dependence was examined by changing the gauge length of

the specimens from 40mm to 180mm. The temperature dependence
was examined by testing specimens maintained for 2 hours at the
ambient temperature of $16^{\circ}C$ whilst a second set were tested at
$25^{\circ}C$. The second set were conditioned in an air oven, maintained
at $25^{\circ}C$, for 2 hours, prior to testing. During testing they
were kept at temperature using a fan heater placed so that an
air temperature of approximately $25^{\circ}C$ was maintained about
the specimens.

Plastics Construction sheet, Placon, was tested using
parallel sided specimens of cross-sectional area $150mm^2$ and
gauge length 90mm.

I.C.I. filled sheet was tested by taking parallel sided
samples parallel to both the length and width of the sheet.
These specimens were prepared with a cross-sectional area of
$90mm^2$ and a gauge length of 100mm.

Yield Stress Determination of the Clear Weld Rod

3.1.2.   Initial tests were carried out with the rod placed directly
in the wedge type grips of the Intron with the result that all
the rods failed in a brittle manner, in the grips, with no signs
of yielding. To circumvent this two approaches were tried, the
first of moulding rod granules into a sheet, from which test
specimens could be machined, and second, the bonding of the ends
of the rods into metal blocks which could then be gripped without
damaging the rod.

For a sheet, 278mm x 202mm x 3mm, the size of the mould available,
it was calculated that approximately 0.23Kgs. of rod material
would be required. Therefore, it was decided that the same
material would be used for each pressing until the correct
pressing conditions were established. Although some degradation
was apparent after the third pressing the same material was
still used.

The rod and the pressed sheet were granulated using a
laboratory granulator which gave granules approximately $20mm^3$.

The compression moulder was a Vinipart with a maximum limit of 20MPa. Before each moulding the mould was preheated to 100°C, in an air oven, and was sprayed with a silicon release agent before the granules were added. Once the pressing was finished the mould was transferred to a water-cooled press where it was allowed to cool to room temperature, see table 7, for pressing conditions tried.

After five attempts at pressing the resultant sheet still retained a granular character, see fig. 34, and cracked along the granule boundaries when flexed. The material was badly degraded and this approach was abandoned.

For the second approach, 12.5mm square cross-section steel bar was cut into 25mm lengths. A 3mm diameter hole was then drilled into the length of each block, to a depth of approximately 15mm.

Initially,Devco epoxy resin, 5 minute cure time was used as the bonding agent. However during trials the rods tended to slip from one of the blocks. Roughening of the ends of the rods only lead to rods fracturing at the block. Some rods were prepared with thinned centre sections to produce dumbbell specimens. The thinning was achieved by careful scraping using a scalpel followed by smoothing with 600grade emery paper. By reducing the diameter of the rod to approximately 2.5mm yielding was observed. However, the difficulties in reproducing the thinning operation and the time required for it lead to other adhesives being used.

A cyanoacrylate adhesive, Superglue 3, was tried, again using rods whose ends had been roughened with the result that the rods still fractured at the blocks.

Two points were noted:

    i) end-roughening of the rods was usually required to
       fit the rods into the holes.

    ii) this adhesive set in approximately 10 seconds and
        block alignment became critical.

The first point suggested that the 3mm diameter hole was too small. Initially a $\frac{1}{8}$ inch diameter drill bit was tried but later 3.1mm and 3.2mm diameter drill bits were used. For as-received rod the 3.1mm diameter hole was found most satisfactory and end-roughening was stopped.

The second point lead to the rod being cemented separately into each block with the second block being accurately aligned with the first, to prevent any twisting force being applied to the rod during the test.

A range of cyanoacrylates were used; Superglue 3, IS.12 and IS.495. All were Loctite products, with the latter giving the most consistent results. The adhesive was usually allowed to cure overnight, prior to testing. Four specimens were prepared using steel rods in place of the weld rod. Tests on these showed that for IS.495 adhesive failure occurred at loads typically, four times greater than the failure load of the weld rods.

With careful manufacturing the number of premature brittle failures was reduced but the fraction of samples which failed during yielding, before cold drawing, remained high.

Using this method it was possible for rods to draw their entire length before failure, see fig. 35. Often two necks would form in different positions along the rod, though only one would draw.

A range of gauge lengths were used, this being the distance between the blocks, with typical lengths being 150, 200 and 250mm although some specimens were prepared with gauge lengths up to 450mm.

3.1.3. Tensile Modulus

Only the 10mm thick Darvic 025 sheet and the clear weld rod were tested.

The sheet was prepared as parallel sided test pieces, as in

section 3.1.1, each with a cross-section of approximately 60mm^2 and a length of approximately 250mm. An initial grip separation distance of 200mm was used.

Once a specimen had been clamped in the grips of the Instron, a clip-on strain gauge extensometer, Instron G-51-14-M-A, with a 50mm gauge length, was attached to the central portion of the specimen. The strain gauge amplifier was set up in accordance with the maker's instruction. This extensometer can be used to measure strains in the range between 0% and either 5%, 10%, 25% or 50% depending on the accuracy required.

After trials using the 0% to 25%, 0% to 10% and 0% to 5% strain ranges a series of 10 specimens were tested using the 0% to 5% strain range. To ensure reasonable accuracy in measuring strain the load full scale deflection was 5000N.

The weld rod tensile modulus was determined both from the load-extension curves obtained during the previous yield stress testing, and by using an Instron clip-on strain gauge extensometer, G-51-16.

During the yield stress testing of the rod, the initial load full-scale deflection was set as 100N and only as the pen reached full-scale deflection was it adjusted to either 500N or 1000N.

For the extensometer measurements the rod was clamped in Houndsfield rod grips, adapted to fit the Instron. The grip separation was 100mm and the load full-scale deflection was 40lbs. This extensometer was used on its minimum measuring range of 0% to 1% strain.

3.1.4. Flexural Modulus

Darvic 025 sheet, 10mm and 3mm thick, and clear rod were tested.

The three-point bend rig used is shown in fig. 36. This rig had

a maximum span of 102mm and a maximum width 20mm. All bearing surfaces have a radius of curvature of 3mm.

For this test an Instron tension-compression load cell was used with the plunger connected to the load cell which was bolted into the top fixed crosshead of the Instron. The frame was taped to the moving crosshead so that the plunger acted through the centre of the span and at right angles to the length of the span.

According to the ASTM D790-66 [171] the ratio of the span to the depth of a specimen should be at least 16:1. This could not be achieved with this rig for the 10mm sheet and so the maximum span available was used. Similarly the width of 3mm sheet should be 25mm which was too large to fit the rig and so the width was cut the same as the 10mm sheet.

Both the 10mm and 3mm thick samples were cut to be 16mm wide and 150mm long. The 10mm samples were tested using a span of 102mm and a crosshead rate of 5mm/min. The 3mm samples were tested using a span of 47.6mm and a crosshead rate of 1.25mm/min. The welding rod was cut into 150mm lengths and tested using a span of 47.6mm and a crosshead rate of 1.25mm/min.

The 10mm sheet specimens were only loaded so as to give the straight line response of load and extension whilst the 3mm sheet and rod specimens were tested through yield.

Eight samples of 10mm sheet, twelve samples of 3mm sheet and twelve samples of rod were used during testing.

3.2. Microstructure

Four aspects of microstructure were studied: the molecular weight distribution, the glass transition temperature, the shrinkage caused by various thermal treatments and the birefringence. Only 10mm clear sheet and the clear weld rod were examined with respect to shrinkage and birefringence whilst I.C.I. weld rod was also included in the molecular weight distribution and glass transition temperature studies.

-51-

3.2.1. Molecular Weight Distribution

These were obtained via the RAPRA Service. Samples were
sent to RAPRA where they were dissolved in tetrahydrofuran (THF)
and analysed using gel permeation chromatography. The RAPRA
service includes a computer analysis of the molecular weight
distribution which gives the number, weight, viscosity and z
averaged molecular weights. Samples sent for testing included
sheet and clear rod, as-received, and sheet, clear rod and I.C.I.
triangular rod both as-received and post a 10 minute, 160°C
thermal treatment.

3.2.2. Glass Transition Temperature, T_g

Initially, the T_g was studied using the technique of
differential thermal analysis, (DTA) with a Du Pont 900 Thermal
Analyser, set up with the DTA head. Samples were taken from
granulated material. However, due to experimental requirements,
only the very fine powder not the granules was used. Glass micro-
spheres were used as the reference material. A starting
temperature of 30°C and a heating rate of 10°C/min were used.
After ten trial runs this method was dropped due to the poor
reproducibility of the results. The T_g analysis was, then,
based on the technique of differential scanning calorimetry (DSC),
again using the Du Pont 900 Thermal Analyser, this time fitted
with the DSC head. Samples were taken either from the granulated
stock, this time using the granules, or from shavings taken
directly from the materials.

Samples, approximately 15mg, were accurately weighed into
aluminium pans which were then hermetically sealed. A pan
containing a similar weight of glass microspheres was prepared
as the reference.

For most of the study a temperature range from 30°C to 100°C
was used, with a heating rate of 10°C/min. In certain cases
this range was extended down to -100°C, using the manufacturer's
cooling attachment, or up to 350°C. In these cases a heating

rate of 20°C/min. was used. Some samples were cycled, that is heated to 100°C, cooled, either in air or in the cell, back to 30°C and then were retested.

It was found necessary to use the machine on its most sensitive range and spurious peaks were sometimes observed due to fluctuations in the purging gas flow. The heating rate was checked with a stop-watch and the temperature calibration checked using a polystyrene standard.

3.2.3. Thermally Induced Shrinkage

Due to differences in manufacturing processes, the sheet and weld rod may be expected to have different residual stresses in their as-received form. To investigate this, their relaxation at elevated temperatures were studied.

The 10mm clear sheet was tested as required in BS3757 pt.1. [172]. For this, a 12inch square of material has a 10inch diameter circle scribed about the centre of the square. The sheet is then placed in a pre-heated air oven set at 120°C, on a glass plate covered with cloth. After 45 minutes the sheet is withdrawn and allowed to cool on the glass plate. Once cooled a second 10inch circle. is scribed about the centre and the difference between the original and second circle is taken as a measure of the relieved internal strain.

A second test used 4inch squares of sheet. About the centre of the square, a grid of four horizontal and four vertical lines, spaced 20mm apart, were scribed, drawing out nine squares in a square pattern. Each block was labelled, and the position of fifteen of the points were measured with respect to one corner point, using a travelling microscope. The thickness was measured at each corner.

One block was then placed in an oven, set at either 110°C, 130°C, 150°C or 170°C, on a PTFE sheet. Then at specified times the block and base were withdrawn and allowed to cool. Once

cool, measurements were made of the grid and the thickness and the block then returned to the oven. At the higher temperatures the blocks were found to stick slightly to the PTFE sheet.

In the case of the weld rod, 150mm lengths were used. Initially tests were done using a 'non-stick' baking tray as the base, however this was later changed to a PTFE sheet and then later still to a bed of glass microspheres. These changes were made as the rod was found to stick to the first two base materials, at higher temperatures. Heat treatments used temperatures between 70°C and 180°C, for a range of times, up to several hours, except where limited by degradation of the rod. Once heated the rod usually became curved, which caused difficulties when measuring the length. To straighten them the rods were allowed to air cool until just flexible and were then held against a wood-former until rigid again. Measurements of the length were made with a 150mm steel rule and of the diameter with a micrometer.

3.2.4. Birefringence

The birefringences of both clear sheet and clear weld rod were determined using a calibrated quartz wedge attachment on a Vickers M55 Microscope. The stress-optic-coefficient of clear sheet was determined using cantilever beam specimens loaded between the crossed polars of a circular polariscope.

3.3. Chemical Analysis

This section is in three parts, the first is concerned with the extraction of the additives from the as-received materials, the second with the analysis of the additive-free polymer and extracted additives and the third with the effects of solvent washes and wipes of weld rods,(sometimes recommended prior to welding).

3.3.1. Extraction of Additives from the As-Received Materials

For the majority of this work a Soxhlet extraction technique, using ether or methanol as a solvent, was used to separate the

polymer from the additives. This method was used on the sheet and both the clear and the I.C.I. weld rods.

A tetrahydrofuran (THF) recovery process was used for the 6mm thick grey sheet and as a cross-check on the sheet.

The materials for the Soxhlet extraction were granulated such that the largest granules were approximately 20mm^3. The weld rod granules were more uniform than the sheet granules as they were generally broken across the diameter.

Two Soxhlet extraction systems were set up so that both sheet and rod could undergo extraction at the same time.

The Soxhlet thimble was weighed and then either an approximate 10gm or 20gm of sample were added to the thimble which was again weighed. The flask, containing 2 or 3 bumping granules was weighed prior to the solvent being added. Approximately 150 - 200ml of solvent was used.

Initial runs were for 2 days, using laboratory ether. Solvent was later evaporated off the extract by gently heating the flasks in isomantles. However, the additives degraded during the evaporation and a second extraction on fresh material was carried out. This time the solvent was removed using a rotary evaporator under a slight vacuum.

Due to doubts concerning the purity of the ether used, a third run was carried out using AR diethyl ether. At the end of 3 days continuous extraction the ether flask was replaced by one containing AR methanol, and a subsequent 3 day extraction was carried out on the same polymer. To check that the majority of the additives had been extracted a 5 day AR diethyl ether extraction was carried out, with a subsequent 5 day AR diethyl ether extraction to confirm that little more could be extracted. Finally the I.C.I. rod and the clear rod were subjected to a 5 day AR diethyl ether extraction.

The solvent removal procedure was extended to include 24 hours

in a vacuum oven at 30°C, after rotary evaporation, as traces
of solvent were detected after rotary evaporation only.

After the solvent was removed, the flasks were weighed and
labelled. To maintain purity, the flasks were kept sealed at all
times, except when samples were being removed for analysis.
These samples were generally retained.

The THF recovery technique was applied both to the clear sheet
and the grey sheet. A sample between 1 and 2gms, was accurately
weighed and then dissolved in THF in a large centrifuge tube. When
fully dissolved the solution was centrifuged at 3000 to 4000 r.p.m.
for 2 hours. The tube was then topped up with fresh THF and
centrifuged for a further 1 hour. The resulting liquid was
poured off and saved. The precipitate was washed with THF, recentri-
fuged and the liquid then added to the previously poured-off liquid.

The precipitate was dried in a vacuum oven at 40°C until
constant weight was achieved. The polymer was precipitated from
the cooled stirred liquid by the dropwise addition of AR methanol.
The precipitated polymer was separated from the remaining liquid
by filtering through a previously weighed sintered glass filter.
Several warm ether washes were used before the polymer was dried
to a constant weight in a vacuum oven at 40°C. The remaining
solution was transferred to a flask of known weight and the solvent
was driven off using a rotary evaporator. The residue was kept
at 30°C in a vacuum oven until a constant weight was achieved.

In the case of the grey sheet the centrifuging procedure failed
to give a clear solution despite extended centrifuging.

3.3.2. Analysis of the Separated polymer and Additives

The polymer granules, after the initial 2 day extraction were
dried in air and then subjected to a sequence of drying programmes
in an attempt to achieve constant weight, see table 8.
The polymer granules from the second 2 day ether extraction were
also subjected to this drying programme excluding the step

where they were dried for 30 minutes at $100^{\circ}C$.

Samples of both the sheet and filler rod granules post the 2 day ether extraction and the 3 day ether, 3 day methanol extraction were examined using the DSC technique described in section 3.2.2.

The additives as extracted, with no further separation, were examined by four methods:infra-red and ultra-violet spectrophotometry (IRS and UVS respectively),nuclear magnetic resonance (NMR)and DSC.

IRS was carried out using a Pye Unicam SP1000. Specimens were taken either direct from the extract or from a solution with carbon tetrachloride and were placed onto one face of a 1 inch diameter sodium chloride crystal. A second crystal was brought into contact with the first and the liquid was squeezed between the two crystals giving an even thickness film. The crystals were clamped together, leaving an area free for the infra-red beam to pass normally through the film. The clamp was placed in the detector and a spectral scan was made using the automatic program. Air was used in the reference beam.

The crystals were regularly run blank, after carbon tetrachloride washes, to ensure they were free of contamination. The spectro- photometer calibration was regularly checked using a polystyrene standard.

UVS was carried out using either a Pye Unicam SP800 or a SP800A. Spectroscopically pure ethanol was used as the sample solvent reference and the samples were made up to a concentration of approximately 550:1 by weight, solvent to extract. Glass cells were used and prior to each run a baseline was recorded, using a second cell of solvent in the sample beam. All records were obtained using the fast automatic programme.

NMR analysis was carried out on a Jeol C60HL which was operated as a service by the Chemistry Department of Sheffield City Polytechnic. Samples were prepared by dissolving the extract in deuterated chloroform. Tetramethyl silane was the reference.

DSC was carried out using the technique described in section 3.2.2. The extracts were cooled to 0°C so as to be solid. Samples were scraped into the aluminum pans which were then sealed. Initially the temperature range examined was 20°C to 100°C but this was extended to -100°C to 100°C. Cycling was not attempted due to sample weight losses after the initial heating.

In those cases where the extract was dissolved in a solvent as part of the sample preparation, once the sample had been taken, the solvent was driven off the extract by rotary evaporation and drying in a vacuum oven at 40°C.

Samples of commercially available additives were examined by the above methods to produce reference spectra. In certain cases solid samples were prepared for IRS by the potassium bromide disc method, the ratio of additive to potassium bromide being adjusted to give the optimum spectrum.

The precipitated powder from the centrifuging of the THF grey sheet solution was examined with respect to its chemical composition and its particle size. As it was suspected to be calcium carbonate a small sample was placed in a test tube to which dilute hydrochloric acid was added. The resulting gas was passed through lime water.

A second sample was placed in a small beaker to which acetone was added. After 5 minutes agitation in an ultrasonic bath, a few drops of the resultant suspension were deposited onto a scanning electron microscope (SEM) sample stub. Once the acetone had evaporated, the stub was coated with gold in a sputter-coater, and then examined in a Cambridge SEM. This SEM was fitted with a wavelength dispersive analyser and this was used to confirm the presence of calcium. A qualitative examination of the powder particle size was also carried out on the sample.

3.3.3.   The Effects of Solvent Washes on Weld Rod

Two effects were studied, the first was solvent absorption and the second the possible extraction of additives from the rod.

The solvent absorption was investigated by immersing four 50mm lengths of clear weld rod in methy-ethyl-ketone (MEK) for 5, 10, 20 and 30 seconds. Their weights prior to immersion, and after a range of evaporation times and procedures were noted. Evaporation times, in air, were up to a week after immersion, followed by 3 days under vacuum, followed by 5 days at 30°C.

The extraction of additives was investigated by immersing twelve 50mm lengths of clear weld rod in 50ml of chloroform contained in a flask of known weight. The flask was gently agitated for approximately 1 minute and the rods removed. The solvent was removed by rotary evaporation and by drying in a vacuum oven at 30°C for 24 hours. After weighing, some chloroform was added and a sample taken for IRS examination.

3.4. Welding of Standard Materials

The work carried out in this section includes the hand welding of sheet using circular and triangular rod, speed welding of sheet using circular rod and the hot plate welding of sheet. Details are given of the design and trial runs of the welding rig built to allow hot gas welding to be carried out under controlled conditions. It also includes the details of the tensile testing of welds, the visual examination of weld interiors and the fracture surface studies.

3.4.1. Hot Gas Welding

Basic training in hot gas welding was obtained from the welders at British Nuclear Fuels Limited, Windscale site, over a 2 week period. Two months were then spent practising the technique at Sheffield City Polytechnic, before any test pieces were prepared. Initially the test pieces were prepared for the fracture toughness testing, see Section 3.5.2., though later work concentrated on tensile strength studies.

The sheet material was prepared into rectangular pieces, 300mm

by 75mm, using a circular saw. The edge of one of the long sides was chamfered either by filing, using a coarse file, or by cutting, using the variable angle cutting facility on the circular saw. Initially, filing was used as this was the method used by industrial welders. This was superseded by cutting on the circular saw as this gave a more accurate and consistent angle of chamfer plus a better surface finish. Two angles were employed, initially a 90° included angle was used but this was changed to a 70° included angle for the majority of the welding to conform to standard recommendations. All welds were produced with a symmetrical double-vee configuration.

Two welding facilities were used, A and B. The early work was carried out using the welding equipment belonging to the Department of Mechanical Engineering, Sheffield City Polytechnic, and hereafter is called system A. This consisted of a Goodburn High Speed Torch connected to a compressed air supply via a gas control board. This board provided both the means of cleaning the gas and regulating both the pressure and flow rate of the gas. The torch was fitted with a 600 watt heater cartridge and the HS/N4 nozzle; this is a standard round nozzle, to which has been added a tack welding tip which is screwed into the end of the torch. The welding gas was always turned on before the torch was switched on and when it was switched off the gas supply was left on for a further 5 - 10 minutes whilst the torch cooled. The compressed air was regulated to a pressure of 0.2 bar and a flow rate of 35L/min. The gas temperature, approximately 3mm from the end of the nozzle, was measured, using a mercury thermometer, and was found to be 280°C.

One of the pieces to be welded was clamped to a wooden bench. The second piece was then held in position, by hand, whilst a tack weld was made to provide the initial fixation. Hand welding was then carried out, using either three or six weld rods each side to fill the weld. The first rod was welded into position and the weld allowed to cool for 2 - 3 minutes. The weld piece was then turned over and, keeping the welding direction the same, the second rod was welded into position. Thereafter the sheet was turned over after each weld run, after a brief

cooling period.

The majority of these welds were made with a 90° included angle and were used for the fracture toughness testing of welds. Welds were produced in 10mm thick clear sheet using the clear weld rods and in 6mm thick filled sheet using 3mm circular filled weld rods. One welded sheet of both the clear and filled materials were used for the tensile tests, the clear sheet weld was completed with six passes of weld rod in each groove and the filled sheet weld with three passes in each groove.

For the majority of the welding of tensile test pieces a second welding set up was used, hereafter called system B. This consisted of a Leister Diode welding torch connected via a flow meter and two way valve to either a nitrogen cylinder or the Leister Minor air compressor. The Diode welding torch had a variable heater control marked 1-13, which controlled a 1300 watt heater cartridge. The torch incorporated a gas flow adjuster which was set in the fully open position at all times. The nozzles available were the speed nozzle (No.27) for 3mm circular rod and the tacking nozzle (No.28), both being a push fit onto the normal round nozzle fitted to the torch. The flow meter was a GEC 1100 Rotameter fitted with the 6-A-150 tube and B6S float. The flow was adjusted so that the float was at a scale reading of 75mm.

A nitrogen gas pressure of 0.14 bar was used, as measured on the cylinder regulator, and according to the flowmeter manual the nitrogen flow rate was approximately 35L/mins.

The two way valve was incorporated so that the Leister Minor air compressor could supply air to the torch whilst the torch was heating up, cooling down, or was not in use between weld runs, thus saving nitrogen. However, the Minor failed to supply the flow rate necessary to keep the gas temperatures stable between weld runs. Therefore, it was only used to supply air whilst the torch was cooling down.

A torch heater control setting of 4.5 was found to give a

gas temperature of 270-280°C when measured 3mm from the end
of the standard round nozzle. When the tacking nozzle was
used a setting of 5.5 was necessary whilst a setting of 5.2
was used when the speed welding nozzle was fitted. When
welding the large triangular cross-section I.C.I. weld rod
the control setting was raised to 7.0. Sheets were prepared
for welding by chamfering to give a symmetrical double-vee
configuration, with an included angle of 70°. Two weld pieces
were clamped to the weld bed of the welding rig, see Section 3.4.6,
leaving a gap of approximately 0.5mm between the chamfered edges.
To conform to industrial practice, one vee was filled first
before the second was started, although a brief cooling period
of approximately 2 minutes was allowed before each run. The
pieces were not tack welded.

During hand welding, standard practices concerning welding
were followed. The starting end of the welding rod was cut to a
30° angle and softened in the welding gas. The start of the vee
was then softened and the rod pressed into the vee. The rod,
under a pressure of approximately 1.3MPa, (equal to a load of
0.9Kgs) was then forced into and along the vee. Once moving
along the vee only a vertical pressure needed to be applied to the
rod.

The welding torch was drawn back along the vee at the same rate
as the rod filled the vee. The torch was held approximately
parallel both to the surface of the sheet and the line of the
weld. The gas jet was mainly directed at the base of the rod
from a distance sufficient to cause a bow wave at the base of
the rod (typically 10mm to 20mm). Only a slight pendulum action
was used directing the gas jet between a point just above the
weld rod base and to a point just along the rod from the weld rod
base. The action was repeated once or twice a second.
Little degradation was observed.

Regular checks on the speed of welding were made by noting
the time taken to complete one length of welding using a stop
watch. The degree of stretching of the weld rod was also checked
by measuring the initial length of rod and the length of rod left

after a known length of welding.

Using the hand welding method, two welded sheets were prepared using three passes of clear rod in each groove. A third welded sheet was prepared with three passes of I.C.I. rod in each groove, and a fourth was prepared with a single pass of I.C.I. triangular weld rod in each groove.

Speed welding was carried out using both clear and I.C.I. blue weld rods. Three welds were prepared, two using clear rod and one with the I.C.I. rod. Each weld was completed with six passes of rod in each groove. One speed weld completed with clear rod and the one with I.C.I. rod were prepared very carefully at a relatively slow speed. The second speed weld, using clear rod, was prepared at a faster rate.

3.4.2. Hot Tool Welding

The hot tool welding of the 10mm thick clear sheet was carried out on a Haxey Engineering pipe welding rig, see fig. 37 The rig consists of one fixed and one moving frame, in which the pipe clamps are fitted, mounted on steel guide rods. The moving frame is driven backwards and forwards by compressed air. The pressure associated with the movement is displayed on the gauge incorporated in the movement control box.

The rig was adapted to weld sheet by using the fittings shown in fig. 38. The cylindrical ends were loosely fitted into the pipe clamps, in the frames, so that the sheet clamp ends faced each other. The fittings were carefully aligned and then the pipe clamps were fully tightened.

The fittings were designed to accept plates 100mm square, up to 15mm thick, leaving 20mm of plate proud for welding. Two plates of 10mm thick clear sheet were prepared, 100mm square, and fitted to the clamps, again ensuring the correct alignment before being clamped .

The hot tool was a circular plate of diameter 250mm.

and thickness 20mm, fitted with PTFE sheet on both faces
It was electrically heated and thermostatically controlled.
The controls were present to give a tool surface temperature of
190°C. The temperature variation across the tool was measured
using a digital thermometer and was found to be $\pm$ 5°C.

Welding was carried out using standard procedures. The
heated tool was placed between the frames and the moving frame
driven forward until both plates were in contact with the tool
surface. A pressure of 0.6 bar, as measured on the gauge, was
applied until a 1-2mm bead of softened material had formed
round both plates. The pressure was dropped to zero and the
material allowed to 'heat soak' for 45 seconds. The moving frame
was then pulled back, the tool removed and the frame brought
forward so that the plates were again in contact. A pressure
of 0.4 bar was applied and maintained for 5 minutes. The
pressure was then reduced to zero and the welded plates removed.

The tensile strength of the weld was determined as in Section 3.4.4.

3.4.3. Examination of the Interior of the Welds

A visual examination of the interior of the welds was made
prior to and during the testing of the welds. The number of
samples required for the testing were cut from the welded sheet,
using a bandsaw. The samples were 15mm wide parallel strips
cut so that the weld lay across the 15mm width, perpendicular
to the length of the sample, see fig. 39. They were cut in
order, starting at the same end as the welding was started.
Each sample had scribed on to it a number which identified both
the welded sheet and the particular sample. This number
also served to identify the orientation of the sample.

The machined surfaces of the piece were ground using a range
of emery papers from 120 to 600 grit. The surfaces were then
polished using 6μm diamond paste. This was normally sufficient
to enable the examination of the interior. However, some were
further polished using 1μm diamond paste.

Internal flaws could be highlighted by viewing at an oblique angle into the polished surface. The interior was examined both visually and through a stereo microscope, photographs were taken using a Canon AE1 fitted with a macro lens.

Certain samples were examined between the crossed polars of the circular polariscope described in section 3.2.4.

3.4.4. Tensile Testing of Welds

At least five samples from each weld were prepared as above. However certain welds had their entire lengths prepared as tensile test pieces. The first specimen, the one which included the start of the weld, was not used in the tensile test programme.

All test pieces were conditioned in the laboratory for at least 2 days prior to testing and ambient temperature were used. The cross-section of each test piece, approximately 20mm either side of the weld, was determined using a micrometer.

All tests were carried out using either the floor model or table top model Instron set up as in section 3.1.0. A gauge length of 90mm was used, i.e. the distance between the grips, and the crosshead rate was 5mm/min. A visual examination of the weld region was maintained during testing. All tests were taken to failure.

3.4.5. Fracture Surface Studies

All fracture surfaces were examined visually and selected ones were further examined using either light or scranning electron microscopy.

The light microscopy was carried out using either the stereo microscope or a Zeiss Ultraphot fitted with a macro head. Photographs were taken using either the Canon AE1 using a macro lens or the Ultraphot. The depth of the unfused region at the centre of fracture initiation, on selected samples, was measured

using a travelling microscope.

Scanning electron microscopy was carried out using a Philips
500 SEM, on samples which had been sputter-coated with gold.

3.4.6. Automatic Hot Gas Welding Rig

The welding rig was required to provide a facility by which
the following welding parameters could be controlled: welding
speed, welding gas temperature, pressure and flowrate, welding
gas jet direction, distance between the torch and the weld and
the pressure and direction of pressure applied to the weld rod.

As such it was divided into three parts:

1) the main chassis and moving weld bed system
2) the welding torch and gas control systems
3) the weld rod feed system.

A moving weld bed system was chosen rather than a moving
torch and rod feed system assembly as it was thought to provide
a more flexible design if changes had to be made. The weld bed
was a combination of steel base plate covered by a 10mm thick
sheet of Sindanyo, an asbestos-cement product of high density.
The base plate of 350mm x 200mm x 20mm, was mounted, lengthwise, on
two steel guide rods, 1m long, using brass bearing rings fitted
beneath each corner. Two guide rods plus two similar rods
were bolted, at both ends, through the corners of two 200mm square
steel end plates thereby forming a long rectangular box frame.
a lead screw was mounted between the centres of the end plates and
was connected to the base plate through a floating coupling.

The asbestos-cement sheet was used to cover the base plate
so that the heat loss, during welding, through the weld bed would
be reduced. This would better simulate welding done on a
wooden bench top. A lengthwise groove 10mm wide by 4mm deep was
machined along the centre of the sheet. This was to allow a double-
vee butt weld to be turned over and clamped without causing distortion
even when the down facing vee had been overfilled. The clamps,

to secure the sheets to be welded, were mounted on the base plate, through holes cut in the Sindanyo sheet.

The weld bed had approximately 600mm of travel between the end plates. The bed was driven by means of a variable speed, high torque, reversible electric motor connected to the lead screw by a drill chuck. Safety stops were mounted on the end plates to prevent the bed being driven into them. Manual positioning of the bed was affected by rotating a handle connected to the lead screw, after the screw was disconnected from the motor by undoing the chuck.

Both the weld bed assembly and the motor were secured to the tubular metal frame chassis, see fig. 40 . It was also intended that the fittings to support the welding torch and the weld rod feed system would be mounted to the chassis.

The welding torch and gas control system were those described in section 3.4.1. as System B, consisting of the Leister Diode torch using nitrogen as the welding gas. During trials the torch was held in position using a retort stand and clamp.

For the trials the weld rod was fed by hand. The maximum speed of the welding bed was found experimentally, to be 300mm Attached to the bed was a marker which pointed down to the chassis. Secured to the chassis, below the marker, was a 300mm rule. This, in conjunction with a clock, allowed the speed of welding to be determined.

Welding trials were carried out using two welding gas temperatures, one of $220^{\circ}C$ and one of $280^{\circ}C$. One double-vee butt weld was made using the $220^{\circ}C$ condition whilst two were made using the $280^{\circ}C$. These welds used three weld rods in each vee.

The gas pressure was 0.14 bar and the flow rate was 35L/min. Each weld was initially tack welded and the tacking nozzle was left on during the subsequent weld runs. After tack welding

the sheets, by hand, the torch was clamped into the welding position. This was predetermined during trial runs made with the torch switched off. The torch was set with a slight downward angle of approximately 15° with the nozzle approximately 10mm to 15mm above the surface of the sheets.

A length of weld rod was welded to a piece of scrap material to determine the approximate speed of welding for the set weld gas temperature.

The weld bed was fitted with the pieces to be welded and was positioned just behind the welding torch. The weld rod was cut to a 350mm length and one end softened in the welding gas. When softened the welding bed motor was turned on, preset for the welding speed, and the weld bed drive engaged. The rod was pressed into the vee and the speed adjusted to maintain the rod in the same position relative to the torch. This was complicated by having to adjust the pressure on the rod to ensure that a good bow wave was being formed.

The remaining weld rods were laid down on alternate sides, after a brief cooling period, using the conditions determined above. The torch position was adjusted to allow for the change in position and height due to the earlier weld runs.

The weld speed found suitable when using a gas temperature of 220°C was 120mm/min $^{+}_{-}$ 14mm/min; when using 280°C the speed was increased to 180mm/min $^{+}_{-}$ 20mm/min.

3.4.7. Commercial Welds

Samples of weld as used in industry were obtained from BNFL, Windscale, Plastics Construction Ltd, Bolton, and Leister, Germany. In addition, a visit to the Plastics Construction factory was arranged so that welding could be observed.

Five BNFL welders each prepared a sample of welded sheet. The sheet was 10mm thick clear Darvic sheet and the weld rod was small triangular I.C.I. rod. They all prepared double-vee butt

welds but they each used a different number of weld rods to
fill the vee's. When received the sheets were coded A - E.

At least five test pieces, from each weld, were prepared as
in section 3.4.3. and tested as in section 3.4.4. A further
five pieces were taken from weld D but were dressed before
testing. This involved filing the weld region flat, parallel
to the sheet surface. Filing was continued until there were no
traces of the original weld surface. The filed surfaces were
then smoothed using 320 and 600 grit paper, see fig. 41.

Plastics Construction Ltd. kindly provided the services of
an experienced welder, who prepared welds from the materials
used in this project as well as from materials provided by
Plastics Construction Ltd.

The welder prepared four welds using 10mm thick clear Darvic
sheet. The first weld was welded using the I.C.I. circular weld rod,
the second was similar except the welder dressed the weld. The
third used I.C.I.'s small triangular rod and the fourth used
the clear weld rod.

The welder was asked to prepare the welds in his usual
manner. The weld configuration was an asymmetric double-vee
butt weld as shown in fig. 42. The sheets were chamfered
using a hand held grinding tool. The chamfer angle, proportioning
of the vee's and the land section were judged by eye. Dressing
of the weld was done using the chamfering tool.

A Leister Diode torch was used. There were no systems for
monitoring or regulating the gas pressure or flow rate. The
welder gauged the gas temperature using the 'palm of the hand'
method.

One sheet was clamped and the other tack welded to it. The
welder used the speed welding technique when welding with
circular rod and the hand welding method when welding with
triangular rod. In both cases he filled the larger vee first
before starting the smaller vee. He used six circular or

-69-

three triangular rods to fill the larger vee and three circular or one triangular rod to fill the smaller vee. The rods were welded one after the other with no time allowed for cooling.

The same welder then prepared three welds using the Plastics Construction Ltd materials. Again the weld configuration was the asymmetric double-vee butt weld. The first two welds were speed welded, one used six weld rods to fill the larger vee whilst the second used ten. Both used three rods to fill the smaller vee. The third weld was done using the hand welding method for the root runs either side, the remaining runs being speed welded. As before the larger vee was filled first before the smaller vee was started, with no time being allowed for the weld to cool.

When hand welding the welder used a pendulum technique and welded at a speed of approximately 180mm/min. When speed welding a welding speed of approximately 1m/min was maintained.

Test pieces for examination were prepared as in section 3.4.3. and were tested as in section 3.4.4.

A single welded sheet, prepared by a Leister welder, was obtained by Dr. D.V. Quayle whilst visiting Germany. The welder used a standard double-vee butt weld configuration, each vee being filled with a single large triangular grey weld rod. These were prepared and tested as above.

3.5. Fracture Mechanics Testing

This section concerns the work carried out in evaluating the fracture mechanic parameters G_{IC} and K_{IC} both for sheet material and welded material. The original work concentrated on methods using cantilever beam systems. However, UPVC appeared to be particularly unsuited to this approach, requiring large quantities of material to obtain only a few results. Later work was then carried out using a single edge notch system. This has the particular advantage of simulating the tensile test conditions applied to welds during normal testing.

The resulting fracture surfaces from both methods, cantilever beam and single edge notch, were examined.

3.5.1. Cantilever Beam Methods

Three variations of this method were used :

1) double cantilever beam (DCB)
2) tapered double cantilever beam (TDCB)
3) double tension (DT)

The original work was carried out using the TDCB method, this being experimentally the more simple. In the course of this study a large number of samples were tried, covering a wide range of designs and test conditions.

The first specimen, shown in fig. 43 was based on a commonly employed design. The taper angle, α, was $\tan^{-1} 0.2$ Shoulders were used to strengthen the specimen at the loading points. Sidegrooves were used to control the crack growth direction.

A rectangular sheet 270mm by 150mm was cut using a circular saw. A line was accurately scored 75mm from one edge along the length of the sheet, on both sides. The specimen geometry was cut from graph paper, to serve as a template. This template was carefully aligned, using the scored line, and taped into position. The design was then scribed onto the sheet. The side grooves were then machined, 2mm deep, into the sheet using a 0. 01 inch diamond slitting saw.

The nett section at the shouldered end was machined, using the saw, to leave a swallow tail section, see fig. 44. The distance from the narrow end of the specimen to the section was approximately 35mm. The section was used to ease crack initiation and to have an initial crack length of 20mm. The specimen was then cut from the plate, using a band saw, and the loading pin holes drilled.

The specimen was conditioned for 2 days in the laboratory, at ambient conditions. A floor model Instron was used for testing with the specimen being fitted to the Instron using special clamps, fig. 45. When clamped the specimen was supported at the far end, as its weight produced a couple on the clamps. The specimen was fractured at a constant cross-head rate of 5mm/min.

A further eleven specimens were prepared as above, except seven were prepared with groove depths between 3-3.5mm. A range of crosshead travel rates were used 0.05 to 5mm/min. In four cases a clamp was applied at the taper end of the shoulder until the crack first jumped, at which point it was removed. For details of the specimen geometry, test conditions and resulting fracture behaviour see table 8.

The design was then changed and a range of taper angles between $\tan^{-1}0.1$ and $\tan^{-1}0.25$ used, see table 8. Samples were prepared as above, except the initial size of the sheet was altered to reduce wastage when using the new designs. To reduce machining time the grooves were inserted using a shaper fitted with a specially prepared tool, only 1.8mm wide. The initial crack length was then prepared using a hacksaw, the nett section being shaped to a vee instead of the swallow tail. The use of strengthening shoulders was abandoned during this part of the work, most samples being prepared as simple tapered design, see fig. 46. A further variable altered was the effective height of the taper at the loading line.

The later work concentrated on the design shown in fig. 46 which used a simple taper design with a taper angle of $\tan^{-1}0.15$ The height of the taper at the loading line was 19mm and the length of the specimen from the loading line to the wide end was 295mm. Groove depths were typically 2mm.

As there was some doubt concerning the reproducibility of cracks sharpened by a scalpel, sharp natural cracks were used as the initial cracks for the tests. These were prepared by sharply tapping a ground file blade into the initial crack nett

section. This method usually produced a single naturally sharp crack approximately 50 to 80mm long.

Due to work reported elsewhere [124] a sample was reverse loaded, i.e. at the thick end of the taper, so that the crack grew towards the narrow end.

As a large part of the initial work was concerned with establishing the conditions for slow crack growth only two compliance calibration curves were prepared, one for the original design and one for the latter design, shown in fig. 43 and 46. Each calibration curve for the change of specimen compliance with crack length was prepared using compliance data obtained for pre-inserted simulated cracks. These cracks were inserted using a hacksaw. At any particular crack length the sample was loaded to produce a load-extension curve. The sample was then unloaded and the crack extended and the sample reloaded. This procedure was then repeated for a range of pre-inserted crack lengths.

As it has been shown [124] that more stable crack growth occurred for reduced taper angles, it was then decided to use the DCB system (taper angle of 0°).

The same methods of sample preparation and testing were used as for the TDCB samples except the specimen design was cut when the original rectangle of sheet was prepared. However, the groove guidelines were accurately scribed down the centre of the sheets. A range of beam heights and groove depths were used. The grooves were machined using either the slitting saw or the shaper. Crosshead travel rates were varied between 0.5 – 250mm. For the details of specimens used see table 10.

The third method of testing, DT, was used both to see if this produced slow crack growth and because it more closely simulated in-service conditions for welded and unwelded sheet.

A specimen rig was designed for this test and is shown in

fig. 47. This rig allowed 150mm wide welded or unwelded sheet to be tested with lengths up to 340mm. For the details of the plunger and support system dimensions see fig. 48. The rig was designed to fit the table top model Instron. The plunger screwed into the load cell and the support bed was bolted to the moving crosshead. The load cell was operated in compression by driving the crosshead up to the plunger.

However, at a later stage, it was discovered that this type of Instron is designed only to apply loads with a downward moving crosshead. The moving crosshead contains anti-whiplash springs which hold the bearing surfaces of the drive components against each other. If loaded incorrectly, at a load of 35Kgs. the springs compress and the load extension curve is distorted. Further, as there was a risk of damage being done to these springs if testing in this manner was continued, the DT test programme was curtailed and there was insufficient time to redesign the rig for proper Instron operation.

During trials 8 specimens were used. These were rectangles 300mm x 150mm with a groove 2mm deep down the centre of the length of one face. During testing the groove was always on the bottom surface. Only a crosshead travel rate of 5mm was used. At the loading end of the specimen the nett section was reduced, as in fig. 49 by hacksawing. Initial crack lengths were typically 10 - 30mm. A naturally sharp starter crack was produced as with the TDCB method. Once the crack has jumped it takes on a characteristic shape and therefore crack lengths were always measured along the bottom surface.

Selected samples of typical fracture surfaces from all three types of specimens were taken for scanning electron microscopy examination.

3.5.2. Weld Fracture Mechanics

The three cantilever beam methods of fracture mechanics testing used with the 10mm thick clear UPVC were applied to hot gas welded clear UPVC. Only welds produced with clear rod were used in this programmme of work.

The programme was divided into two parts, A and B. The initial work, part A, employed the DCB and TDCB methods on sheets welded using welding system A described in section 3.4.1. The latter work, part B, used the DT method to test sheets welded using welding system B described in section 3.4.1.

Specimen preparation for both parts of the programme were similar. Each weld was prepared from two rectangular sheets, typically 300mm x 75mm, which had been chamfered along their lengths to produce a symmetric double-vee butt weld configuration. Specimens produced in part A of the work used an included angle of 90° whilst those prepared in part B used an included angle of 70°. Welds were then carried out using the appropriate welding system and were completed using, as required, either one, three or six passes of rod to fill each groove. For DCB and DT testing the to-be-welded sheets were machined with the width required for the particular test. The welded sheets for the TDCB specimens were prepared with widths sufficient to allow the required TDCB design to be machined from them. The TDCB geometry was scribed onto and cut from the welded sheet as in section 3.5.1, but with the template being referenced to the chamfered edges of the weld groove.

In all the tests carried out, the specimens were loaded so that the crack should have moved along the weld seam, see fig. 50. The starter notch was prepared in the same way for all the specimens tested, with the notch being first prepared with a hacksaw and then sharpened with a scalpel.

As was the case for the DCB and TDCB testing of clear UPVC,

a wide range of specimen designs and crosshead travel rates
were used to establish if slow crack growth were possible,
see table 11 and table 12. During part A of the work it
was observed that over 50% of the specimens failed by arm
break-off or with the crack moving out of the weld zone. Two
methods were used to try to overcome this problem. Initially,
crack path controlling grooves, as used in the unwelded
specimens, were machined along the centre of the weld seams
on both sides of the welds. However, only a slight reduction in
arm break-off was achieved and a second method using bonded
side plates was tried. It was thought that the bonding of
side plates onto welded TDCB's might lead not only to reduced
levels of arm break-off [125] but also to an increased possibility
of slow controlled crack growth [148]. TDCB specimens were
machined, from welded sheets, to the standard TDCB design, shown
in fig. 46. Side plates of the same design, but allowing for
the weld groove, were prepared from 1/16 inch thick steel,
3/16 inch thick aluminium, 6mm thick Perspex and 3mm and 10mm
thick clear UPVC sheeting. Identical side plates were bonded
onto both sides of the test specimen using IS 495, see fig. 51.
After allowing at least 4 hours for the adhesive to cure, the
specimens were tested using a crosshead travel rate in the
range 5-20mm/min, see table 12 for details of the specimens used.
A compliance calibration curve was only produced for a welded
TDCB with 3mm thick clear UPVC side plates.

For part B of this programme only two welded DT specimens
were produced, both were symmetric double-vee butt welds,
having the same dimensions as the unwelded DT specimens, see
section 3.5.1. The first specimen was completed with one pass
of rod in each groove whilst the second was completed with just
one pass of rod in the upper groove and none in the lower.
Both specimens were tested using a crosshead travel rate of 5mm/min.
This part of the programme was curtailed once it was realised
that the continued use of the DT test could have led to the
Instron being damaged.

3.5.3. Single Edge Notch Testing

Materials tested by this technique included 10mm and 6mm thick clear Darvic, and 6mm filled Darvic. The materials were prepared as 12-15mm wide strips approximately 200mm long using a band saw. The machined surfaces were ground smooth using 320-600 grit papers and in some cases were polished using 6μm diamond paste.

At the centre of the length of each strip, a shallow groove was cut across the width, perpendicular to the length. Where the notch was to be a naturally sharp crack, the groove depth was approximately 0.5mm. Where the notch was inserted as a scalpel-sharpened groove, the groove was first cut to the depth required using a hacksaw. The naturally sharp cracks were produced in a similar fashion to those in the cantilever beam systems, i.e. by tapping a sharp wedge into the groove. Varying notch depths were obtained as an inherent feature of this method of production. Generally the razor-sharpened notches were used for the filled sheet and 6mm clear sheet as there was a greater occurrence of through-specimen failure using the other method of notching. For the early work on the 10mm clear UPVC and the 6mm filled UPVC, the notches were introduced into the specimen so that the crack would grow across the width of the specimen. However, to simulate the failure of welded tensile test pieces, latter specimens had notches introduced such that the crack grew into the thickness of the sheet.

Samples were tested either on a table top or floor model Instron, at ambient temperatures. A gauge length of 90mm and a crosshead rate of 5mm/min were used for all tests. Notch depths were measured, using a travelling microscope, from the fracture surfaces. Selected fracture surfaces were examined using scanning electron microscopy.

3.6. Pre-Weld Treatments and Changes to the Weld Rod Composition

From the previous work, the importance of notches and defects

within the weld zone became increasingly apparent. It was decided that, in order to improve the weld strength of hot gas welded clear UPVC, either the size or number of notches had to be reduced, or the materials used had to be made less sensitive to the presence of notches.

Two factors were proposed as being possible causes of the notches or, rather, unfused regions within the weld zone. These were:

1) the presence of frozen-in orientation in the as-received weld rod

2) a possible layer on the surface of the weld rod of either diffused additives or difficult to remove dirt which acts as a physical barrier to fusion.

To make the weld strength less sensitive to the presence of notches in the weld zone, it is necessary to improve the toughness of the materials used to make the weld. It was considered impractical, in the short term, to change the composition of the sheet. However, changes to the weld rod formulation were quite feasible and would allow the incorporation of impact modifiers into the weld rod, thereby improving the toughness of one of the components of the weld.

The work carried out to explore both approaches to improving weld strengths was divided into two parts. In the first varied pre-weld treatments to the weld rod and sheet were used, whilst in the second, materials of different composition were obtained, converted into weld rod and used to produce hot gas welds. As such the second part was concerned not just with improving the toughness of the weld rod but also with trying to prevent the formation of any layer of additives on the surface of the weld rod.

All the welds prepared for this work were prepared as 300mm long symmetric double-vee butt welds with an included angle of

70°. Unless otherwise stated, each groove was filled with
three passes of weld rod. Welding was carried out using
system B described in section 3.4.1. with a gas jet temperature
of approximately 280°C, measured 3mm from the end of the nozzle.
Specimens were cut from the welded sheets and were prepared and
tested as in section 3.4.3. - 3.4.5.

3.6.1. Pre-Weld Treatment of Weld Rod

Hot gas welds were prepared using clear weld rods which had
been subjected to either an annealing treatment or a solvent
wash.

Six weld rods, 390mm long, were annealed for ten minutes
at 150°C, on a bed of glass microspheres. After cooling in air,
their lengths were found to be between 350-355mm, indicating that
some relaxation of orientation had taken place. One weld
sheet was prepared with the annealed rod.

One of two solvents, either methanol or trichloroethylene,
was used to wipe down both the surface of weld rods, and the
surfaces of the grooves and rods already welded in place,
prior to each pass of weld rod. During welding, polyethylene
gloves were worn to avoid re-contaminating the weld rod surface.
Two welded sheets were prepared, one with rod washed with methanol
and one with rod washed in trichloroethylene.

3.6.2. Changes to Weld Rod Composition

In conjunction with I.C.I. various changes to the standard
weld rod composition were decided upon, see table 13. Representatives
of I.C.I. supplied the new compositions in the form of sheets
cut from the hide produced by a two-roll mixer. Approximately
300gms of each composition was supplied.

Weld rods of each composition were prepared by extruding the
granulated sheets using a Davenport Rheometer as a ram extruder.
The sheets were first granulated such that the largest granules

were approximately 20mm^3. The rheometer was allowed to stabilise at 190$\pm$ 5°C and approximately 70gm of granules were used to charge the barrel. The charge was added in 10gm lots which were tamped down after each addition. Once the barrel was full, the ram was lowered until a slight pressure was read and the charge allowed to come to temperature over a 3-4 minute period. Ram extrusion was then carried out with the ram speed being adjusted to the fastest rate consistent with the production of smooth, bubble-free rod. Typical ram speeds were 10mm/min. The rod was allowed to extrude to a length of 350mm before being cut at the die. The extruded rods were then allowed to cool on a wooden bench top and were marked in the order they were extruded.

To extrude 3mm diameter rod it was necessary to manufacture new dies for the rheometer. The widest bore available in the standard set of dies supplied by the manufacturer had an internal diameter of 2mm. During trials, using this die and granules of clear Darvic, the extruded rod was found to have a diameter of 2.5mm. It was calculated that a bore of 2.5mm internal diameter was required, assuming constant die swell, to produce rod with a diameter of 3.1mm. Two stainless steel dies were produced, identical in size to the supplied dies except their bores had an internal diameter of 2.5mm. All extrusion of weld rod of the new compositions was carried out using these dies.

It was normally possible to extrude 13-14 350mm lengths of rod from each 70gm charge. Although the barrel would take a larger charge, degradation of the polymer prevented any further useful rods being produced. The barrel and die were carefully cleaned after each run to prevent contamination of subsequent runs.

Only one welded sheet was prepared using rod of each composition except in the case of formulation No.9, see table 13, for which a second welded sheet was prepared. This second sheet was welded using six passes of rod in each groove, which required two extra batches of rod to be extruded.

Selected samples of extruded rod were subjected to a heat treatment of 170°C for 10 minutes to determine the level of frozen-in orientation caused by the extrusion process. The length of each rod, before and after the heat treatment, was measured. The rods were kept on a bed of glass microspheres during the heat treatment and the subsequent cooling.

4. Results

In the following chapter the results of the previously described experimental work are presented. The results are discussed in the context of the experiment from which they were obtained along with their general significance to the overall programme of work. However, a more detailed discussion relating specifically to the welding and fracture mechanics work is reserved for the next chapter.

4.1. Mechanical Properties

All the stresses reported here are engineering stresses, and are calculated [170] as the load, P, divided by the specimen initial cross-sectional area, A_o,

$$\sigma = P/A_o \qquad -(12)$$

A true stress, σ_T, is defined as the load divided by the instantaneous cross-sectional area, A, and is related to the engineering stress, assuming a constant volume deformation process, by

$$\sigma_T = \sigma \times (1/1_o) \qquad -(13)$$

where 1 is the specimen gauge length under the applied load and 1_o is the specimen's original gauge length. At yield, for UPVC, the true stress is typically 6% higher than the engineering stress [77].

Engineering strain, e, is defined [170] as,

$$e = (1 - 1_o)/1_o \qquad -(14)$$

The tensile modulus, E, is defined [170] as,

$$E = \sigma/e \qquad\qquad -(15)$$

where the ratio σ/e is taken from the initial linear part of the load - extension/strain curve. A secant modulus is defined as the stress required to produce a specific strain divided by that strain.

The flexural modulus, for rectangular cross-section bars, is defined [173] as

$$E_B = (L^3 P)/(4bh^3 y) \qquad -(16)$$

where L is the length of the span between the outer supports of the 3-point bend rig, b is the width of the bar, h is the thickness and y is the deflection induced at the centre of the bar by the applied load, P.

For a circular cross-section rod, the flexural modulus is defined [174] as

$$E_B = (4 L^3 P)/(3\pi d^4 y) \qquad -(17)$$

where d is the diameter of the rod.

4.1.1. <u>Tensile Yield Stress</u>

During the tensile testing programme three types of failure behaviour were observed: necking and cold drawing, necking rupture and brittle fracture. When either of the first two types were seen failure was deemed to have occurred once the load sustained by the specimen began to drop. A yield stress, σ_y, was then calculated from (12) using the maximum load sustained by the specimen. When brittle fracture occurred a fracture stress, σ_F, was calculated from (12) using the load at which fracture occurred. Where the term tensile strength is used it is taken as being either the yield stress or the

fracture stress.

The yield stress of the 10mm thick clear sheet was
determined as 67.5 ± 1.4MPa when the dumbbell specimens were
used and as 61.4 ± 1.4MPa when the parallel sided specimens
were used (as part of the tensile modulus programme). When the
sheet was later examined for orientation, the yield stress
along the length of the sheet was calculated as 64.7 ± 1.6MPa
whilst across the width, it was 65.6 ± 1.4MPa.

A short test programme revealed that the yield stress
was not dependent on specimen cross-sectional area or ageing
but that it was dependent on the strain rate and temperature
of the test. Although the programme was not particularly
detailed it was possible to establish that the yield stress
increased approximately 1.5MPa each time the strain rate was
doubled and that it decreased by approximately 0.8MPa for
each $1^{o}C$ increase in test temperature. These results are
in general agreement with the values reported in the literature
[44,45], allowing for the range of strain rates and
temperatures used. After allowances were made for the
different strain rates used in the various tests there was
still a difference between the yield stresses of approximately
4MPa. This may be explained as being caused by fluctuations
in the test temperature. Although the specimens were
conditioned in the test laboratory for at least 24 hours
prior to testing, the laboratory temperature itself was
observed to change between $12^{o}C$ and $28^{o}C$ over a 12 month
period and even up to $5^{o}C$ over the normal working day.

The weld rod yield stress was determined to be 70.0 ± 1.5MPa
from the specimens bonded into the steel blocks. This value
was calculated assuming a rod diameter of 3.0mm. However, it
was generally observed that the rod cross-section was an ellipse
with a major axis diameter typically 0.1mm greater than the
minor axis diameter. Further, it was noted that there was
a variation in these dimensions along the length of the rod.

After averaging several measurements taken from various positions along different rods, it was found that 3.0mm was a reasonable value for the rod diameter. However, it is probable that by using this value the yield stress is under-estimated by up to 5%.

This implies that the clear rod yield stress is significantly higher than that of the sheet, especially as the strain rate used was usually half that used for sheet testing. Even allowing for small variations in the temperature of testing between the sheet and rod tests there is still a difference in the yield stresses. This difference probably reflects the slightly increased levels of orientation frozen-in the rod during processing.

The yield stress of the Plastics Construction sheet material was found to be 67.0 ± 1.0MPa. The filled UPVC sheet was tested for orientation induced by processing. The yield stress when measured in the direction of the surface texture was 53.3 ± 0.7MPa whilst perpendicular to this it was 50.6 ± 0.7MPa.

4.1.2. <u>Tensile Modulus</u>

When measured for strains less than 0.4%, that is within the initial linear part of the load-strain curve, the 10mm thick sheet was found to have a tensile modulus of 3.60 ± 0.15GPa. However, the secant modulus measured at 0.8%, 2%, and 4% strain was found to be 3.0 ± 0.1GPa and approximately 2.0GPa and 1.5GPa respectively.

The weld rod was observed to have a very much longer linear part for its load-extension curve and the tensile modulus measured at up to 1% strain was 3.42 ± 0.10GPa. A result confirmed by the extensometer measurements. Once again, this value is thought to be an under-estimate on the grounds that the rod was assumed to have a diameter of 3mm. If the cross-sectional area has been over-estimated by 5% then the tensile modulus would really be 3.6GPa. However, if the work of

Rawson and Rider [82] is examined, the fact that the weld
rod yield stress is higher than that of the clear sheet
because of orientation, then the tensile modulus of the weld
rod should also be higher than that for the sheet. From their
work, an approximate relationship between the ratios of yield
stress and tensile modulus for orientated and unorientated
material may be written as

$$(\sigma_o - \sigma_u)/\sigma_u = 1.45 (E_o - E_u)/ E_u$$

-(18)

where subscript o refers to the orientated material property
and subscript u refers to the unorientated material property.
If the yield stress and tensile modulus values for sheet are
representative of unorientated material then from the clear
rod yield stress value, the clear rod tensile modulus would be
expected to be 3.8GPa. Two reasons may be proposed to explain
why this value was not observed:

   1) different test temperatures were used

   2) the rod and sheet materials are not identical
      and the relationship given in (18) does not
      apply.

4.1.3. Flexural Modulus

   The flexural modulus of the 10mm thick clear sheet was found
to be 3.07 ± 0.09GPa, whilst the 3mm thick clear sheet had a
modulus of 2.90 ± 0.10GPa. The clear weld rod had a modulus of
3.12 ± 0.20GPa. As before, the modulus for the rod was
calculated assuming a rod diameter of 3mm and therefore it is
probably an underestimate. Allowing for this and the fact
that the 10mm thick sheet was tested using a strain rate three
times that used for the rod implies that the rod flexural
modulus is significantly higher than the sheet.

   The difference in the values of the flexural modulus for
the sheet and rod is further evidence that the rod contains

frozen-in orientation. The flexural modulus test demonstrates
this better than either the yield stress or tensile modulus
tests since it primarily tests the outer skin of the rod.
It is in just this layer that one would expect any frozen-in
orientation to be concentrated and therefore for it to have
a marked influence on the modulus measurement.

4.2. Microstructure

The following sections, 4.2.1 - 4.2.4, deal with the
results of the microstructural analysis stage of the materials
characterisation programme. The first section deals with
differences in the base polymers used and the effects on
molecular weight distribution caused by heat treating the
materials. The second examines the thermal properties of the
materials and discusses how they are affected by thermal
history and additives. The third and fourth sections examine
the orientation left in the materials by their different
processing histories, through thermally induced shrinkage
and birefringence studies. The fourth section also examines
the dependence of birefringence on the applied stress for
the sheet material.

4.2.1. GPC Results

Although GPC is a quick method to determine the molecular
weight distribution of polymers it suffers from batch to batch
variability. The normal practice was, therefore, to include a
standard sample of clear sheet which could be used as a
reference. The results for the two GPC analyses carried out
are given in table 14.

Despite there being a large scatter in the results it would
seem reasonable to assume that the I.C.I. materials, both
sheet and rod, are based on the same polymer. The clear weld
rod would seem to be based on a different polymer but one
with a similar molecular weight distribution.

The GPC analyses of the heat treated samples would
indicate that they have been little affected, with respect
to molecular weight distributions, by being kept at elevated
temperatures for a time similar to that experienced during
welding.

4.2.2. Determination of T_g

The DTA work was not easily reproducible and as sample
preparation was time consuming it was decided to abandon
this method at an early stage, in favour of DSC.

The DSC method normally gave reproducible results, of a
standard form, for the sheet material examined in the range
$30 - 100^oC$, see fig. 52. Spurious peaks and slight variations
were accounted for by either sample movement within the pans [98]
or erratic purge gas flow. Cycling of the sheet in the range
$30 - 100^oC$ produced no changes in the output thermogram.

However, the clear rod thermograms showed an endothermal
peak over the glass transition region during the first heating
run. Cycling of the rod produced thermograms of the standard
form, see fig. 53.

The glass transition temperatures were determined using the
'crossed-line' method recommended by Griffiths and Maisey [175],
see fig. 54.

The T_g of the sheet was found to be $67.0^{\pm} 1.5^oC$, with no change
with cycling. The clear rod T_g was $64.9^{\pm} 1.9^oC$ for the initial
heating but dropped to $58.6^{\pm} 1.1^oC$ after cycling. This large
difference was due to the presence of the endothermal peak
over the T_g region during the first heating.

The endothermal peak was, at first, thought to be due to
the presence of a lubricant additive, Wax E, a Hoechst product,
which has been observed to cause problems in interpreting the
glass transition curve for PVC. This lubricant has a melting

peak in the region of the polymer T_g. This peak was observed
to decrease in size and the polymer T_g was found to decrease
by several degrees when the sample was cycled [176].

That the endothermal peak would arise as a product of the
heating rate used was originally thought unlikely since to
produce the peak a slow cooling and fast heating cycle is
required [81]. It was thought that in the extrusion process
the extruded rod would be rapidly quenched into a cold water
bath during the haul-off. However, it is a common practice
to extrude into a warm water bath, to prevent the formation of
bubbles within the rod. This may be sufficient, combined with
a long storage time, to give rise to the endothermal peak and to
account for its removal by cycling.

The study of thermal behaviour of the sheet and rod over
the temperature range $-100^{\circ}C$ to $0^{\circ}C$ was of little use as the
curves were masked by excessive noise. This seemed to be a
problem associated with using the thermal analyser on its
most sensitive setting and at low temperatures.

The high temperature study, $30^{\circ}C$ to $350^{\circ}C$, was limited to
two runs to prevent any damage to the DSC cell, caused by the
hydrogen chloride given off by the PVC degrading. The thermograms
for sheet and rod are given in fig. 55. The main difference
appears to be that the exothermic reaction associated with
degradation starts at $170^{\circ}C$ for the rod and at $195^{\circ}C$ for the
sheet. This suggests that during hot gas welding the rod is
more likely to degrade than the sheet. Considerably more work
is required before anything more definite could be concluded
but this technique might prove useful in comparing the sheet
and rod in any further study.

4.2.3. <u>Thermally Induced Shrinkage</u>

The BS shrinkage test [172] for sheet, indicated that
the sheet shrank less than 1% with only a small degree of
orientation being left in the sheet after processing.

-89-

The shrinkages measured using the square block method rose to 3%, for heat treatments of 170°C for 1 hour. See table 15 for details of the measured shrinkages resulting from various heat treatments. The scatter in results prevented any detailed analysis relating to frozen-in orientation. It was estimated that when measuring the blocks the error was up to 0.5% of the measured shrinkage which would mask any small effects due to orientation indicated by the results. However, any orientation would appear to cause less than 5% difference in the shrinkages measured parallel and perpendicular to the sheet length. It is assumed that the maximum difference would be observed when measured in these directions. In all cases the sheet thickness was observed to increase approximately 5% with the first 10 minutes of the heat treatment and remain constant thereafter.

The rod was found to shrink up to 25% along the length of the rod when heated to 180°C for 15 minutes, see fig. 56. The rod did adhere to some of the surfaces used for supporting the rods during the heat treatment and this may explain some of the scatter in the results. See table 16 for the measured shrinkages resulting from various thermal treatments to the rods. Measurement of the shrinkage was made using a 150mm steel rule since the heat treated rods were rarely straight enough to justify the use of a travelling microscope. A feature of all the rods was their tendency to become curved during cooling. Some scatter in the results for the shrinkages may have been induced by the method of straightening the rods as they cooled. The diameter of the heat treated rods was generally found to have increased, after allowing for the variations previously discussed, in the diameter of rods prior to heat treatment. The rod diameter increase appeared consistent with the rod maintaining a constant volume during the shrinkage, although the measurements are not accurate enough to be conclusive. Typically the rod diameter increased 10 - 15% for the rods showing the maximum shrinkage.

4.2.4. Birefringence

The orientation in the sheet and rod was measured using a quartz wedge system on the Vickers M55 microscope. The scale reading, S, at which extinction was observed was converted to the retardation, R, in nm using the quartz wedge calibration.

$$R = 28.36 \, S + 174.19$$

$$-(19)$$

The birefringence, Δn was then calculated using

$$\Delta n = R/t$$

$$-(20)$$

where t is the specimen thickness.

For the 10mm thick clear sheet the birefringence was typically $0.65 \times 10^{-4} - 0.85 \times 10^{-4}$, whilst for the rod it was approximately 1.85×10^{-4}. Although the difference between the sheet and rod birefringences is large both values are small when compared to the values for UPVC showing marked anisotropy in its mechanical properties [77].

The stress optic coefficient, C, was originally determined so that a photoelastic stress analysis of the hot gas welds could be carried out. The value of C was determined, for the sheet, using the cantilever beam method. A cantilever beam of sheet was loaded at its free end, between the crossed polars of a circular polariscope. The stresses along the resulting isochromatic lines were calculated using standard beam equations and C was then calculated from

$$R = n\lambda = C(\sigma_1 - \sigma_2)t$$

$$-(21)$$

Where σ_1 and σ_2 are the principal stresses in the beam (in this method σ_2 is assumed to equal zero), λ is the wavelength of the incident light (in this case a sodium lamp was used with $\lambda = 589$nm) and n is the isochromatic fringe number [177]. For the sheet, C was found to be $6.51 \pm 0.36 \times 10^{-12} m^2/N$.

This result is in good agreement with values reported in the literature [178, 179] and confirms the fact that UPVC is a material unsuited to photoelastic analysis as its birefringence is relatively insensitive to stress.

4.3. Chemical Analysis

The chemical analysis of the sheet and rod materials was considered necessary since the presence or absence of particular additives will affect the mechanical properties of the finished product. Examples of such additives are plasticisers, impact modifiers and certain of the thermal stabilisers.

To carry out an exhaustive quantitative analysis was considered outside the scope of this project, since considerable time and special expertise are required. The basic problem of the analysis is the wide range of materials in use as additives. The analysis of UPVC is further complicated by the relatively large number of additives used in a particular formulation and the low levels at which they are present. In a typical unfilled non-impact modified UPVC the major additive is 1 - 2% thermal stabiliser with a number of lubricants, all at the 0.5% level, a U-V absorber, at the 0.2% level, and sometimes, pigments at the 0.1% level. However, a semi-quantitative analysis, in which most of the additives might be identified, was considered possible.

There were several clues from the previous work on which to base the analysis. The clear sheet was believed to contain an organotin stabiliser: it would be expected as a requirement of clarity. Further, the yield stress and T_g of the sheet would suggest the presence of an anti-plasticising agent such as an organotin [62]. The sheet was unlikely to contain any plasticiser nor would it contain any impact modifiers. These dramatically reduce yield stress when used in their normal concentrations. The rod might have contained a plasticiser, plasticised weld rod being popular in Europe, though the

yield stress suggested otherwise. The presence of a
particular lubricant, the Hoechst product, Wax E, was also
suggested as it provided one explanation for the endothermal
peak seen over the glass transition region of the clear
rod [176].

4.3.1. Extraction

Only the 10mm thick clear Darvic sheet, the I.C.I. weld
rod and the clear weld rod were studied in detail. However,
the filled Darvic sheet was also examined to determine which
filler had been used.

The extraction method used for the clear materials was
an ether extraction using the Soxhlet apparatus, as recommended
by Haslam et al [180]. In their extraction, they start with
a finely divided powder polymer sample and reflux the solvent
over the sample for 6-7 hours. For most additives they found
ether to be an acceptable solvent, although hot methanol was
required when polymeric additives were present.

As there were no facilities to provide a finely divided
sample the materials were granulated using a laboratory
granulator which produced granules approximately 20mm^3. To
allow for the increased volume that the solvent had to extract
through, the extraction time was extended first to 48 hours
and then up to 240 hours. To obtain a reasonable amount of
extract the sample size was increased from 2gms to 20gms.
Although a hot methanol extraction was carried out, subsequent
to the ether extraction, only a minute extract was obtained
and it was not adopted as part of the general extraction
programme. The different extraction conditions and the weight
of extracted materials are given in table 17.

It had been suggested [181] that variations in the weight
of extracted additives probably resulted from the minor
variations in composition, between batches, arising from the
day-to-day changes in processing conditions. Allowing for this,

the sheet contained approximately 2.9% extractable additives whilst both the rod materials contained approximately 4.1% extractable additives. This difference is believed to be due to the different types and levels of additives required for the different processing conditions. These levels are in agreement with those quoted by Cornes and Haward [93]. The levels of additives indicated that neither impact modifiers, plasticisers nor processing aids were used in these materials, since these additives would normally be present at the 10% level.

A second method of separating the polymer from the additives, the THF recovery method also recommended by Haslam et al [180], was used to confirm the levels of additives in the clear sheet and to allow the determination of the filler in the filled sheet. The clear sheet material was found to contain 3.75% soluble additives and 1.3% insoluble additives. Although these values are higher than those from the Soxhlet extraction, they confirm the level of additives as being no higher than the 5% level. The difference is thought to be due to :

1) the granules used in the Soxhlet extraction being of a sufficient size to prevent complete extraction.

2) the insoluble additives centrifuged off probably containing both some crosslinked polymer and the dirt particles trapped in the material during processing (a visual examination of the sheet reveals numerous inclusions within the sheet).

The recovery method was only used to separate the filler from the filled UPVC sheet and the insoluble additive content was found to be 12%.

4.3.2. Analysis of Additive-Free Polymer

After Soxhlet extraction, the polymer granules were subjected to various drying procedures, in an attempt

get a constant weight measurement. However, the granules were found to increase in weight with increasing time of exposure to air, see table 8 for drying conditions used and the resulting granule weights. The granules were found to gain approximately 2% weight compared to the sample weight prior to extraction. This would indicate an increase in polymer weight of approximately 6%, allowing for the removal of additives.

After the ether extraction the granules appeared unchanged. However, the granules of both sheet and clear rod developed a milky white translucence during drying after the methanol extraction. Sample granules, taken after the methanol extraction, were found to contain voids when cut open and examined using a light microscope. It is thought that the hot methanol swells the polymer granules during extraction and during drying the granules are constrained to their swollen shapes. The polymer can return to its normal density only by forming internal voids.

Dried granules of both sheet and clear rod were subjected to a DSC analysis, see fig. 57. The resulting thermograms indicate a reduction in polymer T_g to approximately $45^{\circ}C$. This, combined with the increased weight of the granules, suggests they still retain some solvent which is acting as a plasticiser [182].

4.3.3. Analysis of Extracted Additives

The author would like to take this opportunity to acknowledge the assistance of Dr. G. Corfield and Dr. A. Ellis in the following work and the co-operation extended by the technical services sections of I.C.I., Hoechst Chemicals and Ciba-Geigy.

The analysis programme chosen reflected the need to gather the maximum information in the shortest time. It was expected that some of the additives would remain unidentified and that

no quantitative information concerning the level of the individual additives would be obtained.

The programme consisted of submitting the dried extracts, without further separation, to analysis using standard I-R, U-V, NMR and DSC techniques. The first three are recommended by Haslam et al [183]. The last was expected to provide melting point information and thus allow an estimate of the number of additives present in each extract. The results for the extracts from these methods were then compared against results obtained for pure samples of a range of additives, selected as possibly being present in the extract, and against results given by Haslam et al [184]. It was appreciated that the identification of some of the additives would prove impossible due to chemical changes brought about by processing and that some would be masked by other additives in the extract.

The extracts from both the clear sheet and the I.C.I. rod were similar in appearance. Both were a brown slurry which largely solidified with time, though they melted if warmed in the hand. The clear rod extract was a blue slurry which solidified with time and also melted if warmed in the hand.

The I-R, U-V, and NMR spectra for the sheet and two rod extracts are given in figs. 58-66. The DSC thermogram for the sheet and clear rod extracts is given in fig. 67. Details of additives obtained as standards and with which method they were analysed are given in table 18.

As the extracts are mixtures, a comparison of spectra with standards can only provide indications as to which additives are present.

The I-R spectra of the sheet extract strongly indicated the presence of di-octyl tin di-octyl thioglycollate, an

organotin liquid stabiliser. The U-V spectra was identified
with that for the U-V absorber 2-(2-hydroxy-5-methyl-phenyl)-
2H-benzotriazole. The NMR spectra failed to compare with
any of the standards.

The I-R spectra of the I.C.I. rod extract suggested the
presence of ethyl palmitate, a lubricant with no indications
to the type of thermal stabiliser used. The U-V spectra was
similar to that of the sheet extract, suggesting the same U-V
absorber. Again there was no match of the NMR spectra with
that of any of the standards.

The I-R, U-V and NMR spectra for the clear rod extract
all pointed to a phthalate-containing additive. This would
usually indicate a plasticiser such as di-octyl phthalate. However,
it was suggested that at these levels, i.e. less than 5%, it
was probably a phthalate type lubricant such as stearyl phthalate
[185]. The standard produced similar I-R and U-V spectra but
IRS and UVS do not readily differentiate between the octyl and
stearyl forms. [186].

The DSC thermograms for both the sheet and clear rod
extracts indicated several melting points. However, the DSC
equipment failed before all the standards could be examined.
The limited temperature range used for the extracts does not
include temperatures at which most lubricants melt, i.e. above
100°C, and no results were obtained for the liquid additives.

The stabiliser in the clear rod was determined to be a
di-butyl tin di-octyl maleate by R.Clarkson using a Mössbauer
technique [187]. He concluded that there was considerably
more stabiliser in the clear rod than in the sheet.

During the consultations with I.C.I. concerning new weld
rod formulations the additives identified in the I.C.I.
materials were confirmed. The weld rod stabiliser was given
as a di-butyl tin maleate with the lubricant systems

in the sheet and I.C.I. rod similar although the levels in
the sheet were lower.

The insoluble additives separated from the filled sheet
using the THF recovery method mainly consisted of a fine
greyish-white powder. The powder was analysed, using a
wavelength dispersive analyser, as containing only calcium in
significant quantities. However, this system was not able to
detect elements of atomic number less than twelve. The powder
was observed to consist of particles with dimensions up to
$20\mu m$, see fig. 68. The gas evolved after hydrochloric acid
was added to the powder was identified as being carbon dioxide.
It was concluded that the filler was mainly calcium carbonate
which was added to reduce cost rather than to improve impact
properties.

4.3.4. The Effects of Solvent Washes on the Weld Rod

It had been suggested that wiping the weld rod with a
solvent prior to welding leads to an improved weld strength [188].
Two experiments were carried out to examine whether such an
improvement was due to either the removal of an additive from
the surface of the rod or to the absorption of the solvent into
the rod leading to a surface layer of plasticised material.

For the first experiment clear weld rod was soaked in a
flask of chloroform for 1 minute. After the rod was removed,
the chloroform was driven off and the flask weighed. Approximately
0.15% by weight of additive was found to have been extracted.
Examination of the extract using infra-red spectrophotometry
indicated that the extract was similar to that obtained during
Soxhlet extraction.

For the second experiment clear weld rod was immersed in
methyl ethyl ketone for various times. The weight of the rod
before immersion and after various drying procedures was

recorded, see table 19.

From the experiments it would seem that solvent washes can lead to both the extraction of additives and the absorption of solvent into the rod. Although both effects are small they may be significant since they are localised to the surface of the rod and it is the condition of the surface of the rod which critically controls the fusion obtained during welding.

4.4.   Weld Results

The weld failure stress was calculated using (12) with the cross-sectional area defined as the width of the specimen, at the weld, times the average thickness of the sheet, away from the weld. The stress, so defined, is the gross specimen stress and not the stress experienced at the weld. However, this definition of stress permits the assessment of the load bearing capacity of the welded sheet and is also the same stress normally used in fracture mechanics analysis. The drawback of this stress is that it does not permit an assessment of differences in bond strength due to technique when different weld configurations are used.

The efficiencies of the welds were calculated using

$$\text{Weld efficiency} = \frac{\text{Weld failure stress}}{\text{sheet yield stress}}$$

-(22)

with the sheet yield stress being taken as 65.0MPa for welds using clear sheet and 53.0MPa where grey sheet was used. As Alf et al [168] have shown that weld failure stress is relatively insensitive to variations in temperature, for temperatures about $20^{\circ}C$, no allowances were made for variations in the temperature of testing. The choice of the materials' yield stress values were based on the results of tensile tests on similar sized specimens of unwelded sheet.

The description of differences observed between welds
during the examination of their interiors is only qualitative
as it was not considered possible to make it quantitative.

At least one specimen from each weld tested was examined
between the crossed polars of a circular polariscope. A
typical isochromatic fringe pattern is shown in fig. 69.
As can be seen, the poor photoelastic response of UPVC combined
with the complex stress system resulting from the welding
process and the interference of lines due to the etching of the
boundaries of the foils makes analysis extremely difficult.
It was decided that such an analysis was beyond the scope of
this work.

4.4.1. Polytechnic Welds

 In the majority of cases the main feature of the examination
of the interiors of hot gas welds was that the various weld
boundaries, i.e. rod/rod and rod/sheet, were invisible when
viewed from an oblique angle.

The usual indication of a weld boundary was the presence of
slightly degraded material, showing up as light green/brown
streaks, within the weld zone. Sometimes trapped particles of
dirt or more heavily degraded material were present along a
boundary. Sometimes a weld rod was observed to have bubbles
within it. However, in virtually every welded tensile test
specimen at least one boundary would be revealed by having a
silver streak along it. These streaks had the characteristics
of planar cracks in that they had sharply defined but irregular
boundaries in the plane of the streak and were very thin along
the plane. A typical hot gas weld interior showing all the above
features is shown in fig. 70.

When the weld interior was viewed head-on the weld boundaries
were more clearly indicated, since the presence of degraded
material along the boundaries reduced the amount of light
transmitted along them, see fig. 71.

A further feature observed in welded specimens when
viewed in this direction was the presence of a zone of
changed refractive index in the sheet about the weld, see fig. 72.
It would seem reasonable to associate this with a heat affected
zone (HAZ), as found in metal welding. The horizontal lines
seen in the sheet appear to be boundaries between the foils of
UPVC, which are pressed together to form the thickness of the
sheet, which have been preferentially etched during the final
stages of polishing.

The filled sheet welds examined in this way showed good
homogeneity across the weld zone except at the root, see fig. 73.
There was no evidence of an HAZ.

The hot tool welded specimens viewed at an oblique angle
gave little indication as to the position of the weld
boundary. Only when viewed head-on could the boundary be
seen and then only as a very thin dark line. There was in this case
evidence of an HAZ, see fig. 74.

During tensile testing of the welds, the silver streaks
were observed to form or grow in a jerky manner accompanied by
audible clicks. This growth usually occurred at loads
approximately 25% that of the failure load.

The results of the tensile tests are given in table 20.

4.4.2. <u>Commercial Welds</u>

As described in section 3.4.7. a wide range of weld config-
urations and conditions were used by the industrial welders.

In most respects the features seen in the interiors of the
industrial welds were little different from those observed in welds
prepared by the author. However, two differences were noted:

      1)   for all the Plastic Construction welds there
           had been no attempt to achieve weld root pen-
           etration, see fig. 75

2) the general number and size of internal
   flaws (silver streaks) were smaller than
   those seen in the author's welds, discounting
   the flaw at the root of the Plastic
   Construction welds.

The large flaws at the root of the Plastics Construction
welds were the result of a deliberate policy in which a large
flat is left at the root of the weld to allow easier alignment
of the parts during welding. The second point noted in the
industrial welds would appear to result from the greater skill
and experience of the industrial welders. However, the silver
streaks were, again, observed to form and grow during the
tensile testing of the welds.

The results of the tensile tests are given in table 20.

In almost all cases failure occurred with one crack growing
straight across the specimen. However, in three specimens, one
Plastics Construction and two BNFL, failure occurred with the
entire weld region being ejected, in one piece, from the
specimen, see fig. 76.

4.4.3.   Fracture Surface Studies

Light and scanning electron microscopy of the weld fracture
surfaces revealed the presence of regions within the weld zone
which acted as fracture initiation sites. These regions had
irregular but sharply defined boundaries, see fig.77, and
appeared to be related to the silver streaks seen in the interior
of welds prior to and during testing. The surfaces of these
regions had a characteristic smooth appearance which was
consistent with them being surfaces at which little or zero
fusion had occurred, see fig. 78.

A measurement of the size of the region at the fracture
initiation site, for selected welds, was made using a travelling
microscope. The surface of the region was assumed to be
horizontal for the purposes of this measurement although it
was most often ridge-like or at an angle to the horizontal, see

-102-

fig. 79. The average flaw size for each of the welds examined is given in table 21. In nearly 80% of the weld fractures examined, the initiation site appeared along either a rod/rod or rod/sheet boundary near or at the surface of the weld. In some cases, this proximity to the surface prevented the measurement of the size of the region, as it was impossible to distinguish where the region ended and the surface began.

Several features became apparent during this work:

1) fracture initiation did not always occur at the widest part of the region, see fig. 80.

2) examination of the fracture initiation sites revealed no slow fracture and little evidence of crazing, see fig. 77.

3) the fracture surfaces were typical of fast brittle fracture, see fig. 81.

4) the morphology of the fracture surface was related to the failure stress. For low failure stresses the fracture surface was planar and very smooth but as failure stress increased the degree of surface roughness also increased. At the high failure stresses the surfaces were extremely rough with extensive hackle and crack bifurcation, see fig. 82 and fig. 83.

5) once the crack propagated it moved perpendicular to the loading direction with no tendency to follow weld boundaries at which fusion had occurred, see fig. 84.

6) the fracture surfaces of welds in which the weld zone was completely separated from the two sheets were distinctive in that one surface was rough whilst the other was extremely smooth, see fig. 85 and fig. 86.

7) only rarely was the same flaw found to run through more than two adjacent test pieces of a weld.

4.4.4. Weld Rig

Although only a few trials were carried out using the rig it became obvious early on that it was very difficult to produce welds when all the parameters were held constant. The two

-103-

parameters which appeared to have the greatest influence on welding were the welding speed and the pressure being applied to the rod. In other welding rigs the welding speed is usually left as a free variable as the rig is effectively moved along by the weld rod being pushed into the groove. With the welding speed held constant, the base of the weld rod was found to gradually move out of the heated gas jet, if the bow wave was being maintained. It seemed that the speed of welding needed constant re-adjustment to maintain proper welding conditions and as this was impractical the work on the rig was stopped.

4.5. Fracture Mechanics

As described in the previous section flaws or notches within the weld zone appeared to be an important feature of the failure of welds. The effects of such flaws on weld strength can be estimated through the theories of fracture mechanics. In the case of hot gas welded UPVC the fact that failure occurs at stresses typically less than half the unwelded sheet yield stress and the fact that the load-extension curves are generally linear up to failure allows the methods of linear elastic fracture mechanics to be used.

In the first part of this programme the notch sensitivity of unwelded UPVC was studied both for filled and unfilled UPVC. The second part examined how the welding process had affected the notch sensitivity of the UPVC, whilst the third part was an examination of how the fracture surfaces differed between unwelded and welded specimens.

4.5.1. Unwelded Sheet Fracture Mechanics

It was originally expected that both the initiation and the propagation values of the stress intensity factor, K, and the strain energy release rate, G, could be determined. In the case of most polymers it is possible to observe first slow stable crack growth, from which propagation values are determined, followed by fast unstable crack growth, from which initiation values are determined (see section 2.5). However, in this work

using UPVC, it was impossible to achieve reproducible slow stable crack growth and the work concentrated on determining the initiation values for K and G.

The initial approach was that of determining G using crack line loaded tapered double cantilever beams. When this type of test has been used with other polymers it has been possible to get considerable data from each specimen. However, with clear UPVC, as slow crack growth occurred only rarely and as the cracks tended to jump over 100mm at each propagation, only two or three results were generated from each specimen. Of these only one result could be obtained using the simplified experimental procedure permitted by the use of this type of test. The compliance calibration curves for the two main TDCB designs used are shown in fig. 87 and fig. 88. Through these it was possible to get results from the data for crack propagations outside the region over which the specimen compliance changes linearly with crack length. All the results were calculated using the dC/da factor appropriate to the particular crack length at which the crack propagated, instead of using the approximation of constant dC/da and (11)

$$G_{IC} = \frac{P_f^2}{2b_c} \quad x \quad \frac{dC}{da}$$

where b_c is the nett section thickness of the specimen in the plane of the groove. The results of the G_{IC} analysis are given in table. 22.

Designs of TDCB other than the two standard designs were only tried to examine if more slow crack growth or an increased number of crack propagations were possible. Within the TDCB programme no particular design was found to give rise to either of these conditions. For all the designs used slow crack growth was only observed for one or two specimens out of each set of ten specimens tested. It did appear that if a crosshead rate of 10mm/min was used, then slow crack growth was more probable but the evidence was inconclusive. For the majority of

this programme it was assumed that slow crack growth was more probable the slower the crosshead rate used, as is the case for PMMA [131]. However, it would seem that in this respect UPVC is more like epoxy resin and requires higher crosshead rates to produce slow crack growth.

The use of reverse-end loaded TDCBs as suggested by Mai et al [124] to achieve more controlled crack growth was tried. The initial crack propagated to within a 30mm of the end of the specimen and did not appear to offer any advantages over the standard TDCB work.

The data from the TDCB programme was also treated using a similar analysis to that used for the DCB programme to derive K_{IC} through (9)

$$K_{IC} = \sigma_f Y \sqrt{a} \ .$$

with the calibration factor, Y, being derived from beam theory. The actual equation used was

$$K_{IC} = P_f \ Y/ \ (b \ b_c)^{\frac{1}{2}}$$

$$-(23)$$

where P_f is the load at failure and b is the sheet thickness. The calibration factor was calculated from

$$Y = (12a^2/H^3 + 4/H)^{\frac{1}{2}}$$

$$-(24)$$

where a is the crack length and H is the height of one of the tapered arms at that crack length [131]. The results are given in table 22, fewer results are given than for the G_{IC} analysis as the above equations were assumed to be only valid for crack propagations in the range.

$$2H < a < W-H$$

$$-(25)$$

where W is the length of the specimen.[131]. A similar analysis

based on boundary collocation methods [119] was also used and was found to give results typically 5 - 10% higher than above.

The DCB programme was only used to generate K_{IC} results as no compliance calibration curves were prepared. The data was analysed using (23) but with Y given by

$$Y = (2.38 + 3.46 \ a/H) \ /H^{\frac{1}{2}}$$

-(26)

this factor being derived from boundary collocation methods [118]. The results are given in table 22, again the boundary condition (25) applies. Using the DCB specimens slow fracture was observed in eight tests out of the seventeen carried out. No analysis was attempted on the slow fracture as it was only observed late in the programme and after it was realised that slow fracture was not observed in welded specimens. However, some points were noted:

1) crack speeds were typically 80mm/min

2) crack lengths were unpredictable, varying between 50 - 200mm

3) all slow fractures terminated in arm break-off.

The DT data were analysed using (23) with Y given by

$$Y = 1 \ (3 \ (1 + \nu) \ / \ (b^2 \ W) \ )^{\frac{1}{2}}$$

-(27)

Where 1 is the moment arm of the applied load and W is the width of the specimen [120,132], see fig. 17. The results are given in table 22. Each DT specimen gave two results, with the crack first propagating 90 - 120mm and then completely severing the specimen. There was no evidence of slow fracture for any of the specimens. The cracks had the distinctive shape normal for this method and all crack lengths were measured along the bottom surface of the specimen.

Throughout the cantilever beam test programme there was
no evidence of plane stress effects, nor that changes in the
notching procedure significantly affected the results.

To supplement the cantilever beam programme an SEN programme
was initiated, this having the advantage of more closely
simulating the tensile test on welds. Results from this
programme were analysed using (9) with Y given by

$$Y = 1.99 - 0.41d + 18.7d^2 - 38.48d^3 + 53.85d^4$$

$$-(28)$$

where d equals a/W and W is the specimen width [114] see fig. 15.
To actually determine K_{IC} the data was plotted as failure stress,
σ_f, against the reciprocal corrected crack length $(Y \sqrt{a})^{-1}$,
and the best straight line fit determined using standard
least squares analysis, see fig. 89 for the graph of clear
UPVC SEN data and fig. 90 for the graph for filled UPVC
SEN data. Two straight line fits were used:

$$y = Ax + B$$

$$-(29)$$

and

$$y = Ax$$

$$-(30)$$

with y equal to the failure stress and x equal to the recriprocal
corrected crack length. The constant A is then equal to K_{IC}
and the constant B the intercept of the stress axis. The
second equation (30) is the solution to (9), but the first
equation (29) allows an extra degree of freedom in the analysis.
The first equation was preferred since for most of the SEN tests
the boundary conditions (10)

$$a, W, t > 2.5 \ (K_{IC} / \sigma y)^2$$

could not be met and the analysis based on (29) would allow for
this better than (30). The results, for both analyses, of the

SEN tests for clear UPVC for specimens with W = 15mm and
W = 9.5mm and for the filled UPVC with W = 6mm are given
in table 22.

In the case of clear UPVC SENs, the requirements for valid
plane strain fracture toughness testing appear to have been
met. Fracture stresses were typically less than half the
sheet yield stress; the load-extension curve showed little
sign of non-linearity and the fracture surfaces showed only
cleavage fracture markings. In general there was no
evidence to suggest that any of the test geometries used have,
in fact, infringed (10).

However, the filled UPVC SENs clearly infringed the
requirements for plane strain fracture toughness testing.
For all the geometries used in which the crack grew along
the thickness of the sheet, failure occurred by through-section
yielding with gross stress whitening. Only in the case where
cracks grew into the thickness of the sheet did brittle
fracture occur. In this case fracture stresses were usually
over 90% of the sheet yield stress; the load-extension curve
showed gross non-linearity and stress whitening could be seen
on the fracture surface about the fracture initiation site.

4.5.2. Weld Fracture Mechanics

The main feature of the welded TDCB test programme was the
lack of results. Of the twenty-nine specimens prepared and
tested, eighteen failed by arm break-off, three failed with the
crack moving out of the weld zone and three failed with the
first propagation completely severing the specimen. Further,
the only specimens to show more than one useful crack propagation
were those to which side-plates had been bonded, see table 12.
The only compliance calibration curve prepared for the welded
TDCBs was for the design incorporating 3mm thick clear UPVC
side plates. see fig. 91. Only one specimen of this design

was tested and this only gave one result, see table 22.

When the calibration curves for the 10mm thick clear UPVC, fig. 88, and the welded TDCB with 3mm thick clear UPVC side plates, fig. 91, are compared it seems that over the linear range, i.e. for crack lengths 70 - 150mm, the ratios of dC/da are inversely related to the effective beam thickness. This implies that any effects due to welding are constrained to a very small volume about the weld zone. This might. permit the calibration curve for unwelded specimens to be used for welded specimens of the same design if results could be obtained from the welded specimens.

Although the use of side plates bonded to welded TDCB specimens gave more control of the crack growth, difficulties and the time involved in specimen preparation lead to the curtailment of this work.

The DCB method generated more results in that only four of the eight specimens tested failed to produce a result. However, the four specimens which gave results only gave one result per specimen. These results were analysed using the boundary collocation method via (23) and (26) and the result is given in table 22. This result is the average of the results obtained from three DCBs welded with one weld pass in each groove and from one DCB welded with three passes of rod in each groove. However, the value of these results is undermined in that the load measurement, at the significant crack propagation, was made from charts for which the full scale deflection was that necessary to measure the initial crack failure load, which was typically ten times greater than the relevant crack failure load.

The DT method was only applied to two welded specimens but generated seven results, see table 22. Again two weld types were used but the results were averaged.

Two features were noted concerning the weld fracture
mechanics work:

1) there was no evidence of slow crack growth

2) the arms separated either by arm break-off or
   the severance of a specimen were so distorted
   after fracture they could not be fully mated
   together. This distortion was in the form of
   a bowing in the plane of the arms which caused
   a gap at the centre of the specimen, see fig. 92.

The first feature lead to the fracture mechanics work for
both unwelded and welded specimens concentrating solely on
fracture initiation values of G and K. The second feature would
seem to indicate the presence of residual stresses within the
weld and might form the basis of a future study of hot gas
welding.

4.5.3.   Fracture Surface Studies

The fracture surfaces of the TDCB and DCB specimens showed
the usual features associated with brittle fracture, that is
mirror, haze and hackle zones. However, because of the constraints
of these tests, in that the crack comes to a halt subsequent
to the hackle zone, the remaining fracture surface up to the
next crack arrest had a mirror-like surface. Typically the
initial fracture surface features appeared over the first 5 - 10mm
of crack growth with the following 100 - 200mm showing just the
mirror features.

A microscopical examination of this mirror-like surface
revealed that it was covered with fine striations. These were
typical of the striations previously discussed, see section 2.4.2.
They had a leading edge followed by what appeared to be craze
material which gradually faded into a featureless band prior to
the start of the next striation, see fig. 93. These striations
were typically 10 - 12μm wide and were extremely regular and
parallel down the length of the specimen. A detailed examination
of two TDCBs suggested that this spacing was constant and

independent of crack length. Occasionally two sets of bands
were observed across the crack front. They did not intersect
or overlap as did the Wallner lines seen in the haze and hackle
zones, but rather they gradually merged into one single set
of striations. It is thought these striations are intimately
associated with the crack front and that two or more sets
are created when different parts of the crack front are
moving at different speeds. The sets merge as the crack front
comes to equilibrium. Two further features of these striations
are that they do not appear to be affected by crack velocity
as they appeared within the hackle and haze zone, and they are
not dependent on specimen size or design as they appear on
the SEN fracture surfaces and could be seen on the fracture
surfaces of scrap UPVC which had been randomly fractured.

Although these striations have been previously reported
they have not been seen on such a large scale. As the reason
for their existence has not yet been ascertained, these
cantilever beam methods might be a useful way of generating
them for a more detailed study.

The fracture surfaces of specimens which had regions of
slow crack growth were also examined. Despite examination at
up to x 800 magnification these slow crack growth surfaces
appeared devoid of any significant regular features.

The DT specimens' fracture surfaces also showed characteristic
brittle fracture features, though modified by the crack geometry,
see fig. 94. Again, after the usual sequence of mirror-haze-
hackle zones there was a further haze and mirror zone. The
mirror zone was covered with the fine striations but the
larger number of minor crack arrest bands prevented such large
areas of uninterrupted striations being seen.

The clear UPVC SENs showed brittle fracture markings,
although this time they were characteristic of complete
catastrophic failure. Following the mirror and haze zones, the

hackle region was usually extremely rough and showed no
signs of abating before the crack severed the sample. The
degree of roughness was generally related to the failure
stress in that higher failure stresses gave rougher surfaces.

The filled UPVC SENs showed both types of failure behaviour,
yielding and brittle fracture. Brittle fracture was only
observed when the crack grew through the thickness of the sheet.
These brittle fracture surfaces showed, in general, 1 - 2mm of
stress whitening about the fracture initiation site before
showing the cleavage markings of fast fracture, see fig. 95.
As such these surfaces only showed coarse fracture markings
presumably because of the presence of the filler. The necking
rupture surfaces (yielding failure) showed the usual features
of gross stress whitening, reduction of specimen cross-section
and occasional advance fractures.

The major feature of the failure of welded TDCBs and DCBs
was the large number of specimens in which the crack grew
through the unwelded sheet rather than through the weld zone.
Where the crack did grow along the weld and through the weld rod
fracture surface markings were very similar to those seen
for unwelded specimens. However, one difference was the
increased amount of haze observed between the hackle and the
subsequent mirror zone. This would suggest that fracture speeds
are somewhat higher than in unwelded specimens. This might
explain the high levels of arm break-off since high crack
velocities encourage crack bifurcation [151] and explain also
why cracks tended to completely sever the specimen from the
first crack propagation.

4.6. Pre-Weld Treatments and Changes to the Weld Rod Composition

As already briefly discussed in section 3.6., and further
discussed in section 5.2., the previous work lead to the
conclusion that the major cause of the poor weld strength in
hot gas welded clear UPVC sheet was the presence of flaws or
cracks within the weld. On this basis, two approaches were

adopted to improve the weld strength:

1) to reduce the size and number of these flaws.
2) to reduce the notch sensitivity of the materials used.

The flaws were assumed to arise either from some incompatibility between the sheet and rod or from the contamination of the surface of the materials, probably by additives in the materials, which created a physical barrier to welding. As a result of the materials characterisation programme the major difference between the sheet and rod, except for additive content, appeared to be in the degree of orientation left in by processing. To reduce the difference, weld rod was annealed prior to welding, to thermally relax the excess orientation. To reduce any contamination of the weld surfaces, two methods were explored:

1) solvent cleaning of the weld surfaces just prior to welding
2) the removal or replacement of various lubricant additives in the rod composition.

As such, the second method overlapped with the approach of reducing the notch sensitivity of the materials in that again the rod composition was altered but this time by adding an impact modifier at various loadings.

Pre-weld treatments therefore cover the annealing of weld rod and the solvent cleaning of the rod. Changes to the rod composition includes both the changes to the lubricant package and the addition of an impact modifier.

4.6.1. Pre-Weld Treatments

The tensile test results for the welds which had undergone the various pre-weld treatments are given in table 23.

The annealed rod was observed to be particularly susceptible

-114-

to degradation during welding and this caused a significant quantity of degraded material to be left within the weld zone. However, no systematic fault was noted in the fractured specimens which suggests that the low weld strengths are a feature of welds prepared with annealed rod.

The weld prepared with a methanol wash treatment was not noticeably different during welding or in testing. The poor failure stress, has been mainly caused by two low results, less than 12MPa, which result from a systematic fault across two test pieces. If these results are excluded, the average weld strength improves to 17.6 ± 2.2 MPa.

As was the case with annealing the weld rod, the trichloro-ethylene wash treatment lead to excessive degradation of the weld rod, particularly in rod which was being heated by a second pass of rod. However, the main cause of failure was the presence of a systematic flaw between one of the outer rods and the sheet material. This makes the interpretation of this result difficult, as the poor weld strength may result from poor welding technique.

4.6.2.   Changes   to the Weld Rod Composition   .

During the granulation stage, formulations 8 - 12, see table 13, all exhibited marked toughness in that the hides were extremely difficult to break up for granulation. All the hides of these formulations were prone to yielding with gross stress whitening. The hides of the remaining formulations all failed in a brittle manner.

There appeared to be no major differences between the formulations in their extrusion behaviour or their susceptibility to degrade during extrusion. Randomly selected rods showed less than 1% shrinkage when subjected to an annealing treatment of $170^{\circ}C$ for 10 minutes. When this is compared to commercially available rod, which showed typically 10%

shrinkage when subjected to the same treatment, it indicates that the new formulation rods contain much less frozen-in orientation than the standard rods.

The examination of the interiors of the welds, prepared with the new rod materials, was hindered by the fact the rods of some of the compositions were opaque or only translucent. This problem particularly affected those rods containing either MBS or ESBO. However, those features seen in the interiors were typical of those seen in the standard welds.

The results of the tensile tests are given in table 13.

The average flaw sizes, as measured on the fracture surfaces, are given in table 13. A flaw size could not be determined for all the welds since some flaws occurred at the surface of the weld, which made determining the flaw boundaries difficult. In the case of those welds prepared with rod containing MBS, the fracture surfaces were extremely rough and difficult to interpret. Almost all these welds failed from internal flaws but it was impossible to determine, with any degree of accuracy, the flaw boundary which bordered against the weld rod. Stress whitening about the fracture initiation site was common, see fig. 96. For those welds prepared with rod not containing MBS fracture usually occurred at or near to the weld surface.

One interesting feature of the fracture behaviour of these welds was that in two specimens the weld zone was completely ejected. In one case the weld zone was ejected from a specimen, prepared with rod formulation 9, which failed at 30.5MPa, whilst in the second it was ejected from a specimen, prepared with formulation 6, which failed at only 19.7MPa. Previously it had been thought that the ejection of a weld zone was associated with high failure stresses but the above indicates otherwise. The fracture surfaces, characteristic of these types of fracture, see section 4.4.3., were observed for both the specimens.

5. <u>Discussion</u>

This chapter is divided into three sections: standard welds, fracture mechanics and modified weld procedure and rod composition. This follows the basic diagrammatic layout of fig. 32, with the materials characterisation programme being treated as support work rather than a main section in its own right. Thus, the discussion follows the progress and reasoning behind each stage of the work,will describe the conclusions drawn at each stage and show how the sections are linked together.

5.1. <u>Standard Welds</u>

The tensile test results for the standard hot gas welds produced by the author and by industry confirm that low weld efficiencies are a feature of hot gas welds made with clear UPVC. Hot gas welds produced with filled UPVC have weld efficiencies typical of those quoted in the literature. This fact and the fact that the amount of clear UPVC hot gas welded by industry is relatively small suggests that the literature values are only applicable to welds produced with filled UPVC.

Filled UPVC hot gas weld efficiencies can be over 100% greater than those for clear UPVC welds. However, this difference is reduced when weld strengths are compared as the efficiency is defined as the weld strength divided by the sheet yield stress. In the case of filled UPVC the sheet yield stress is 20% lower than that of the clear UPVC and this alone means that even if the weld strengths were equal, clear UPVC would have a poorer weld efficiency. It is therefore felt that weld strength is a more meaningful parameter for comparison than efficiency.

Throughout the remainder of this section where a weld number is given,this number identifies a weld whose tensile test results are given in table 20 under that number.

The definition of weld strength, is that of the load
at failure divided by the specimen cross-section area,
measured away from the weld. This is a useful design
parameter, as far as the load bearing capacity of the weld
is concerned, but does not provide a true insight into the
strength of the fusion bond. The definition ignores the
fact that different weld configurations can have different
load bearing capacities but may have similar weld bond
strengths. This is demonstrated when the weld strengths of
weld no.7 and no.8 are compared. Weld no.7 was completed
with three passes of rod in each groove and had an average
weld strength of 18.5MPa. Weld no.8 was completed with six
passes of rod in each groove and had an average weld strength
of 22.4MPa. Although both welds were prepared using identical
materials and techniques, by increasing the number of rods
used, and hence the degree of overfill, an increase in weld
strength of 20% is achieved. Therefore, caution is required
when comparing welds of different configurations, in terms
of weld strength alone.

In general the author's welds have lower weld strengths
when compared with those produced by industrial welders
and this is explained in two ways. In the first instance,
as just described, differences in weld configuration can lead
to differences in weld strength. All the welds produced by
industrial welders had a considerable amount of overfill, when
compared with those of the author. They normally used more
than twice the number of rods used by the author to complete
their welds when using circular rod, and when using triangular
rod, which has a larger cross-section, used at least the same
number and often more, see fig. 42. Weld no.8, produced by
the author, with six passes of rod in each groove, more closely
matches the degree of overfill used by the industrial welders
and the weld strength obtained is within the range observed
for the industrial welds. However, a second cause is undoubt-
edly the author's inexperience when compared with industrial
welders. This is reflected in the size and number of faults
within the weld zone. Qualitative evidence of this was seen
when weld interiors were examined prior to and during testing.

More quantitative evidence is seen in data for the average
size of the fracture initiation sites, for various welds,
given in table 21. An approximate relationship between
average flaw size and average weld strength can be seen in
that as the flaw size decreases the weld strength increases.
The author's welds are found to contain, generally, large flaws
and these result from the lack of experience in welding.

Of the industrial welds tested, those produced by the
Plastics Construction welder seem to have the higher weld
strengths and smaller flaw sizes. One major difference in the
way these welds were produced was that the speed welding
technique was used instead of the hand welding method. In
the past speed welding has been associated with faster welding
but poorer weld strengths. The Plastics Construction welds
indicate that not only can speed welding reduce weld times
but in skilled hands can also increase the weld strengths.
Three speed welds were prepared by the author, weld numbers
3, 4 and 5. Two were produced using the clear rod but were
welded using different speeds and one was produced using the
I.C.I. rod using a slow weld speed. As can be seen, weld no.3
and no.5, both carried out using a low speed, are clearly
stronger than weld no.8 which was only hand welded, and are
comparable to the Plastics Construction welds. Weld no.4
was welded at a faster rate and the decreased weld strength
indicates how sensitive weld strength is to weld speed.

It should be noted that weld numbers 15, 16, 17 and 24 show
that high weld strengths may be achieved using the hand welding
technique but it is felt that the speed welding method, when
used with care, may permit these levels of strengths to be
achieved by the less skilled welder. This is thought to be due
to the way in which speed welding reduces the control required
by the welder on certain weld variables. For example, the
distance of the torch from the weld zone is controlled by the
use of the speed welding nozzle, which also serves to give better
control of the pressure applied to the rod.

One interesting feature of the welds prepared by the author is the difference in the average weld strength for welds prepared using clear rod, no.7, and the I.C.I. rod, no.9. The clear rod weld has an average strength of 18.5MPa whilst the I.C.I. rod weld had an average strength of 24.2MPa. The scatter in the results means there is some overlap, but the difference would appear to be significant. There would seem to be three possible explanations:

1) there are major differences between the rods due either to composition or processing

2) the weld technique was modified to allow for the curved nature of the I.C.I. rod

3) the author's general technique significantly improved for the time when the I.C.I rod weld was being prepared.

The third explanation is discounted on the basis that weld no.9 was prepared after weld no.6 and before weld no.8 and therefore one would, reasonably, expect any improvement in general technique to be reflected in weld no.8. The first explanation may account for part of the difference since the welds produced by the Plastics Construction welder show a similar though smaller difference. However, the second explanation appears to be the more relevant, as the curved nature of the I.C.I. rod would prevent excess pressure being applied to the rod. An excess pressure might be used to obtain the bow wave condition when the weld thermal conditions are incorrectly adjusted. This would explain the reduced difference between the welds produced by the Plastics Construction welder since he used the speed welding technique which would suppress this factor.

When looking at how the differences in rod composition might affect weld strengths it is interesting to observe that the Leister produced weld, no.25, was prepared using a filled weld rod. As the mechanical properties of filled UPVC are significantly different to that of clear UPVC, a marked change in the weld strength might have been expected. The average weld strength, however, is typical of the values obtained with the standard clear materials.

The use of only five tensile test pieces being taken
from a weld for testing was adopted so that sufficient welded
material would be left to carry out the double torsion
fracture mechanics test on the weld. Both BS 4994 [166] and
ASTM D1789 [167] recommend the use of three test pieces but
it was decided that, since the hot gas weld strengths showed
a considerable degree of scatter, more pieces were required.
A comparison of the results for weld no.6 and no.8 show that
using five test pieces gives a reasonable measure of the weld
strength. In some cases, where more scatter was observed
or further results were felt necessary, the number of tests
were increased.

The weld efficiency of 95% obtained for hot tool welded
clear UPVC, weld no.10, is a value typically quoted for
UPVC [1]. The fact that such a high efficiency may be
obtained suggests that when a good thermal bond is achieved
the bond strength is comparable to that of the sheet.

One reason for such a high efficiency may be that only
identical materials are being joined without the introduction
of an intermediate rod material. This would imply that the
rod/sheet bond is much weaker than the sheet/sheet bond or that
some incompatibility between the sheet and rod prevents a
uniform bond forming.

A second reason may be that the hot tool welding process
is a much more controlled one than the hot gas welding process.
During hot tool welding, a uniform thermal cycle is applied
over the weld faces and a constant pressure is applied across
the weld interface. During hot gas welding the welder continually
adjusts the thermal energy supplied to the weld zone and the
pressure applied to the rod to achieve the optimum bow wave
condition. Distractions and tiredness can lead to the welder
varying these parameters thereby causing variations in the
uniformity of the weld process. At points in the weld where
this occurs a poor bond, or no bond at all, may result.

Observations of the fracture surface of hot gas welds indicate that normally the rod/sheet bond has a strength comparable to that of the sheet. If this bond was significantly weaker than the sheet then the crack would tend to move along this interface, as it would be the path of least resistance to crack growth. However, the crack once started moves perpendicularly to the applied force and not along any of the weld boundaries. The fracture surfaces do show that the fracture initiation sites are areas at which either very poor bonding or no bonding has occurred between either rod/sheet, rod/rod, or even sheet/sheet. The fact that little or no bonding has occurred is indicated by either the presence of pre-weld machining marks on the sheet or by the shiny undistorted surfaces of the rod.

Three further observations, which support the suggestion that it is not some basic weakness in the rod/sheet bond which leads to low weld strengths, are:

1) some weld pieces had weld efficiencies as high as 70%

2) the internal flaws commonly seen in the hot gas weld test pieces were not seen in the hot tool test pieces

3) the large standard deviation in the results for the hot gas welds is not consistent with a uniform weakness being a cause of low efficiencies.

The following observations were made during the above work:

1) using clear sheet and standard weld rod, average hot gas weld efficiencies were not greater than 51%

2) using filled sheet and rod, average hot gas weld efficiencies of 85% may readily be achieved

3) hot tool welded clear sheet may be welded with average efficiencies of 94%

4) the internal flaws seen in hot gas welds

in clear materials are not present in
hot tool welded clear sheet. Also, in
general, they have a random distribution

5) these internal flaws form and grow during
tensile testing and have the characteristics
of sharp cracks

6) fracture initiation occurs at sites where
little or no fusion has occurred across the
rod/rod, sheet/rod or sheet/sheet interfaces
in both clear and filled hot gas welds.

7) the fracture initiation sites and the
internal flaws observed in clear welds
are of a comparable size and geometry

8) that speed welding may improve weld
efficiencies by increasing the uniformity
of the hot gas welding process.

It was therefore concluded that the hot gas welded clear
materials failed from areas of poor fusion which arise during
welding. Where fusion occurred, the bond across the various
interfaces could have a strength of nearly 95% that of the
sheet. These areas of poor fusion were an inherent feature of
hot gas welds occurring in both clear and filled UPVC welds.
The clear sheet, however, was much more sensitive to the
presence of these flaws than was the filled sheet.

5.2. Fracture Mechanics

As described, weld fractures appear to be initiated at
the boundaries of areas of poor or zero fusion across the
weld interfaces. The unfused region may be treated as a
crack and its effect on weld strength analysed using linear
elastic fracture mechanics (LEFM).

Using a number of methods both K_{IC} and G_{IC} were determined
for the 10mm clear sheet and for welded clear 10mm sheet.
Only K_{IC} was determined for the 6mm clear and filled sheet.
Despite using several test geometries and test rates no test
conditions were found which would give reproducible slow

-123-

stable fracture. The analysis therefore concentrated on the crack initiation values of K and G.

The values of these parameters for the clear sheet, as shown in table 22, are in agreement with values reported by Mills and Walker [94] and Cornes and Howard [93]. The higher values reported by other workers are thought to be the result of either using specimen geometries and sizes which infringe the plane strain boundary conditions [114] or of using poor notching techniques. The higher scatter in the results, i.e. 15% compared to 10% reported by Mills and Walker [94], may be explained by variations in testing temperature as the test laboratory was not temperature controlled. Mills and Walker [94] suggested that slow fracture was impossible with clear UPVC but slow fracture was observed in twenty-one tests, however, this behaviour was extremely erratic.

The DCB, TDCB and DT methods gave K_{IC} results for the 10mm clear sheet in good agreement. However, using the standard equations, the SEN method gave results nearly 20% higher. If the SEN data was analysed using the least squares fit for a straight line of equation (29)

$$y = Ax + B$$

where $y = \sigma_f$, $A \equiv K_{IC}$, $x = {}^1/ (Y \sqrt{a})$ and $B \equiv \sigma_o$ the intercept of the line with the stress axis, the K_{IC} obtained was a much better fit with the results from the other methods, see table 22. The reason for this might be that the reduced specimen sizes used for the SEN method infringed the plane strain boundary conditions. However, the similarity between the results for 10mm and 6mm clear sheet would suggest otherwise and the reason may lie in the notch geometry.

From section 2.5.1, K_{IC} and G_{IC} are related through (7)

$$K_{IC}^2 = G_{IC} E /(1 - \nu^2)$$

If the experimentally determined values of G_{IC} and E are inserted into the equation and a Poisson's ratio of 0.4 assumed [189] then a value of $K_{IC} = 2.87$ MPam$^{\frac{1}{2}}$ is obtained. The value taken for the tensile modulus , 3.6GPa,is that appropriate for strains less than 0.4%. However, in the SEN tests failure strains were typically 1.5% at which level the tensile modulus has decreased to approximately 2.2GPa. When this value is used, a value of $K_{IC} = 2.3$MPam$^{\frac{1}{2}}$ is obtained, in much better agreement with the experimentally determined value of K_{IC}.

The filled sheet was only tested using the SEN method and two features were noted:

1) when the crack moved perpendicular to the thickness failure only occurred by ductile tearing

2) when the crack moved parallel to the thickness of the sheet brittle fracture occurred but the fracture surface showed evidence of a large plastic zone with stress whitening and failure occurred at loads just lower than those expected for yield.

It was therefore concluded that plane stress effects were much more significant in the failure of notched filled materials, causing in most cases through-thickness or nett-section yielding. These effects were so important that even when brittle failure occurred the failure stress was insensitive to notch size. Therefore, the basic requirements for LEFM analysis were not met and no analysis was possible.

This therefore supports the conclusion drawn from work on standard welds, that the clear UPVC sheet is an extremely notch sensitive material, when compared to the filled UPVC sheet, and that this, combined with the existence of flaws

left in the weld region, by the nature of the weld process, leads to the low weld strengths seen in hot gas welded clear UPVC sheet.

A simplistic analysis, based on the assumption that these flaws act as surface notches, may be carried out using flaw sizes and weld strengths typical of both clear and filled UPVC welds. In over 80% of all welds tested failure was initiated from flaws at or very near to one surface. Assuming a flaw size of 1mm and a failure stress of 22MPa, values typical of welds produced by the author, the value of K_{IC} for welded sheet is calculated to be $1.5\mathrm{MPam}^{\frac{1}{2}}$, using the standard SEN equations. The same analysis using the average flaw sizes and average weld strengths observed for each of the industrial welds gives a value $K_{IC} = 1.4 \overset{+}{-} 0.2\mathrm{MPam}^{\frac{1}{2}}$. In the case of the filled UPVC a flaw size of 0.75mm and a weld strength of 42MPa may be used which gives $K_{IC} = 2.5\mathrm{MPam}^{\frac{1}{2}}$, but since the requirements of LEFM are not met for this material the result is not very meaningful.

Although the above SEN analysis is crude, variations in shape, size, position, and tip radius of the unfused regions, combined with the irregular weld cross-section and the thermal history of the weld material, make a more refined analysis impractical. However, some justification for the use of the SEN analysis may be seen if the results for weld no.11 are examined. This was the only standard weld to fail predominantly from the weld root. If a centre notch model is used [114] then, using the measured flaw sizes and weld strengths, a value of $K_{IC} = 1.4 \overset{+}{-} 0.2\mathrm{MPam}^{\frac{1}{2}}$ is obtained. Both these analyses support the conclusion that poor weld strengths are due to the presence of unfused regions, but also imply that embrittlement of the UPVC has taken place during welding.

One particular result of LEFM is that a flaw well within a sample has to be nearly twice the size of one at the surface to cause the same reduction in failure stress. Therefore,

even if one assumes the flaws within the welds are the same
size as those at the surface, the removal of the surface
flaw should lead to a significant improvement in the failure
stress. Two welds, no.16 and no.19 (see table 20) were
prepared with the weld surface dressed, either by filing
or by grinding, until there was no sign of the original
weld surface remaining. Weld no.16 test pieces were in
fact taken from weld no.15, this weld already having been
shown to have a high failure strength, whilst weld no.19
was prepared in an identical manner to weld no.18. Both
welds were prepared by experienced industrial welders. As
can be seen from the results the apparent removal of surface
flaws did not lead to any major improvement in weld strength.
An examination of the fracture surfaces revealed that
weld no.16 had failed from surface flaws and weld no.19
had failed from both surface flaws and internal flaws. The
internal flaws in weld no.19 were usually associated with
the weld root which, following normal Plastics Construction
practice, was typically 1.7mm deep. However, two of the
test pieces, from weld no.19, had internal flaws approximately
0.3 - 0.5mm deep and these pieces had failure stresses over
40MPa. It seems, therefore, that the dressing of a weld
does not lead to improved weld strengths due to difficulties
in ensuring the complete removal of surface flaws.

Both the experimentally determined values of G_{IC} and
K_{IC} for clear welded UPVC support the above analyses and confirming
the increased notch sensitivity of the clear UPVC, see table 22.
Both G_{IC} and K_{IC} are found to drop to values between 60 - 70%
of those for unwelded material. The fact that both K_{IC} and
G_{IC} drop by similar amounts may be accounted for if one
assumes that the tensile modulus of the UPVC is also reduced by
the welding process.

Observations of the fracture surfaces of the filled hot
gas welds support the suggestion that the material is embrittled
during welding since there is no evidence of stress whitening

nor of a plastic zone in the region of the fracture initiation
sites.

Mills and Walker [94] examined the effects of different
thermal histories on K_{IC} for clear UPVC and found that
except for freshly quenched material, quenched from $90^{\circ}C$,
K_{IC} did not change. However, none of their thermal treatments
involved temperatures greater than $90^{\circ}C$. Certain processes
which are rate or temperature dependent may not show changes
over the time for which their samples were heat treated.
During the hot gas welding process, temperatures over $180^{\circ}C$
may be experienced by the materials. They then air cool,
but may experience a further heat treatment. At these
temperatures three effects may become pronounced:

1) densification of material and an increase
   in yield stress

2) degradation

3) the setting up of internal stresses due
   to thermally induced expansion and contraction.

Illers [74] has reported the occurrence of the first but
this was compared with quenched material. It is felt that,
except for a small increase in crystallinity, the heat treatment
is unlikely to result in significant increases in either
density or yield stress compared to that of the as-received
material.

Degradation leads to both chain scission and cross-linking
and both of these can cause embrittlement. However, the results
of the GPC analysis for heat treated and as-received sheet and
rod reveal no significant changes in the molecular weight
averages. The work of Vincent [44] indicates that a major
change in molecular weight is required to produce significant
changes in the mechanical properties of UPVC. Furthermore, a
general observation made [25, 29] is that degradation has to
proceed beyond the colour change stage before the mechanical
properties of UPVC are affected. Therefore, it would appear

that degradation although occurring during welding is not
the major cause of embrittlement.

Thermally induced internal stresses have been reported
in hot gas welded UPVC by Voigt [159]. They arise from the
expansion and contraction induced in the material as it is
heated and then cooled during welding. They may also arise
from the relaxation of the residual orientation of the weld
rod or the stretching of the weld rod resulting from a poor
welding technique. They may be demonstrated when clear
welds are examined between crossed polars. A complex pattern
of isochromatic fringes is observed, within and around the
weld zone, which is difficult to analyse due to the weak
photoelastic response of clear UPVC causing poor resolution,
see fig. 69. They are also demonstrated by the fact that
the severed arms of TDCB, DCB and DT specimens cannot be
mated together, see fig. 92. They are distorted in the plane
of the sheet and this distortion is typical of that seen in
samples containing residual stresses which have had layers
of material removed [190]. No analysis was attempted as it
was considered beyond the scope of this work.

However, assuming the degree of embrittlement is similar
in both clear and filled hot gas welds and in clear hot tool
welds, the overriding cause of low weld strengths is the
presence of unfused regions in a notch sensitive material.
This would suggest that two approaches may be made to improve
weld strengths:

1) reduction in the size and number of
   unfused regions

2) a reduction in the notch sensitivity
   of the materials in use.

5.3. Modified Welding Procedure and Changes to Weld Rod Composition

Before proceeding with an investigation into the ways to
reduce the number and size of the unfused regions within the

weld, it is first necessary to understand how they arise.
Four causes were proposed:

1) they are an inherent feature of the type of welding method

2) they are the result of poor welding technique

3) they are the result of a mismatch in the properties between the rod and sheet

4) they are the result of a physical barrier to fusion which is formed during the welding process.

In over 200 tensile tests of welds produced by eight different welders, using a range of rod profiles and materials and both welding methods only three weld pieces had weld strengths greater than 40MPa. This would indicate that there is, inherent in the welding process, a minimum level of size and number of unfused regions which will occur. This further suggests that it may be possible under the most closely controlled conditions to produce welds with this minimum level. However, it is felt that the welds produced contain the minimum level of unfused regions which it is practically possible to produce within industrially acceptable constraints.

As a result of the materials characterisation programme, the only significant mismatch in properties, between the rod and sheet, arises from the residual orientation in the rod caused by extrusion. The differences in properties might be expected to be reduced after the welding process has annealed the orientation out of the rod. This would only be the case if the rod is allowed to relax the orientation in an unconstrained fashion, but during welding the rod is prevented from a free relaxation by the fusion with the sheet and other rods. However, it is not the differences in mechanical properties which would cause the unfused region but the residual orientation itself. Therefore a weld was prepared using rods which had been given a heat treatment of 150°C for 10 minutes on a bed of glass microspheres to relax

the orientation. These rods showed a shrinkage of 12% in
their length. This weld, see table 23, weld no.1, had an
average weld strength of only 13.8MPa.

This result suggests that either the residual orientation
has a beneficial effect on weld strength or that the heat
treatment has lead to either an increase in notch sensitivity
or an increase in the number and size of the unfused regions.
It is difficult to see how,in the context of hot gas welds,
residual orientation could have a beneficial effect on weld
strengths and therefore more attention was directed to the
effects of the heat treatment. The means whereby the heat
treatment might lead to an increase in notch sensitivity have
already been considered when discussing the embrittlement of
hot gas welds. It is felt that the main effect of this
thermal treatment would be degradation and that this would
not, on its own, account for such a dramatic drop in the
weld strength. It would, therefore, appear that the thermal
treatment gives rise to an increase in the number and size
of unfused regions.

This then leaves only the fourth suggested cause of
unfused regions, that is, that some physical barrier to
fusion arises during the welding process. Examples of such
barriers which may arise when insufficient care is taken
during welding are layers of either grease, dirt or water
deposited on the to-be-welded surfaces which then prevent
good fusion.

On the basis of the assumption that the surfaces of the
weld materials and the weld gas were uncontaminated, and the
result for the weld strength of the weld made with heat treated
rod, it was decided that the most likely cause was the
thermally activated diffusion of an additive to the surface
of the materials.

If it is assumed, for such a process to occur, that the
additive would need to be incompatible with the polymer, the

first additive to be examined has to be the external lubricant.
Two investigations were made:

1) all the to-be-welded surfaces were wiped
   before and between welding with either
   trichloroethylene or methanol to remove
   any additives on the surfaces

2) in conjunction with I.C.I., the lubricant
   package of the rod was modified.

Trichloroethylene was chosen as one solvent as it is one of
the few solvents capable of dissolving Wax E, a Hoechst product,
[185] which was originally thought to be present in the rod.
Methanol was chosen in place of di-ethyl ether on the grounds
of availability and on the basis that it was a solvent
recommended for the Soxhlet extraction of additives from PVC [180].

The results of the weld strengths for welds produced using
the solvent wash procedures are given in table 23, weld no.2
and no.3. When the fracture surfaces of the methanol washed
weld were examined, two adjacent test pieces were found to
have a particularly bad flaw which appeared to have resulted
from poor weld technique. If these results are excluded from
the analysis, the average weld strength then improves to that
obtained for other welds produced by the author. Therefore,
a methanol wash appears to have little effect on weld strength.
The trichloroethylene washed weld fracture surfaces indicated
the presence of a systematic flaw throughout the test pieces.
This is probably the result of poor weld technique but in any
case the use of a trichloroethylene wash does not lead to an
improvement in weld strength. An observation, made at the
time of welding, was the increased tendency of the weld
surfaces to degrade, which indicated the removal of the
thermal stabiliser. However, the fact that unfused regions
occur in filled materials which use a non-liquid, non-organotin
stabiliser [66] would indicate that the stabiliser is not the
cause of a barrier to fusion.

The second investigation was combined with the work on

changing the notch sensitivity of the rod material used.
In conjunction with I.C.I., material was prepared with
modifications to the standard rod formulation and then ram
extruded into weld rods. The method of extrusion gave an
added advantage in that the rods were found to suffer little
thermally induced shrinkage. The formulations used and the
results for welds prepared with these materials are given
in table 13. Formulation 1 was the standard formulation
used as the reference, formulations 2 - 7 involved changes
to the lubricant system of the rod. Formulations 8 - 11
were designed to alter the notch sensitivity of the weld
rod via the addition of methyl methacrylate-butadiene-styrene
(MBS) terpolymer. Formulation 12 was an attempt to incorporate
both a change to the lubricant system and a reduction in
notch sensitivity to achieve the best possible weld strength.
In the remainder of this section any references to particular
weld numbers are based upon the weld and formulation number
in table 13.

In formulations 2 - 4, the levels of both internal and
external lubricants were step wise reduced to zero. The
results of the tensile tests indicate that by reducing the
external lubricant level to zero the average weld strength
goes up by over 30%. However the reduction of the internal
lubricant level to zero appears to have no significant effect
on weld strength. In formulation 5 the standard lubricants
were replaced with 3phr epoxidised soya bean oil (ESBO) since
it was considered impractical to manufacture weld rod,
without any lubricant, on a commercial scale. As can be
seen, the improved weld strength was retained. To examine
how ESBO affected the standard formulation, as it acts not
only as a lubricant but also as a plasticiser, ESBO was added
to it at both the 3phr and 10phr level, formulations 6 and 7
respectively. The weld strength results indicate that these
have slightly improved weld strengths but that they do not
have any major effect on weld strength. A feature of the
welds prepared with rod of formulations 2 - 6 was the very
high degree of scatter in the weld strengths.

-133-

The fracture surface examination revealed that for weld numbers 2 - 7 failure occurred from surface flaws. Although there were no systematic flaws, the majority of flaws were found in the boundary between one of the outer weld rods and the sheet material. In these cases, the crack moved into and through the sheet material rather than into the weld. It was not possible to correlate flaw size with failure stress. It is felt that this was partly due to the difficulties in obtaining an accurate measure of the size of flaws at the surface of the weld. Furthermore, a positive correlation would imply that the fracture toughness for the different welds was similar. The fact that the rods were prepared from material of different compositions and in a batch process would make this unlikely. However, if a SEN analysis is carried out for these welds using the flaw sizes and failure stresses as measured, then the values of K_{IC} calculated all fall within the range, of $1.4 \pm 0.2 MPa^{\frac{1}{2}}$, found for standard welds. The fact that the average flaw sizes for weld numbers 2 - 4 do not decrease as the lubricant level is decreased would suggest that the improvement in weld strengths is not due to a reduction in flaw size. But this cannot be stated conclusively as the measurement of the flaw size is relatively crude and does not take into account the shape of the flaw. Furthermore, the small sample size used only permits one to draw the more general conclusion that the removal of the standard external lubricant leads to improved weld strengths.

If one assumes that either through the use of solvent washes or through the changing of the lubricant system of the rod, welds were produced with the minimum practically obtainable flaw size then the observed flaws must be inherent to and be a result of the welding process. If this is the case, then, despite the fact that the average inherent flaw size may be reduced by improved welding technique, on the basis of the results of the work·on standard welds, the smallest average inherent flaw will still cause low weld strengths in clear hot gas welded UPVC.

Therefore, if there is an inherent flaw which cannot be reduced or removed, then the only way to obtain high weld strengths is to increase the toughness of the welded material. This was attempted by adding MBS to the standard rod formulation, see formulations 8 - 11.

As can be seen, the average weld strength increases up to 60% as the level of MBS is increased up to 10phr, but weld no.11, containing 15phr MBS, has a weld strength only 60% that of the standard. However, an examination of the fracture surfaces of weld no.11 showed large, approximately 4mm deep, internal flaws. These were associated with the poor bonding of the root weld rod in each groove. Therefore it is suggested that the low weld strength reflects a faulty welding technique rather than being a feature of the rod material.

A significant feature of the results for the welds toughened with 10 - 15phr MBS was the reduction in the standard deviations for the weld strengths. The exception to this was weld no.10 which was prepared with rod of the same formulation used for weld no.9 but was prepared with six passes of rod in each groove. The results for this weld are even more unusual in that the weld strength does not show the expected improvement, over that of weld no.9, considering the increased amount of overfill. The fracture surfaces also indicated that the fracture behaviour was not the same as for the other MBS toughened welds. The crack was observed to have generally moved into and through sheet material, having started from small flaws at the boundary between the outer layer of rods and the sheet material. Large sections of the weld zone were found to be ejected as major secondary fractures were common. It is felt that the above effects are not the cause of a faulty welding technique but rather reflect the different thermal histories involved. It has been reported the MBS modified UPVC loses its improved toughness when subjected to weathering [19] and one might assume that this loss is accelerated when modified UPVC is subjected to elevated

temperatures. The major difference between weld no.9 and
weld no.10 is the increased exposure to elevated temperatures
due to the extra passes of rod, suffered by weld no.10.

The main feature of the fracture surfaces of weld no.8
and weld no.9 was that fracture appeared to be initiated
within the weld, away from the surfaces, and to have
propagated through or around the weld rods. In both welds
fracture initiated from flaws associated with the weld root
and the poor bonding of the root weld rods. In weld no.9,
as for all welds prepared using rod containing 10phr or
more MBS, bands of stress-whitened material could be seen
at the points where the crack started into the weld rods.
Furthermore, for both weld no.8 and weld no.9, the fracture
surfaces showed that either the crack was prone to following
weld boundaries, i.e. the rod/rod or rod/sheet interfaces,
or the initial flaws were extremely large, of the order
2 - 4mm deep. It may be that the blunting of the edges of
initially small flaws prevents cracks growing into the
sheet material, which would result in a low stress fracture,
but forces them to grow along poorly bonded weld interfaces
until they are large enough to cause fracture through the
weld rods. However, interpretation of the fracture surfaces
was made difficult by the lack of detail shown on the
surfaces where the crack propagated through the weld rods.

It was therefore concluded that the addition of MBS to
the weld rod formulation has a beneficial effect on weld
strength in that it was both improved and more reproducible.
However, the addition of MBS does not lead to the same levels
of weld strengths as achieved for filled UPVC and it is
probably necessary to modify the sheet material before these
will be achieved.

Weld rod formulation 12 was an attempt to combine the
improvements obtained by the replacing of the standard
external lubricant with ESBO and the addition of MBS to the
standard rod formulation. But, by accident, the standard

lubricant was still added to the formulation. The average
weld strength obtained was over 20% lower than that for
weld no.9 but was still 30% higher than the standard. The
results for weld no.8, the standard plus 3 phr ESBO, indicated
that the addition of ESBO to the standard formulation had
no major effect on weld strength. Therefore, the poor weld
strength must result from the combination of MBS and ESBO.
The fracture surfaces revealed that all the fractures resulted
from the crack moving directly into the sheet and not through
the rod, normally from a small surface flaw. It is not
understood why this happens, nor why the combination of MBS
and ESBO should lead to it.

Two major points concerning the work on the modified
weld rod and welding procedure need to be emphasised:

1) the work was only an initial study and
the conclusions are based on the result
of only one weld per modification

2) all the welds were prepared by the author
and it may be that experienced welders
would obtain even better results for some
of the materials tested.

The first point means that only general conclusions may
be drawn from this work. Many more welds need to be prepared
for each modification to both reduce the effects of variations
in the welding technique and to allow a more detailed explanation
of how the modifications affect the weld strength. The second
point affects the conclusion that the inherent flaws present
in hot gas welded clear UPVC limit the practically achievable
weld strength to a value of the order, only 30MPa. It is
probable that a more skillful welding technique would leave
smaller inherent flaws and this might lead to higher weld
strengths. Therefore, in any future study, welds should be
prepared by a number of skilled welders, to ensure that both
the optimum result and a typical range of results are obtained.

However, after taking these points into consideration, it
is felt that the results do justify the conclusions that

a general solvent wash does not lead to improved weld strengths but that, independently, both the changing of the rod lubricant system and the addition of MBS impact modifier do lead to improved weld strengths.

6. Conclusions and Further Work

6.1. Conclusions

1) Low weld strengths, typically less than 30MPa, are a
feature of hot gas welded clear UPVC. Weld strength
achieved is dependent on the skill of the welder, the
welding method used (hand or speed), and the weld config-
uration and degree of overfill used. Using the same
welding technique, the author was able to obtain a weld
strength of 45MPa for filled UPVC.

2) Weld failure occurs by brittle fracture initiated at sites
of poor or zero fusion along either the rod/rod, rod/sheet
or sheet/sheet interfaces. Fracture usually occurs from
those sites located at or near to the weld surface.

3) The sites of poor or zero fusion may be considered to
be flaws and are an inherent feature in hot gas welded
UPVC, both clear and filled. They are not found in
hot tool welded clear UPVC.

4) Clear UPVC is more notch sensitive than filled UPVC.
Using the methods of linear elastic fracture mechanics,
K_{IC} for clear UPVC was found to be approximately $2.1 MPam^{\frac{1}{2}}$,
but filled UPVC proved to be too tough to measure using
these methods.

5) The low weld strength for hot gas welded clear UPVC is a
result of the existence of flaws and the high notch
sensitivity of clear UPVC.

6) The notch sensitivity of UPVC is increased by the hot gas
welding process. The K_{IC} for hot gas welded clear UPVC,
was found to be nearly 30% lower than for unwelded clear
UPVC when measured directly and when calculated using a
simplistic single edge notch model.

7) The removal of surface notches by the dressing of
the weld failed to improve weld strength. Flaws at
the surface are the most common cause of failure
but the removal of surface flaws by dressing causes
what were internal flaws to become surface flaws.

8) The use of solvent washes prior to and during welding
does not lead to improved weld strengths.

9) Modifying the lubricant system used in the standard
weld rod may lead to an improvement in weld strengths.
In particular, by replacing the standard external
lubricant with 3 phr epoxidised soya bean oil a
30% increase in weld strength was achieved.

10) Higher and more consistent weld strengths are achieved
when methacrylate-butadiene-styrene impact modifier
is added to the rod composition. An improvement of
66% over the standard welds is achieved through the
addition of 10 phr MBS.

11) Modifications to the rod formulation still only give weld
strengths of up to 30MPa. To achieve a major improvement
in weld strength, the sheet notch sensitivity needs to
be greatly reduced.

6.2. Further Work

1) Any future work on hot gas welded UPVC would benefit greatly
if a facility to manufacture well characterised and controlled
welds were available. To do this a controlled welding rig
is necessary but as realised during this work, too much
control makes the production of welds extremely difficult
and a major re-think on the design of such a rig is
required. However, such a rig would not only remove the
human factor from welding, but would also permit a study
into how changes in weld parameters, such as gas temperature,

distance of the torch from the weld, the pressure applied
to the weld rod and speed of welding affect the weld
strength.

2) As stated in the Conclusions, the welded UPVC appears to
be more notch sensitive than the unwelded UPVC. This
conclusion was partly based on the direct measurement
of K_{IC} and G_{IC} for welded UPVC. However, the number of
results was small and further work is required to confirm
this conclusion. The author would recommend that any such
study be based upon the double torsion test method.
Furthermore, since slow crack growth was observed during
the testing of unwelded material, the test conditions
should be varied to see whether slow crack growth is
possible in welded UPVC.

3) One suggested cause of the increased brittleness of welded
UPVC was the setting up of internal stresses in the weld
zone during welding. A study into the parameters affecting
the levels of internal stresses and the ways to reduce
them may lead to improved weld strengths.

4) The work described under Changes to the Weld Rod Composition
can only be considered an initial study. This work needs
to be expanded to give more comprehensive data on how
changes to the lubricant system and the addition of impact
modifiers affect the weld strength. It would be of
particular interest to determine whether or not the same
kind of improvement, provided by these changes, as seen
in the author's welds are reflected in welds prepared by
more experienced welders.

5) One part of the initial planned programme of work which
was not carried out in this study was to determine how
the weld strength is affected after the weld has been
immersed in various chemicals. In view of the possible
changes to the weld rod composition, this work takes on
a new importance in ensuring that any improvements in weld

strength are not lost if the weld is subject to
immersion in particular chemicals.

References

1) "Thermal and Chemical Welding of Plastics Materials"
(EEUA Handbook No.35), Engineering Equipment Users
Association, London, 1976, Sect. 6.

2) G.A.R. Matthews, "Vinyl and Allied Polymers Vol.2",
Iliffe, London, 1972.

3) H.A. Sarvetnick, "Polyvinyl Chloride", Reinhold,
New York, 1969.

4) W.S. Penn, "PVC Technology", 2nd.Ed., Maclaren,
London, 1966.

5) J.A. Brydson, "Plastics Materials", 2nd.Ed., Iliffe,
London, 1969.

6) A.W. Birley, in "Thermoplastics : Properties and Design",
(Ed. R.M. Ogorkiewicz), Wiley Interscience, London,
1974, p. 24 - 26.

7) G.A.R. Matthews, "Vinyl and Allied Polymers Vol.2",
Iliffe, London, 1972, Ch. 3.

8) G.C. Marks, in "Developments in PVC Technology",
(Ed. J.H.L. Henson and A. Whelan), Applied Science, London,
1973, Ch. 2.

9) G.A.R. Matthews, "Vinyl and Allied Polymers Vol.2",
Iliffe, London, 1972, p. 57 - 59.

10) S.A. Iobst, Ph. D. thesis, Lehigh University, U.S.A, 1970.

11) M.E. Carrega, Pure Appl. Chem., 49 (1977), 569.

12) R.S. Straff and D.R. Uhlmann, J.Polym. Sci. Phys.Ed.,
14 (1976), 353.

13) G.A.R. Matthews, "Vinyl and Allied Polymers Vol.2",
Iliffe, London, 1972, p. 42.

14) M.J.R. Cantow and J.F. Johnson, in "Encyclopedia of Polymer Science and Technology Vol.9", Wiley Interscience, New York, 1968, p. 182.

15) G.A.R. Matthews, "Vinyl and Allied Polymers Vol.2", Iliffe, London, 1972, p. 43 - 45.

16) ISO/R174 - 1961 (E).

17) G.A.R. Matthews, "Vinyl and Allied Polymers Vol.2", Iliffe. London, 1972, p. 320.

18) D.D. Bly, Science, 168 (1970), 527.

19) F.W. Billmeyer, Jr ., "Textbook of Polymer Science", 2nd. Ed., Wiley Interscience, New York,1971, p. 53 - 56.

20) J. Lyngaae-Jørgensen, J. Polym. Sci., C33 (1971), 39.

21) N.G. McCrum, B.E. Read and G. Williams, "Anelastic and Dielectric Effects inPolymeric Solids", Wiley, London, 1967, Ch. 11.

22) G. Pezzin, F. Zilio-Grandi and P. Sanmartin, Eur. Polym. J., 6 (1970), 1053.

23) E.R. Harrell, Jr., and R.P. Chartoff, J. Macromol. Sci.Phys., B14 (1977), 277.

24) R. Diaz Calleja, Polym. Eng. Sci., 19 (1979), 596.

25) G.A.R. Matthews, "Vinyl and Allied Polymers Vol.2", Iliffe, London, 1972, Ch. 5.

26) F. Tüdos, T. Kelen and T.T. Nagy, in "Developments in Polymer Degradation Vol.2" (Ed. N. Grassie),Applied Science, London, 1979, Ch. 7.

27) H.O. Wirth and H. Andreas, Pure Appl. Chem., 49 (1977), 627.

28) G. Ayrey, B.C. Head and R.C. Poller, J. Polym. Sci. Macromol Revs., 8 (1974), 1.

29) J. Stepek and C. Jirkal, Chem. Listy, $\underline{59}$ (1965), 1201.

30) C.A. Brighton, in "Encylcopedia of Polymer Science and Technology Vol.14.", Wiley Interscience, New York, 1971, p. 414.

31) W.V. Titow, in "Developments in PVC Production and Technology Vol. 1", (Ed. A. Whelan and J.L. Croft), Applied Science, London, 1977, Ch. 4.

32) L. Mascia, "The Role of Additives in Plastics", Edward Arnold, London, 1974, Ch. 3.

33) A. Guyot and A. Michel, in "Developments in Polymer Stabilisation Vol. 2", (Ed. G. Scott), Applied Science, London, 1979,Ch. 3.

34) G. Ayrey and R Poller, in "Developments in Polymer Stabilisation Vol.2", (Ed. G. Scott), Applied Science,London, 1979, Ch. 1.

35) R.K. Khanna, Plast. and Polym., $\underline{42}$ (1974), 80.

36) C.W. Fletcher and D. Dieckmann, 39th SPE ANTEC, 1981, p. 529.

37) K. Mathur and S. Driscoll, 39th SPE ANTEC, 1981, p. 912.

38) G.A.R. Matthews, "Vinyl and Allied Polymers Vol. 2", Iliffe, London, 1972, Ch. 6.

39) C.A. Brighton, in "Encyclopedia of Polymer Science and Technology Vol.14", Wiley Interscience, New York, 1971, p. 434.

40) E.A. Collins and C.A. Krier, J. Appl. Polym. Sci., $\underline{10}$ (1966), 1573.

41) G. Pezzin and G. Zinelli, J. Appl. Polym. Sci., $\underline{12}$ (1968), 1119.

42) P.B. Bowden,in "The Physics of Glassy Polymers", (Ed. R.N. Haward), Applied Science, London 1973, p. 306.

43) E. Jones Parry and D. Tabor, Polymer, $\underline{14}$ (1973), 623.

44) P.I. Vincent, Plastics, 28 (1963), 120.

45) C. Bauwens-Crowet, J.C. Bauwens and G. Homes, J. Polym. Sci.
A - 2, 7 (1969), 735.

46) H. Eyring, J. Chem. Phys., 4 (1936), 283.

47) D.P. Isherwood and J.G. Williams, Eng. Frac. Mech., 2 (1970),19.

48) F.F. Rawson and J.G. Rider, J. Polym. Sci., C33 (1971), 87.

49) G. Pezzin, G. Ajroldi, T. Casiraghi, C. Garbuglio and
G. Vittadini, J. Appl. Polym. Sci., 16 (1972), 1839.

50) D.M. Shinozaki, K. Woo, J. Vlachopoulos and A. Hamielec,
J. Appl. Polym. Sci., 21 (1977), 3345.

51) P.I. Vincent, Plastics, 26 (1961), 141.

52) P.I. Vincent, Polymer, 1 (1960), 425.

53) W. Retting, Eur. Polym. J., 6 (1970), 853.

54) H. Oberst and W. Retting, J. Macromol. Sci. Phys., B5 (1971),
559.

55) J.R. Martin and J.F. Johnson, J. Appl. Polym. Sci., 18
(1974), 257.

56) M.D. Skibo, R.W. Hertzberg, J.A. Manson and S.L. Kim,
J.Mater.Sci., 12 (1977), 531.

57) M. Skibo, J.A. Manson, R.W. Hertzberg and E.A. Collins,
J. Macromonol. Sci. Phys., B14 (1977), 525.

58) R.P. Kambour, J. Polym. Sci. Macromol. Rev. , 7 (1973), 1.

59) L.H.P. Weldon, Plast. Inst. Trans., 24 (1956), 303.

60) P.I. Vincent, in "Encyclopedia of Polymer Science and Technology
Vol.7", Wiley Interscience, New York, 1967, p. 336.

61) W.J. Jackson and J.R. Caldwell, J. Appl. Polym. Sci., 11 (1967), 211.

62) L. Mascia, Polymer, 19 (1978), 325.

63) H. Penkert, Kunststoffe, 45 (1955), 257.

64) J.C. Chauffoureaux, Pure Appl. Chem., 51 (1979), 1125.

65) G.A. Baum, Appl. Polym. Symp., 4 (1967), 189.

66) I.C.I. Technical Service Note W121. 2nd. ed. 1980, p.14.

67) K.V. Gotham and S. Turner, Polym. Eng. Sci., 13 (1973), 113.

68) L.H. Dunlap, C.R. Foltz and A.G. Mitchell, J. Polym. Sci. Phys. Ed., 10 (1972), 2223.

69) J.A. Duiser and A.E.M. Keijzers, Polymer, 19 (1978), 889.

70) S. Turner, Brit. Plastics, 37 (1964), 682.

71) C.M.R. Dunn and S. Turner, Polymer, 15 (1974), 451.

72) D.C. Wright, Polymer, 17 (1976), 77.

73) L.C.E. Struik, 3rd. Int. Conf. Deformation, Yield and Fracture of Polymers, Cambridge, Mar. 1976, 2/1.

74) K.H. Illers, Makromol. Chem., 127 (1969), 1.

75) N.J. Mills, 2nd. Int. Conf. Deformation, Yield and Fracture of Polymers, Cambridge, Mar. 1973, 6/1.

76) A. Cross and R.N. Haward, Polymer, 19 (1978), 677.

77) J.G. Rider and E. Hargreaves, J. Polym. Sci. A - 2, 7 (1969), 829.

78) K.H. Illers, J. Macromol. Sci. Phys., B14 (1977), 471.

79) P.V. McKinney and C.R. Foltz, J. Appl. Polym. Sci., 11 (1967), 1189.

80) A. Gray and M. Gilbert, Polymer, 17 (1976), 44.

81) S.M. Wolpert, A. Weitz and B. Wunderlich, J. Polym. Sci. A - 2, 9 (1971), 1887.

82) F.F. Rawson and J.G. Rider, Polymer, 15 (1974), 107.

83) F.F. Rawson and J.G. Rider, J. Phys. D. Appl. Phys., 7 (1974), 41.

84) T.E. Brady and S.A. Jabain, Polym. Eng. Sci., 17 (1977), 686.

85) E.H. Andrews, in "The Physics of Glassy Polymers" (Ed. R.N Haward), Applied Science, London, 1973, p. 423 - 424.

86) R.P. Kambour, J. Polym. Sci. A, 2 (1964), 4159.

87) R.P. Kambour, J. Polym. Sci. A -2, 4 (1966), 17.

88) M.J. Doyle, A. Maranci, E. Orowan and S.T. Stark, Proc. Roy. Soc., Lond., A329 (1972), 137.

89) P. Beahan, M. Bevis and D. Hull, Phil. Mag., 24 (1971), 1267.

90) J.E. Field, Contemp. Phys., 12 (1971), 1.

91) B.R. Lawn and T.R. Wilshaw, "Fracture of Brittle Solids", Cambridge University Press, Cambridge, 1975, p. 100.

92) K.V. Gotham, Plast. and Polym. 37 (1969), 303.

93) P.L. Cornes and R.N. Haward, Polymer, 15 (1974), 149.

94) N.J. Mills and N. Walker, Polymer, 17 (1976), 335.

95) I.Wolock and S.B. Neumann, in "Fracture Processes in
    Polymeric Solids" (Ed. B. Rosen), Wiley Interscience,
    New York, 1964, p. 235.

96) E.H. Andrews, J. Appl. Phys., $\underline{30}$ (1959), 740.

97) P. Beahan, M. Bevis and D. Hull, Proc. Roy. Soc. Lond,
    $\underline{A343}$ (1975), 525.

98) N. Walker, Ph.D. thesis, Birmingham University, Birmingham, 1976.

99) H. Wallner, Z. Physik, $\underline{114}$ (1939), 368.

100) K. Takahashi, M. Kimura and S. Hyodo, J. Mater. Sci. Letters, $\underline{13}$
     (1978), 2718.

101) M. Skibo, J.A. Manson, R.W. Hertzberg and E.A. Collins,
     J. Macromol. Sci. Phys., $\underline{B14}$ (1977), 525.

102) A. Weill and R. Pixa, J. Polym. Sci., $\underline{C58}$ (1977), 381,

103) M.J. Doyle, J. Mater. Sci., $\underline{10}$ (1975), 159.

104) G.H. Jacoby, ASTM STP 453, 1969, p. 147.

105) B.R. Lawn and T.R. Wilshaw, "Fracture of Brittle Solids",
     Cambridge University Press, Cambridge, 1975.

106) J.F. Knott, "Fundamentals of Fracture Mechanics", Butterworths,
     London, 1973.

107) D. Broek, "Elementary Engineering Fracture Mechanics",
     Noordhoff, Leyden, 1974.

108) C.E. Inglis, Trans. Inst. Naval Archit., $\underline{55}$ (1913), 219.

109) A.A. Griffith, Phil. Trans. Roy. Soc. Lond., $\underline{A221}$ (1920), 163.

110) A.A. Griffith, Proc. 1st Int. Cong. Appl. Mech., Delft, 1924, p. 55.

111) G. Irwin, in "Handbuch der Physik Vol.6", Springer-Verlag, Berlin,
     1958, p. 551.

112) E. Orowan, Welding J. Res. Supp., 34 (1955), 157.

113) D.S. Dugdale, J. Mech. Phys. Solids, 8 (1960), 100.

114) W.F. Brown Jr., and J.E. Srawley, ASTM STP 410, 1966.

115) D.P. Rooke and D.J. Cartwright, "Compendium of Stress Intensity Factors", HMSO, London, 1976.

116) J.F. Knott, "Fundamentals of Fracture Mechanics", Butterworths, London, 1973, p. 116.

117) J.F. Knott, "Fundamentals of Fracture Mechanics", Butterworths, London, 1973, p. 136.

118) B. Gross and J.E. Srawley, NASA TN D3295, 1966.

119) J.E. Srawley and B. Gross, NASA TN D3820, 1967.

120) J.O. Outwater, M.C. Murphy, R.G. Kumble and J.T. Berry, ASTM STP 559, 1974, p.127.

121) S. Mostovoy, C.F. Bersch and E.J. Ripling, Nat. SAMPE Tech. Conf. 1970, Vol. 2, p. 273.

122) J.G. Williams, "Stress Analysis of Polymers", Longman, London, 1973, p. 264 - 265.

123) J.G. Williams, J.C. Radon and C.E. Turner, Polym. Eng. Sci., 8 (1968), 130.

124) Y.M. Mai, A.G. Atkins and R.M. Caddell, Int. J. Frac., 11 (1975), 939.

125) T. Koboyashi and L.J. Broutman, J. Appl. Polym. Sci., 17 (1973), 1909.

126) G.P. Marshall, L.E. Culver and J.G. Williams, Int. J. Frac., 9 (1973), 295.

127) J.J. Benbow, Proc. Phys. Soc., 78 (1961), 970.

128) J.P. Berry, J. Appl. Phys., 34 (1963), 62.

129) J.P. Berry, J. Polym. Sci. A, 1 (1963), 993.

130) L.J. Broutman and F.J. McGarry, J. Appl. Polym. Sci. 9 (1965), 589.

131) G.P. Marshall, L.E. Culver and J.G. Williams, Plast. and Polym. 37 (1969), 75.

132) G.P. Marshall, L.H. Coutts and J.G. Williams, J. Mater. Sci. 9 (1974), 1409.

133) P.W.R. Beaumont and R.J. Young, J. Mater. Sci., 10 (1975), 1334.

134) J.P. Berry, J. Polym. Sci., 1 (1961), 313.

135) D. Kells, Ph.D. thesis, Birmingham University, Birmingham, 1976.

136) A. van den Boogaart and C.E. Turner, J. Plast. Inst., 31 (1963), 109.

137) M. Parvin and J.G. Williams, Int. J. Frac., 11 (1975), 963.

138) M. Parvin and J.G. Williams, J. Mater. Sci., 10 (1975), 1883.

139) R.P. Kambour and S. Miller, J. Mater. Sci., 11 (1976), 823.

140) S. Mostovoy, P.B. Crosley and E.J. Ripling, J. Materials, 2 (1967), 661.

141) S. Mostovoy and E.J. Ripling, J. Appl. Polym. Sci., 10 (1966) 1351.

142) G.G. Trantina, J. Composite Mater., 6 (1972), 192.

143) W.T. Evans and B.I.G. Barr, J. Strain Anal., 9 (1974), 166.

144) K. Selby and L.E. Miller, J. Mater. Sci., 10 (1975), 12.

145)   S. Yamini and R.J. Young, Polymer, 18 (1977), 1075.

146)   R.A. Glendhill, A.J. Kinloch, S. Yamini and R.J. Young,
        Polymer, 19 (1978), 574.

147)   R.J. Young, in "Developments in Polymer Fracture Vol.1"
        (Ed. E.H. Andrews), Applied Science, London, 1979, Ch. 6.

148)   F.J. Guild, B. Harris and A.G. Atkins, J. Mater. Sci., 13
        (1978), 2295.

149)   N.J. Mills, Eng. Frac. Mech., 6 (1974), 537.

150)   H.R. Brown and T.H. Chin, J. Mater. Sci., 15 (1980), 677.

151)   A.K. Green and P.L. Pratt, 5th Int. Conf. Experimental Stress
        Analysis, Udine, 1974, paper 19.

152)   E. Plati and J.G. Williams, Polymer, 16 (1975), 915.

153)   J.C. Radon, Polym. Eng. Sci., 12 (1972), 425.

154)   F.A. Johnson and J.C. Radon, J. Polym. Sci. Chem. Ed.,
        13 (1975), 495.

155)   L.E. Miller, K.E. Puttick and J.G. Rider, J. Polym. Sci., C33
        (1971), 13.

156)   A.Y. Darwish, J.F. Mandell and F.J. McGarry, 39th SPE ANTEC,
        1981, p. 2.

157)   R.C. Reinhardt, U.S. Patent, 2,220,545, 1937.

158)   A. Henning, D.R. Patent, 739,340, 1938.

159)   P. Voigt, Plastics, 13 (1949), 307.

160)   A. Henning, Kunststoffe, 32 (1942), 103.

161)   F.L. Connors, Australian Plastics, May (1954), 6.

162) F.L. Connors, Australian Plastics, April (1954), 6.

163) J.A. Neumann and F.J. Bockhoff, "Welding of Plastics",
Reinhold, New York, 1959, Ch. 2.

164) J. Parker, Welwyn Tool Co., Private Communication.

165) G. Haim, "Manual for Plastic Welding Vol.3. Polyvinyl Chloride",
Crosby Lockwood, London, 1959, Ch. 9.

166) BS 4994 : Section 5.5. : 1973.

167) ASTM 1789 - 65 (Reapproved 1977).

168) E. Alf, H. Potente and G. Menges, 5th Cranfield Conf. Designing
to Avoid Mechanical Failure, Plast. Inst., 1973, paper 6.

169) M.W. Birch, J.G. Williams and G.P. Marshall, 3rd Int. Conf.
Deformation, Yield and Fracture of Polymers, Cambridge, Mar. 1976,
paper 6.

170) BS 2782: Part 3: Methods 320A to 320F : 1976.

171) ASTM 790 - 66.

172) BS 3757 :Part 1 : Appendix E : 1964.

173) BS 2782 :Part 3 : Method 335A : 1978.

174) "Handbook of Chemistry and Physics", Chemical Rubber Co.,
Cleveland, 1964, F 39 (Elastic Moduli).

175) M.D. Griffiths and L.J. Maisey, Polymer, 17 (1976), 869.

176) L.F. King and F. Noel, Polym. Eng. Sci., 12 (1972), 112.

177) A. Kuske and G. Robertson, "Photoelastic Stress Analysis", Wiley,
New York,1974, Ch. 5.

178) R.D. Andrews and Y. Kazama, J. Appl. Phys., 39 (1968), 4891.

179) A. Utsuo and R.S. Stein, J. Polym. Sci. A-2, $\underline{5}$ (1967), 583.

180) J. Haslam, H.A. Willis and D.C.M. Squirrell, "Identification and Analysis of Plastics", 2nd Ed, Iliffe, London ,1972, p. 144.

181) D. Ardern, Technical Services, Ciba-Geigy Plastics and Additives Co., Private Communication.

182) A. Packter and M.S. Nerurkar, Kolloid Z.,$\underline{229}$ (1967), 7.

183) J. Haslam, H.A. Willis and D.C.M. Squirrell, "Identification and Analysis of Plastics", 2nd Ed., Iliffe, London 1972, Ch. 1 and 2.

184) J. Haslam, H.A. Willis and D.C.M. Squirrell, "Identification and Analysis of Plastics", 2nd Ed., Iliffe, London, 1972, p 721-729.

185) R. Miller, Technical Services, Hoechst Chemicals Ltd, Private Communication.

186) G.C. Corfield, Dept. of Chemistry, Sheffield City Polytechnic, Private Communication.

187) D.W. Allen, J.S. Brookes, R.W. Clarkson, M.T.J. Mellor and A.G. Williamson, J. Organometallic Chem., $\underline{199}$ (1980), 299.

188) C.R. Bailey, British Nuclear Fuels Ltd., Sellafield, Private Communication.

189) I.C.I. Technical Service Note D113, 1974, Table 4.

190) B. Haworth, C.S. Hindle, G.J. Sandilands and J.R. White, Plastics and Rubber Processing and Applications, $\underline{2}$ (1982), 59.

191) G. Scott and M. Tahan, Eur. Polym. J., $\underline{13}$ (1977), 997.

Table 1. Correlations for a number of different common methods of characterising molecular weights of vinyl chloride polymers, see [17].

Viscosity number ISO/R174-1961(E)	I.C.I. K-value	K-value 0.5gm/100cc cyclohexanone at 25°C	Specific viscosity 0.5gm/100cc cyclohexanone at 25°C	Weight average molecular weight	Number average molecular weight
50	42	45	0.25	40,000	20,000
54	44	47	0.27	50,000	24,000
57	45	48	0.28	54,000	26,000
61	47	50.5	0.31	60,000	30,000
67	49	52.7	0.34	67,000	34,000
73	51	55	0.37	74,000	38,000
80	53	57.2	0.40	86,000	42,000
83	54	58.3	0.42	92,000	43,500
87	55	59.5	0.44	100,000	45,500
90	56	60.6	0.45	105,000	47,500
94	57	61.9	0.47	114,000	50,000
98	58	62.9	0.49	122,000	52,000
102	59	64	0.51	132,000	53,500
105	60	65.2	0.53	140,000	55,000
109	61	66.3	0.55	150,000	57,000
121	64	69.7	0.61	182,000	62,500
130	66	71.2	0.65	209,000	66,500
149	71	75.5	0.75	272,000	75,000

Table 2   Formulations for the extrusion and calendering
           of clear rigid polyvinyl chloride.

Extrusion formulation[1]

Suspension homopolymer of ISO Viscosity No.90	100 parts
Sulphur containing organotin stabiliser	2-3 parts
Acrylic processing aid	2 parts
Montan ester wax	0.6 parts
Cetyl stearyl alcohol	0.6 parts
Mineral oil	0.1 parts
Low molecular weight polythene	0.1 parts

Calendering formulation[2]

Suspension homopolymer, K[3] value 58-62	100 parts
Sulphur containing organotin stabiliser	1.2 parts
Montan ester wax	0.5 parts
Amide wax	0.1 parts
Glycerine monostearate	0.3 parts

1) See [2], p 149.

2) Taken from "Hoechst Waxes as lubricants in plastics
   processing", Hoechst leaflet W 219 e, 1974, formulation
   no. FK. 3434.

3) Method of determining K not given.

Table 3   Summary of physical properties of cold formed polyvinyl chloride (see [84]).

Mechanical treatment	None	None	Drawn 2:1 at $23^{\circ}C$ 12.7mm/min	Drawn 2:1 at $23^{\circ}C$ 12.7mm/min	Drawn 2:1 at $23^{\circ}C$ 12.7mm/min
Thermal treatment	None	3 days @ $70^{\circ}C$	None	3 Days @ $70^{\circ}C$ restrained	3 Days @ $70^{\circ}C$ unrestrained
PROPERTY Shrinkage					
Onset T, $^{\circ}C$	–	–	45	75	74
Total,%	–	–	42	35	33
Mechanical Yield stress MPa	71.7	65.5	88.3	89.6	75.8
Modulus, GPa	2.3	1.8	3.8	2.8	2.0
Thermal T_g, $^{\circ}C$	78	86	81	87	86

Table 4   Gas conditions used for hot gas welding of UPVC. Gas used: compressed air.

Reference	Gas T ($^{\circ}C$)	Distance measured from nozzle (mm)	Gas flow (L/min)	Gas Pressure (KPa)
Voigt [159]	250	5	–	–
Connors [161]	270-280	6	40	35
Neumann and Bockhoff [163]	290	–	15-50	35
Haim [165]	280	6	15-30	36-60
EEUA [1]	300	3	15-40	20-100
ASTM 1789 [167]	280	6	–	–
Alf et al [168]	315	0	45-50	–

Table 5   Influence of correct heating of parent material and weld rod on strength of "Vinidur" welds (see [159]).

Heating Conditions	State of Bond	Position of Fracture	Appearance when fractured	Weld strength
Both weld rod and sheet insufficiently heated.	Little or no bonding on edges	Along edges of sheet	Along surface of weld rod or edges.	30%
Weld rod correctly heated, sheet insufficiently heated.	Proper bonding between layers of weld rod, insufficient bonding between weld rod and sheet.	Along edges of sheet.	Chamfering still visible.	30 - 50%
Weld rod overheated sheet properly heated.	Charred sections within the weld and between sheet and rod	In weld.	Fracture occurs in weld, charred section.	50%
Weld rod properly heated, sheet overheated	Charred sections in weld deposit and at chamfered edges of sheet.	Either in weld or along the edges of the sheet.	Fracture occurs between weld deposit and sheet.	50%
Weld rod and sheet properly heated.	Proper bonding between layers of weld rod and weld rod and sheet.	Either in weld or in transition zone.	Fracture in weld or sheet.	100%

Table 6   Efficiency of hot gas welded UPVC, subject to
           chemical environment (see [161]).

Environment	Conc. (%)	Weld efficiency (%)
Air	–	48
Nitric acid	10	42
Acetic acid	5	51
Hydrochloric acid	10	46
Sulphuric acid	3	61
Sodium hydroxide	10	53
Ammonium hydroxide	10	41
Ethyl alcohol	50	58
Carbon tetrachloride	–	49
Distilled water	–	47

Table 7   Details of compression moulding conditions used
           in attempts to produce sheets of clear weld
           rod material.

Material form	Mould Temp. (^{o}C)	Pressure (MPa)	Time (Mins)
20cm lengths of rod	160	10	15
20cm lengths of rod	165	15	15
Granules	170	15	20
Granules	180	20	20
Granules	190	20	30

Table 8.

   a)   Initial two-day ether extraction (mass of extracted additives: sheet = 0.08gm; clear weld rod = 0.10gm.)

Details of drying	Mass of thimble + sheet (gm)	Mass of thimble (gm)	Mass of sheet (gm)	Mass of thimble + weld rod (gm)	Mass of thimble (gm)	Mass of weld rod (gm)
Before initial extraction	12.59	2.84	9.75	12.61	2.71	9.9
30 mins. at 100°C + 90mins. at 50°C.	12.79	-	-	12.95	-	-
+ 5 days in air	12.86	-	-	12.97	-	-
+ 36 hrs in vac.	12.79	-	-	12.88	-	-
+ 5 days in vac. at 40°C	12.73	-	-	12.76	-	-
+ 10 mins. in air	12.75	-	-	12.78	-	-
+ 30 mins in air	12.79	2.77	10.02	-	-	-

   b)   Second two-day ether extraction (mass of extracted additives: sheet = 0.21gm; clear weld rod = 0.26gm.)

Details of drying	Thimble + sheet (gm)	Thimble (gm)	Sheet (gm)	Thimble + weld rod (gm)	Thimble (gm)	Weld rod (gm)
Before initial extraction	12.57	2.58	9.99	12.54	2.55	9.99
5 days in vac. at 40°C	12.89	-	-	12.80	-	-
+ 20mins in air	12.90	-	-	12.81	-	-
+ 30 mins in air	-	-	-	12.83	2.53	10.31

Table 9. Specifications and details of crack growth for tapered
double cantilever beam (TDCB) specimens tested.

TDCB taper angle, $\alpha = \mathrm{TAN}^{-1}\ 0.1$

H_o (mm)	b_c (mm)	G_w (mm)	ICL (mm)	LLL (mm)	CHR (mm/min)	Comments Fracture + crack length (mm)
10╫	2.5	1.3	47	295	0.5	FF 152;185;210;285
10╫	2.5	1.3	20	295	5	FF 112;121;245
10╫	5.6	1.3	55	295	0.1	FF 71; 95; AB
10╫	7.0	1.3	15	290	–	FF 40; AB
10╫	7.0	1.3	63	290	0.5	FF 83;116;166;177; AB
15	3.0	1.3	7	290	10	SF 185; AB
35*	3.0	1.3	15	95	–	SF 90
18	6.4	5.0	10	245	12.5	SF 35; AB
18	8.5	5.0	15	235	–	AB

╫ specimen shouldered, shoulder height 15mm.
* specimen prepared from remains of previous test specimen

TDCB, $\alpha = \mathrm{TAN}^{-1}\ 0.15$

H_o (mm)	b_c (mm)	G_w (mm)	ICL (mm)	LLL (mm)	CHR (mm/min)	Comments Fracture + crack length (mm)
15╫	3.2	1.3	5	295	–	FF 37;95;157;280
15╫	3.0	1.3	5	290	10	SF 20; AB
24*	3.0	1.3	10	230	10	SF 165; AB, also severed remainder
15╫	3.6	1.3	15	275	0.5	FF 90;148;222;265;TTE
15╫	6.1	1.3	60	255	20	FF 107;248; CW
15╫	6.7	1.3	35	280	0.5	FF 93; AB
19	6.2	0.9	52	294	5	FF 188
19	6.0	0.9	65	283	5	FF 274
19	5.3	0.9	82	283	5	FF TTE
19	5.5	0.9	10	283	5	SF 50; AB
19	5.5	0.9	37	283	5	AB
19	6.3	0.9	65	283	5	AB
19	5.2	0.9	55	283	5	FF 145; TTE
19	5.1	0.9	70	283	5	FF 270;280
19a	5.0	0.9	82	283	5	FF 28; TTE
19a	5.1	0.9	72	283	5	FF TTE
57	4.6	0.9	32	283	5	FF 232; AB
19	4.6	0.9	80	283	5	FF 250; TTE

Table 9. (continued)

H_o (mm)	b_c (mm)	G_w (mm)	ICL (mm)	LLL (mm)	CHR (mm/min)	Comments Fracture + crack length(mm)
19	5.1	0.9	71	283	5	FF 280; TTE
19	4.9	0.9	17	283	5	AB
19	5.3	0.9	53	283	5	FF 165;275
19	5.3	0.9	110	283	5	FF 175,280;CW
19	4.9	0.9	17	273	5	FF 78;215
19	4.9	0.9	17	273	5	FF 127;185;TTE
19	5.2	0.9	18	273	5	FF 81; AB
19	4.8	0.9	55	273	5	FF 265; TTE
19	5.1	0.9	65	275	5	FF 267; TTE
19	5.0	0.9	71	273	5	FF AB
19	5.4	0.9	72	273	5	FF 153;CW
19	5.0	0.9	69	273	5	FF 267;TTE
19	5.0	0.9	7	273	5	AB
19	5.1	0.9	71	273	5	FF 184
19	4.9	0.9	72	273	5	FF TTE
19	5.3	0.9	72	273	5	FF 256
19	5.3	0.9	72	273	5	FF 124;255;267; TTE
19	5.1	0.9	69	273	5	FF 255
19	4.9	0.9	70	273	5	FF 189;258;265
19	5.5	0.25	40	273	5	AB
19	5.2	0.25	45	273	5	FF 145; AB
19	5.5	0.9	47	273	5	AB
19	5.5	0.25	54	273	5	AB

* specimen prepared from remainder of previous specimen.

⊥ specimen shouldered, shoulder height 19mm

a.reverse end loaded

TDCB, α = TAN^{-1} 0.20

H_o (mm)	b_c (mm)	G_w (mm)	ICL (mm)	LLL (mm)	CHR (mm/min)	Comments Fracture + crack length(mm)
15⊥	2.5	0.25	10	250	–	AB
15⊥	3.0	0.25	15	250	2	FF 126;174;245
15⊥	3.0	0.25	20	250	5	SF 45; AB
15⊥	4.0	0.25	15	250	0.2	Crack wandered about groove

Continued/.....

Table 9. (continued)

H_o (mm)	b_c (mm)	G_w (mm)	ICL (mm)	LLL (mm)	CHR (mm/min)	Comments Fracture + crack length(mm)
15†	4.0	0.25	15	250	2	FF 110;133;193;240
15†	4.0	0.25	20	250	0.2	FF 77;117;155;283
15†	4.0	0.25	10	250	2	FF 60;173;242
15†	5.6	0.25	15	250	1	FF 51;131;240
15†	6.0	0.25	10	250	0.5	FF 32;110; AB
15†	6.0	0.25	10	250	5	SF 40; AB
15†	6.0	0.25	10	250	5	FF 95;145;245
15†	6.5	0.25	20	250	0.5	FF 69;240
15†	6.5	0.25	22	250	5	FF 50;174;240

† specimen shouldered, shoulder height 30mm

TDCB, $\alpha = TAN^{-1} \ 0.25$

H_o (mm)	b_c (mm)	G_w (mm)	ICL (mm)	LLL (mm)	CHR (mm/min)	Comments Fracture + crack length(mm)
15	2.5	1.3	5	295	0.5	FF 40; 131;287
39	2.3	1.3	0	130	–	FF TTE

Key.

H_o : taper height at loading line

b_c : crack width

G_w : groove width

ICL : initial crack length

LLL : specimen length from loading line

CHR : crosshead rate

V_g : V groove

AB : arm break-off

SF : slow fracture

FF : fast fracture

TTE : through-to-end

Table 10. Specifications and details of crack growth for
double cantilever beam (DCB) specimens tested.

H_o (mm)	b_c (mm)	G_w (mm)	ICL (mm)	LLL (mm)	CHR (mm)	Comments Fracture and crack length (mm)
18	3.0	Vg	15	230	5	SF 50; AB
25	3.3	1.8	10	280	5	SF 185; AB
25	6.0	1.8	7	285	125	FF 65;95; AB
25	5.7	1.8	5	285	5	FF 65;195
25	6.0	1.8	5	285	10	SF 13; AB
25	7.0	1.8	5	285	10	AB
25	7.7	1.8	5	285	5	FF 64;83; AB
25	8.0	1.8	5	285	–	AB
25	8.7	1.8	7	285	20	AB
30	3.2	1.8	10	280	2	FF 75;195;225;243;274; TTE
32.5	3.5	1.8	5	280	5	SF 20; AB
33	3.0	1.8	5	280	10	SF 140;AB
33	3.0	1.8	25	125	10	SF 50; AB
33	3.7	1.8	5	285	5	FF 65;275; TTE
33	5.5	1.8	5	285	5	SF 85; AB
40	5.5	Vg	15	130	5	SF 85; AB; also FF into remaining material
40	5.5	Vg	15	130	0.5	FF 105; TTE

For key see end of Table 9.

Table 11.   Specifications and details of crack growth for welded double cantilever beam (DCB) specimens tested.

2V11C* Welded DCB

H_o (mm)	b_c (mm)	G_w (mm)	ICL (mm)	LLL (mm)	CHR (mm/min)	Comments Fracture + crack length (mm)
25	–	–	15	255	10	AB
31	3.8	1.0	20	285	5	FF 150; TTE
32.5	3.2	1.0	43	280	5	FF 52; TTE
33	4.8	1.0	0	285	5	FF 206; TTE
37.5	–	–	5	295	5	FF 66; AB

2V33C* Welded DCB

27	–	–	15	245	10	AB
37	–	–	5	290	5	FF 170; AB
64	–	–	5	255	20	AB

For key see end of table 9.

* 2V : double-vee butt weld
  11 : one pass of rod in each groove
  33 : three passes of rod in each groove
   C : circular cross-section weld rod

Table 12. Specifications and details of crack growth for welded tapered double cantilever beam (TDCB) specimens tested.

2V11C Welded TDCB, $\alpha = \mathrm{TAN}^{-1}\ 0.1$

H_o (mm)	b_c (mm)	G_w (mm)	ICL (mm)	LLL (mm)	CHR (mm/min)	Comments Fracture + crack length (mm)
25	–	–	0	290	–	FF 30; AB
37	–	–	63	165	10	FF TTE

2V11C Welded TDCB, $\alpha = \mathrm{TAN}^{-1}\ 0.15$, with side plates

H_o (mm)	Side Plates	ICL (mm)	LLL (mm)	CHR (mm/min)	Comments Fracture + crack length (mm)
20	3mm DC	5	250	5	FF 20;65;115;235
22	10mm DC	0	275	5	FF 60;220

DC = Darvic clear grade sheet.

DC = Darvic clear grade sheet.

2V33C Welded TDCB, $\alpha = \mathrm{TAN}^{-1}\ 0.15$, with side plates

H_o (mm)	Side Plates	ICL (mm)	LLL (mm)	CHR (mm/min)	Comments Fracture + crack length (mm)
23	3mm DC	50	230	–	FF 145; AB
23	6mm P	00	230	–	FF AB
20	3mm AL	15	265	20	FF 43; AB
20	3mm AL	15	270	10	FF 68; Crack wandered out of weld.
20	3mm AL	17	265	10	FF 80; 245
20	0.8mm S	12	265	10	FF 48; 130 ;Crack wandered out of weld.
20	0.8mm S	35	265	1	FF 47; 255; Crack wandered out of weld.

P = Perspex; AL = Aluminium; S = Steel

Table 12 (continued)

2V11C Welded TDCB, $\alpha = TAN^{-1}\ 0.2$

H_o (mm)	b_c (mm)	G_w (mm)	ICL (mm)	LLL (mm)	CHR (mm/min)	Comments Fracture + crack length(mm)
14	–	–	40	225	25	FF 60; AB
15†	–	–	5	250	–	FF 35; AB
15†	5.0	1.5	17	250	–	FF 75; AB
32*	–	–	72	195	25	FF 110; AB
39	5.0	1.5	0	123	–	FF TTE

† These specimens had rectangular shoulders at height 30mm at loading line.

* Prepared from remainder of previous specimen.

2V33C Welded TDCB, $\alpha = TAN^{-1}\ 0.2$

H_o (mm)	b_c (mm)	G_w (mm)	ICL (mm)	LLL (mm)	CHR (mm/min)	Comments Fracture + crack length(mm)
15†	–	–	0	250	–	FF 50; AB
15†	–	–	0	250	–	FF 70; AB
15†	5.0	1.5	15	250	5	FF 60;68;82;93; AB
20††	–	–	0	250	0.5	FF 15;45; AB
20††	5.5	1.5	22	250	5	FF 70; AB
20††	5.5	1.5	25	250	–	FF 95; AB
20††	5.5	1.5	33	250	–	FF 90; TTE

† Specimens shouldered, shoulder height 30mm

†† Specimens shouldered, shoulder height 35mm

Table 12 (continued)

2V11C welded TDCB, $\alpha = TAN^{-1}\ 0.25$

H_o (mm)	b_c (mm)	G_w (mm)	ICL (mm)	LLL (mm)	CHR (mm/min)	Comments Fracture + crack length (mm)
$14_{\dagger}$	–	–	65	245	–	AB
$15^{\dagger}$	–	–	60	195	–	FF 90; AB but crack also severed remainder of specimen
$15^{\dagger}$	–	–	70	195	–	FF but crack wandered about weld
$15^{\dagger}$	–	–	70	230	–	AB
20	–	–	0	265	–	AB
27*	–	–	75	240	–	FF 100; AB

$\dagger$ Specimen shouldered, shoulder height 35mm

* Prepared from remainder of previous specimen

For key see end of table 9.

Table 13 . Formulations for modified weld rod material and the weld tensile strengths for welds prepared with the modified rod, details of the average flaw size, and type are also included. All welds were prepared using Darvic UP 025 clear sheet with 3 passes of rod in each vee, except 10 which used six passes of rod.

Weld No.	Formulation	Av.flaw size.mm	Flaw type*	Av.σ_F MPa	S.D MPa	Eff.%	Min.σ_F MPa	Max σ_F MPa	Number Samples
1	Std.(Darvic rod)	0.9	S	18.4	3.3	28	15.0	25.7	8
2	50% reduction in ext. and int. lubricants	0.7	S	22.0	5.9	34	14.8	28.5	9
3	0% ext. lubricant	0.6	S	25.6	6.0	40	19.1	32.9	5
4	0% ext. and int. lubricants	0.9	S	25.4	4.8	39	17.3	32.9	10
5	0% ext. and int. lubricants + 3phr ESBO	-†	S	24.0	4.0	37	17.0	27.4	5
6	Std. + 3phr ESBO	-	S	20.3	4.3	31	16.0	27.1	5
7	Std. + 10phr ESBO	-	C/S	19.5	3.1	30	15.9	24.2	5
8	Std. + 5phr MBS	-	C	24.1	4.5	37	18.7	30.5	5
9	Std. + 10phr MBS	-	C	32.0	2.2	49	29.1	33.9	5
10	Std. + 10phr MBS	-	C/S	29.7	3.6	46	22.9	36.4	10
11	Std. + 15phr MBS	-	C/S	13.0	1.4	20	10.5	14.2	5
12	Std. + 10phr MBS + 3 ESBO	-	S	24.2	2.1	37	21.4	26.2	5

Av. = average, σ_F = failure stress, S.D = standard deviation, Eff. = efficiency based on a sheet yield stress of 65MPa, Std. = standard, ext. = external, int. = internal, phr = parts pe hundred resin (PVC polymer)weight ESBO = epoxidised soya bean oil, MBS = methyl methacrylate-butadiene-styrene impact modifier, S = surface flaw C = centre flaw.

* the predominant type of flaw. † an irregular surface or the proximity of the surface prevented a measurement being taken.

Table 14. Results of the RAPRA GPC analysis of molecular weights for the polyvinyl chloride materials used for hot gas welding

Sample	$\bar{M}_n$	$\bar{M}_w$	$\bar{M}_v$	$\bar{M}_z$	$\bar{M}_w / \bar{M}_n$
First series					
I.C.I. Darvic UP 025 sheet	35,000	78,000	72,000	160,000	2.27
Clear weld rod	31,000	87,000	76,000	250,000	2.8
Second series					
I.C.I. Darvic UP 025 sheet	38,000	77,000	71,000	140,000	2.04
I.C.I. Darvic UP 025 sheet annealed @ 160°C 10mins.	36,000	76,000	71,000	130,000	2.09
I.C.I. clear triangular weld rod	35,000	72,000	68,000	120,000	2.08
I.C.I. clear triangular weld rod annealed @ 160°C 10mins.	35,000	74,000	69,000	130,000	2.10
Clear weld rod	43,000	96,000	88,000	180,000	2.21
Clear weld rod annealed @ 180°C 2 mins.	47,000	94,000	88,000	170,000	1.99

Table 15 Effect of various thermal treatments on the dimensional stability of clear Darvic sheet.

Time (mins)		Temperature			
		110°C	130°C	150°C	170°C
0	VM	59.8	60.1	60.0	59.6
	HM	60.1	59.6	60.0	59.9
5	VM	–	–	–	59.1
	HM	–	–	–	59.3
10	VM	59.8	59.6	59.3	59.0
	HM	59.3	61.3*	59.5	59.2
30	VM	–	–	–	57.9
	HM	–	–	–	59.3
90	VM	–	–	58.8	–
	HM	–	–	59.2	–
190	VM	59.2	–	–	–
	HM	59.5	–	–	–
337	VM	59.1	–	–	–
	HM	59.5	–	–	–
1020	VM	–	59.3	–	–
	HM	–	59.4	–	–
1140	VM	–	–	58.6	–
	HM	–	–	59.0	–

VM = Vertical measurement from identification mark (mm)

HM = Horizontal measurement from identification mark (mm)

Thickness measurement was approximately 10.65mm after 10 mins. heating at all temperatures

* This appears to be the result of a systematic error in the taking of the measurement.

Table 16.   Effect of various thermal treatments on the dimensional stability of clear weld rod. (initial length of rods, 150mm).

| Temperature (°C) | Support surface during thermal treatment | | | | | |
| | Baking Tray | | Teflon Sheet | | Glass Microspheres | |
	Time (mins)	Length (mm)	Time (mins)	Length (mm)	Time (mins)	Length (mm)
70	–	–	–	–	1	149.5
	–	–	–	–	2	149.5
	5	149.0	–	–	5	148.5
	10	148.7	–	–	10	148.5
	15	148.5	–	–	–	–
	20	148.5	–	–	–	–
80	–	–	–	–	1	149.5
	–	–	–	–	2	146.5
	–	–	–	–	5	146.5
	–	–	–	–	10	146
90	–	–	–	–	1	146.5
	–	–	–	–	2	145.5
	–	–	–	–	5	145.7
	10	148.0	–	–	10	145.0
	20	147.5	–	–	–	–
	30	148.0	–	–	–	–
	40	147.7	–	–	–	–
100	–	–	–	–	1	145.5
	–	–	–	–	2	145.5
	–	–	–	–	5	145
	–	–	–	–	10	145
110	5	147.7	5	147.2	–	–
	10	147.2	–	–	–	–
	15	147.0	–	–	–	–
	20	147.0	20	146.5	–	–
	–	–	90	–	–	–
	–	–	330	145.7	–	–
120	–	–	–	–	1	144.5
	–	–	–	–	2	144.0
	5	146.7	–	–	5	143.5
	10	147.0	–	–	–	–
	20	146.5	–	–	–	–
	30	146.3	–	–	–	–

Table 16 (continued)

Temperature (°C)	Baking Tray		Teflon Sheet		Glass Microspheres	
	Time (mins)	Length (mm)	Time (mins)	Length (mm)	Time (mins)	Length (mm)
130	–	–	5	146.0	–	–
	–	–	20	145.5	–	–
	–	–	90	144.5	–	–
	–	–	180	143.6	–	–
140	–	–	–	–	1	143.0
	–	–	–	–	2	141.8
	5	144.0	–	–	5	139.7
	10	142.5	–	–	–	–
	15	142.0	–	–	–	–
	20	141.7	–	–	–	–
	30	141.0	–	–	–	–
150	5	139.0	5	143.0	–	–
	10	138.0	–	–	–	–
	15	137.5	–	–	–	–
	20	137.7	20	139.0	–	–
	–	–	90	133.0	–	–
160	–	–	–	–	1	140.5
	–	–	–	–	2	138.3
	5	131.0	–	–	5	136.5
170	5	125.0	–	–	–	–
	10	122.0	–	–	–	–
	25	116.0	–	–	–	–
	35	115.0	–	–	–	–
175	3	117.5	–	–	–	–
	6	115.0	–	–	–	–
	9	113.0	–	–	–	–
	12	111.7	–	–	–	–
	15	111.0	–	–	–	–
	18	110.7	–	–	–	–

Table 16. (continued)

Temperature (^{o}C)	Support surface during thermal treatment					
	Baking Tray		Teflon Sheet		Glass Microspheres	
	Time (mins)	Length (mm)	Time (mins)	Length (mm)	Time (mins)	Length (mm)
180	–	–	–	–	1	135.5
	–	–	–	–	2	132.0
	–	–	–	–	5	121.6
	16	114.0	–	–	–	–

Table 17. Weight of additives extracted after different extraction processes from I.C.I. sheet and weld rod and from clear weld rod

Batch	Extraction time (days)	Solvent	Mass and percentage of additives extracted (gm) and (%)					
			Clear rod		Sheet		I.C.I. rod	
			(gm)	(%)	(gm)	(%)	(gm)	(%)
1	2	Ether	0.10	1.01	0.08	0.8	–	–
2	2	Ether	0.26	2.6	0.21	2.1	–	–
3a	3	AR Ether	0.41	4.1	0.23	2.3	–	–
3b	3	AR Methanol	0.01	0.1	0.02	0.2	–	–
4a	5	AR Ether	0.76	3.8	0.53	2.6	–	–
4b	5	AR Ether	0.09	0.5	0.06	0.3	–	–
5	5	AR Ether	0.82	4.1	–	–	0.82	4.1

3b and 4b were subsequent extractions carried out on the same materials as used in 3a and 4a.

Table 18. List of additives obtained as standards and the methods with which they were examined.

Additive	Chemical Composition	IRS	UVS	NMR	DSC
Lubricants					
Wax E	Ester wax from montanic acids.	✓	✓	✓	✓
Wax OP	Partly saponified ester wax from montanic acids.	✓	✓	✓	✓
VPARE 1	Stearyl phthalate.[+]	✓	✓	–	✓
PE 190	Polyethylene wax MW approx. 9000.	✓	–	–	✓
UV absorbers					
Tinuvin P	2-(2-hydroxy-5-methyl-phenyl)- benzotriazole	✓	✓	✓	✓
Tinuvin 320	2-(2-hydroxy-3,5-di-tertiary-butyl-phenyl)-benzotriazole.	✓	✓	✓	✓
Thermal Stabilisers					
Irgastab 17MOK	Di-n-octyl tin dithiogly-collic acid esters	✓	✓	✓	–
Irgastab 17M	Dibutyl tin mercaptides	✓	✓	–	–
Irgastab DBTM	Dibutyl tin maleate	✓	–	–	–
Plasticiser					
Reomol DOP	Dioctyl phthalate	✓	✓	✓	–

NB. All lubricants were supplied by Hoechst Chemicals Ltd. and all other additives by Ciba-Geigy Plastics and Additives Co.

[+] See [185].

Table 19.   Methyl ethyl ketone absorption measurements on
            50mm lengths of clear weld rod.

Immersion Time (s)	5	10	20	30
Sample mass before immersion (gm)	0.482	0.499	0.502	0.492
Sample mass after drying under various conditions (gm)				
2 mins in Air	0.482	0.501	0.509	0.498
20 mins in Air	0.482	0.500	0.506	0.496
1 week in Air	0.482	0.499	0.504	0.493
3 days in vacuum	0.482	0.499	0.504	0.493
5 days at 30°C	0.482	0.499	0.504	0.492

Weighings accurate to $\pm$ 0.0005 gm.

-177-

Table 20. Summary of weld tensile strengths.

Weld No.	Number of rods and weld type	Weld details	Weld Properties						
			Av.σ_F MPa	S.D. MPa	Eff %	Min.σ_F MPa	Max.σ_F MPa	No of samples
	Author's welds							
1.	2V33C	Filled Darvic sheet(6mm) σ_y = 53MPa,filled rod	44.9	2.6	85	40.6	47.0	5
2	2V11ΔL	Darvic sheet and ICI rod	15.6	3.8	24	7.1	19.1	10
3	2Y66C	Darvic sheet, clear rod, speed welded	27.1	2.2	42	23.7	28.8	5
4	2V66C	As above(but speed weld- ed at a faster rate.	18.7	2.9	29	14.7	21.9	5
5	2V66C	Darvic sheet,ICI rod, speed welded	27.1	5.1	42	21.5	34.1	5
6	2V33C	Darvic sheet,clear rod	18.6	5.2	29	12.6	25.4	5
7	2V33C	As above(separate weld)	18.5	3.0	28	14.1	24.4	14
8	2V66C	Darvic sheet,clear rod	22.4	4.0	33	17.4	29.5	18
9	2V33C	Darvic sheet,ICI rod	24.2	6.8	37	16.0	34.7	10
10	–	Darvic sheet,hot tool welded	61.1	0.9	94	60.3	62.4	4

Continued/......

Table 20. (continued)

Weld No.	Number of rods and weld type	Weld details	Weld Properties Av.σ_F MPa	S.D. MPa	Eff %	Min.σ_F MPa	Max.σ_F MPa	No of Samples
BNFL - Windscale Welds: all welds were prepared using unfilled ICI materials								
11	2V63△S	Weld A	25.6	3.0	39	20.8	28.7	5
12	2V33△S	Weld B	23.7	4.1	36	20.1	28.7	4
13	2V4△S1,△L	Weld C	18.3	3.1	28	14.5	22.3	5
14	2V33△S	Weld D	21.1	9.5	32.5	9.5	30.8	5
15	2V66△S	Weld E	32.1	3.7	49	27.9	37.3	5
16	2V66△S	Weld E(dressed before testing)	31.2	2.3	48	28.9	34.3	5
17	2V66△S	Weld F	29.7	9.7	46	21.3	45.3	5
Plastics Construction Welds: all welds were prepared by the same welder who used an asymmetric weld configuration.								
18	2V63C	Darvic sheet, ICI rod, speed welded	26.5	3.3	41	23.9	31.2	4
19	2V63C	As above but dressed	33.2	7.7	51	20.2	44.1	10

Continued/.....

Table 20 (continued)

Weld No.	Number of rods and weld type	Weld details	Weld Properties					
			Av.σ_F MPa	S.D. MPa	Eff. %	Min.σ_F MPa	Max.σ_F MPa	No.of Samples
Plastics Construction Welds (continued)								
20	2V63C	Darvic sheet,clear rod, speed welded	24.8	3.6	38	21.9	30.0	4
21	2V10,3C	P.C. materials,speed welded	31.8	4.3	49	27.8	35.6	4
22	2V63C	As above,root rod hand welded,rest speed welded	25.1	4.1	39	21.9	32.1	5
23	2V63C	P,C,materials,speed welded	22.2	3.8	34	18.8	28.2	5
24	2V31ΔS	Darvic sheet, ICI rod, hand welded	32.3	5.7	50	25.2	39.5	8
Leister Weld								
25	2V11ΔL	Darvic sheet,filled rod	26.6	4.3	41	16.9	30.5	8

Continued/....

Table 20. (continued)

Glossary of terms used

Number of weld rod and weld type

2V : Double-vee weld configuration.

33 : For example, means 3 rods laid down in each vee on either side of the weld.

C   : Circular section rod

ΔL : Large triangular rod

ΔS : Small triangular rod

Av = average, σ_F = failure stress, S.D. = standard deviation, Eff. = efficiency based on a clear UPVC sheet yield stress of 65MPa, except No.1 which is based on a filled UPVC sheet yield stress of 53MPa.

NB. Except where otherwise stated, the hand welding method was used and Darvic sheet refers to the clear grade UP 025.

Table 21. Details of sizes of flaws as observed on the fracture surfaces of the standard welds tensile test pieces.

Weld[a] No.	Av. σ_f MPa	Av. flaw size, mm	S.D mm	Type of flaw	Number of samples
Author's welds					
1	44.9	0.75	0.55	C	5
2	15.6	0.90	0.35	S	5
3[b]	27.1	--	-	S	-
4	18.7	2.05	1.10	C	5
5[c]	27.1	..	-	C/S	-
6	18.6	0.85	0.30	S	5
7	18.5	1.05	0.30	S	9
8	22.4	1.15	0.35	C/S	9
9	24.2	0.80	0.40	S	5
10	61.1	No flaws observed			
BNFL welds					
11	25.6	1.95	0.50	C	5
12	23.7	0.90	0.30	S	5
13	18.3	1.50	0.60	S	5
14	21.1	1.40	0.65	S	5
15	32.1	0.40	0.05	S	5
16[b]	31.2	--	-	S	-
17	29.7	1.00	0.65	S	5
Plastic Construction Welds					
18	26.5	0.50	0.20	S	4
19[c]	33.2	-	-	C/S	-
20	24.8	0.80	0.50	S	4
21	31.8	0.74	0.25	S	4
22	25.1	0.75	0.30	S	4
23[b]	22.2	-	-	S	-
24	32.3	0.55	0.20	S	5
Leister weld					
25	26.6	0.70	0.25	S	3

a) for details of weld type see table 20.
b) the proximity of the surface of the weld prevented the flaw size being determined.
c) surfaces were too rough to allow flaws to be defined.

/Continued......

Table 21. (continued)

Glossary

Av. = average, S.D. = standard deviation, C = centre flaw,
S = surface flaw.

NB. the type of notch refers to the dominant type of flaw,
flaws occurring at the surface of the weld and those with
a boundary within 1-2mm of the weld surface are considered
to be surface flaws.

Table 22. Summary of the results for the fracture mechanics test programme

Test method	G_{IC} KN/m		K_{IC} MPa m$^{\frac{1}{2}}$		σ_o MPa		Number of samples
	Mean	S.D.	Mean	S.D	Mean	S.D.	
Clear UPVC sheet.							
TDCB (α = tan^{-1} 0.15)	1.92	0.33	2.13[a]	0.25	–	–	29
TDCB (α = tan^{-1} 0.20)	2.00	0.29	2.34	0.23	–	–	5
DCB	–	–	2.14	0.30	–	–	7
DT	–	–	2.44	0.30[d]	–	–	16
SEN[b] (W = 15mm)	–	–	1.87	0.31[d]	6.74	2.22[d]	14
(W = 9.5mm)	–	–	2.17	0.71[d]	6.46	8.36[d]	5
(W = 6mm)	–	–	2.36	2.00[d]	4.24	30.32[d]	5
(all SEN samples)	–	–	2.27	0.18[d]	4.72	1.80[d]	24
SEN[c] (W = 15mm)	–	–	2.72	0.17[d]	–	–	14
(W = 9.5mm)	–	–	2.72	0.12[d]	–	–	5
(W = 6mm)	–	–	2.64	0.15[d]	–	–	5
(all SEN samples)	–	–	2.68	0.08[d]	–	–	24
Welded clear UPVC sheet							
TDCB (α = tan^{-1} 0.15)	1.30[e]	–	1.39	0.22	–	–	6
DCB	–	–	1.65	0.15	–	–	4
DT	–	–	1.34	0.21	–	–	7
Filled UPVC sheet							
SEN (W = 6mm)	–	–	1.46	0.20[d]	20.14	2.90[d]	9
SEN (W = 6mm)	–	–	2.77	0.13[d]	–	–	9

Continued/.........

-184-

Table 22. (continued)

a) analysis based on 24 results.

b) linear regression analysis assuming $y = Ax + B$, σ_o is the resulting intercept of the straight line with the stress axis and corresponds to B in the analysis.

c) linear regression analysis assuming $y = Ax$.

d) these are standard errors and not standard deviations.

e) there was only one result.

NB. all linear regression analysis was carried out using the GLIM 3.12 ((c) 1977 Royal Statistical Society, London) statistical analysis package.

Table 23.   Summary of weld tensile strength results for welds prepared using pre-weld rod treatments.

Weld No.	No of rods and weld type	Pre-weld treatment	Av.σ_F MPa	S.D. MPa	Eff. %	Min.σ_F MPa	Max.σ_F MPa	No.of Samples
1	2V33C	Rod annealed before welding	13.8	4.1	21	8.0	17.8	5
2	2V33C	Weld surfaces washed with trichloroethylene	14.3	1.7	22	12.2	16.8	7
3	2V33C	Weld surfaces washed with methanol	16.7	3.3	26	9.3	20.3	14

For glossary of terms used and the key to the table, see bottom of table 20.

NB. All welds were prepared with the hand welding method and used clear Darvic UP025 and clear weld ro
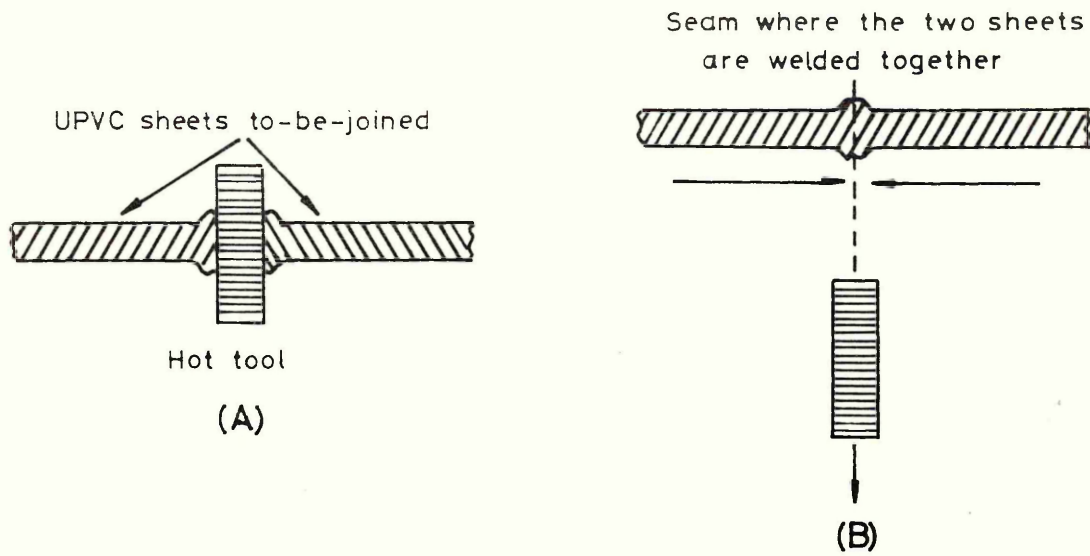
Fig. 1. Hot tool butt welding: A, the parts are pressed against
the tool until softened; B, the tool is removed and
the sheets are pressed together to form a fusion joint.
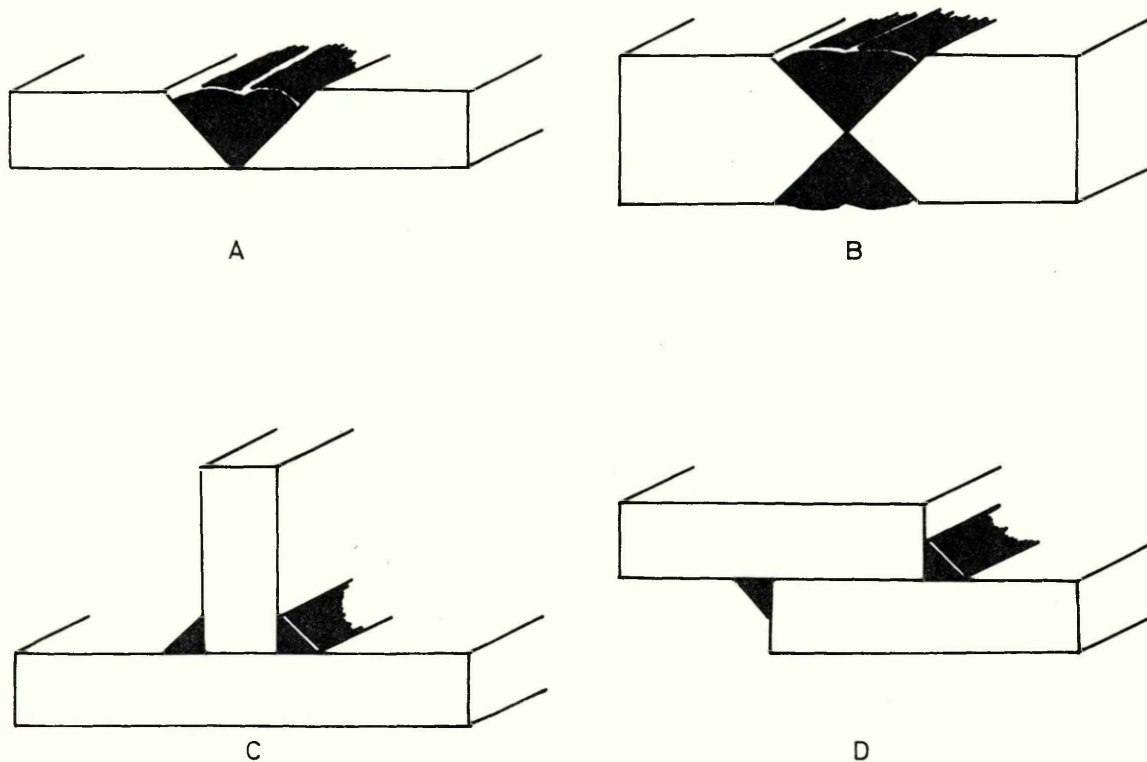
Fig. 2. Different types of welds practised in the fabrication
of UPVC: A, single-vee butt weld; B, double-vee butt
weld; C, fillet weld; D, lap weld.
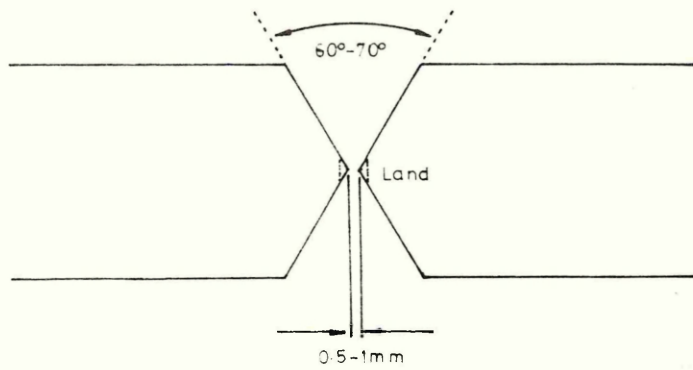
Fig. 3. Preparation of sheet for double-vee butt weld, note sometimes the apex of the chamfer is squared-off to aid sheet alignment and this is called land.
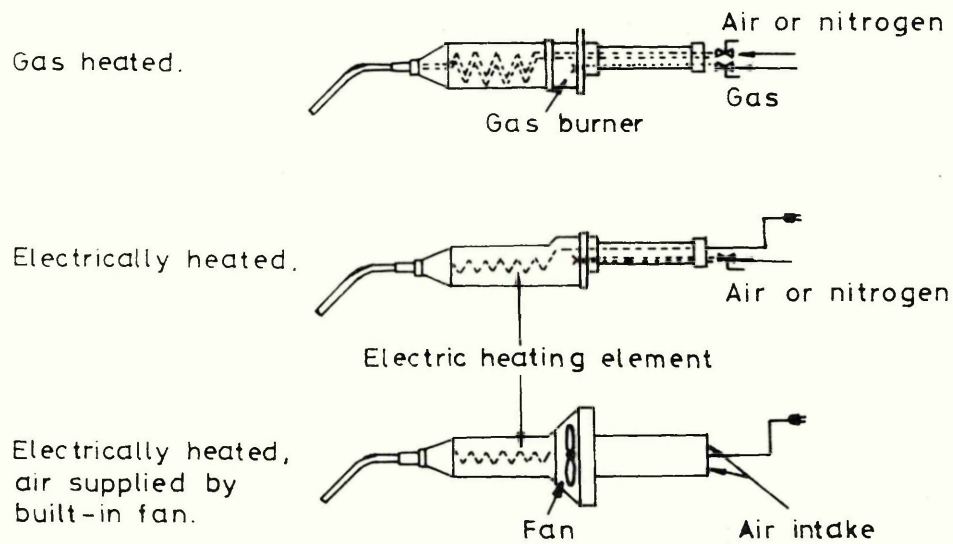
Fig. 4. Basic designs of welding torch.

Fig. 5. Typical nozzles for hot gas welding torches.
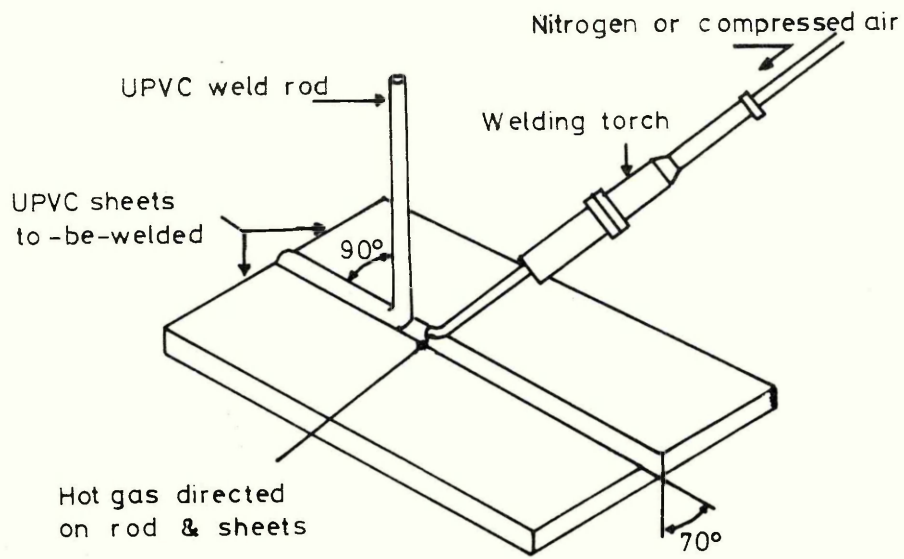
Fig. 6. Hot gas welding of UPVC.
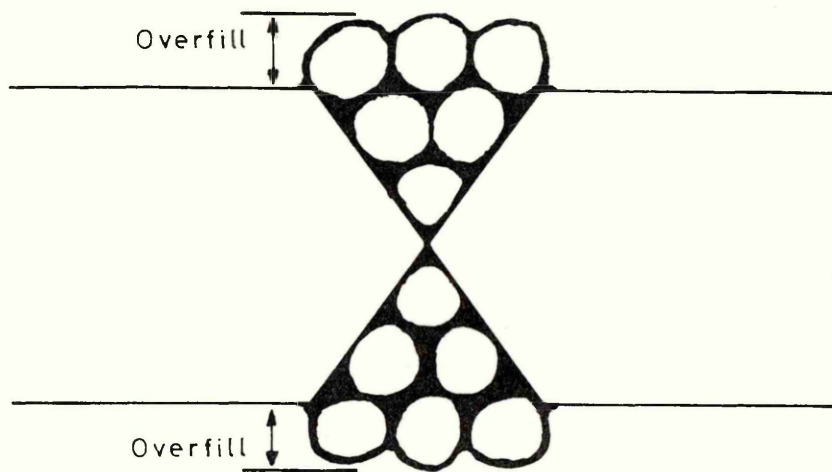
Fig. 7. Overfilling of weld grooves.
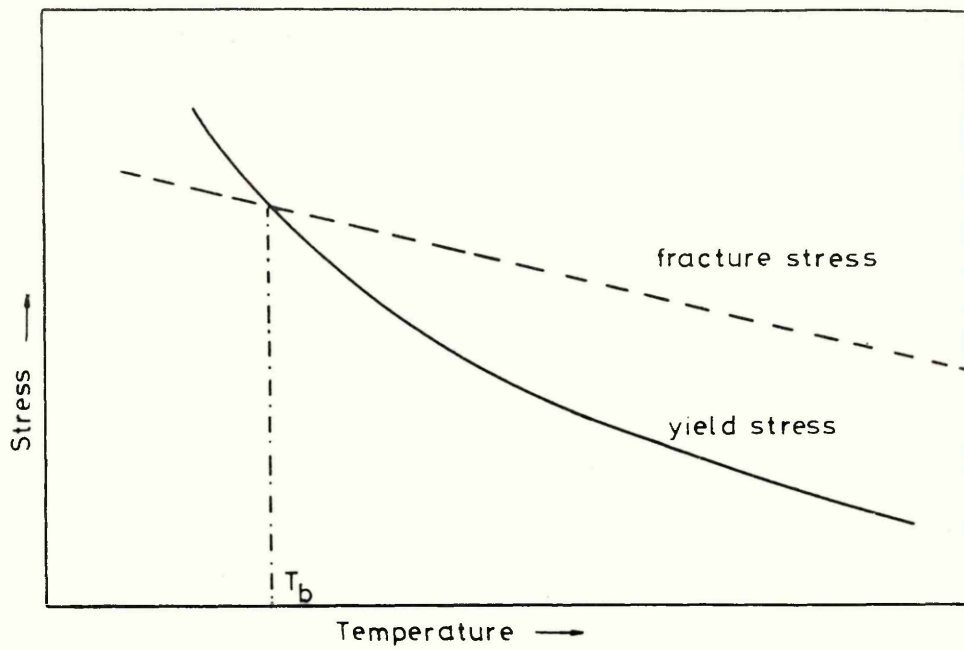
Fig. 8. The effect of temperature on the fracture and yield stresses of thermoplastics and the brittle-ductile transition temperature.
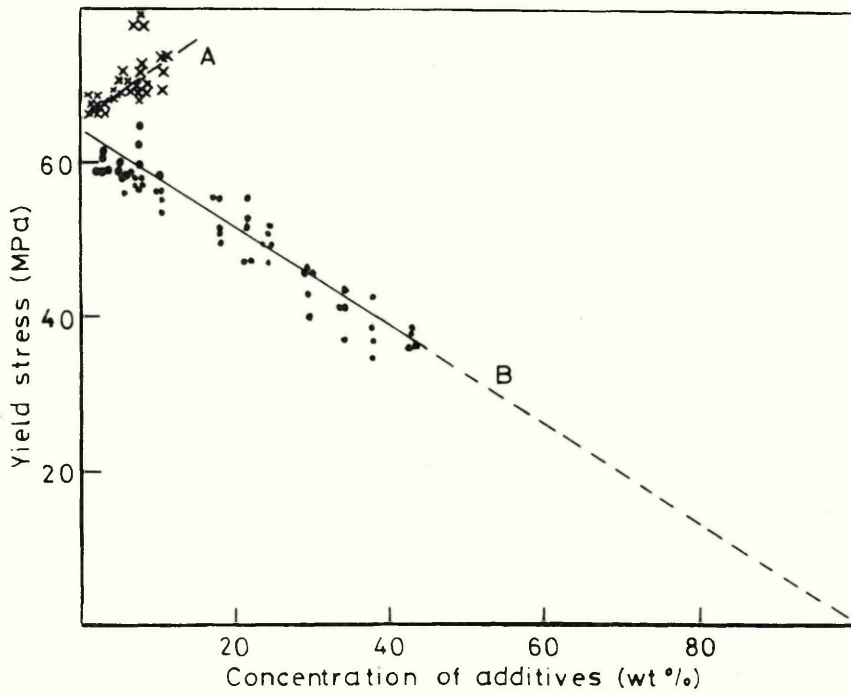
Fig. 9. Effect of additives on the tensile yield stress for UPVC: A, soluble additives; B, insoluble additives (see [60]).
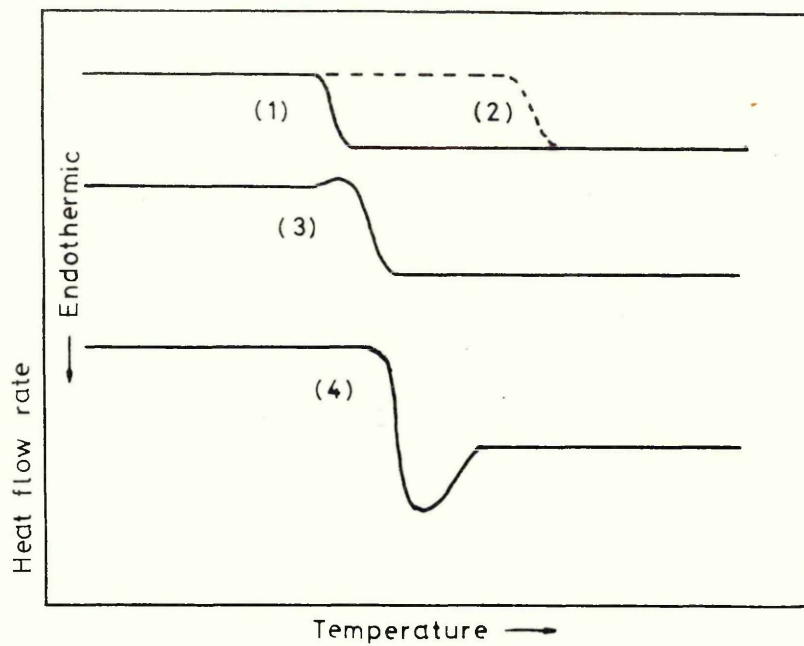
Fig.10. Changes to the glass transition curve due to differences in cooling and heating rates:

(1) slow cooling and slow heating; (2) fast cooling and fast heating; (3) fast cooling and slow heating; (4) slow cooling and fast heating.
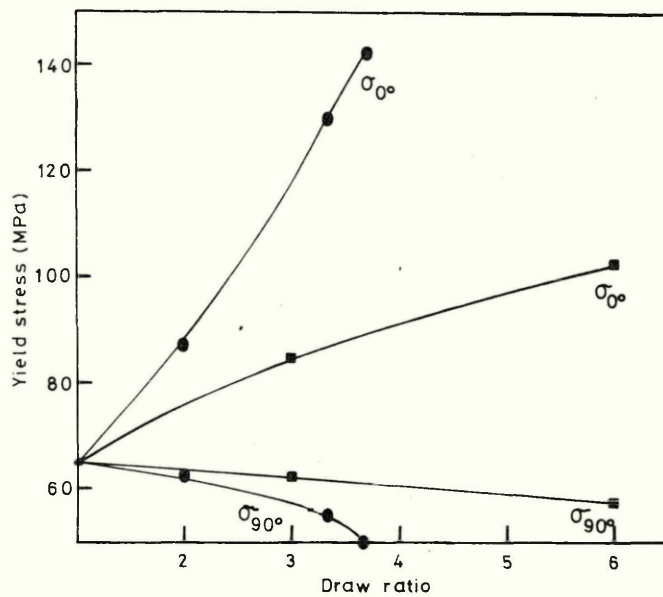
Fig.11. Variation of yield stress for UPVC measured at $\lambda = 0^{o}$ (σ_{o}) and at $\lambda = 90^{o}$ (σ_{90}) with prior draw ratio, for prior drawing at $71^{o}C$ (●) and $90^{o}C$ (■). λ is the angle between the tensile test axis and the direction of drawing (see [77]).
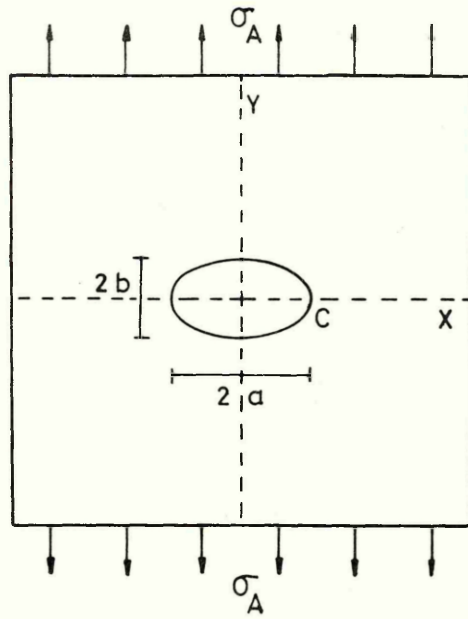
Fig. 12. Plate containing an elliptical hole, semiaxes, a and b, subjected to uniform applied tension, σ_A.
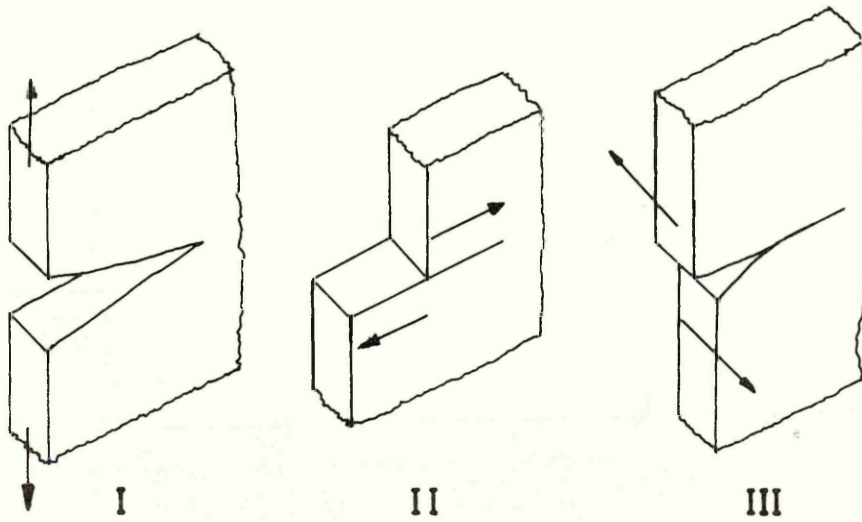
Fig. 13. Crack opening modes.
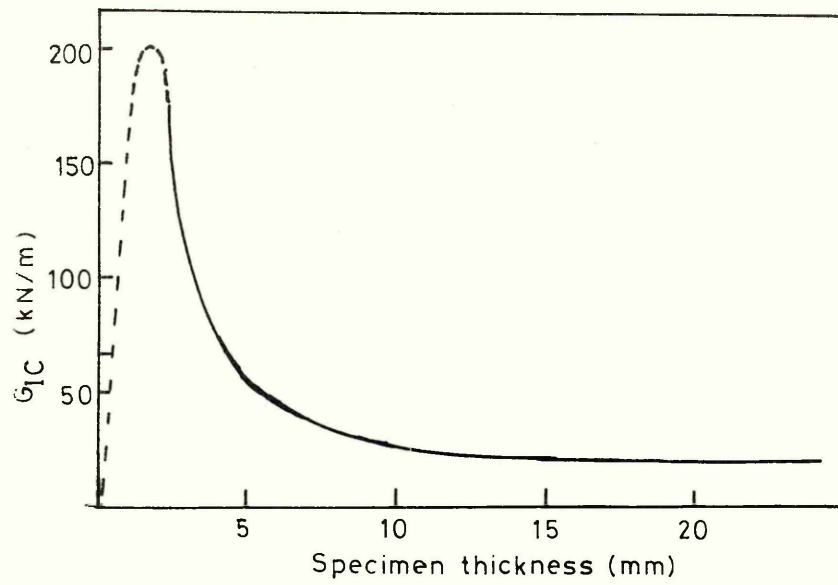
Fig. 14. Variation of G_{IC} with thickness for 7075 Alloy (Al-Zn-Mg) -T6 (See [116]).
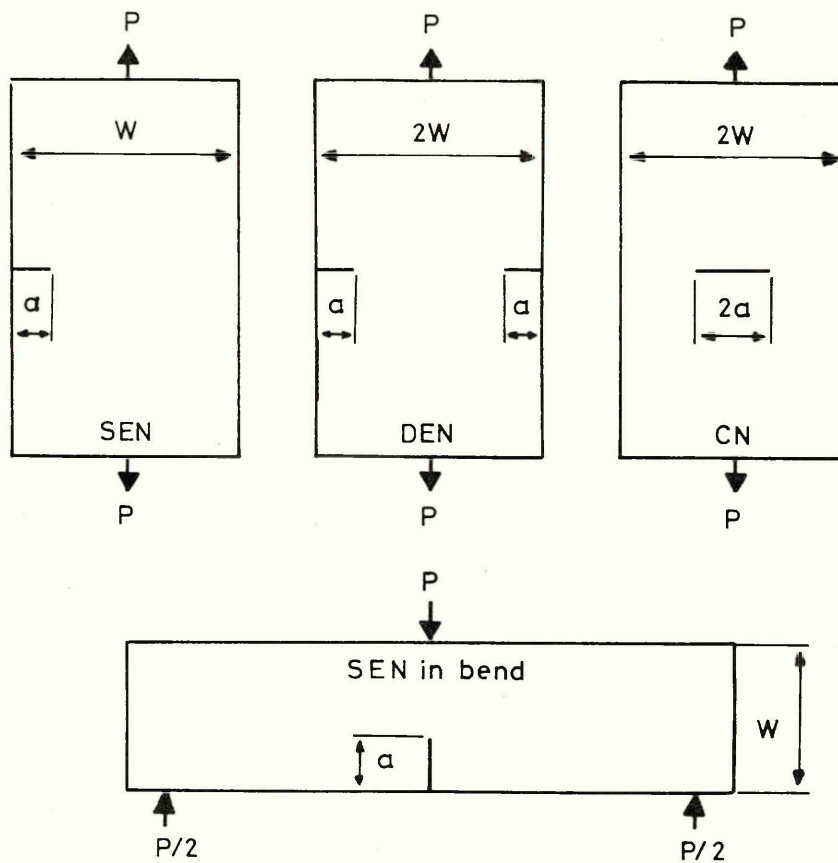
Fig. 15. Single edge notch (SEN), double edge notch (DEN), centre notch (CN) and SEN in bend test geometries.
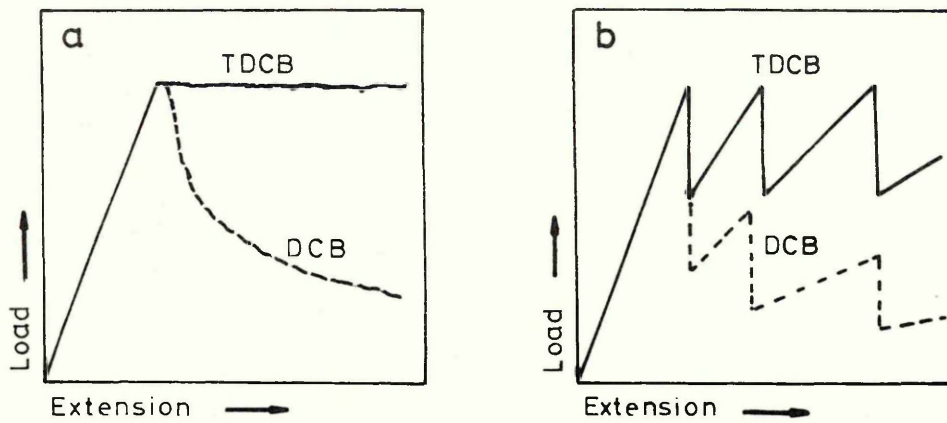
Fig. 16. Typical load extension curves for (a) slow stable crack growth and (b) stick-slip fracture for both tapered double cantilever beam (TDCB) and double cantilever beam (DCB) specimen geometries.
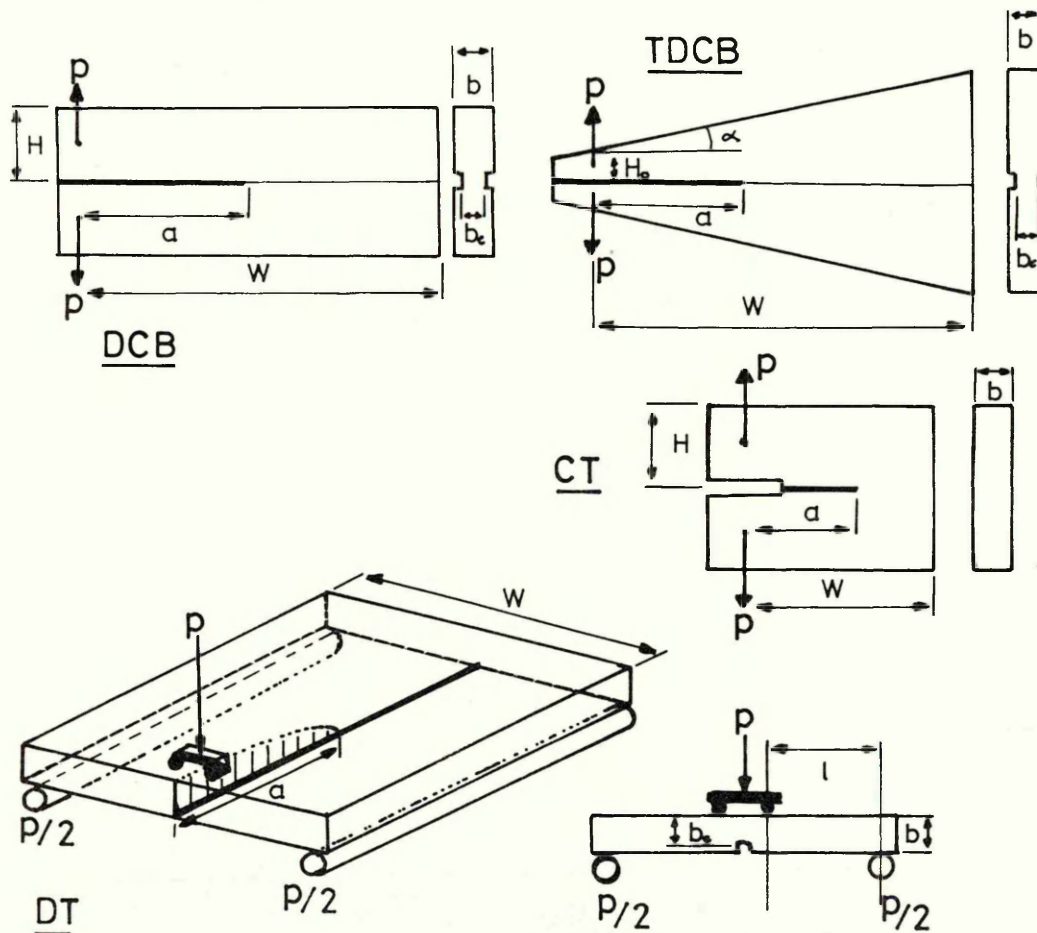
Fig. 17. Double cantilever beam (DCB), tapered double cantilever beam (TDCB), double torsion (DT) and compact tension (CT) test geometries.

-194-
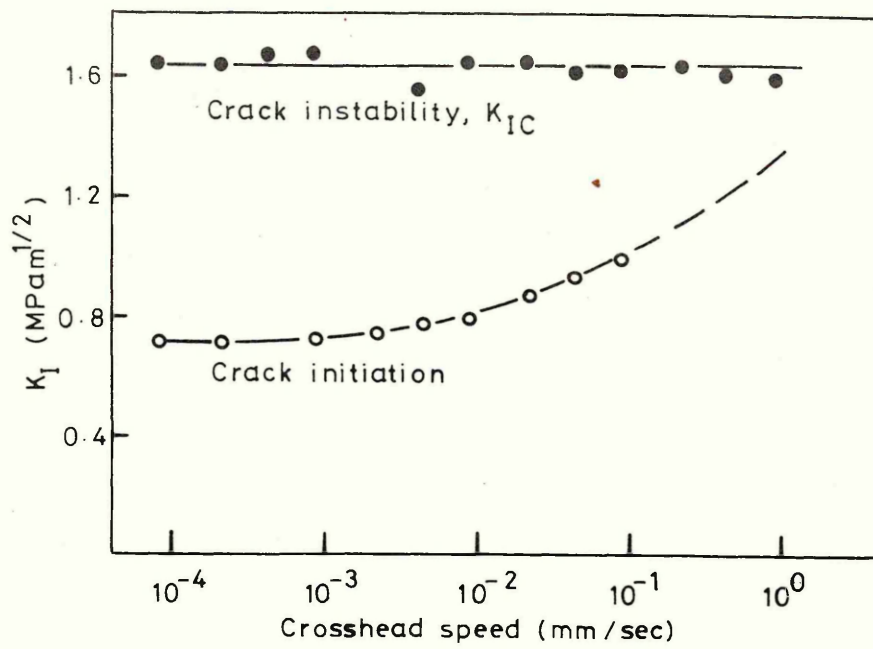
Fig. 18. Variation of K_I with crosshead speed for PMMA; (O)
crack initiation and (●) crack instability (see
[132]).
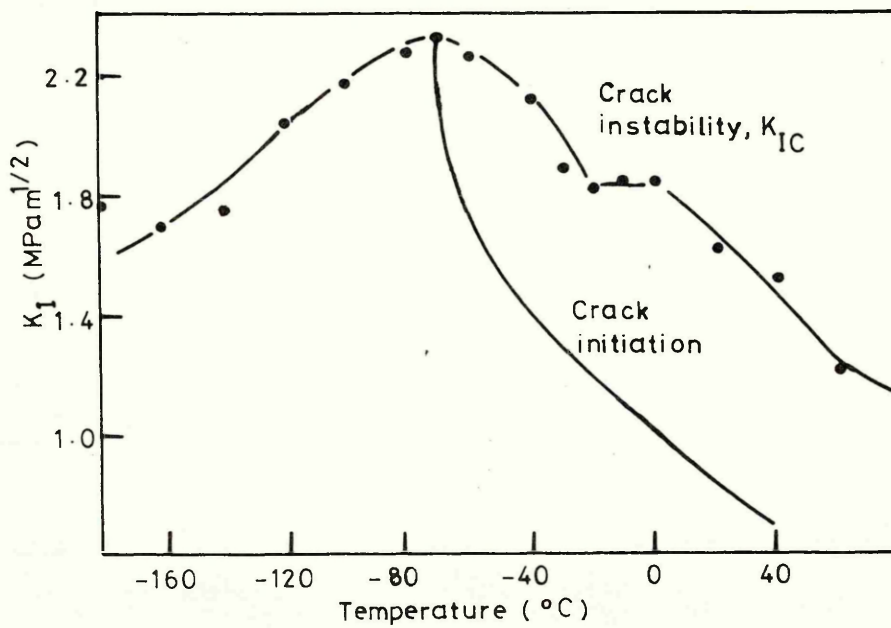
Fig. 19. Variation of K_I with temperature for PMMA (see [132]).
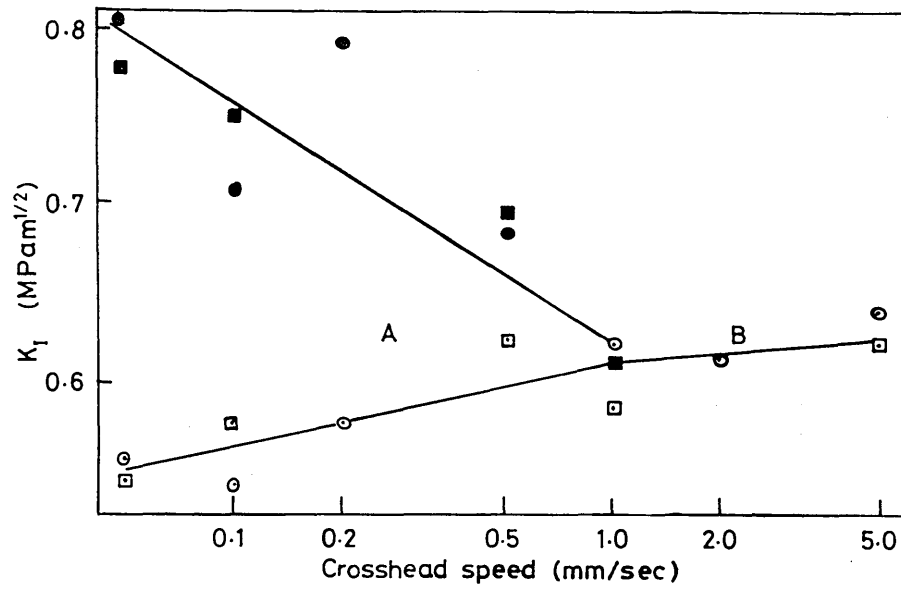
Fig. 20. Variation of K_I with crosshead speed for epoxy resin:
(▫ , ■) 6mm thick specimen, (⊙ , ●) 3.7mm thick
specimens, region A stick slip fracture, region B
continuous crack growth (see [145]).
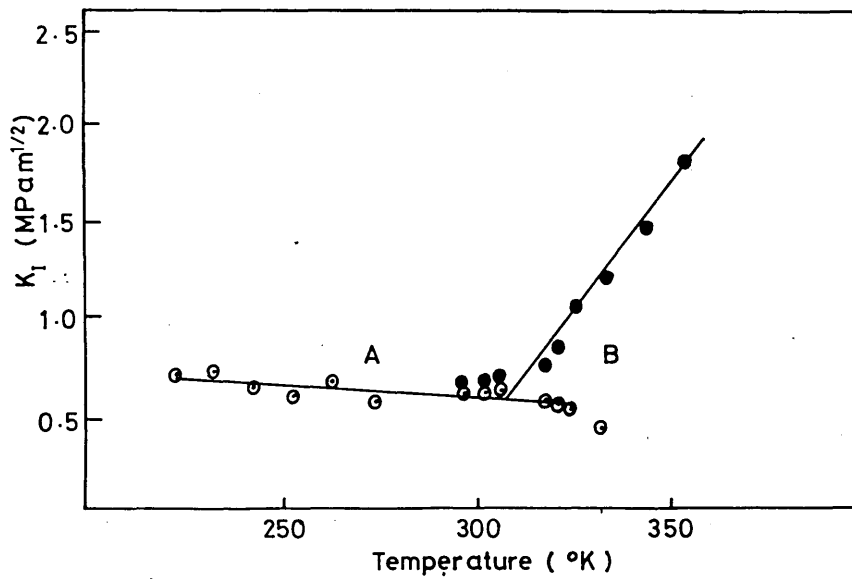
Fig. 21. Variation of K_I with temperature for epoxy resin:
region A continuous crack growth, B stick-slip fracture
(see [145]).
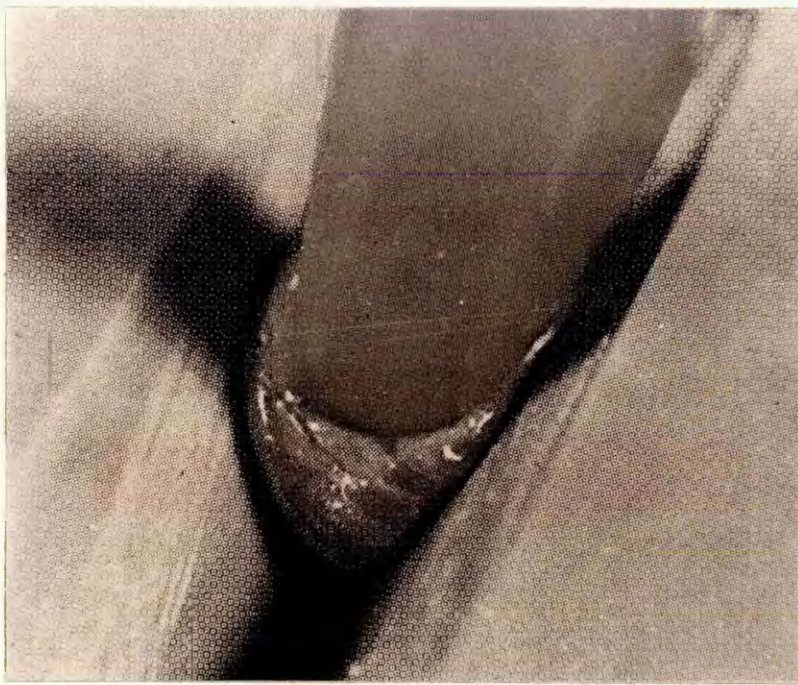
Fig. 22. Bow wave of softened material at the base of the weld
rod during hot gas welding UPVC, this is taken to
indicate that the correct welding conditions are
being used (see [165]   ).
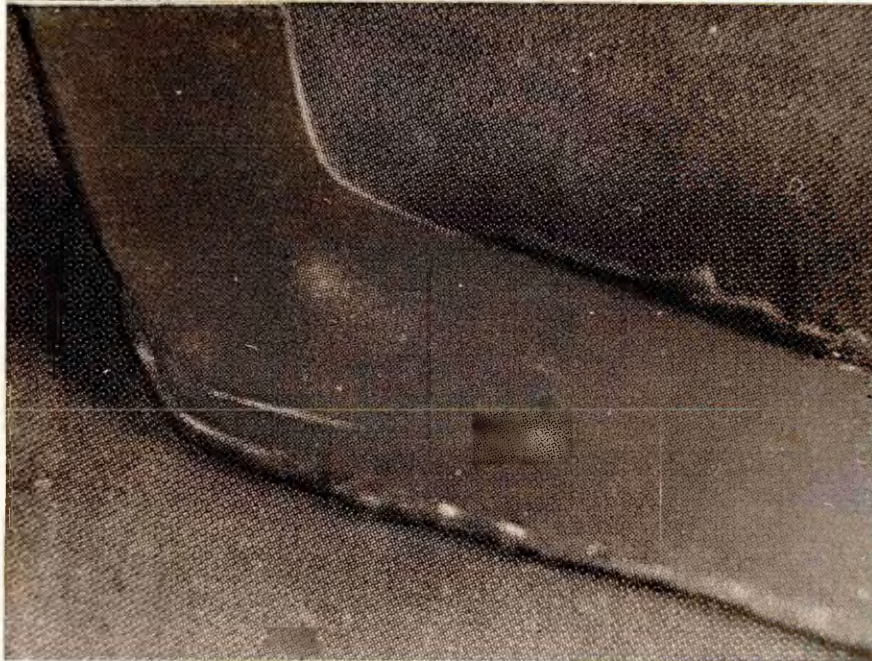
Fig. 23. Ripple of softened weld rod material along both sides
of the weld rod as seen after correct welding
(see   [165]   ).
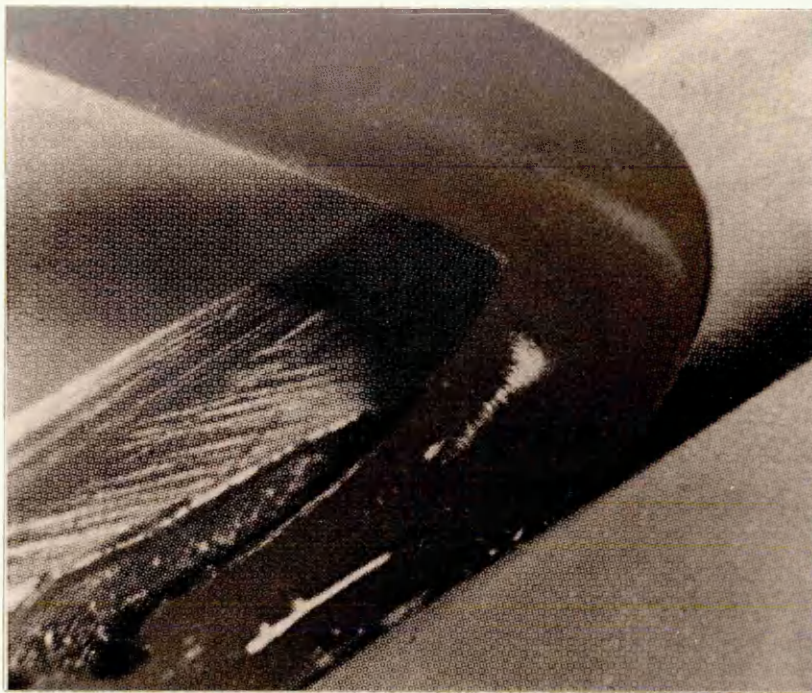
Fig. 24. Stretching of the weld rod will result if the weld
rod is pushed into the weld at an angle less than 90°,
(see [165]).

Fig. 25. In cases where the weld rod has been stretched fracture
of the rod may occur either when it is being welded
or during latter passes of rod (see [165]).
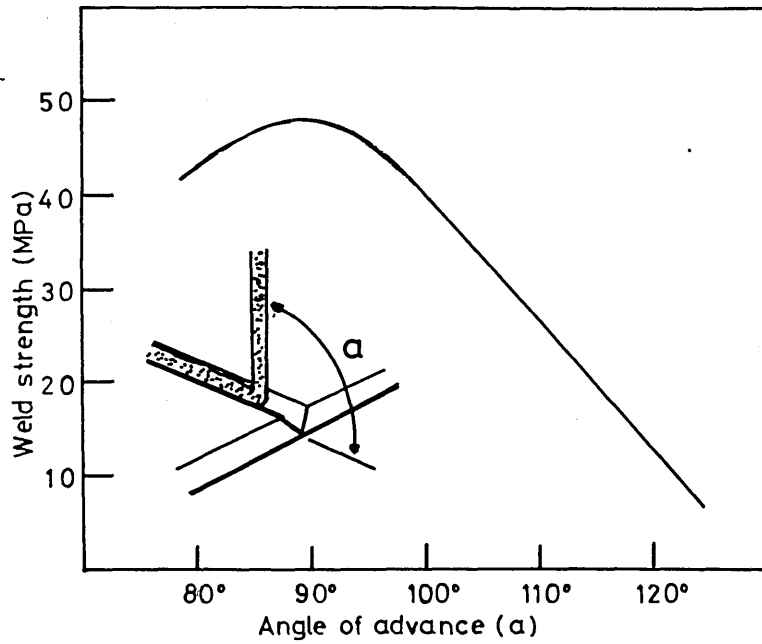
Fig. 26. Variation of UPVC weld strength with the angle at which the weld rod is held during welding (see [1]).
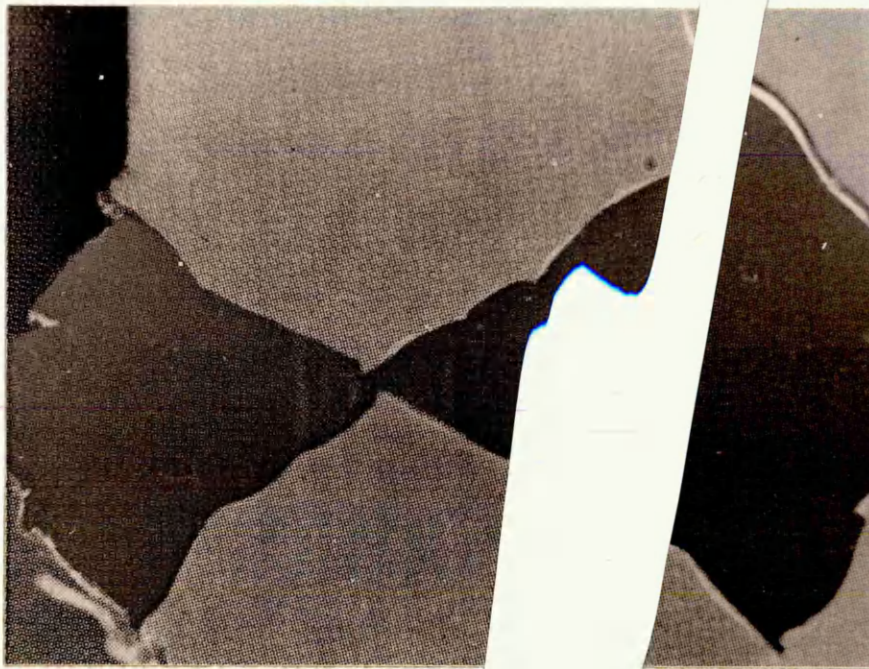
Fig. 27.   Satisfactory double-vee butt   see [165]   ).
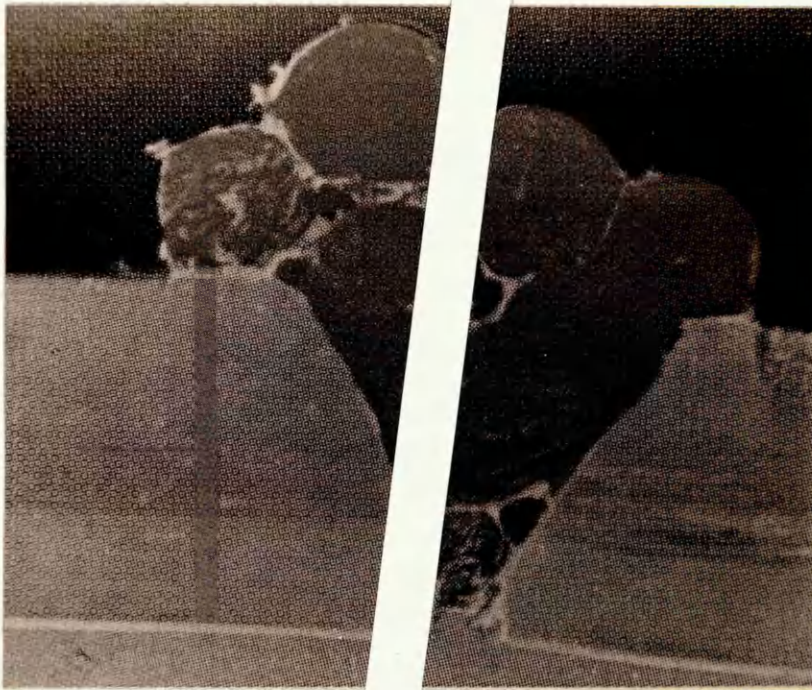
Fig. 28.   Single-vee butt weld   ried out with too low a gas
           temperature, note li   deformation and fusion of
           the rods (see   [165]

Fig. 29. Single-vee butt weld carried out with too high a gas temperature, note charring of rod and sheet at the weld root (see [165]).
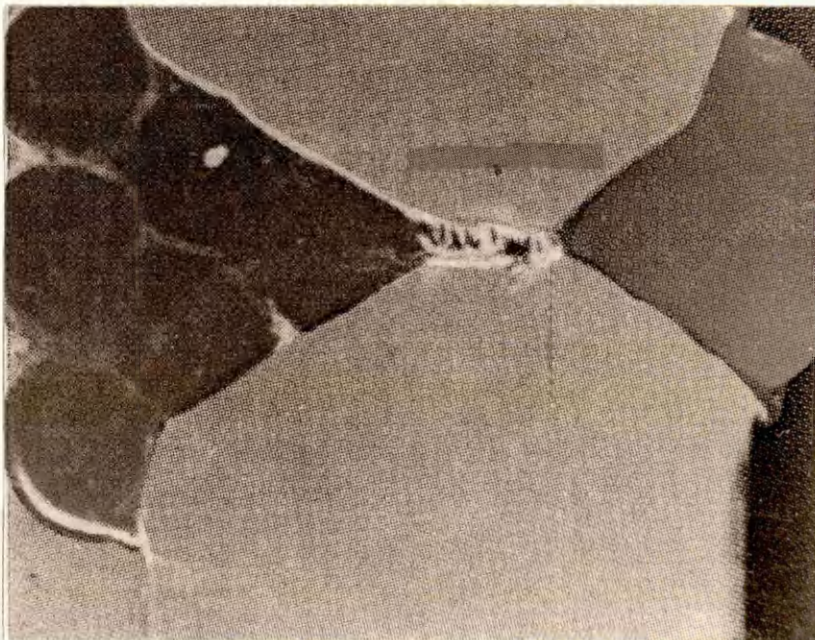
Fig. 30. Double-vee butt weld, unsatisfactory because of insufficient root penetration (see [165]).
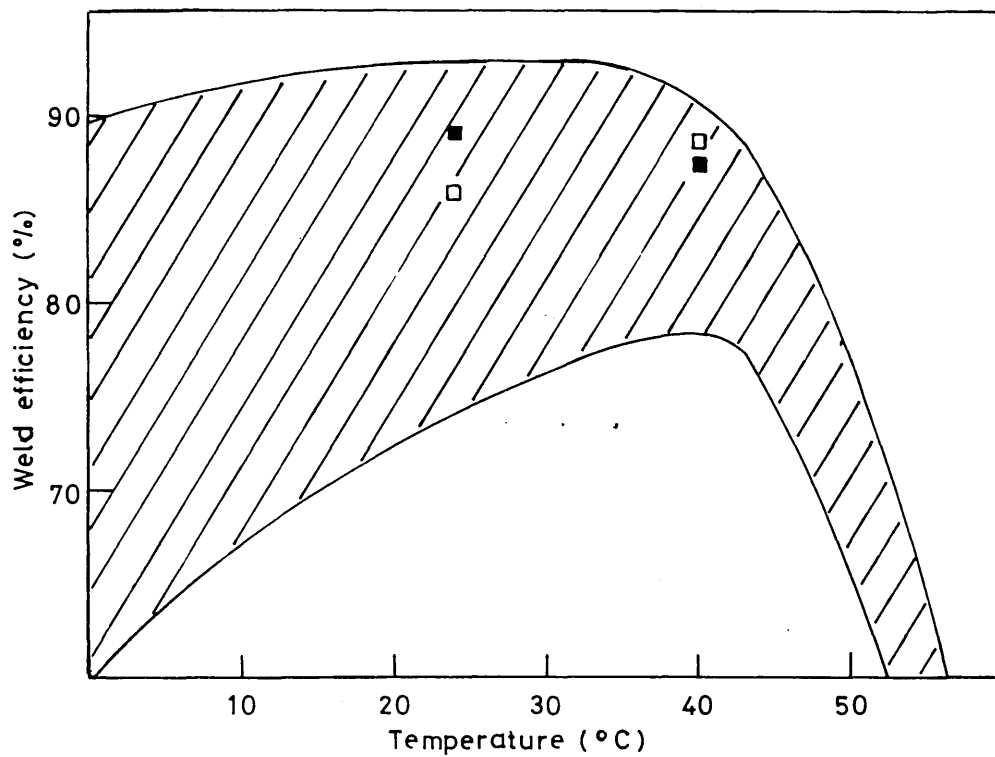
Fig. 31. Variation of emulsion polymerised UPVC weld strength
with temperature : (□) double-vee butt weld in 8mm
thick sheet, (■) single-vee butt weld in 4mm thick
sheet (see [168]).
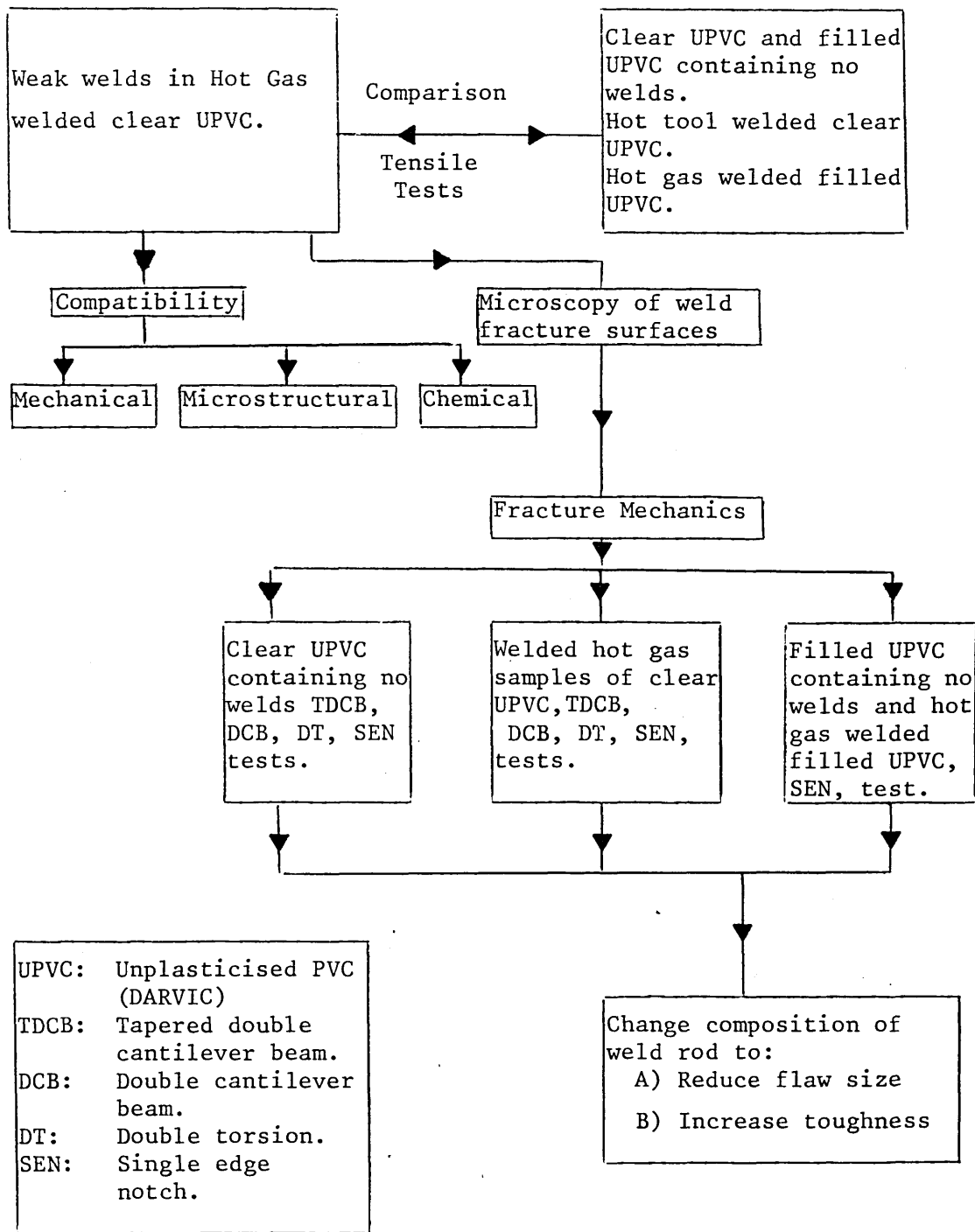
Fig. 32. Flow chart of the work programme.
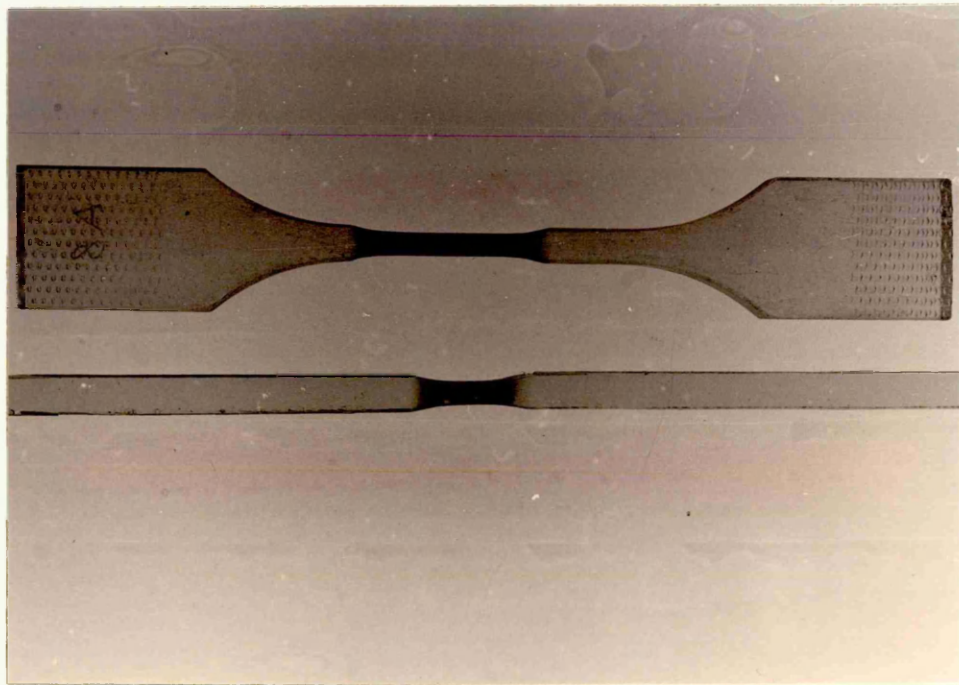
Fig. 33. Dumbbell and parallel-sided tensile test specimen,
note yielding occurring at centre of both specimens.
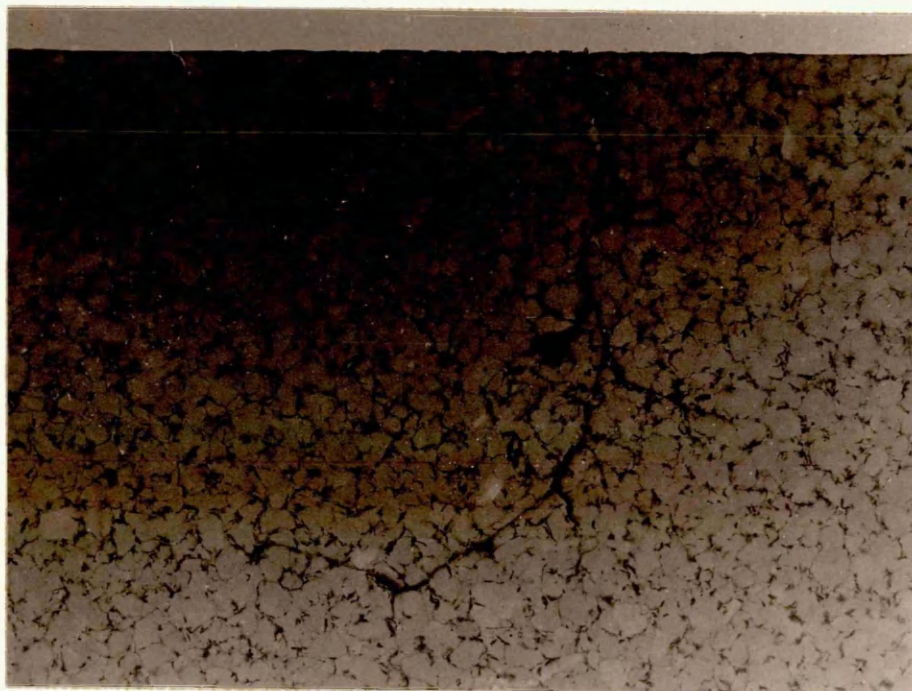
Fig. 34. Pressed sheet of weld rod material showing its retained
granular nature.
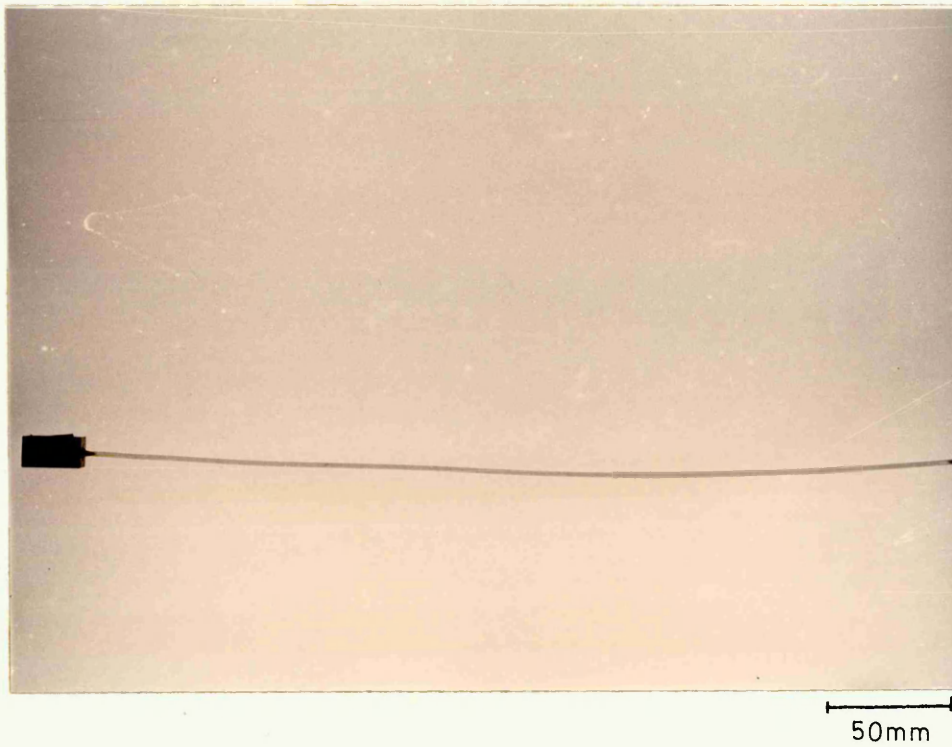
Fig. 35.   Weld rod, bonded into a steel block, which has drawn
           its entire length before failure.
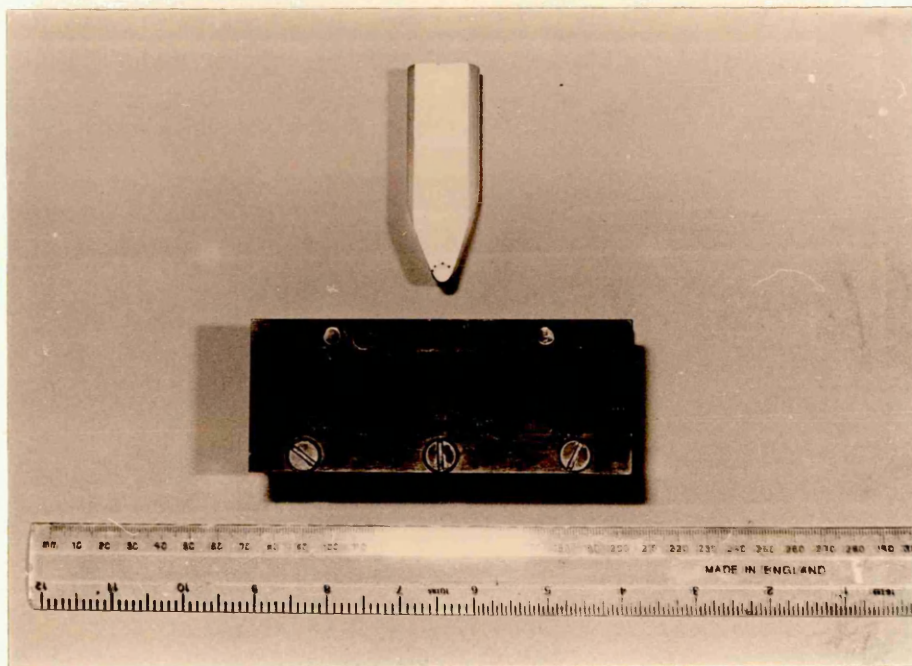
Fig. 36.   Three-point bend rig.
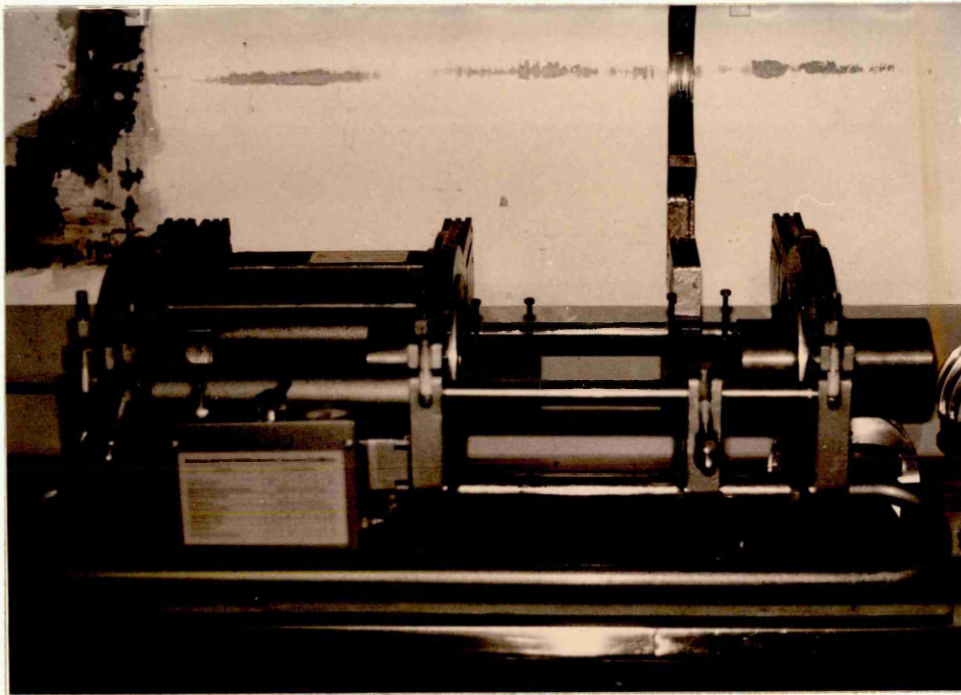
Fig. 37.   Hot tool pipe welding rig.
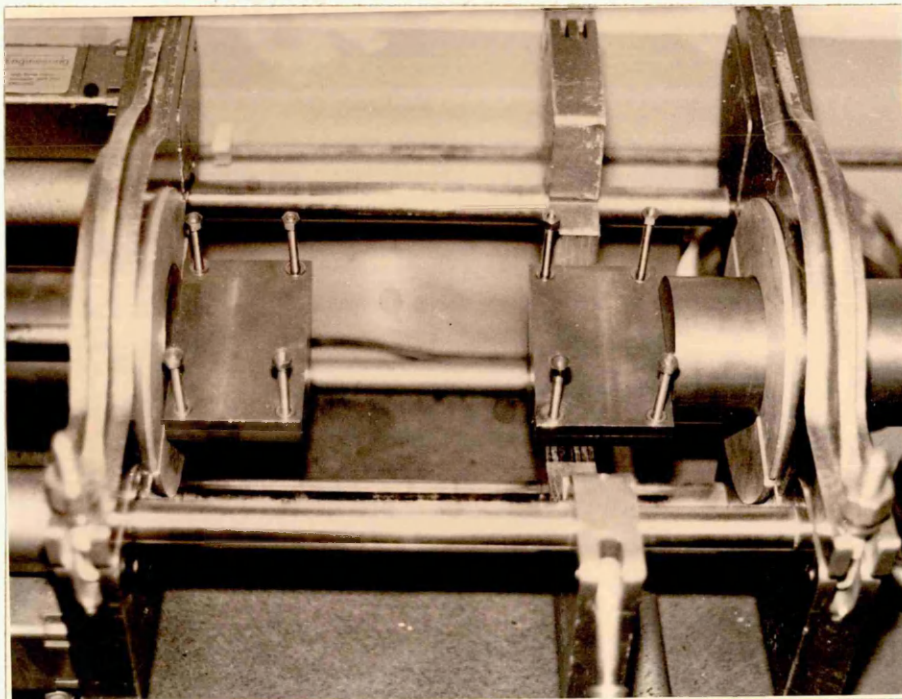
Fig. 38.   Plate holders fitted into pipe clamps.
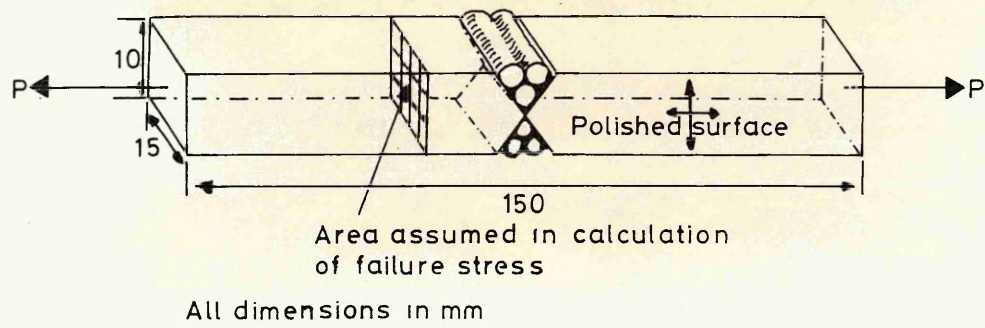
Fig. 39.   Weld tensile test piece.
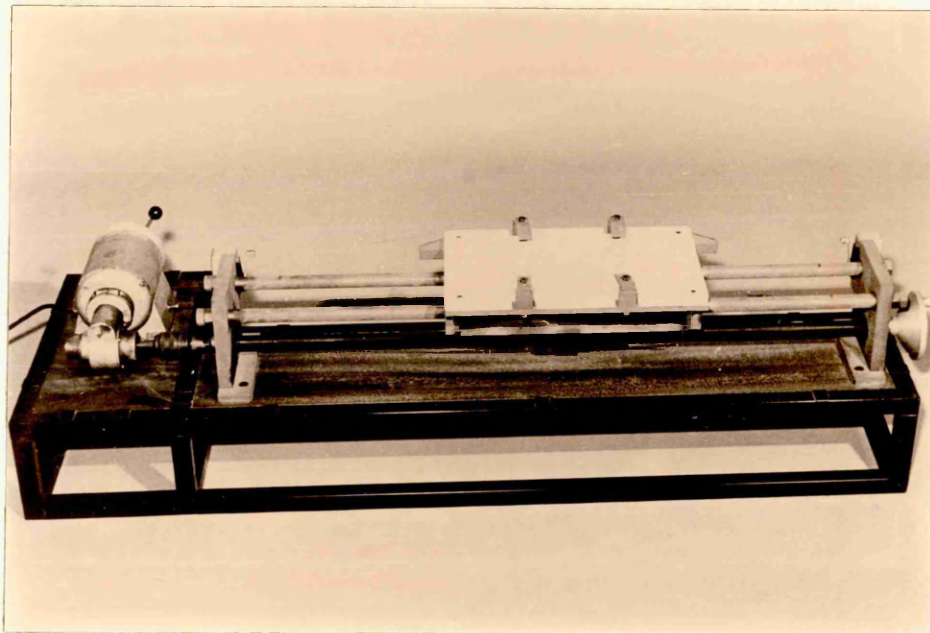
Fig. 40.   Automatic weld rig, weld bed and drive assembly.
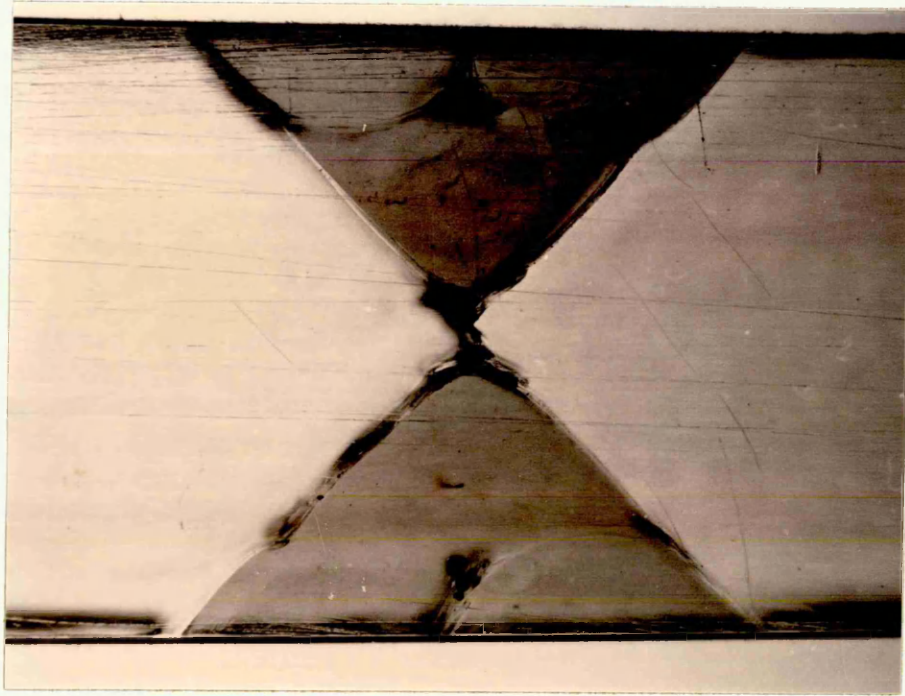
Fig. 41. Weld tensile test piece, dressed.
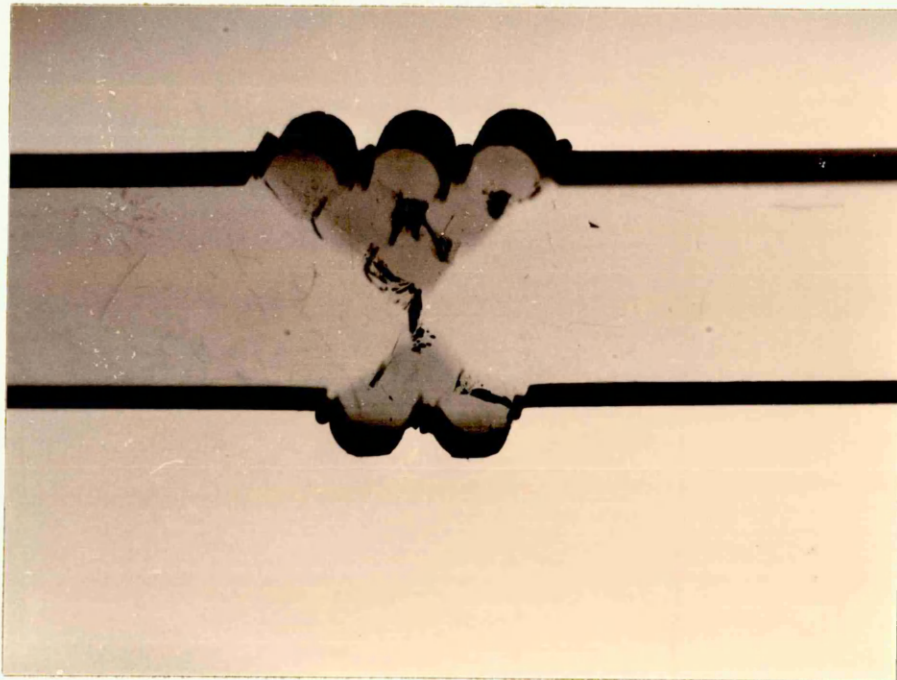
Fig. 42. Asymmetric weld configuration as used by the Plastics
Construction welder.
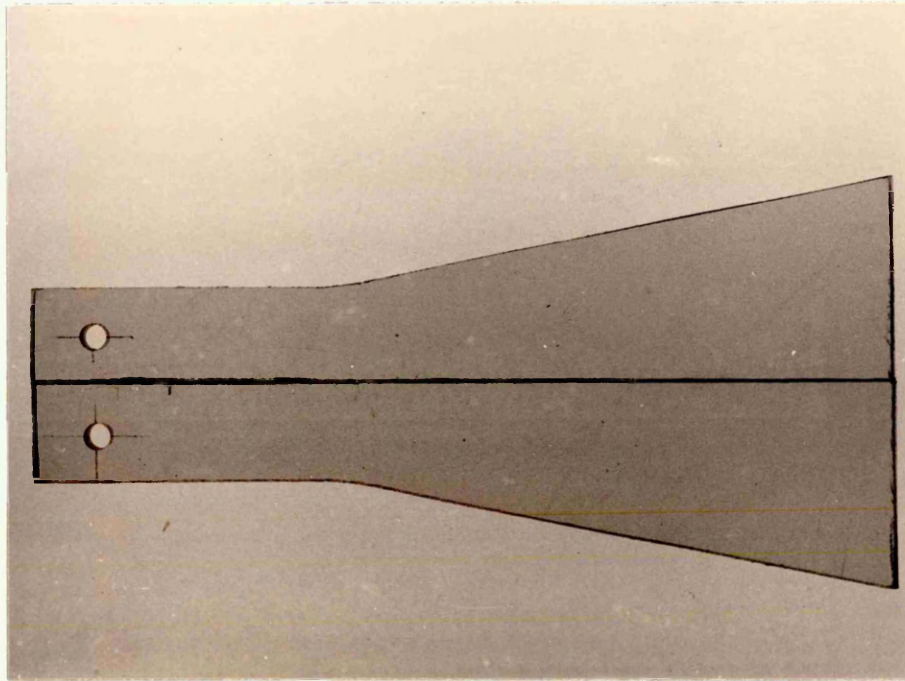
Fig. 43.   Tapered double cantilever beam test specimen;
$\alpha = \tan^{-1} 0.2$, H_o = 15mm, shoulder height 30mm,
length of specimen, from the loading line, 250mm.
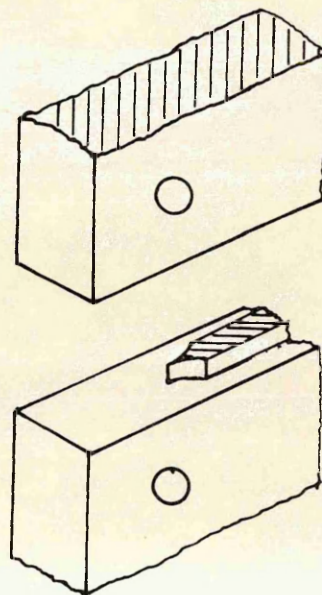
Fig. 44.   Swallow tail section used to ease crack growth in
tapered double cantilever beam specimen.
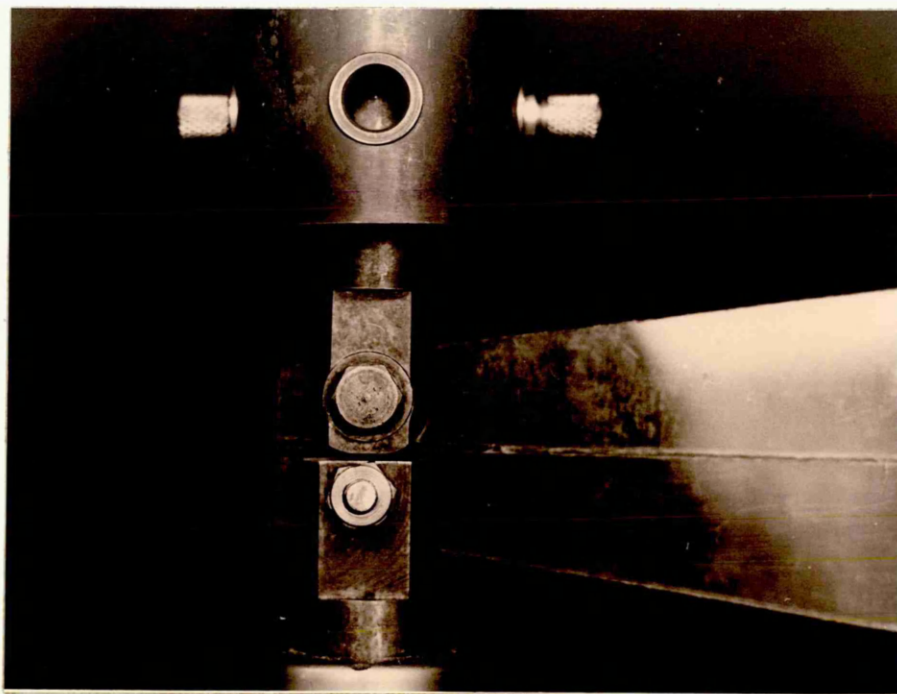
Fig. 45.   Clamps used to apply the load to the tapered double
           cantilever beam and double cantilever beam specimens.
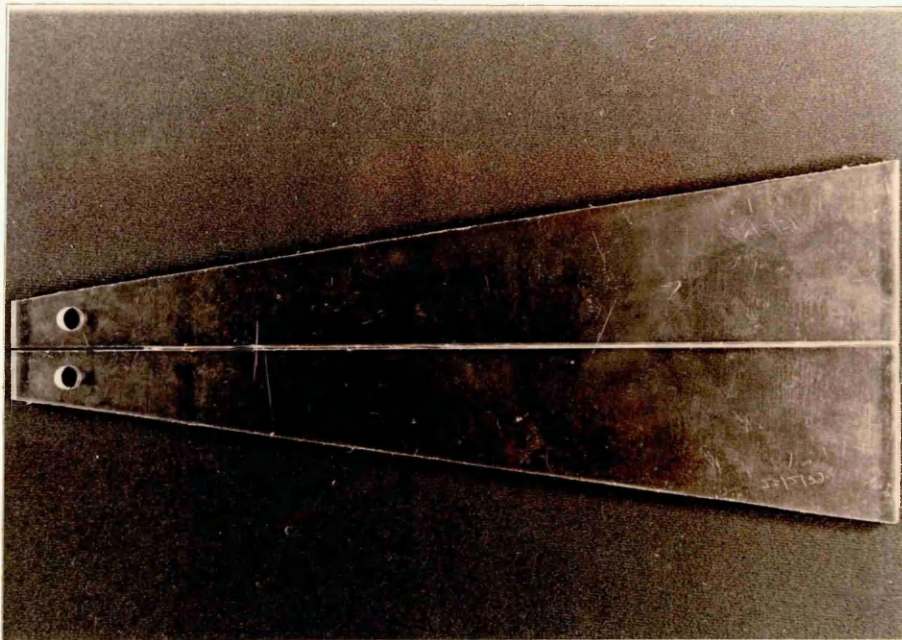
Fig. 46.   Tapered double cantilever beam test specimen:
           $\alpha = \tan^{-1} 0.15$, $H_O = 19mm$, length of specimen,
           from the loading line, 295mm.
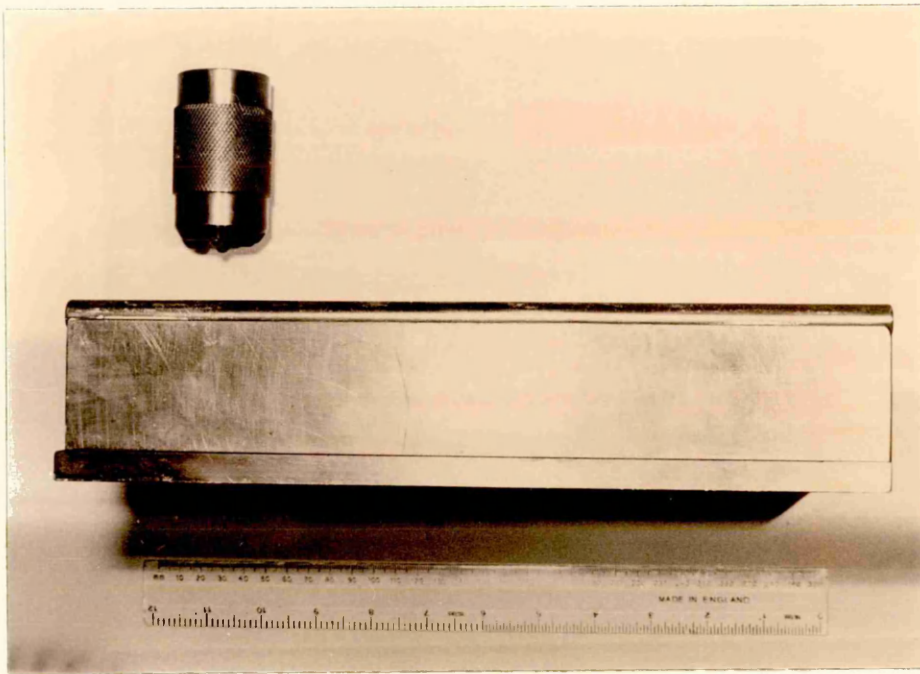
Fig. 47.   Double torsion test rig.
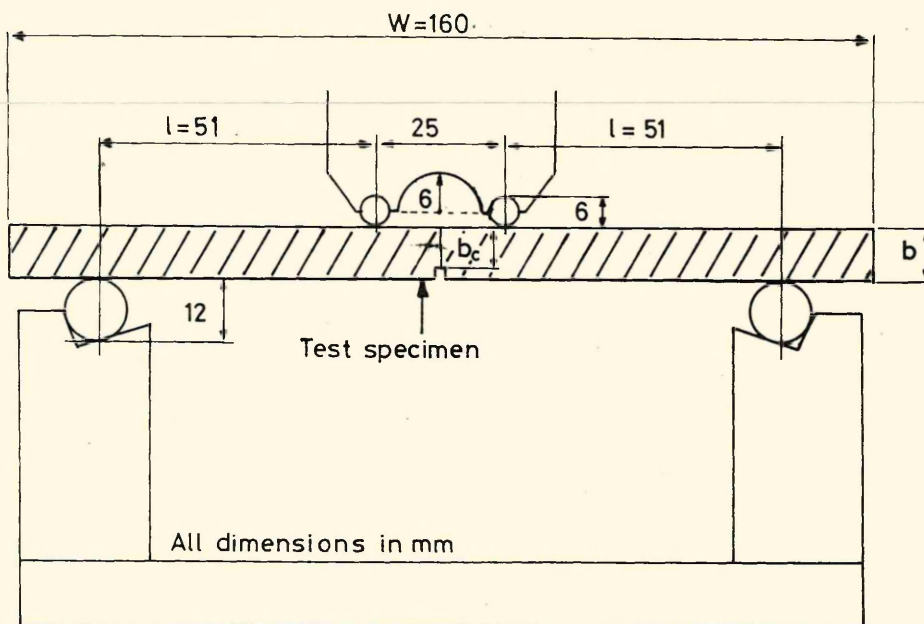
Fig. 48.   Details of the loading plunger and support system
for the double torsion test rig.
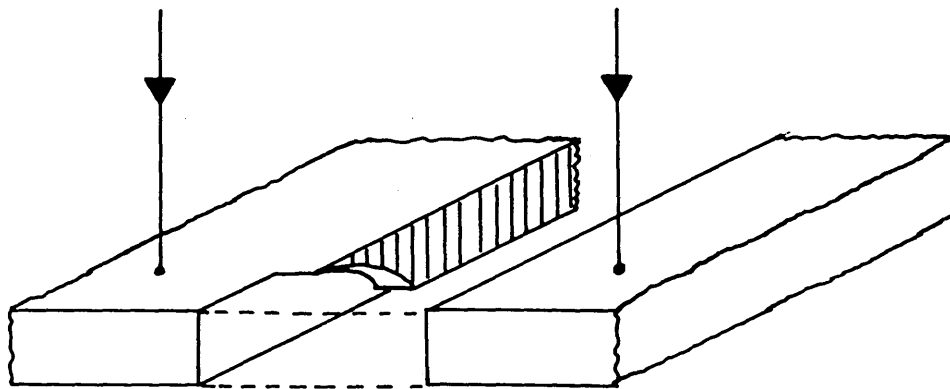
Fig. 49. Reduced groove section at the initial crack position
for double torsion test specimens.
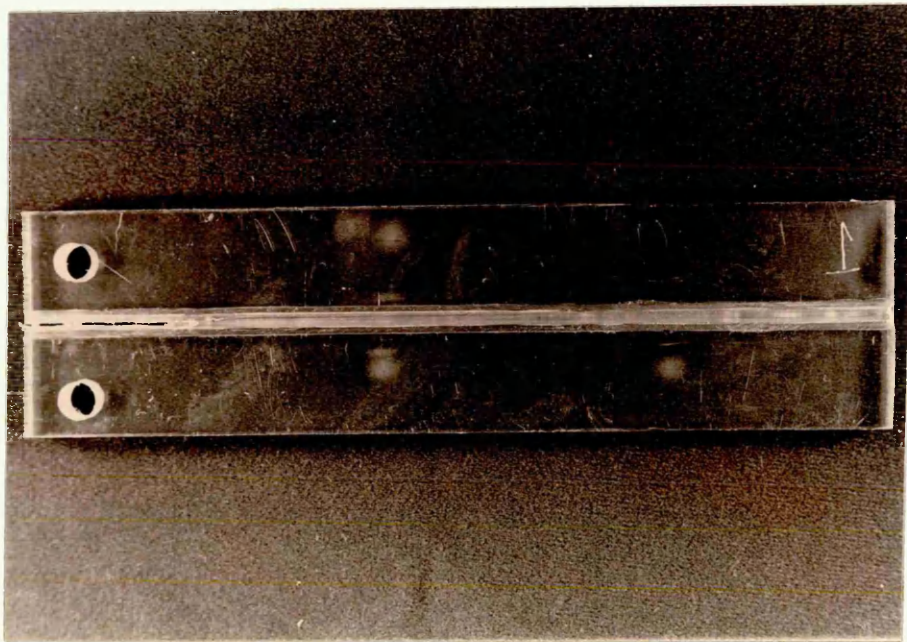
Fig. 50.   Welded double cantilever beam test specimen: H = 25mm.
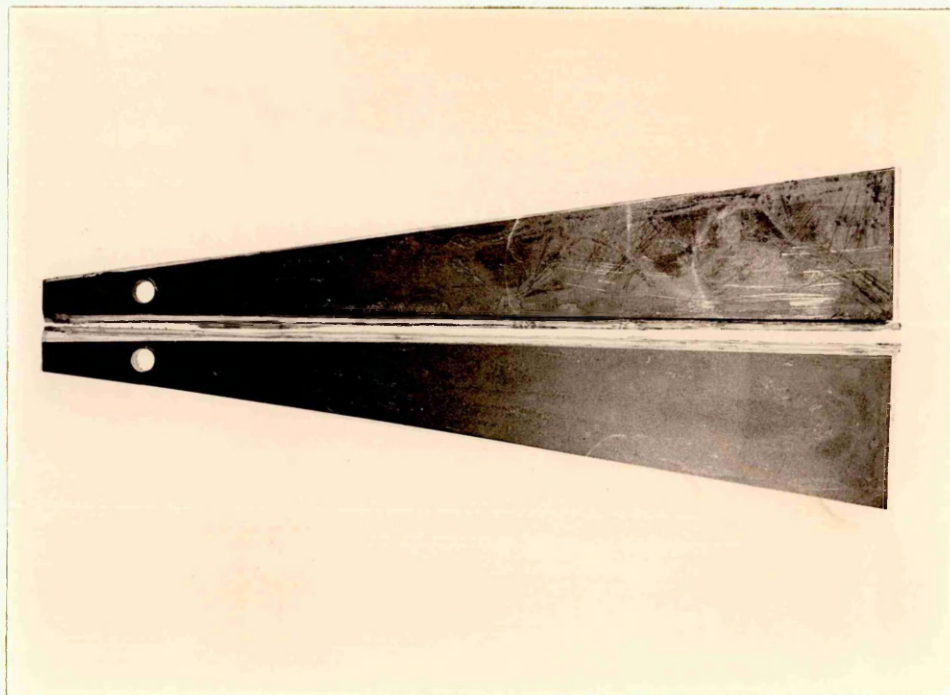
Fig. 51.   Welded tapered double cantilever beam tests specimen
           with bonded steel side plates; $\alpha = \tan^{-1} 0.15$, H_o = 20mm,
           length of specimen, from loading line, 265mm.

-213-
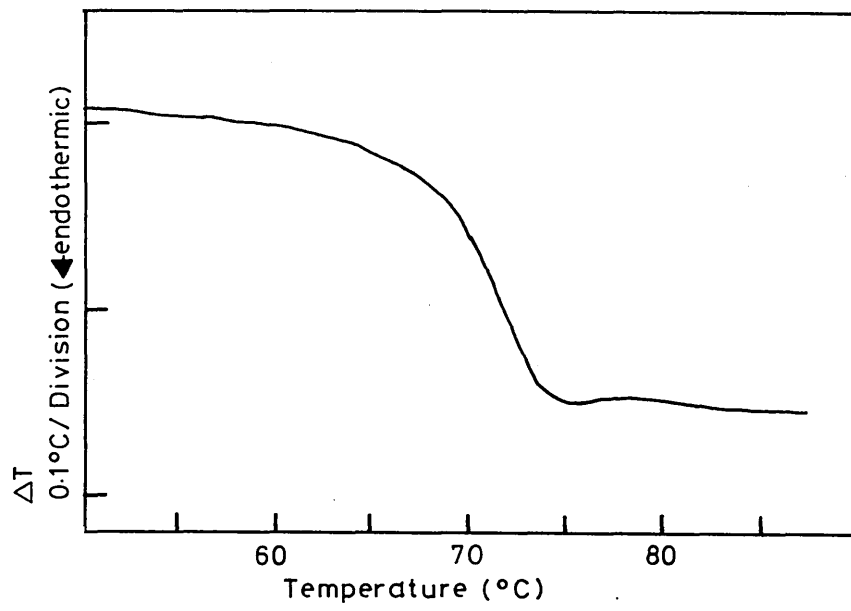
Fig. 52.   DSC thermogram for clear UPVC sheet.
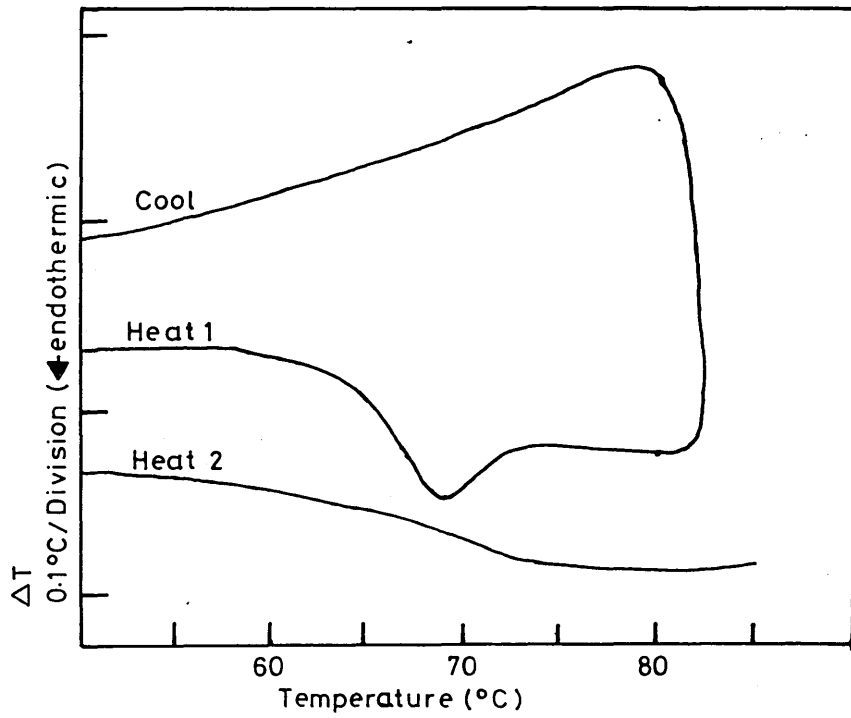
Fig. 53.   DSC thermogram for clear UPVC weld rod showing the
effect of cycling.
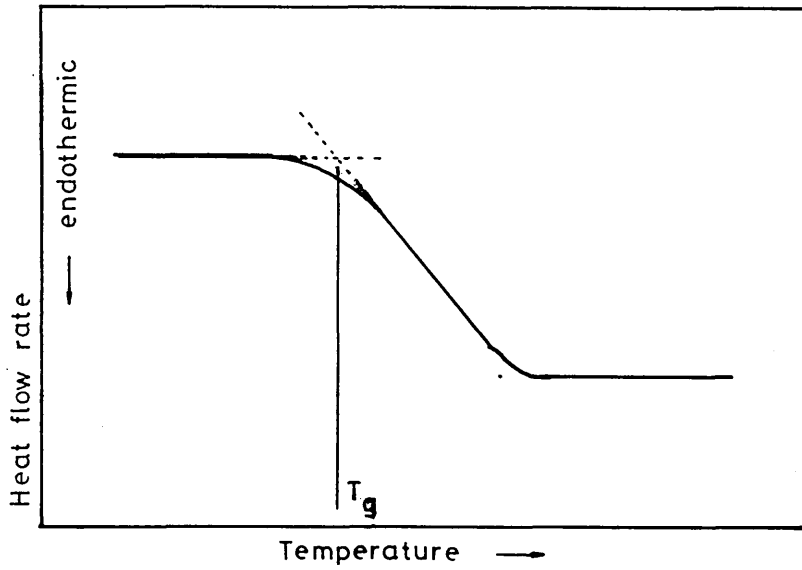
Fig. 54. Crossed line method of determining T_g from the DSC thermogram (see [175]).
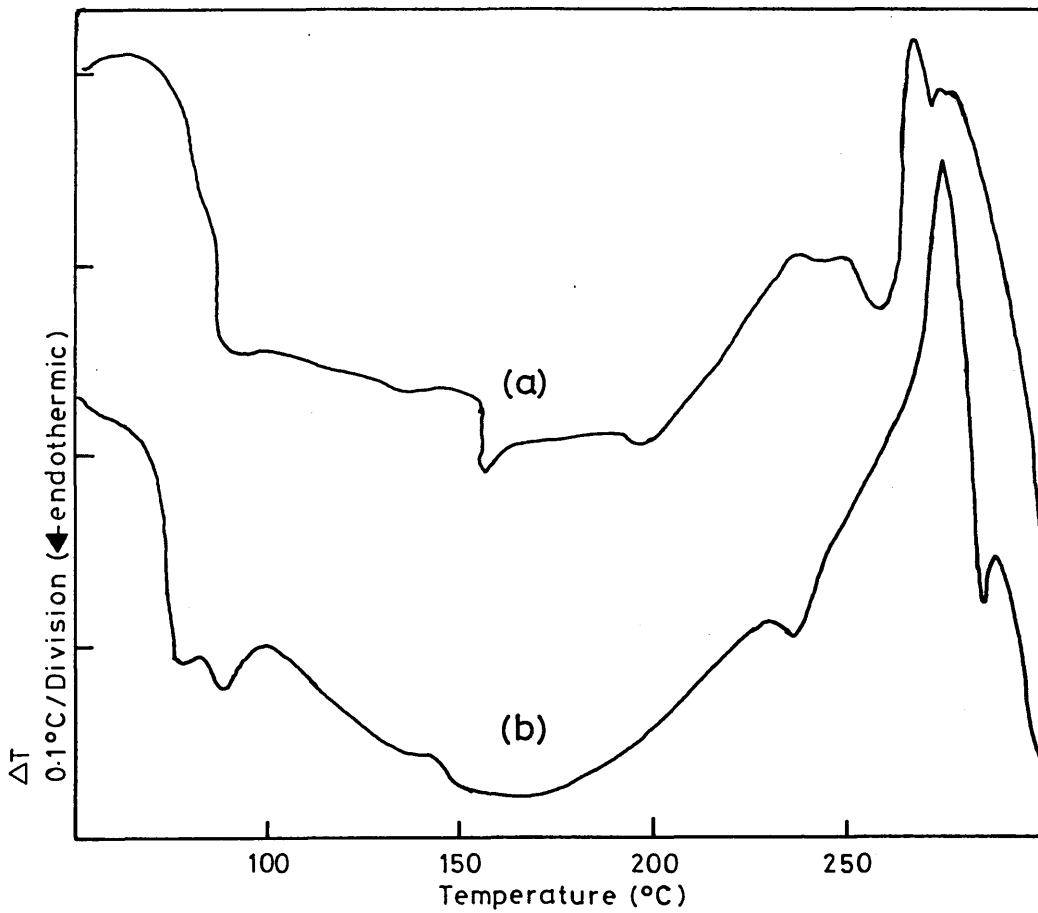
Fig. 55. DSC thermogram for clear UPVC sheet and clear weld rod over the temperature range 30-300°C.
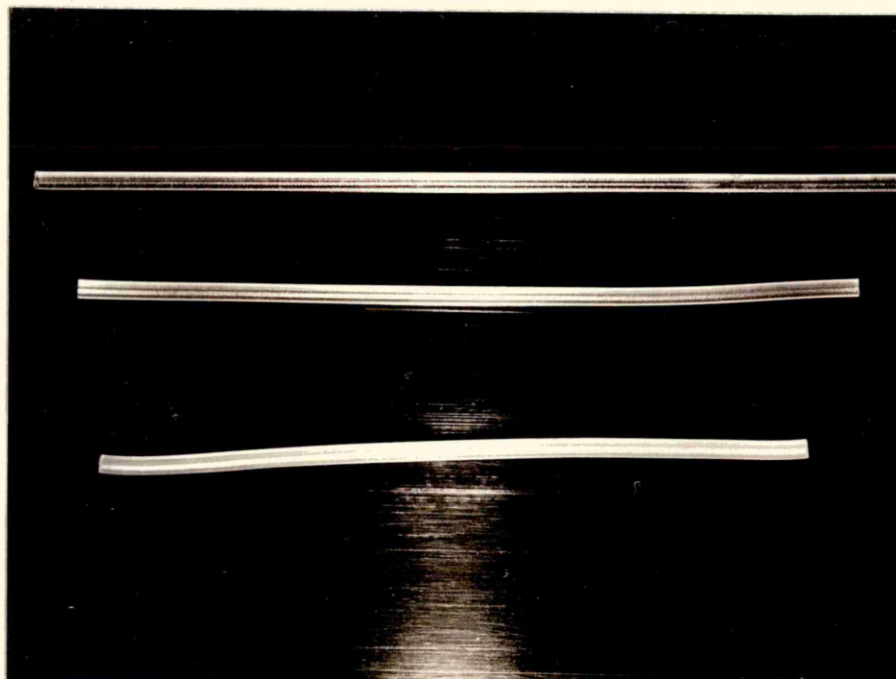
Fig. 56. Length shrinkage in weld rod. Top, 150mm length of rod; middle, 150mm length of rod after 1 min at 180°C; bottom, 150mm length of rod after 5 min at 180°C.
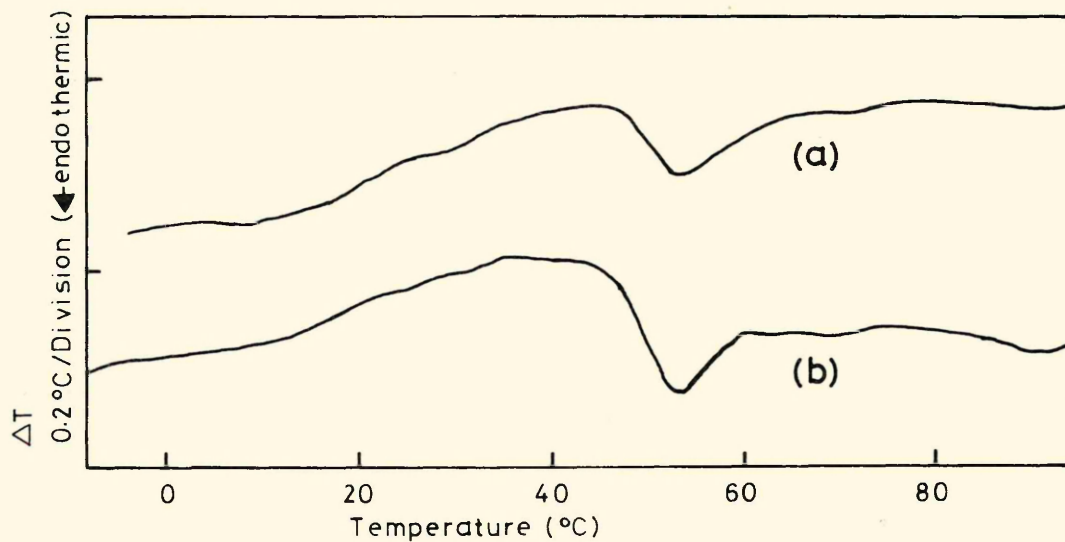
Fig. 57. DSC thermograms for the post-Soxhlet extraction PVC granules: (a) sheet and (b) clear weld rod after the second 2 day ether extraction.
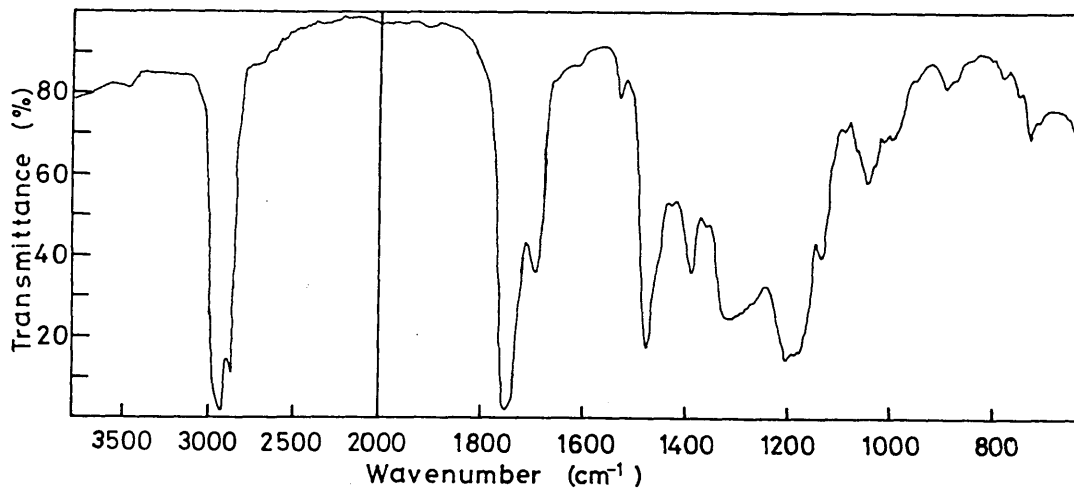
Fig. 58. I-R spectrum for additives extracted from clear UPVC sheet.
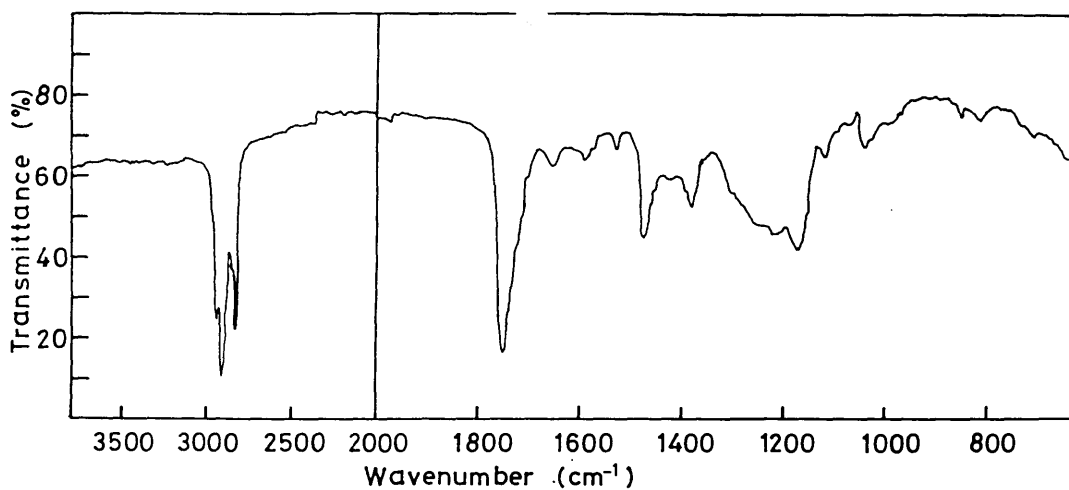
Fig. 59. I-R spectrum for additives extracted from ICI weld rod.
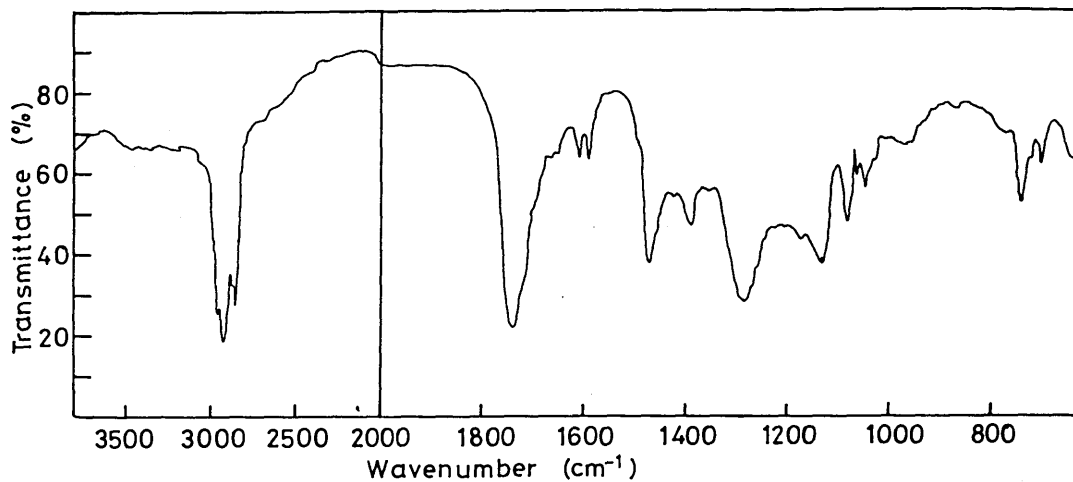
Fig. 60. I-R spectrum for additives extracted from clear weld rod.
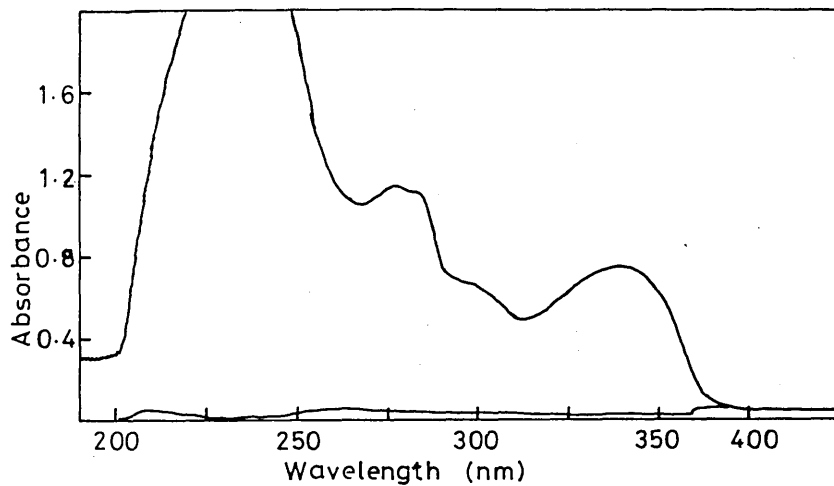
Fig. 61. U-V spectrum for additives extracted from clear UPVC sheet.
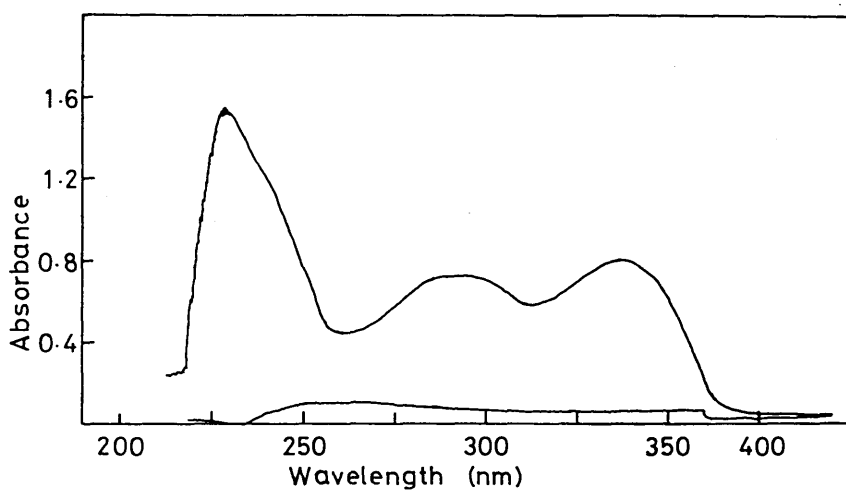
Fig. 62. U-V spectrum for additives extracted from ICI weld rod.
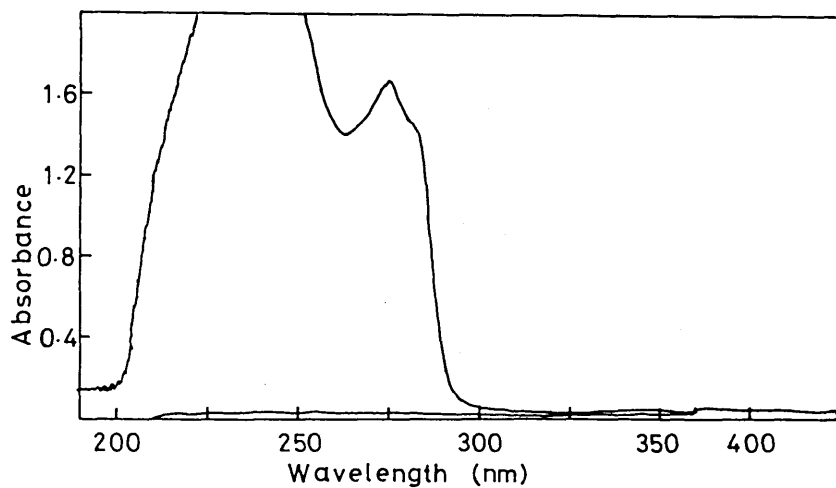
Fig. 63. U-V spectrum for additives extracted from clear weld rod.
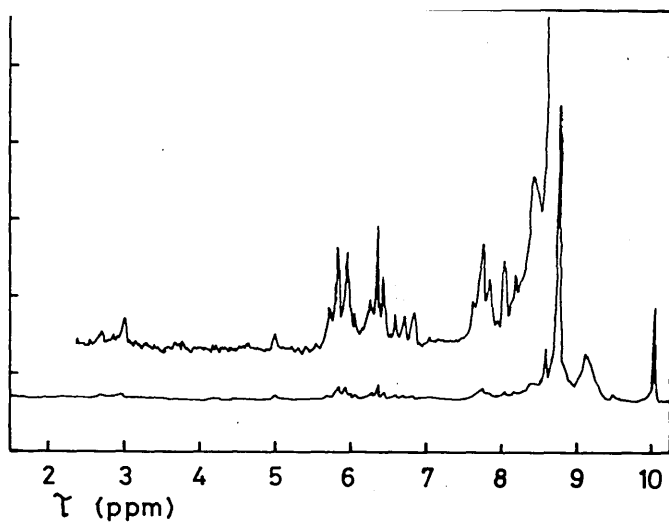
Fig. 64. NMR spectrum for additives extracted from clear UPVC sheet.
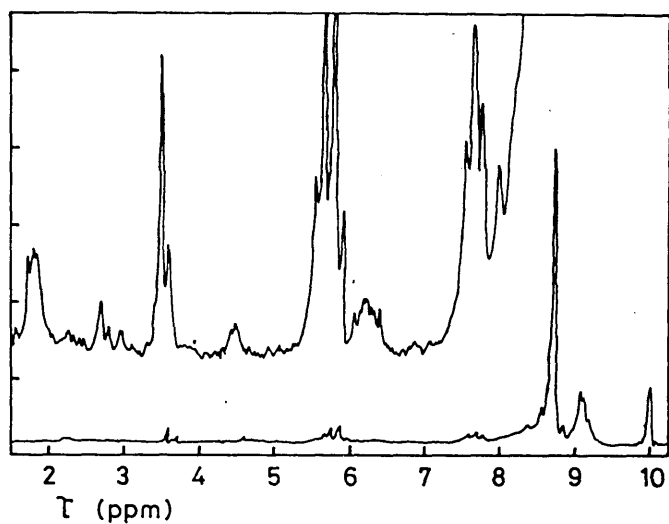
Fig. 65. NMR spectrum for additives extracted from ICI weld rod.
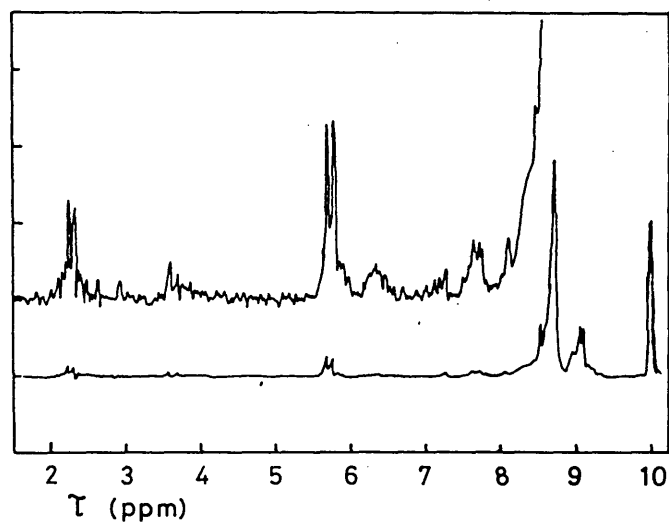
Fig. 66. NMR spectrum for additives extracted from clear weld rod.
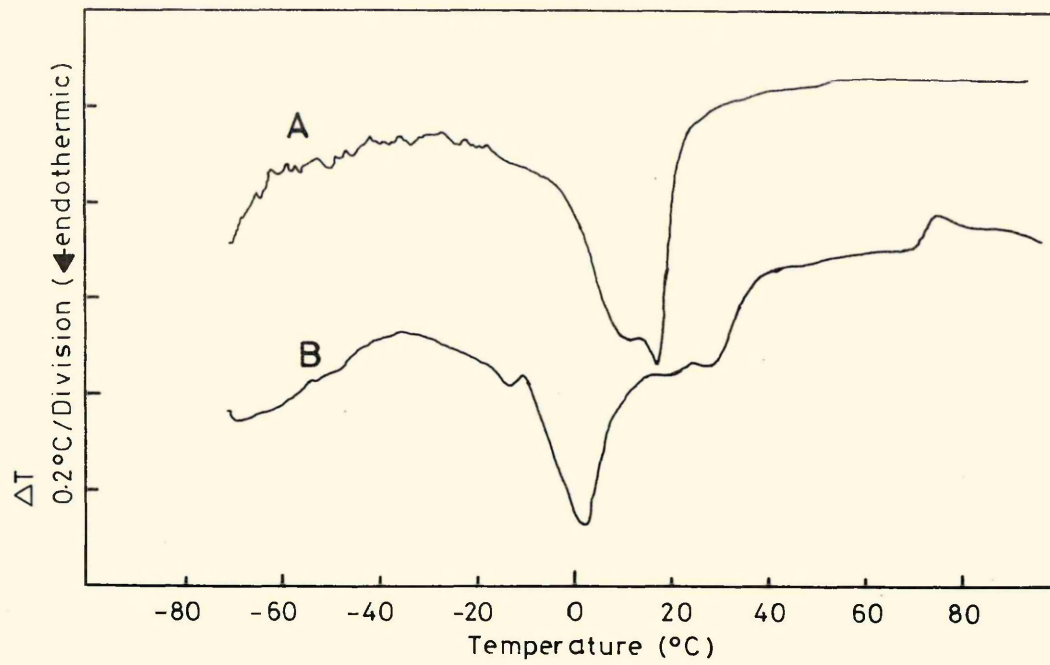
Fig. 67. DSC thermogram for additives extracted from: A, clear UPVC sheet and B, clear weld rod.
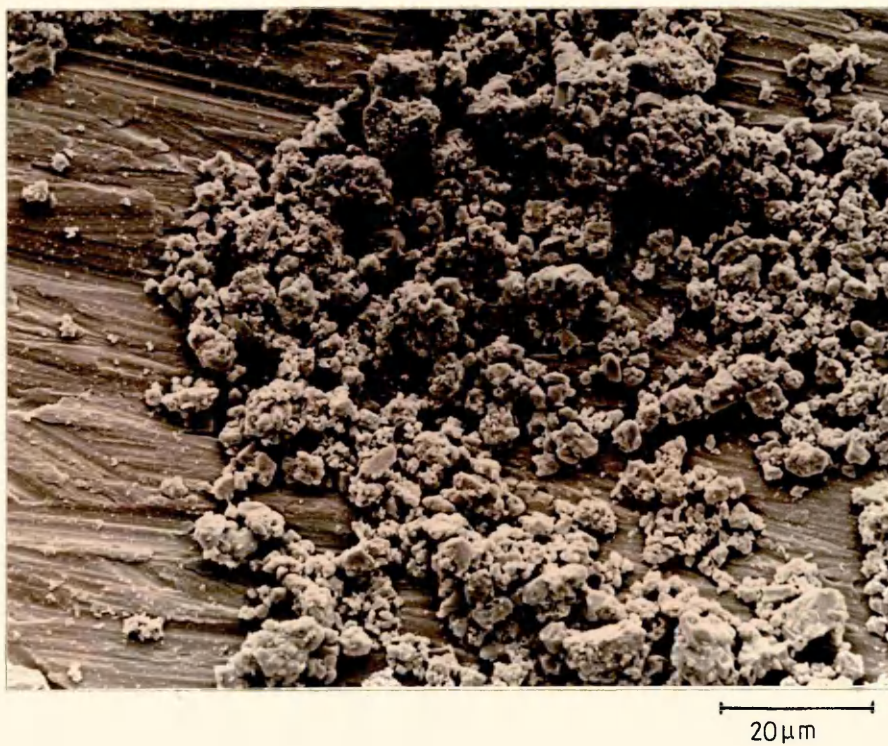
Fig. 68. Filler particles after separation from filled UPVC.
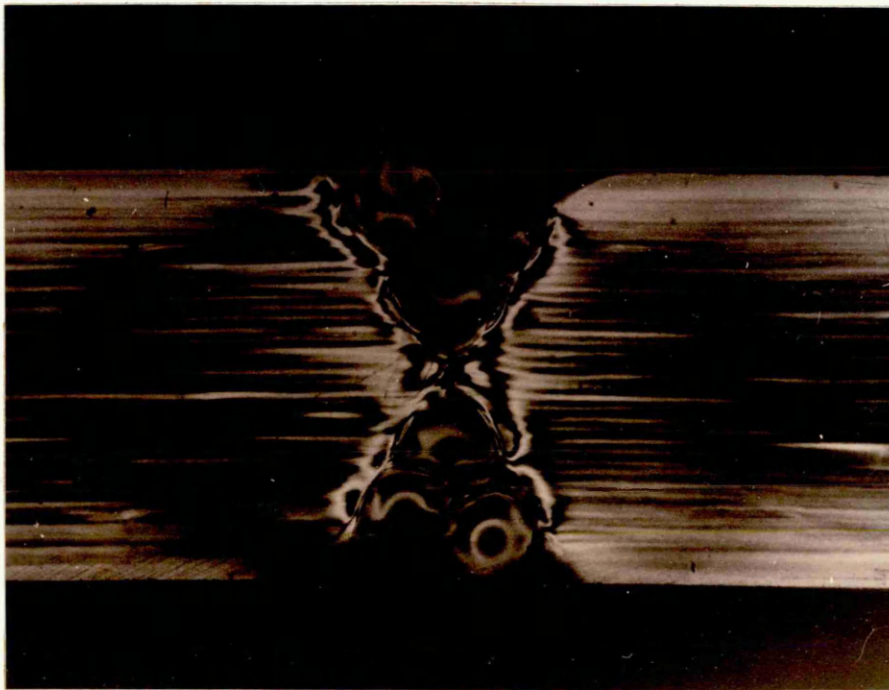
Fig. 69. Typical hot gas welded clear UPVC tensile test piece
          as viewed between the crossed polars of a circular
          polariscope.
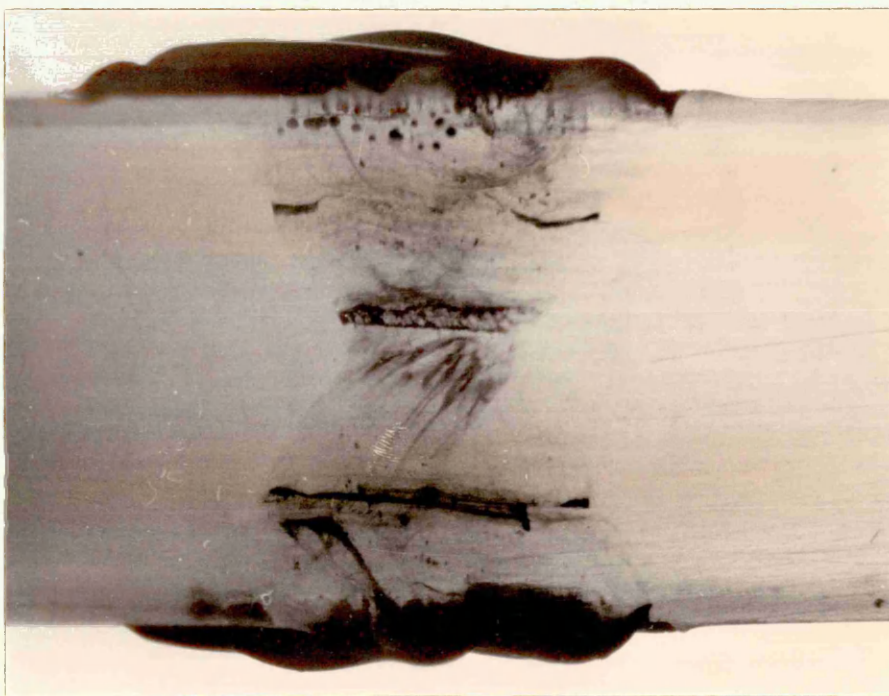
Fig. 70. Interior of a hot gas welded clear UPVC tensile test piece
          as viewed from an oblique angle.
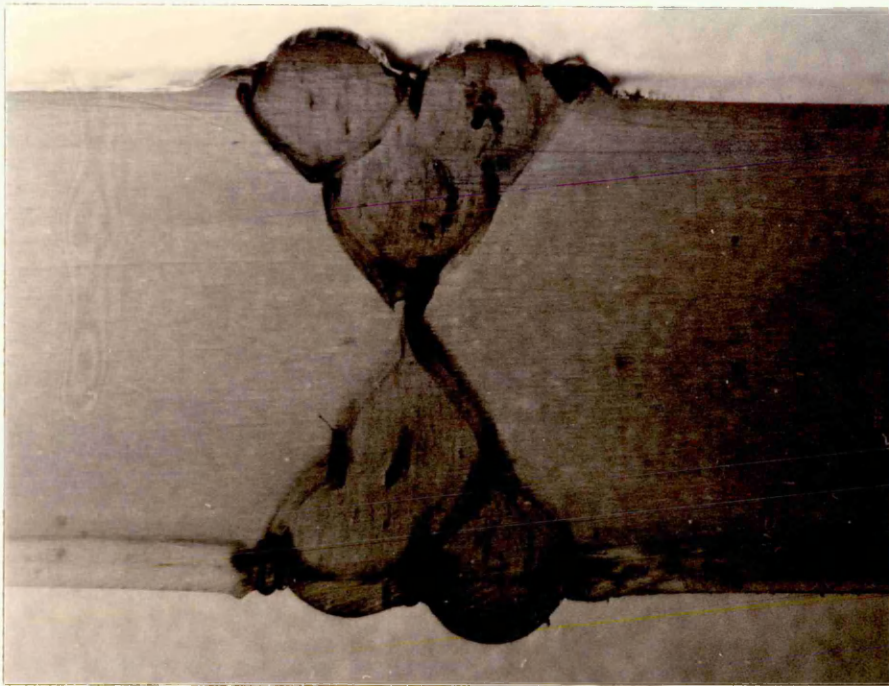
Fig. 71. Hot gas welded clear UPVC tensile test piece viewed head-on.
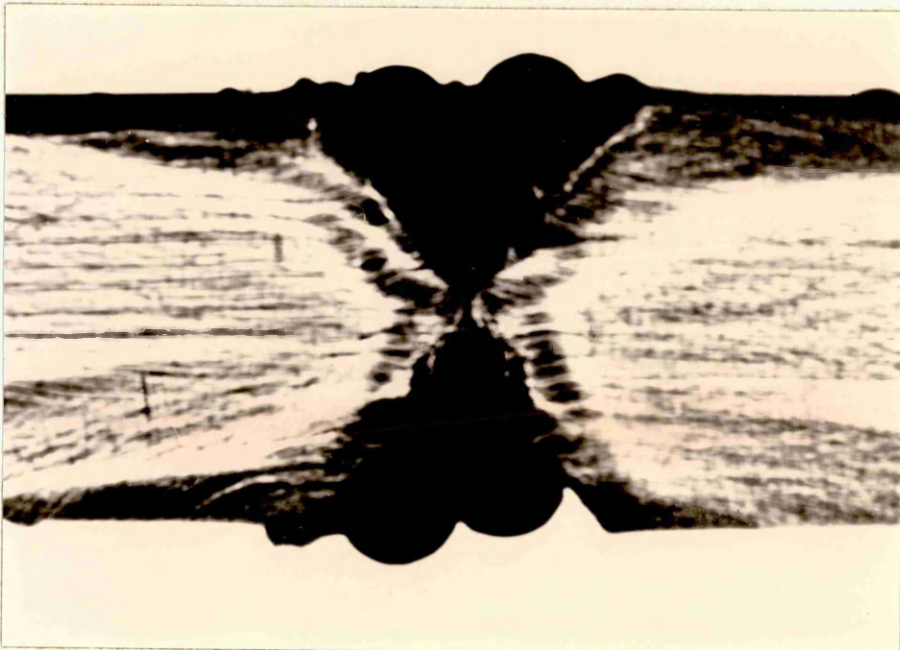
Fig. 72. Heat affected zone either side of the weld zone.
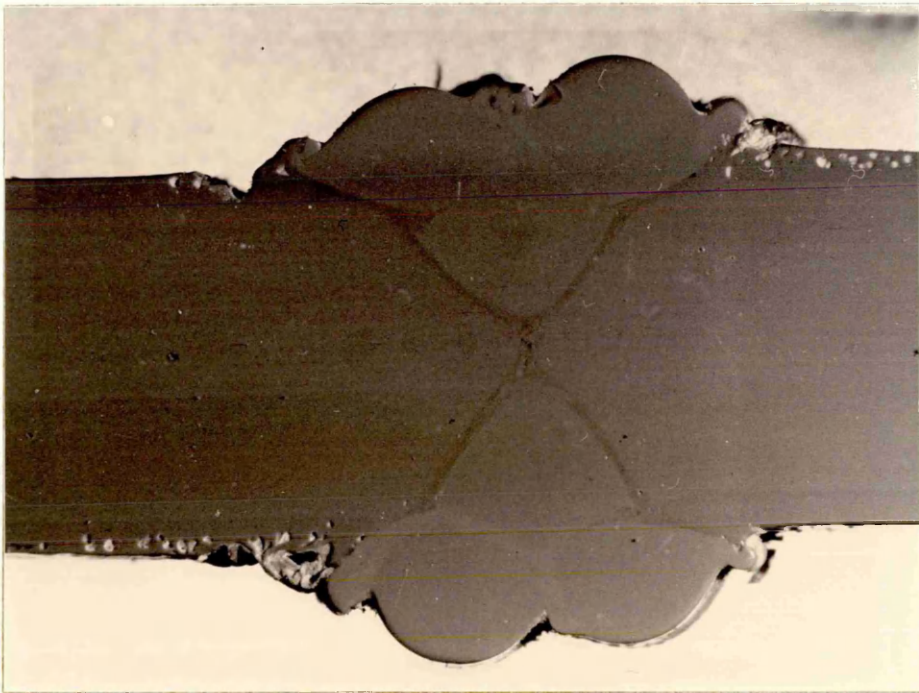
Fig. 73. Hot gas weld prepared using filled UPVC sheet and rod;
6mm thick.

Fig. 74. Hot tool welded clear UPVC, note thin dark line between
weld beads.

Fig. 75. Poor root penetration typical of the Plastic Construction
welds, weld viewed from an oblique angle.
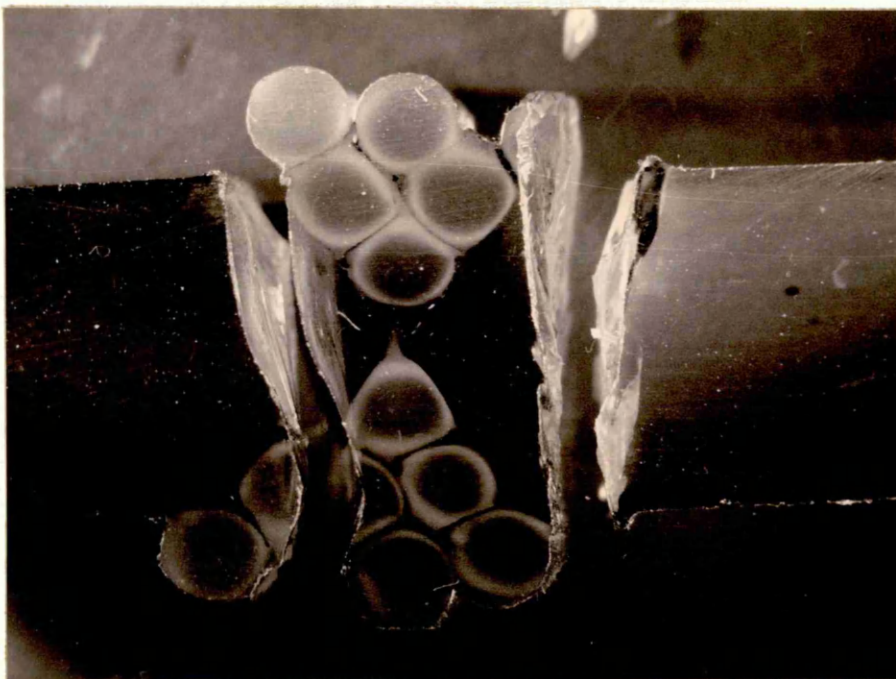
Fig. 76. Complete separation of weld zone from UPVC sheets.

Fig. 77. Fracture initiation site on weld fracture surface, note
no evidence of slow crack growth.

500μm

Fig. 78. Surface of fracture initiation site, indicating that this
surface has not been fused with another.
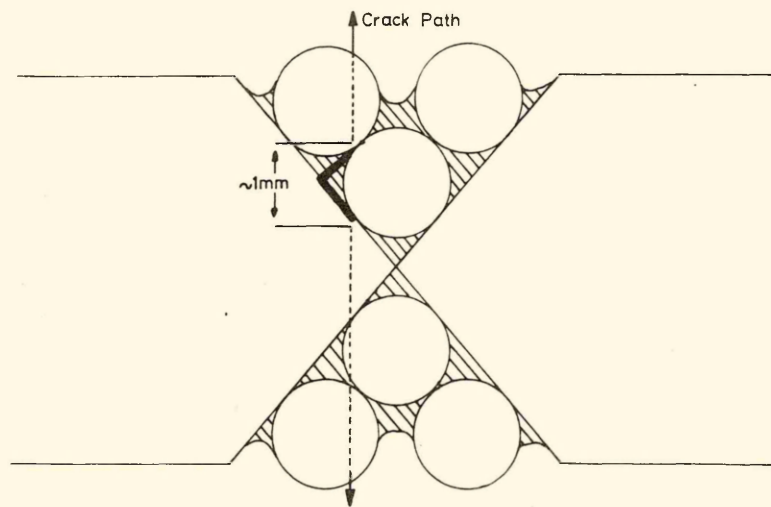
Fig. 79. Schematic of weld failure initiating at a ridge-like flaw within the weld.

1mm
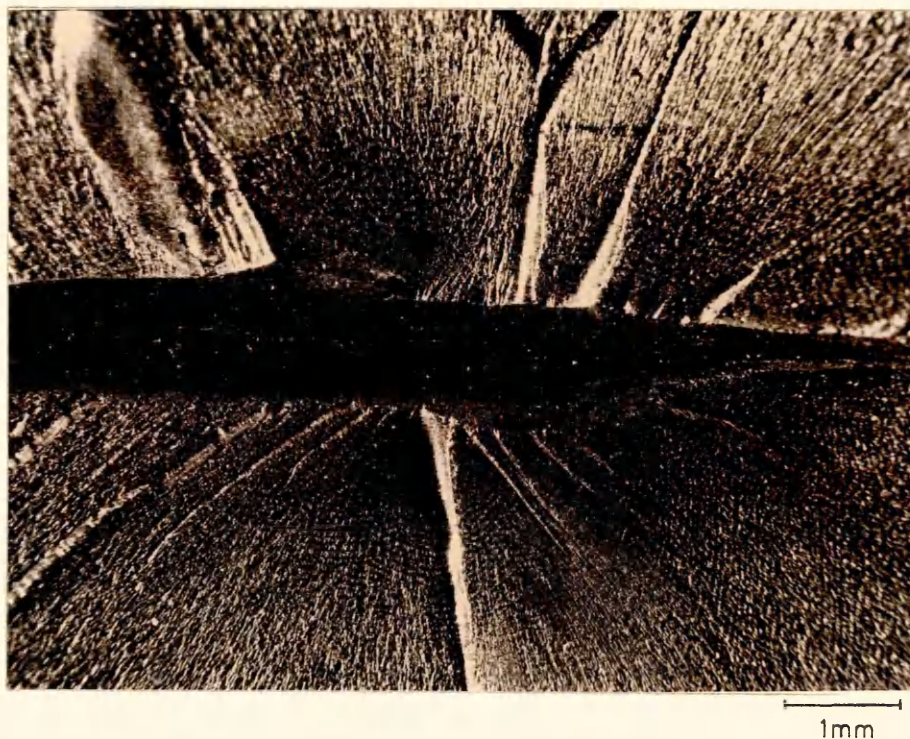
Fig. 80. Fracture initiation (see arrows) did not always occur at the widest part of the flaw.
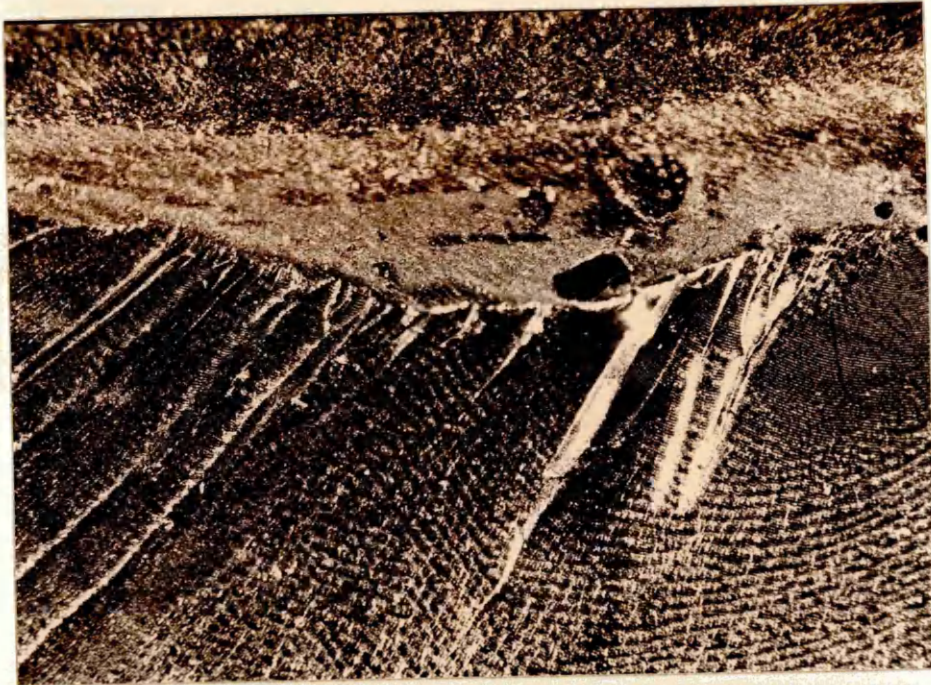
500μm

Fig. 81   Weld fracture surface showing typical fast fracture
features (Wallner lines, hackle bands and river markings)
emanating down from the fracture initiation site in the
top right hand corner.

Fig. 82. Smooth planar fracture surface typical of low stress weld failures.
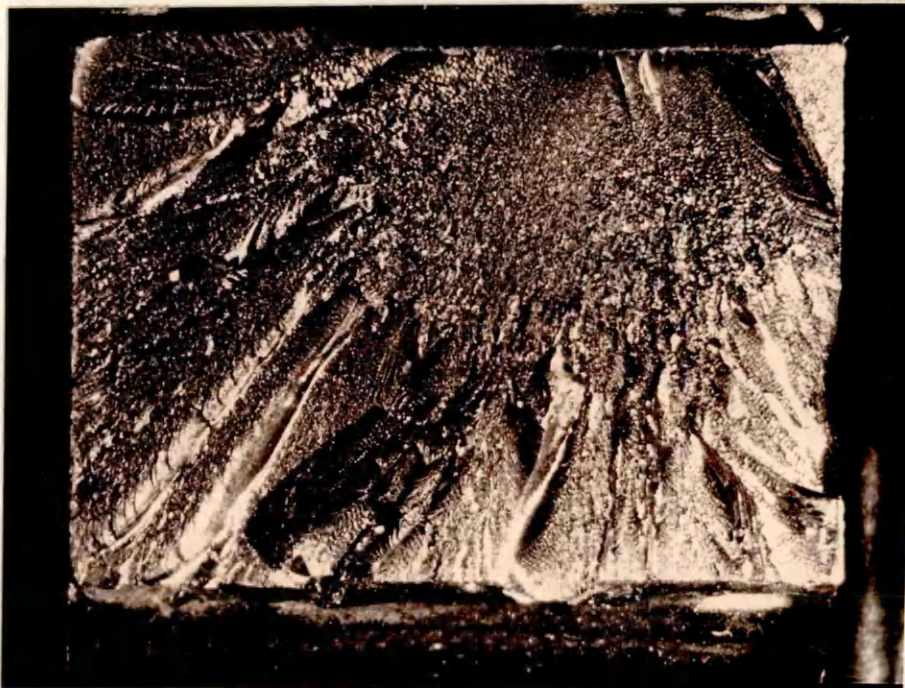
Fig. 83. Rough fracture surface associated with high stress weld failures.
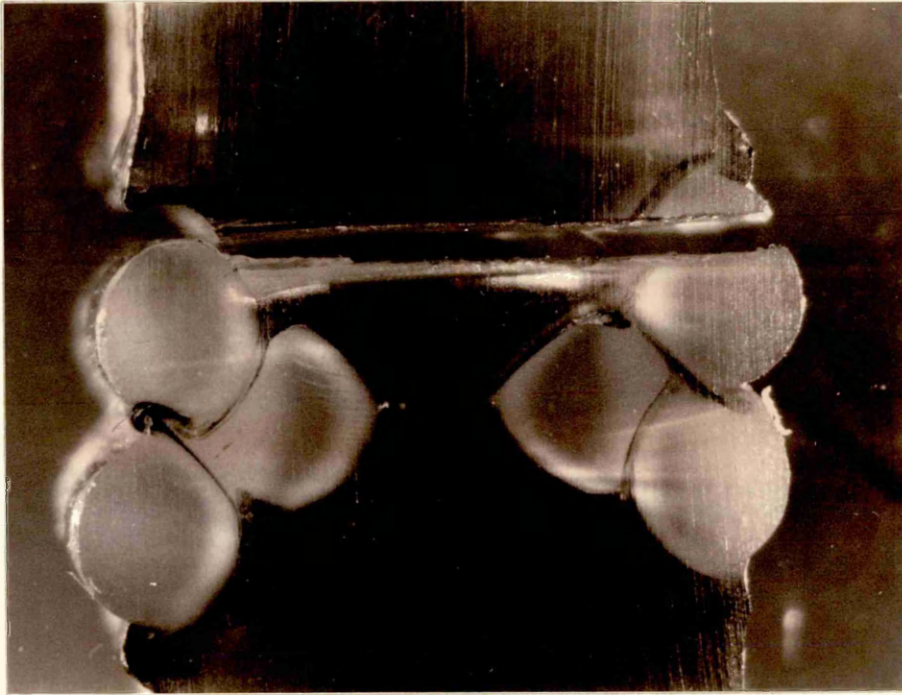
Fig. 84. Crack propagation perpendicular to the tensile axis, note
crack moves back into weld zone with no deviation of path.
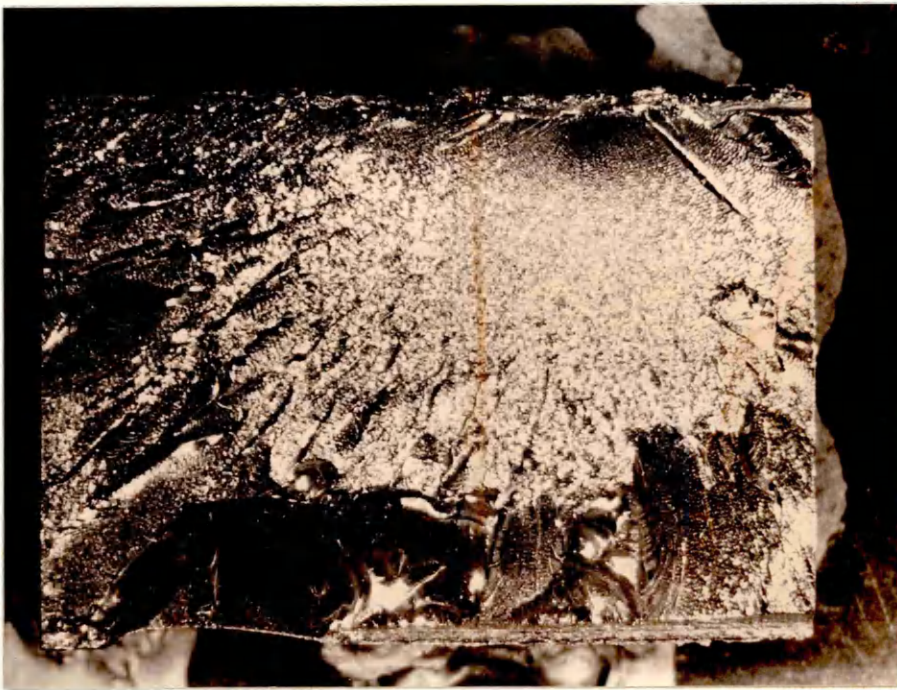
Fig. 85.   Rough fracture surface characteristic of one of the fracture
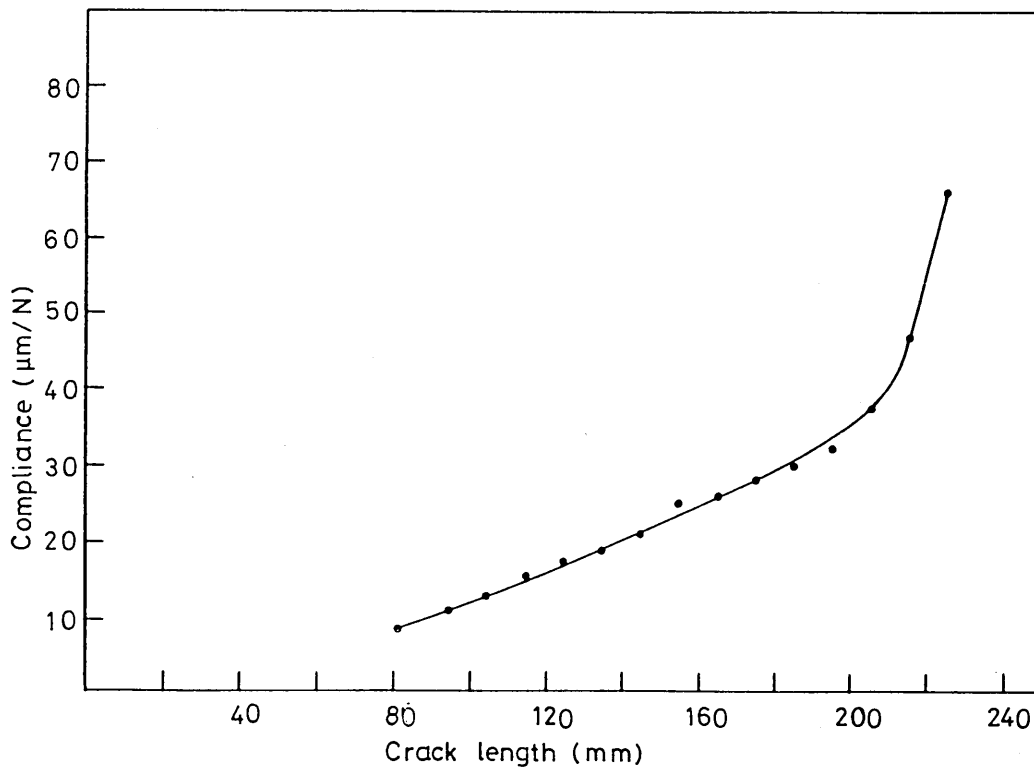surfaces in the case where the complete weld zone was ejected.

Fig. 86.   Smooth fracture surface characteristic of one of the fracture
surfaces in cases where the complete weld zone was ejected.

-230-

Fig. 87.   Compliance calibration curve for the geometry with
H_O = 15mm, α = $\tan^{-1}$ 0.2, specimen length, from
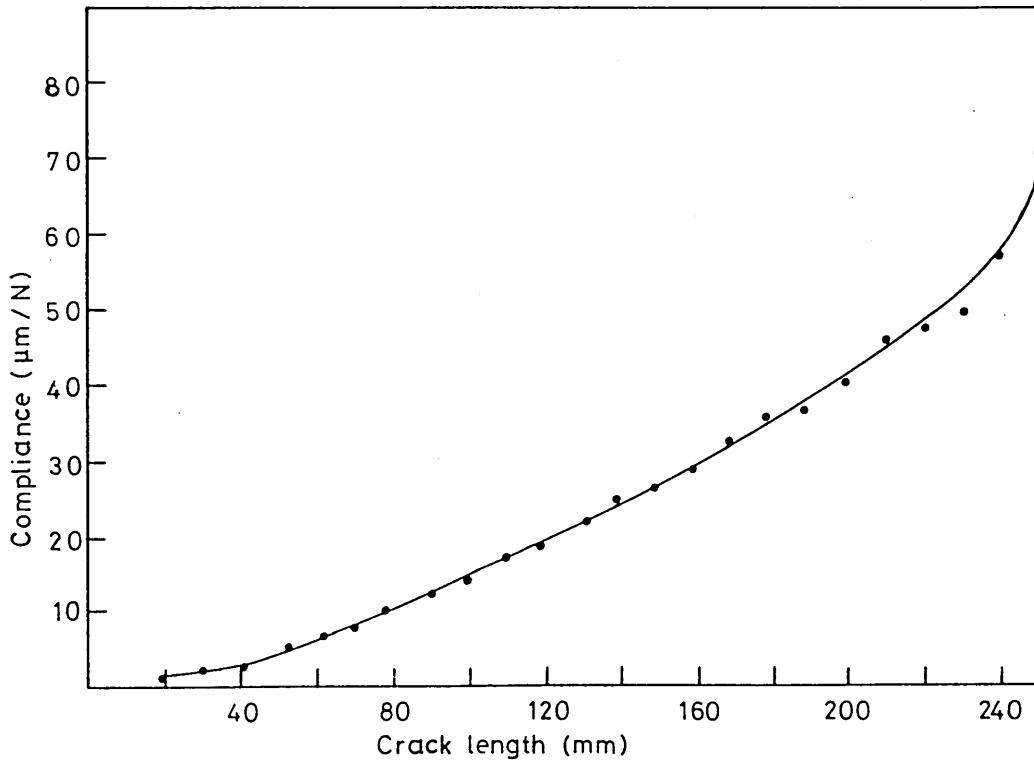loading line, 250mm, note this design used shoulders
30mm high at the loading line.

Fig. 88.   Compliance calibration curve for the TDCB geometry with
H_O = 19mm, α = $\tan^{-1}$ 0.15, specimen length, from loading
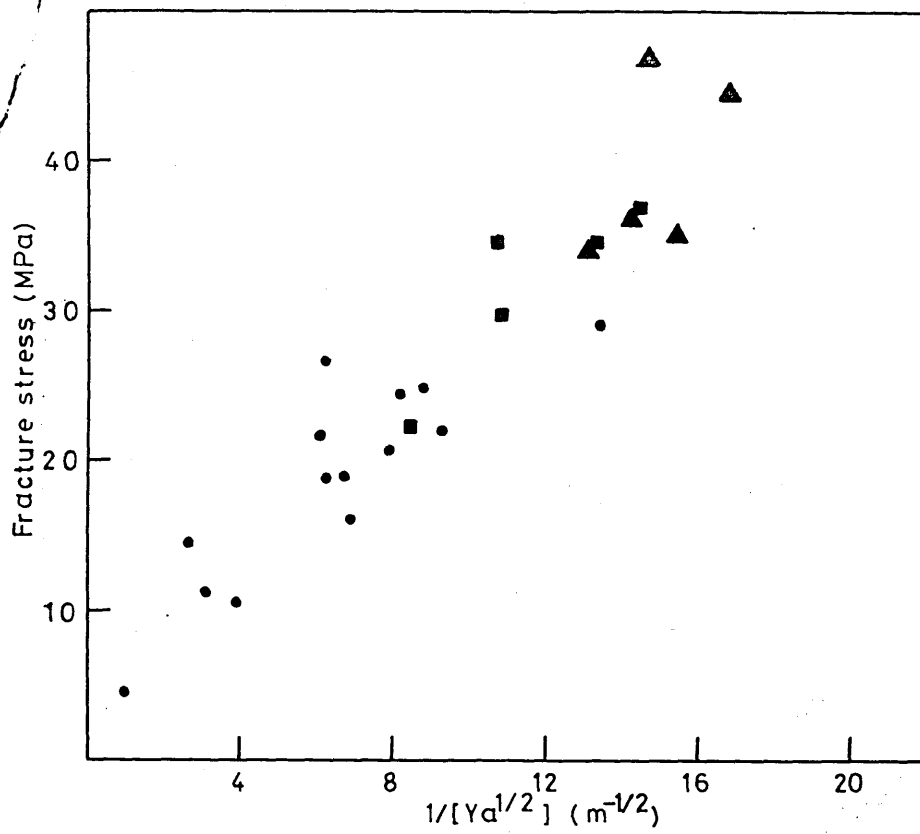line, 295mm.

-231-

Fig. 89. SEN data for clear UPVC sheet: (▲), W = 6mm; (■),
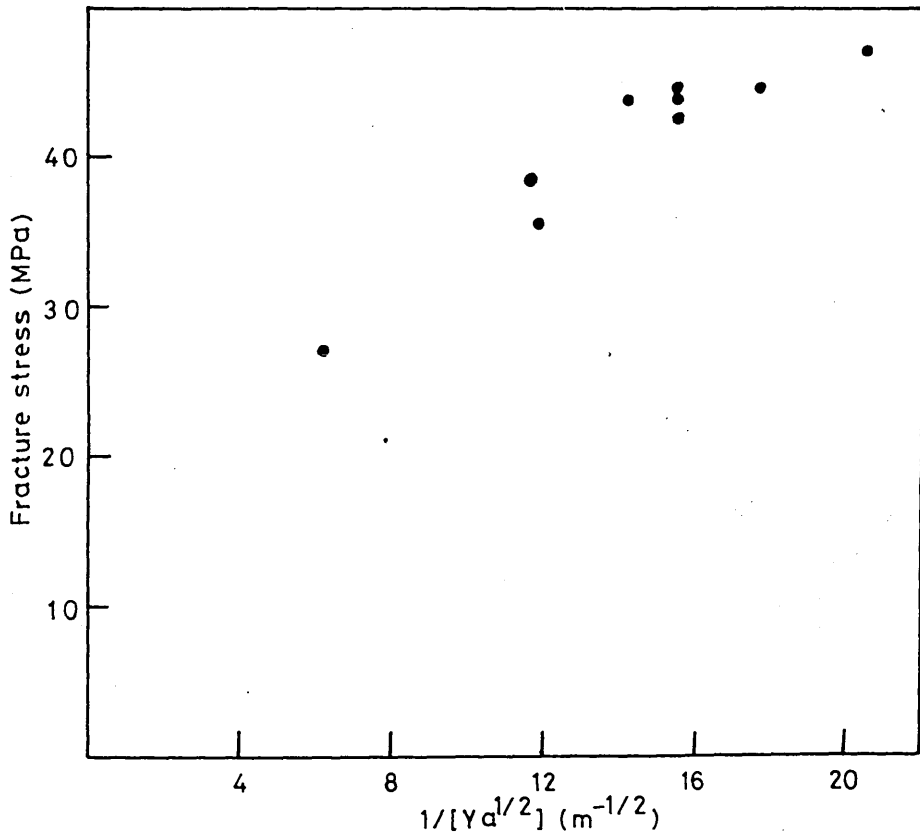W = 9.5mm; (●), W = 15mm.
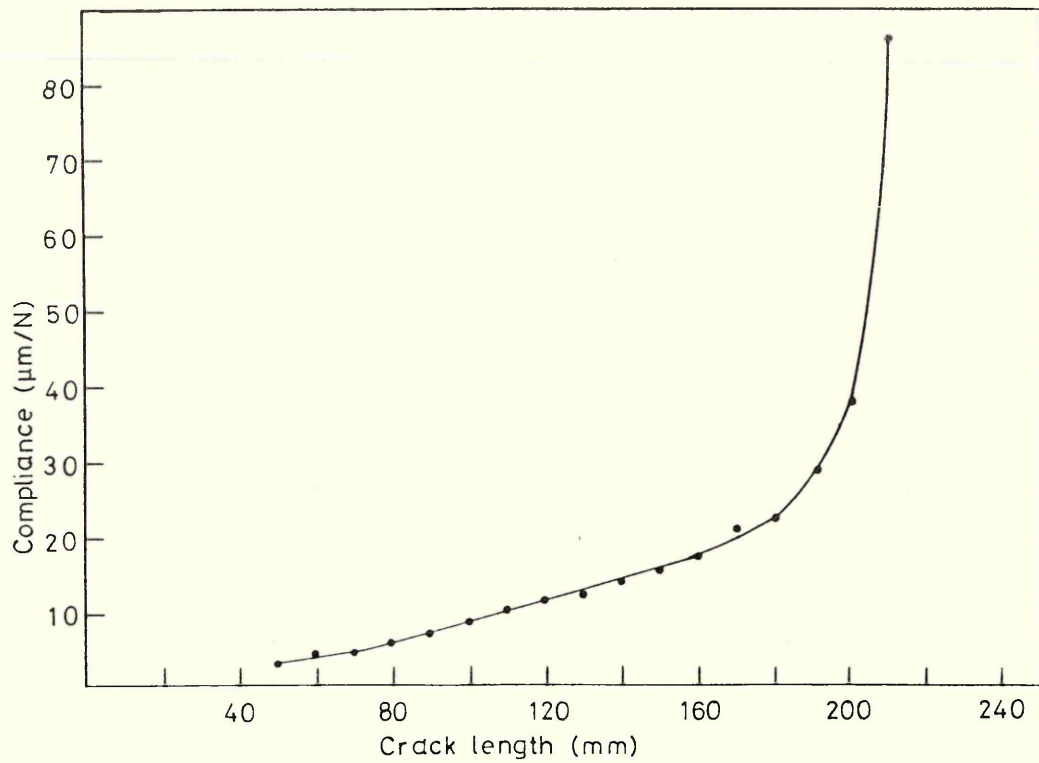

Fig. 90. SEN data for filled UPVC sheet, W = 6mm.

Fig. 91.   Compliance calibration curve for welded TDCB with 3mm thick
clear UPVC side plates: H_O = 20mm, $\alpha = \tan^{-1}$ 0.15; length of
specimen, from loading line, 230mm.

Fig. 92.   Completely severed welded DCB showing the specimen distortion
preventing the fracture surfaces mating together.

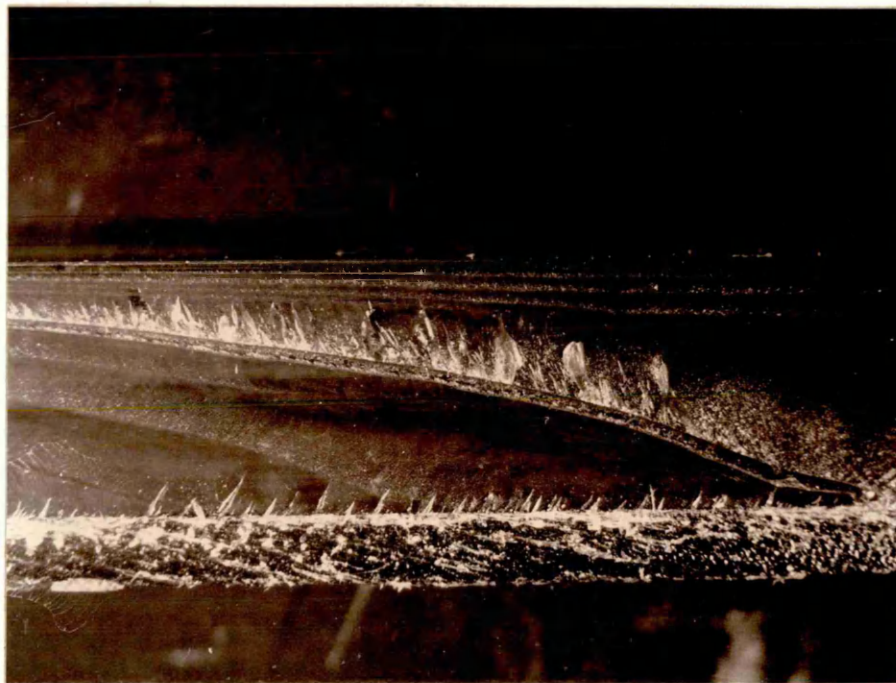Fig. 93. Striations on the fracture surface of a clear UPVC TDCB specimen, crack moving left to right.

Fig. 94. Characteristic crack front for the DT test geometry.

-234-
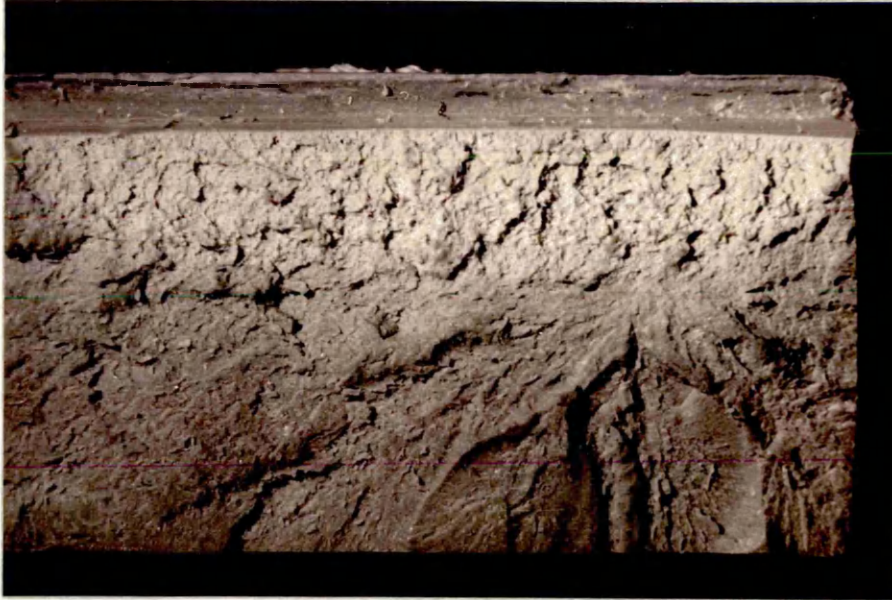
Fig. 95. Fracture surface of filled UPVC SEN, the notch is at the top
and W = 6mm, note plastic zone prior to the main crack
initiation.

Fig. 96. Fracture surface of failed welded tensile test piece
prepared with MBS modified weld rod (10 phr MBS).

The strength of welds in uPVC

J Abram, D W Clegg and D V Quayle

Unplasticized PVC (uPVC) is available in a wide range of formulations designed to meet various specific requirements; such as clarity. However, one of the few common factors between clear and opaque grades of uPVC is that they contain no plasticizer. In other respects varying amounts of types of reinforcing fillers, extenders, processing aids and stabilizers may be present resulting in materials with varying mechanical and physical properties. One notable difference is that water-clear grades contain no reinforcing or extending fillers.

Joining of uPVC is often necessary and hot gas welding is a commonly used process capable of producing satisfactory joints. While hot plate welding is capable of producing higher strength joints it is applicable only to fabrications such as pipework where the joint geometry is simple and reasonably symmetrical. In more complex and 'one off' fabrications hot gas welding is the most suitable process.

This article considers the problems involved in obtaining high joint strengths when hot gas welding clear grades of uPVC and discusses the factors contributing to these difficulties.

Experimental results
Materials

ICI Darvic 025 uPVC was chosen for this study. This material is available as a clear grade and also as an opaque grey grade. Both of these were investigated together with weld filler rods of similar materials. However, the majority of welds made were between clear Darvic sheets. This material was 10 mm thick and in common with grey Darvic is manufactured by hot pressing calendered PVC foils.

Chemical characterization

Chemical analyses and molecular weight measurements were carried out on all the materials used in the study and the main results are summarized in Tables 1 and 2.

While molecular weights were found to be similar for grey and clear Darvic, the constitution of these materials was found to be significantly different. This is because, in the interests of clarity, fillers and extenders are omitted in the clear grade and organo-tin stabilizers are used instead of the more commonly used lead, barium-cadmium and calcium-zinc types. In general additives are kept to a minimum in clear Darvic and in all other types of clear uPVC. The weld filler rods were found to contain greater amounts of the thermal stabilizers than the sheet materials in order to stabilize the material during the welding operation, as well as during manufacture by extrusion. The

David Clegg graduated in Metallurgy from Sheffield University and was later awarded a PhD. Since then he has been a Senior Lecturer in Materials in the Department of Metallurgy at Sheffield City Polytechnic. He is currently researching into radiation resistant elastomers and high performance rubber toughened thermoplastics.
Donald Quayle graduated in Physics while working in the plastics industry. He was awarded a PhD while lecturing at Derby Lonsdale College before his appointment as Principal Lecturer in Polymer Technology to the Department of Metallurgy at Sheffield City Polytechnic. He is now Head of Science at Cambridgeshire College of Arts and Technology.
John Abram graduated in Physics from Warwick University and was then appointed research assistant in the Department of Metallurgy at Sheffield City Polytechnic. He is now a research fellow in the Department of Non-Metallic Materials at Brunel University.
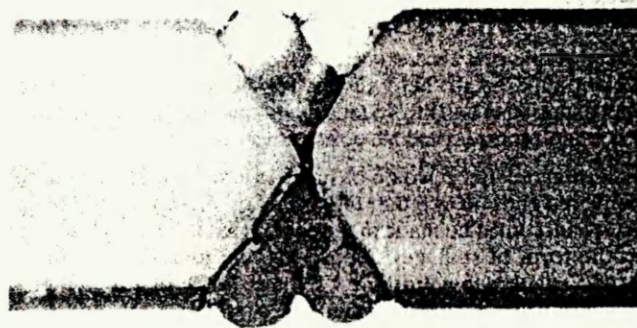
Fig 1 Cross-section of a hot gas weld in uPVC

glass transition temperature was found by differential scanning calorimetry to be 64.5°C compared with a value of 67°C for the sheet material.[1] This difference was attributed to the plasticizing effect of the increased levels of organo-tin stabilizer in the welding rod.[2] The sheet material contains sufficient stabilizer for protection during processing. Little remains for stabilization during the welding process.

Mechanical properties

The tensile strengths of weld filler rods and sheet materials were measured. The clear Darvic sheet was found to have a tensile yield strength of 67 MPa[3] showing little directionality. Only minor changes in tensile strengths were detected on annealing the sheet, varying the strain rate or varying the sample cross-sectional area. However, it should be noted that the tensile strength of PVC is dependent on testing temperature.

Grey Darvic sheet was observed to have a tensile yield strength of 53 MPa significantly less than that of the clear grade reflecting the contribution of extending agents to strength reduction.[4]

Clear Darvic weld filler rod was tested by cementing lengths of the rod into steel blocks with IS495 adhesive and then mounting the blocks into the jaws of the tensile testing machine. This avoided premature failure due to stress concentration effects experienced when samples were mounted directly in the jaws of the testing machine. A tensile yield strength of 71 MPa was observed, significantly higher than that of the sheet Darvic. It was also noted that annealing

Table 1. Molecular weight determinations for clear and grey Darvic sheet and for weld filler rod material

	Molecular weight	
	Sheet	Weld filler rod
Mn	3.46×10^4	3.06×10^4
Mw	7.85×10^4	8.57×10^4
Mw/Mn	2.27	2.80

Table 2, Chemical constitution of ICI Darvic uPVC clear and grey sheet and clear weld filler rod

Main constituents and function	Approximate composition (weight %)		
	Clear sheet	Grey sheet	Weld filler rod
ICI Corvic	bal	bal	bal
Organo tin thermal and uv stabilizers	1.5	—	4.0
Calcium zinc stearate thermal stabilizer	—	1.5	—
External and internal lubricants, uv absorbers, pigments	1%	1%	1%
Calcium carbonate filler	—	15%	—

Fig 2 Angled view of weld in clear uPVC showing interior defects in weld zone

of the rod produced shrinkages of as great as 25%. The general conclusion was that severe orientation was present in the weld filler rod due to its manufacture by extrusion, whereas little orientation existed in Darvic sheet.[5]

Hot gas welding

Manual welding was employed in which weld filler rods were laid down in the previously prepared joint by hand. This method has been extensively described elsewhere.[6,7] A simple design of electrically heated gun was used to heat the rod and surrounding sheet material. Nitrogen gas at a temperature of 280°C, measured 3 mm from the nozzle, and a flow rate of 35 l/min was used in conjunction with a double vee edge preparation with an included angle of 70 degrees. Three filler rods were laid down on either side of the joints as can be seen in Fig 1. Operator skill is crucial in obtaining high quality welds. In order to ensure that the best possible welds were obtained skilled welders from several different establishments each produced test welds during the course of the investigation.

Mechanical properties of welds

Each test weld was sliced across the joint into strips which were tested to assess tensile strength. Several tensile strength values per weld were thus obtained. Results of typical tests are shown in Table 3. These are for welds made by one of the authors. Values for a hot plate weld of clear sheet and for a hot gas weld of grey Darvic sheet carried out by the same person are included for comparison. Weld efficiences have been caluclated as a percentage of the tensile strength values of the sheet materials. It can be seen that efficiencies for the case of clear Darvic welds were at best 29% and that the scatter in results of tests on the same weld was considerable.

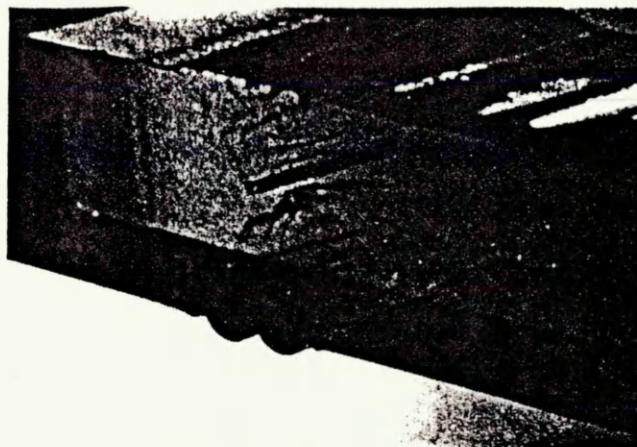Industrial welders using the speed welding technique or more extensive filling of the weld achieved results of up to 50% average efficiency, using clear Darvic.

Visual examination of welds

The sides of the tensile test pieces were polished and the weld zones examined using a low power microscope both before and during testing. This was fairly straight-forward in the case of the clear Darvic where unfused regions, which appear as black lines along the weld, could be seen, see Fig 2. Other defects present are streaks due to flow of degraded material along the weld zone. Even in apparently defect-free welds flaws were generated under low tensile loading, typically 25% of the failure stress. Although the opacity of the grey Darvic made visual examinatioin of the hot gas welds in this material impractical it was concluded from the nature of fracture surfaces examined by SEM, in both clear and grey Darvic that similar infused regions were also present in grey Darvic and that fracture initiated from them, see Figs 3a, b. However, the small reduction in the net section of the welds due to unfused material in clear Darvic was not sufficient to account for the low weld effiences observed. On the other hand no unfused zones were observed in the case of hot plate welds.

Discussion

No distinction is made in the literature between the strengths ar welds made in clear and filled grades of uPVC.[6,7,8] The results quoted are presumably applicable to the filled grades only.

A critical factor in producing high strength welds in uPVC is the production of an intimately fused defect free weld zone. This appears to be obtainable in the case of clear Darvic by hot plate welding resulting in excellent weld efficiencies. However, greater difficulty is encountered in the case of hot gas

Table 3. Mechanical properties of typical welds in uPVC

Materials	Tensile strength (MPa)*				Efficiency (%)	Number of samples	Weld type
	Min	Max	Standard deviation	Average			
Grey uPVC	40.6	47.0	2.6	44.9	85	5	Hot gas
Clear uPVC	12.6	25.4	5.2	18.6	29	5	Hot gas
Clear uPVC	14.1	24.4	3.0	18.5	28	14	Hot gas
Clear uPVC	60.2	61.9	0.4	61.0	94	5	Hot plate

*Calculated from $\dfrac{\text{load at failure}}{\text{width of weld} \times \text{thickness of sheet}}$
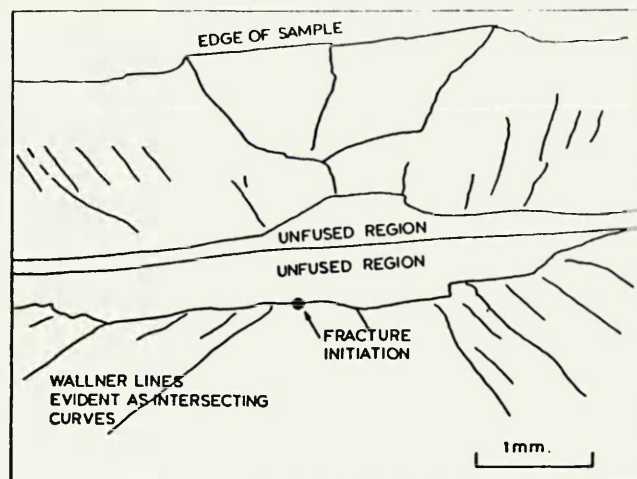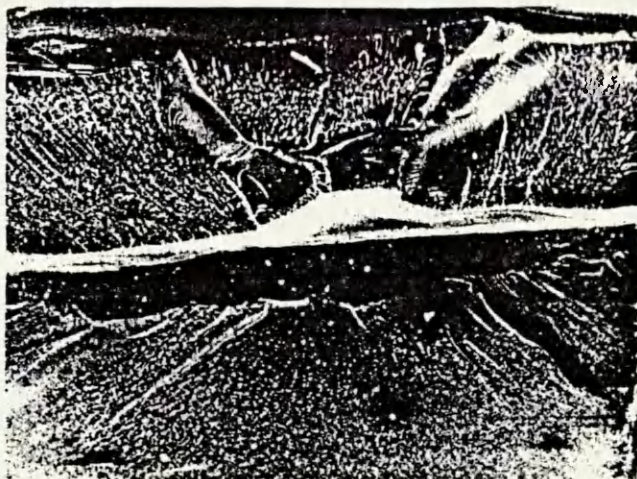
Fig 3a Scanning electron micrograph of a weld fracture surface in clear uPVC showing unfused regions; b diagram of Fig 3a showing location of fracture initiation and unfused regions

welding and weld zones in both clear and grey Darvic contain defects in the form of unfused regions. The important questions to be answered are first of all why do these unfused regions develop and secondly why are weld efficiencies so much poorer in the case of clear Darvic than in the case of grey Darvic. Some of the possible factors contributing to these observations will be discussed.

In view of the similar microstructure of welds in both clear and grey Darvic, the differences in weld properties indicate that the underlying causes are associated with differences in bulk material properties originating in differences in formulation. One important difference in properties is the higher notch sensitivity of the clear Darvic attributable to the soluble organo tin stabilizer.[10] Coupled with the presence of internal unfused regions and surface irregularities at the welded joints an analysis based on fracture mechanics is desirable.[11] However, it should be noted that the removal of surface irregularities by weld dressing was not found to increase weld strength significantly. Consequently, the unfused regions within the joints are almost certainly more important than surface defects. In addition the high degree of orientation present in the weld filler rods may contribute to significant residual stress levels in the welds. Degradation may also play an important part and the common practice of allowing visible discolouration to develop during hot gas welding as an indication of good fusion may in fact produce regions of embrittled material within the weld zone. This aspect is being investigated in detail at the present time by the authors using techniques previously employed in the study of thermal degradation in bulk PVC.[12] Clearly thermal degradation during welding is a potentially more serious problem in the sheet than in the welding rod material as at this stage the former contains very little active thermal stabilizer.

Possible methods of improving hot-gas weld strengths in clear Darvic are being explored. The obvious approach is to ensure that unfused regions do not occur in the weld zones. Out of 200 tests one industrial weld achieved a failure stress of 45.3 MPa and fracture did not originate within the weld interior. This result exceeds the next highest failure stress by 8 MPa. Presumably in this one sample no flaw was present in the weld. Statistically it is very unlikely that no unfused region would occur in a weld run. The overall strength of the weld would depend on the severest flaw. However, the method of hot gas welding, the poor thermal stability of PVC and its high pseudomelt viscosity all make perfect fusion very difficult and highly unlikely.

An alternative approach is to improve the toughness of the weld zone in some way without sacrificing tensile strength at normal and elevated temperatures. This precludes the use of plasticized rod which is in fact commercially available.[9] The use of toughened grades of PVC in the weld zone is a more attractive approach and the construction of welds using toughened filler rods is a subject of a continuing investigation at Sheffield City Polytechnic.

Conclusions

Hot gas welds in clear unplasticized PVC possess significantly lower strengths than in comparable filled grades. Considerable scatter exists in the strengths of hot gas welds in clear uPVC. However, hot plate welds in clear and hot gas welds in filled uPVC exhibit satisfactory strengths and reduced scatter about a mean value.

Unfused regions are invariably present in hot gas weld zones in both clear and filled grades of uPVC and these flaws are a main cause for the low tensile strengths of welds in clear uPVC due to its high notch sensitivity.

References

1 Cross, A and Haward, R N Polymer 19 (1978) 677
2 Dunlap, I H, Folz, C R and Mitchell, A G J Polym Sci: Phys Ed 10 (1972) 2223
3 ICI Ltd, Tech Man D106, 3rd ed (Sept 1980)
4 Vincent, P I 'Fracture', Enc Polymer Science and Tech 7, Fig 31, 336
5 Brady, T E and Jabarin, S A Polymer Eng Sci 17 (1977) 686
6 EEUA Handbook, Thermal and Chemical Welding of Plastics Materials. No 35 (1976)
7 Haim G Manual for Plastic Welding: Vol 3 PVC (1956)
8 Connors, F L Australian Plastics (May 1954) 6
9 Alf, E, Potentes, H and Menges G Designing to Avoid Mechanical Failure. PI Conference (1973)
10 ICI Ltd, Tech Service Note W121, 2nd Edn (1980)
11 Clegg, D W and Abram, J To be published
12 Allen, D W, Brooks, J S and Clarkson, R W J Organometal Chem 199 (1980) 299-310

THE MECHANICAL PROPERTIES OF WELDS IN U-PVC

J Abram*, D W Clegg and D V Quayle[+]
Department of Metallurgy, Sheffield City Polytechnic
*now at Brunel University
[+]now at Cambridgeshire College of Arts & Technology

Tensile strengths of hot gas and hot plate welds in
clear and filled grades of unplasticised PVC have been
determined. The mechanical properties of hot gas
welds have been assessed using linear elastic fracture
mechanics. Attempts have been made to relate variat-
ions in observed mechanical properties to microstruct-
ural features in the weld zones, material constitution
and differences between the welding processes.

INTRODUCTION

Unplasticised PVC (U-PVC) is available in a wide range of formulations
designed to meet various specific requirements. Such a requirement is
clarity and clear grades of U-PVC may be used as part of, or for the whole
of, welded fabrications. However, one of the few common factors between
clear and opaque grades of U-PVC is that they contain no plasticiser.
In other respects varying amounts and types of reinforcing fillers, ex-
tenders, processing aids and stabilisers may be present resulting in mat-
erials with varying mechanical and physical properties. One notable diff-
erence is that water clear grades contain no reinforcing or extending
fillers.

Joining of U-PVC is often necessary and hot gas welding is a commonly used
process capable of producing satisfactory joints. While hot plate weld-
ing is capable of producing higher strength joints it is applicable only
to fabrications such as pipework where the joint geometry is simple and
reasonably symmetical. In more complex and 'one off' fabrications hot
gas welding is the most suitable process.

This paper draws attention to the problems of obtaining high joint streng-
ths when hot gas welding clear grades of U-PVC and discusses the factors
contributing to these difficulties. The properties of welds in clear
grades are compared with those of the more commonly used filled grades.

EXPERIMENTAL

Materials

ICI Darvic 025 U-PVC was chosen for this study. This material is available as a clear grade and also as an opaque grey grade. Both of these were investigated together with weld filler rods of similar materials. However, the majority of welds made were between clear Darvic sheets, 10mm in thickness.

Chemical Characterisation

The materials used were chemically analysed and the main results are summarised in Table 1.

While molecular weights were found to be similar for grey and clear Darvic the constitution of these materials was found to be significantly different. This is because fillers and extenders are omitted in the clear grade and organo-tin stabilisers are used instead of the more commonly used lead, barium-cadmium and calcium-zinc types. In general additives are kept to a minimum in clear Darvic and in all other types of clear U-PVC. The weld filler rods were found to contain greater amounts of the thermal stabilisers than the sheet materials in order to stabilise the material during the welding operation as well as during manufacture by extrusion.

The sheet material contains sufficient stabiliser for protection against degradation during manufacture. Little remains for stabilisation during the welding process.

Table 1 – Chemical Constitution of I.C.I. Darvic U-PVC Clear and Grey Sheet and Weld Filler Rod

Main Constituents and Function	Approximate Composition (weight %)		
	Clear sheet	Grey sheet	Weld filler rod (clear)
ICI Corvic.	bal.	bal.	bal.
Organo tin thermal and U-V stabilisers.	1.5		4.0
Calcium zinc stearate thermal stabiliser.	–	1.5	–
External and internal lubricants U-V absorbers, pigments.	1%	1%	1%
Calcium carbonate filler.	–	15%	–
Number average molecular weight, Mn (determined by gel permeation chromatography).	3.5×10^4	3.5×10^4	3.0×10^4

Mechanical Properties

The tensile strengths of weld filler rods and sheet materials were measured. The clear Darvic sheet was found to have a tensile yield strength of 67 MPa[1] showing little directionality.

Grey Darvic sheet was found to have a tensile yield strength of 53 MPa significantly less than that of the clear grade reflecting the contribution of extending agents to strength reduction[2].

However, clear Darvic weld filler rod was found to have a tensile yield strength of 71 MPa, significantly higher than that of the sheet Darvic. It was also noted that annealing of the rod produced shrinkages of as great as 25%. The general conclusion was that severe orientation was present in the weld filler rod due to being manufactured by extrusion, whereas little orientation existed in Darvic sheet[3].

Hot Gas Welding

A manual welding method was employed in which weld filler rods were laid down in the previously prepared joint by hand. This method has been extensively described elsewhere[4,5]. An electrically heated gun was used to heat the rod and surrounding sheet material. Nitrogren gas at a temperature of 280°C, measured 3mm from the nozzle, and a flow rate of 35 l/min was used in conjunction with a double vee edge preparation with an included angle of 70 degrees. Three filler rods were laid down on either side of the joints as can be seen in Fig.1. Operator skill is crucial in obtaining high quality welds. In order to ensure that the best possible welds were obtained skilled welders from several different establishments each produced test welds during the course of the investigation. Some welds were produced by a high speed welding method and a few were overfilled. However, welds consisting of the type described above formed the main area of investigation.

Tensile Properties of Welds

Each test weld was sliced across the joint into strips which were tested to assess tensile strength. Several tensile strength values per weld were thus obtained. Results of typical tests are shown in Table 2. These are for welds made by one of the authors. Values for a hot plate weld of clear sheet and for a hot gas weld of grey Darvic sheet carried out by the same person are included for comparison. Weld efficiencies have been calculated as a percentage of the tensile strength values of the sheet materials. It can be seen that efficiencies for the case of clear Darvic welds were at best 29% and that the scatter in results of tests from the same weld run was considerable. However, the hot gas weld in grey Darvic exhibited an efficiency of 80% and the hot plate weld in clear Darvic an efficiency of 94%.

Industrial welders using the speed welding technique or more extensive filling of the weld achieved results of up to 50% maximum average efficiency, using clear Darvic.

Table 2 - Mechanical Properties of Typical Welds in U-PVC

| Materials | Tensile Strength (MPa)* | | | | Efficiency (%) | Number of Samples | Weld Type |
	Min.	Max.	Standard Deviation	Average			
Grey U-PVC	40.6	47.0	2.6	44.9	85	5	Hot gas
Clear U-PVC	12.6	25.4	5.2	18.6	29	5	Hot gas
Clear U-PVC	14.1	24.4	3.0	18.5	28	14	Hot gas
Clear U-PVC	60.2	61.9	0.4	61.0	94	5	Hot plate

$$*\text{calculated from } \frac{\text{load at Failure}}{\text{width of weld} \times \text{thickness of sheet}}$$

Visual Examination of Welds

The sides of the tensile test pieces were polished and the weld zones examined using a low power microscope both before and during testing. This was fairly straight forward in the case of the clear Darvic where unfused regions, which appear as black lines along the weld, could be seen, See Fig.2. Other defects usually present are streaks due to flow of degraded material along the weld zone. One weld was found to contain a sharp crack running within a weld filler rod along the length of the weld, see Fig.3. Even in apparently defect-free welds, flaws were generated under low tensile loading, typically 25% of the failure stress. Although the opacity of the grey Darvic made visual examination of the hot gas welds in this material impractical it was concluded from the nature of fracture surfaces examined by S.E.M., in both clear and grey Darvic that similar unfused regions were also present in grey Darvic and that fracture initiated from them, see Fig.4. However, the small reduction in the net section of the welds due to unfused material in clear Darvic was not sufficient to account for the low weld efficiencies observed. On the other hand no unfused zones were observed in the case of hot plate welds.

Fracture mechanics

As described, weld fractures appear to be initiated at the boundaries of unfused weld rod. The crack shown in Fig.3 is also a prime initiation site. The unfused region may be treated as a crack and its effect on the weld strength analysed using linear elastic fracture mechanics (LEFM)[6].

LEFM uses two parameters, the stress intensity factor K and the strain energy release rate, G, to characterise the stress state within a loaded body containing a crack. The fracture criterion is that the crack will propagate catastrophically when these two reach a particular value which is characteristic of the material. For mode I opening these values are denoted K_{Ic} and G_{Ic} and are called the fracture toughness and fracture surface energy respectively.

The two are related, under plane strain conditions, by:

$$K^2_c = E \, G_{ic} / (1-\nu^2) \qquad \dots\dots\dots\dots\dots\dots\dots\dots\dots\dots\dots\dots\dots \quad (1)$$

Where E is the materials Young's modulus and ν the Poisson's ratio.

The fracture toughness may be determined by a notched bar method using the following equation:

$$K_{ic} = \sigma_F \sqrt{a} \, Y \quad \dots\dots\dots\dots\dots\dots\dots\dots\dots\dots (2)$$

where σ_F is the gross section failure stress, a is the notch depth and Y is a geometric factor which takes into account different specimen geometries, sizes and loading conditions. For methods based on the cantilever beam, specific equations have been calculated and data are available[7].

The fracture surface energy is derived from

$$G_{ic} = \frac{P_f^2}{2b} \, dc/da \quad \dots\dots\dots\dots\dots\dots\dots\dots\dots\dots (3)$$

where P_f is the failure load, b is the specimen thickness and dc/da is the rate of change of the specimen compliance, C, with crack length, a. A calibration curve of compliance with crack length is prepared using a dummy specimen and during actual testing a record of both load and crack length is required.

The fracture toughness of the 10 mm clear sheet was determined using single-edge-notch (SEN), double-cantilever-beam (DCB) and double torsion (DT) methods whilst the fracture surface energy was determined using a tapered-double-cantilever-beam (TDCB) method. Typical specimen dimensions are given in fig.5. Only the fracture toughness was determined, using the SEM method, for the 6mm clear and filled material.

The DCB, DT and TDCB methods were used since with other materials it is usually possible to obtain many results, up to 20, from each specimen. When used in 'fixed-grip' loading the crack growth is stable in that the crack should stop again as once it is growing no more energy is delivered by the loading system. Normally crack growth is either slow stable or in short sudden jumps. However, with this material (U-PVC) it was only possible to get at best 2 or 3 results per specimen. Slow stable crack growth only occurred for cross head rates between 0.5-2 cm min^{-1} and even then it only occurred with some specimens. The normal behaviour was for the frist crack to jump to within a few centimetres of the end of the specimen where the equations become invalid.

For the SEN specimens K_{Ic} was calculated using equation (2) with Y given by:-

$$Y = 1.99 - 0.41(a/w) + 18.7 (a/w)^2 - 38.48(a/w)^3 + 53.85(a/w)^4 \quad (4)$$

Where w is the depth of the specimen.

For the DCB specimens K_{Ic} was calculated[8] using

$$K_{Ic} = P_f \frac{3.46 \, (a/H + 0.7)}{b_c \, H^{\frac{1}{2}}} \quad \dots\dots\dots\dots\dots\dots\dots\dots (5)$$

where H is the height of the arm of the specimen and b_c is the net section thickness in the plane of the crack, in the case where a groove is used to control the crack path[9].

For the DT specimens K_{ic} is calculated[10] using

$$K_{ic} = P_f \, L \, \left(\frac{3(1 + \nu)}{b_c \, b^3 D}\right)^{\frac{1}{2}} \quad \dots\dots\dots\dots\dots\dots\dots\dots\dots\dots\dots\dots\dots(6)$$

Where L is the distance between the loading points and D is the width of the specimen.

The TDCB method was used since by careful design the factor dc/da can be made nearly constant for a large range of crack lengths, thus removing the need to monitor crack length whilst the crack is in this range.

The size requirements for valid plane strain fracture toughness testing[11] could only be met for the DCB, DT and TDCB specimens. In the case of the SEN's it was decided to simulate weld failure by having the crack grow through the thickness of the sheet which meant that either the initial crack length or the length of material left infringed the size requirements. It has been shown that the size requirement is conservative for the clear material but evidence for the filled material suggested that for unwelded material plane stress effects were becoming important but were not so important for the welded material.

The DCB, DT and TDCB methods were used in the same way to study the welded material by preparing specimens with the hot-gas weld seam arranged along the crack growth direction. The specimens were in other respects as shown in fig.5.

The results from these techniques are given in Table 3.

Table 3 - K_{Ic} and G_{Ic} Data for Unwelded + Welded Material

Sample type and thickness	SEN K_{Ic}(MPa m$^{\frac{1}{2}}$)	DCB K_{Ic}(MPa m$^{\frac{1}{2}}$)	DCB$_{corr}$ K_{Ic}(MPa m$^{\frac{1}{2}}$)	DT K_{Ic}(MPa m$^{\frac{1}{2}}$)	TDCB G_c(Nm^{-1})
Clear 10 mm	2.1	3.0	2.1	2.9	2100
Clear 6 mm	2.3	-	-	-	-
Filled 6 mm	2.9	-	-	-	-
Clear 10 mm hot gas welded	1.5*	2.4	1.6	2.6	1400
Filled 6 mm hot gas welded	2.5*	-	-	-	-

*Estimated using SEN analysis

The value of K_{Ic}, for 10 mm clear sheet, determined by the DCB method using equation (5) is much larger than that calculated from the SEN method, however other workers[9] have found that the presence of the crack controlling grooves used in DCB specimens causes calculated values of K_{Ic} to be 50% too high. The corrected value shown in Table 3 shows much better agreement. The DT method also gives a higher value of K_{Ic} but this may be due to the different notch geometry found with these specimens.

The fracture surface energy value may be used with values of the materials Young's Modulus, appropriate to the testing conditions, and equation (1) to cross check the fracture toughness. The quoted Young's Modulus of E = 3.6 GPa is that measured at 0.2% strain. However, at the strains observed for fracture in SEN specimens (1.5%) this value has dropped to E = 2.2 GPa and when this is used the calculated fracture toughness is K_{Ic} = 2.3 MPam$^{\frac{1}{2}}$.

When the values of K_{Ic} for the welded DCB's are corrected, for grooving, they suggest that the welding process has lead to a 40% decrease in fracture toughness. This drop is reflected in the fracture surface energy though the decrease is not as big as expected if calculated from equation (1). This is thought to be due to the effects of welding on the materials Young's Modulus.

If a welded tensile test piece is analysed as if it were an SEN specimen with a notch depth the same length as an unfused region as observed in the weld, then the welded material's fracture toughness can be estimated. Using typical values of a = 1 mm and σ_F = 22 MPa (for welds in 10 mm clear sheet) then a fracture toughness of K_{Ic} = 1.5 MPam$^{\frac{1}{2}}$ is derived. If the same is done for the filled material welds using a = 0.75 mm and σ_F = 42 MPa then a fracture toughness K_{Ic} = 2.5 MPam$^{\frac{1}{2}}$ is obtained.

Although the SEN analysis is crude, the variation in notch shape shape, size, position and notch tip radius of the unfused region combined with the irregular weld cross section and the thermal history of the weld material make a more refined analysis impractical. It does indicate that the poor weld strengths are due to the embrittlement of welded structures and the presence of unfused weld rod.

DISCUSSION

No distinction is made in the literature between the strengths of welds made in clear and filled grades of U-PVC[4,12,13]. The results quoted are presumably applicable to the filled grades only.

A critical factor in producing high strength welds in U-PVC and the thermoplastics in general is the production of an intimately fused defect free weld zone. This appears to be obtainable in the case of clear Darvic by hot plate welding resulting in excellent weld efficiencies. Far greater difficulty is encountered in the case of hot gas welding and weld zones in both clear and grey Darvic contain several types of defects including those in the form of unfused regions.

In view of the similar microstructures of welds in both clear and grey Darvic the differences in weld properties indicate that the underlying causes are associated with differences in bulk material properties origina-

ting from differences in formulation. One important difference in propert-
ies is the higher notch sensitivity of the clear Darvic attributable to the
soluble organo-tin stabiliser[14]. Coupled with the presence of internal
unfused regions and surface irregularities at the welded joints an analysis
based on fracture mechanics is clearly appropriate. The analogy between
tensile test samples and SEN fracture toughness samples yields direct evid-
ence that internal defects of the sizes observed are responsible for the
low values of fracture toughness measured.

It should be noted that the removal of surface irregularities by weld dress-
ing was not found to significantly increase weld strength. Consequently,
the unfused regions within the joints are almost certainly more important
than surface defects. In addition the high degree of orientation present
in the weld filler rods may contribute to significant residual stress levels
in the welds. Degradation may also play an important part and the common
practice of allowing visible discolouration to develop during hot gas weld-
ing as an indication of good fusion may in fact produce regions of embritt-
led material within the weld zone. Clearly thermal degradation during
welding is a potentially more serious problem in the sheet than in the weld-
ing rod material as at this stage the former contains very little active
thermal stabiliser. Increasing the level of stabiliser in the sheet is an
economically unattractive proposition.

Possible methods of improving hot-gas weld strengths in clear Darvic are
being explored. The obvious approach is to ensure that unfused regions do
not occur in the weld zones. Out of 200 tests one industrial weld achieved
a failure stress of 45.3MPa and fracture did not originate within the weld
interior. This result exceeds the next highest failure stress by 8MPa.
Presumably in this one sample no flaw was present in the weld. Statistic-
ally it is very unlikely that no unfused region would occur in a weld run.
The overall strength of the weld would depend on the severest flaw. How-
ever, the method of hot gas welding, the poor thermal stability of PVC and
its high melt viscosity make perfect fusion highly unlikely. As a result
the weld zone is a complex region and potential source of weakness. An
alternative approach is to improve the toughness of the weld zone in some
way without sacrificing tensile strength at normal and elevated temperat-
ures. This precludes the use of plasticised rod which is in fact commer-
cially available. The use of toughened grades of PVC in the weld zone is
a more attractive approach and is being investigated.

CONCLUSIONS

Hot gas welding is a convenient and economic method of joining U-PVC and
other thermoplastics. It is a flexible process allowing complex fabric-
ations to be produced. However, in general lower joint efficiencies are
produced than in other welding methods, notably hot plate welding. The
weld region is complex and contains various types of defect, such as de-
graded zones and unfused areas. The effect of these on weld strengths
depends on the precise material formulation, even minor changes in comp-
osition leading to serious reductions in some cases.

Hot gas welds in clear U-PVC have significantly lower strengths and eff-
iciencies than in similar filled grades. In the case of clear U-PVC con-
siderable scatter in the strength of a weld exists along its length. Hot
gas welds in filled U-PVC and hot plate welds in U-PVC have high strengths
and efficiencies and reduced scatter.

Unfused regions are present in hot gas weld zones in clear and filled U-PVC and are the major factor in the production of low strengths and fraction toughness values in the case of clear U-PVC welds. This is probably due to the high notch sensitivity of clear U-PVC brought about by the use of organo-tin thermal stabilisers.

Considerable care is required in hot gas welding PVC to minimise weld flaws and to ensure optimum fusion. The use of weld filler rods manufactured from toughened U-PVC is an attractive proposition.

Tensile testing gives a useful indication of weld properties and fracture mechanics offers a promising basis for complementary testing procedures.

ACKNOWLEDGEMENTS

REFERENCES

1.   I.C.I. Ltd. Tech. Man. D106. 3rd Ed. Sept. 1980.

2.   Vincent, P.I. 'Fracture', Fig.31 Enc. Polymer Science and Tech. 7, 336.

3.   Brady, T.E. and Jabarin, S.A.   'Polymer Eng.Sci.' 1977, 17, 686

4.   E.E.U.A. Handbook,'Thermal and Chemical Welding of Plastics Materials'. No.35 1976.

5.   Haim, G.'Manual for Plastic Welding'. vol.3 PVC, 1956.

6.   Bucknall, C.B., Drinkwater, I.C. and Smith, G.R. 'Polymer Eng. Sci.' 1980 20 432.

7.   Rooke, D.P. and Cartwright, D.J. 'Compendium of Stress Intensity Factors'. HMSO 1976.

8.   Gross,B and Srawley,J.E. NASA TN D 3295, 1966.

9.   Marshall, G.P., Culver, L.E. and Williams, J.G. Plastics and Polymers Feb. 1969, 75.

10.   Marshall, G.P., Coutts, L.H. and Williams, J.G. J. Mat. Sci. 1974, 9 1409.

11.   ASTM. STP 410.

12.   Connors, F.L. Australian Plastics, May 1954, 6.

13.   Alf, E. Potentes, H. and Menges, G. 'Designing to Avoid Mechanical Failure'. Plastics Inst. Conf. 1973.

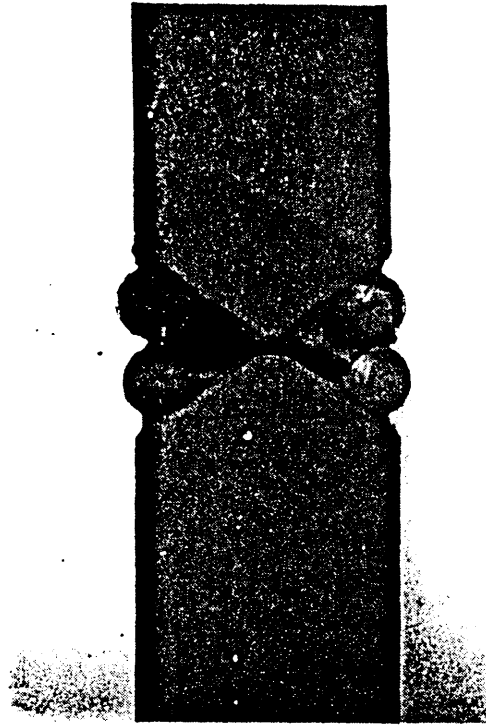14.   I.C.I. Ltd., Tech. Service Note W121 2nd Ed. 1980.

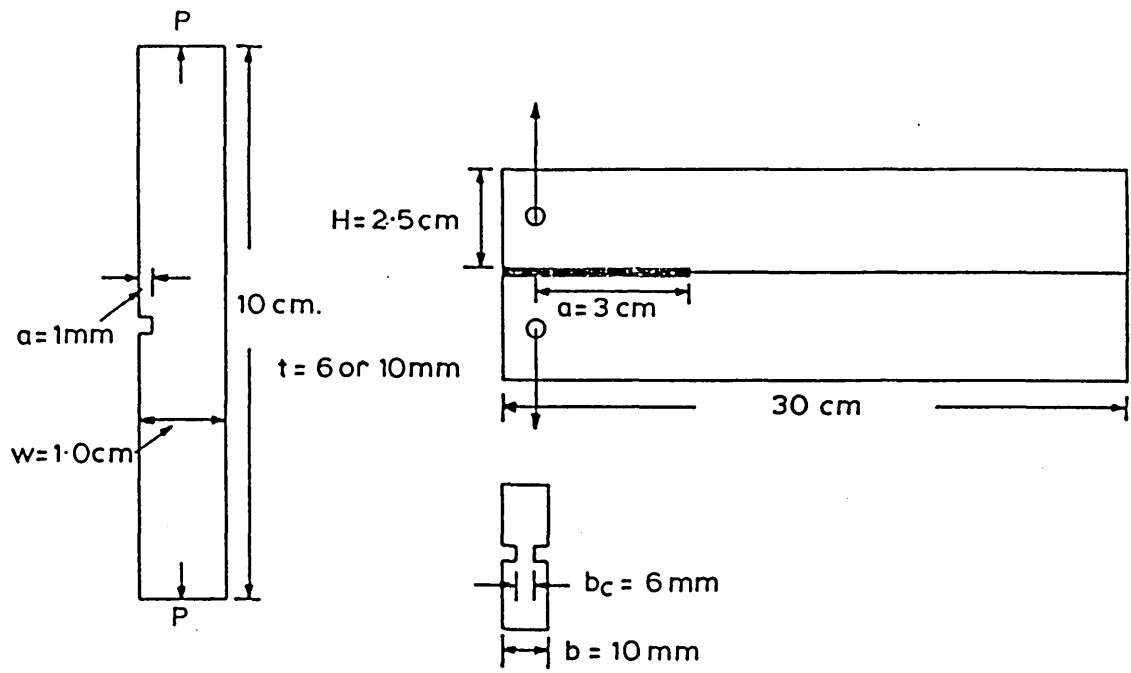Fig.1 Cross-section of a hot gas weld in clear U-PVC

Fig.2 View through hot gass weld in clear U-PVC showing interior defects

Fig.3 Sharp crack within a weld filler rod
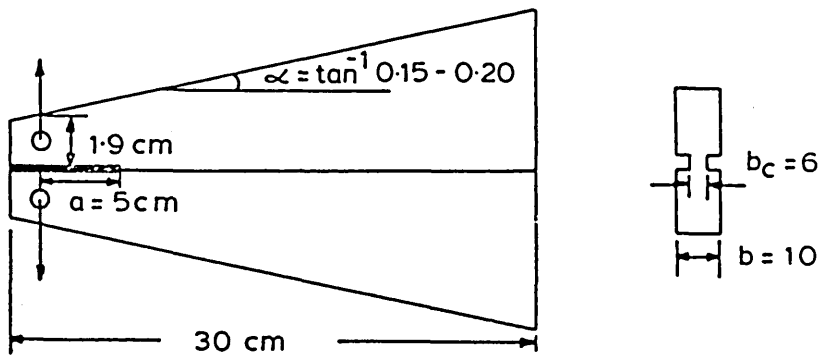

Fig.4 Scanning electron micrograph of a weld fracture surface in U-PVC
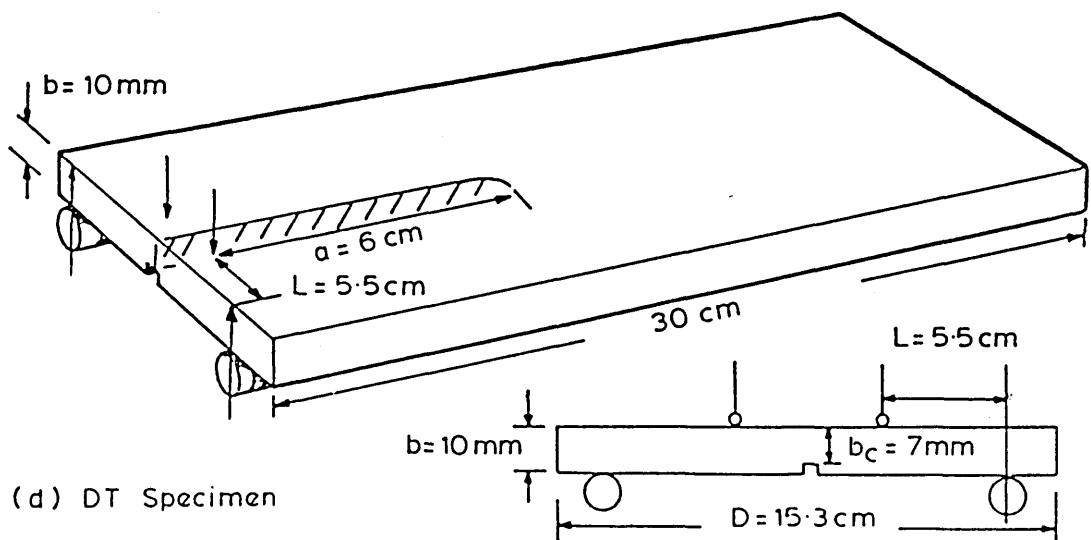
(a)   SEN Specimens

(b)   DCB Specimens

(c) TDCB Specimen

(d) DT Specimen

Fig.5 Details of fracture mechanics specimens